Toxicologic and pharmacologic properties of the dodecaborate cluster: Synthetic, physical-chemical and biological studies

Dissertation

zur Erlangung des Doktorgrades der Naturwissenschaften

- Dr. rer. nat. -

vorgelegt dem Promotionsausschuss

des Fachbereichs 2 (Biologie/Chemie) der Universität Bremen

von

Tanja Schaffran

Universität Bremen 2009

Tag des öffentlichen Kolloqiums: 12.06.2009

Gutachter der Dissertation

1. Gutachter: Prof. Dr. Detlef Gabel
2. Gutachter: Prof. Dr. Bernd Jastorff

Danksagung

Herrn Prof. Dr. Detlef Gabel danke ich für die Überlassung der interessanten und abwechslungsreichen Themen und die Möglichkeit frei forschen zu können, außerdem für die Bereitstellung des Arbeitsplatzes. Auch möchte ich mich herzlich für die stete Diskussionsbereitschaft und für seine Geduld mit meinem Englisch bedanken!

Für die Erstellung des Zweitgutachtens danke ich Herrn Prof. Dr. Bernd Jastorff. Für die Übernahme des Prüferamtes möchte ich mich bei Prof. Dr. Dietmar Beyersmann und Prof. Dr. Horst Diehl bedanken.

Den Mitgliedern und ehemaligen Mitgliedern der Arbeitsgruppe von Prof. Dr. Detlef Gabel, hier insbesondere Frau Andrea Vöge, Frau Katy Penk und Herr Dr. Eugen Justus, danke ich für die sehr angenehme Arbeitsatmosphäre, für die anregenden Diskussionen, die gute Zusammenarbeit und die Hilfsbereitschaft. Hiermit möchte ich mich auch bei Herrn Dr. Eugen Justus für die gute Einführung in die Borclusterchemie bedanken.

Ich bedanke mich bei Prof. Dr. Katarina Edwards von der Universität von Uppsala (Schweden) für die exzellente Zusammenarbeit und die vielen wissenschaftlichen Anregungen. Ich konnte während meiner Promotionszeit viel von ihr lernen.

Ich möchte mich herzlich bei Göran Karlsson von der Universität Uppsala (Schweden) für die Aufnahme und Bearbeitung der cryo-TEM Bilder bedanken.

Bei Prof. Dr. Rolf Schubert und Prof. Regine Peschka-Süss bedanke ich mich für die Zusammenarbeit zu den borhaltigen Lipiden.

Für die Aufnahme der Massenspektren bedanke ich mich bei Herrn Dr. Thomas Dülcks und Frau Dorit Kempken.

Ein Dank geht auch an die vielen Studenten, die mit ihren Forschungsberichten/–arbeiten, Diplomarbeiten und Masterarbeiten einiges zu meiner Doktorarbeit beigetragen haben.

Ein besonderer Dank geht an meinen Lebensgefährten Nico Frische und an meine Eltern, die mich während des Studiums und der Dissertation immer unterstützt haben. Ohne Euch wäre diese Arbeit sicherlich nicht möglich gewesen.

Meinen vierbeinigen Mitbewohnern danke ich für ihre schnurrige Anteilnahme.

List of abbreviations

A	Acceptor
AB	*N,N,N*-trialkylammonioundecahydrododecaborates
AChE	Acetylcholinesterase
B-6-14	S-(N,N-(2-dimyristoyloxyethyl)-acetamido)-thioundecahydro-closo-dodecaborate
B-6-16	S-(N,N-(2-dipalmitoyloxyethyl)-acetamido)-thioundecahydro-closo-dodecaborate
B12NH3	Ammonioundecahydro-*closo*-dodecaborate
BBB	Blood brain barrier
B-Dioxan-14	4-(N,N-bis(2-myristoyloxyethyl)-N-ethoxy-ammonium)-ethoxyundecahydro-closo-dodecaborate (-1), cesium salt
BNCT	Boron neutron capture therapy
BOPP	tetrakis-carboranecarboxylate ester of 2,4-bis-(*α,β*-dihydroxyethyl)deuterioporphyrin IX
BPA	4-dihydroxyborylphenylalanine
BSH	Mercaptoundecahydrododecaborate ($Na_2B_{12}H_{11}SH$)
B-THF-14	4-(N,N-bis(2-myristoyloxyethyl)ammonium)-butoxyundecahydro-closo-dodecaborate (-1), cesium salt
BuAB	*N,N,N*-tributylammonio-undecahydro-*closo*-dodecaborate
Cryo-TEM	Cryo-transmission electron microscopy
D	Donor
DBDU	5-(dihydroxyboryl)-2'-deoxyuridine
Dioxan-SAINT-12	4-(Bisdodecylmethyl)pyridinio-N-ethoxy-ethoxy-undecahydro-closo-dodecaborate (-1), cesium salt
Dioxan-SAINT-14	4-(Bistetradecylmethyl)pyridinio-N-ethoxy-ethoxy-undecahydro-closo-dodecaborate (-1), cesium salt
Dioxan-SAINT-16	4-(Bishexadecylmethyl)pyridinio-N-ethoxy-ethoxy-undecahydro-closo-dodecaborate (-1), cesium salt
DMPC	Dimyristoylphosphatidylcholine
DMPG	Dimyristoylphosphatidylglycerol
DNA	Deoxyribonucleic acid
DPH	1,6-diphenyl-1,3,5-hexatriene
DPPC	Dipalmitoylphosphatidylcholine
DPPE	Dipalmitoylphosphatidylethanolamine
DSC	Differential scanning calorimetry
DSPC	Distearoylphosphatidylcholine
DTNB	5,5'-dithio-bis-(2-nitrobenzoic acid)

EC_{50}	Half maximal effective concentration (induces 50% cell death)
EDCI	1-(3-dimethylaminopropyl)-3-ethylcarbodiimide hydrochloride
EGF	Epidermal growth factor
EINS	Electrophile-induced nucleophilic substitution
EPG	Egg phosphatidylglycerol
EtAB	*N,N,N*-triethylammonio-undecahydro-*closo*-dodecaborate
Et2AB	*N,N*-diethyl-*N*-benzylammonio-undecahydro-*closo*-dodecaborate
FA	Folic acid
FR	Folate receptor
FRET	Fluorescence resonance energy transfer
FTIC	Fluoresceinisothiocyanato
H_{II}	Inverted hexagonal phase
HA	Hyaluronic acid
HxAB	*N,N,N*-trihexylammonio-undecahydro-*closo*-dodecaborate
Ils	Ionic liquids
Kow	Octanol/water coefficient
mPMS	1-methoxy-5-methyl-phenazinium methyl sulfate
NADH	Nicotinamide adenine dinucleotide (hydrogen)
NBD-PE	N-(7-nitrobenz-2-oxa-1,3-diazol(-4-yl)-1,2-di-hexadecanoyl-sn-glycero-3-phospho-ethanolamine, triethylammonium salt
iPen	*N,N,N*-triisopentylammonio-undecahydro-*closo*-dodecaborate
LDLs	Low-density lipoproteins
LUV	Large unilamellar vesicles
MeAB	*N,N,N*-trimethylammonio-undecahydro-*closo*-dodecaborate
MLV	Multilamellar vesicles
PAS	Peripheral anionic site
PE	Phosphatidyl ethanolamine
PEG	Polyethylene glycol
PFOS	Perfluorinated drugs
PrAB	*N,N,N*-tripropylammonio-undecahydro-*closo*-dodecaborate
Pyran-SAINT-12	4-(Bisdodecylmethyl)pyridinio-N-pentoxy-undecahydro-closo-dodecaborate (-1), cesium salt
Pyran-SAINT-14	4-(Bistetradecylmethyl)pyridinio-N-pentoxy-undecahydro-closo-dodecaborate (-1), cesium salt
Pyran-SAINT-16	4-(Bishexadecylmethyl)pyridinio-N-pentoxy-undecahydro-closo-dodecaborate (-1), cesium salt
Q	Cubic phase

RES	Reticuloendothelial system
Rh-PE	Rhodamine B 1,2-dihexadecanoyl-sn-glycero-3-phospho-ethanolamine, trimethylammonium salt
RORs	Ring opening reactions
SUV	Small unilamellar vesicles
TF	Transferrin
THF-SAINT-12	4-(Bisdodecylmethyl)pyridinio-N-butoxy-undecahydro-closo-dodecaborate (-1), cesium salt
THF-SAINT-14	4-(Bistetradecylmethyl)pyridinio-N-butoxy-undecahydro-closo-dodecaborate (-1), cesium salt
THF-SAINT-16	4-(Bistetradecylmethyl)pyridinio-N-butoxy-undecahydro-closo-dodecaborate (-1), cesium salt
THF	Tetrahydrofurane
THP	Tetrahydropyrane
TNFα	Tumor necrosis factor α
WST-1	4-[3-(4-iodophenyl)-2-(4-nitrophenyl)-2*H*-5-tetrazolio]-1,3-benzene disulfonate

Summary

General aspects for dodecaborate cluster compounds

The dodecaborate cluster unit $B_{12}H_{12}^{2-}$ exhibits properties of a pharmacophor and consequently causes certain pharmacological interactions. It is responsible for a firm binding to membrane surfaces due to interactions with the head groups of phosphatidylcholine lipids. Compounds containing the dodecaborate cluster adopt this unexpected behavior which is not known for other ionic species.

Amphiphilic derivatives of the dodecaborate cluster cause a different pharmacologic effect than pure ionic substances. Depending on their lipophilic part they can react as detergent or can incorporate into existing membranes without any disturbances of the membrane.

High molecular weight compounds induce pharmacological effects which are unexpected and so far not understood in molecular detail.

Ionic liquids

The toxicological hazard potentials of different *N,N,N*-trialkylammonioundeca-hydrododecaborates (ABs), a novel class of compounds of interest for use as anions in ionic liquids, are determined for Man and environment. The test strategy comprises the mammalian cell line V79, the limnic green algae *Scenedesmus vacuolatus* and the enzyme acetylcholineesterase. Qualitative trends of toxicity are established for all ABs with *n*-alkyl chains and can be applied to all named biological systems. The toxic potential of the ABs increases with increasing lipophilicity of the ABs resulting from longer alkyl chains. The length of the chains influences drastically the properties of the ABs which show an increasing surfactant-like behavior with longer alkyl chains.

A quantitative prediction of the toxicity for ABs with longer *n*-alkyl chains was only successful for mammalian cells. Qualitative conclusions or quantitative predictions for asymmetrically substitution or branched side chains could not be drawn.

The cell membrane is proposed as target site for toxic interactions. A model for the AB binding to the membrane is devised on the basis of zeta potentials and DSC data obtained by liposomes as model a cell membrane. We suggest that the dodecaborate cluster unit interacts electrostatically with the lipid head groups and that the ammonium group is probably in contact with the deeper-lying phosphate group. The alkyl chains of the ABs form hydrophobic interactions with the non-polar hydrocarbon part of the membrane. The latter interactions are an important driving force for the binding to the membrane surface.

Different toxic modes of action are feasible for the ABs and might concern changes in the membrane potential of cells, permeabilization of the membrane by pore formation or the complete disruption of the membrane.

A potential mechanism for AChE inhibition was theoretically developed for ABs with *n*-alkyl chains on the basis of thinking in terms of structure activity relationships. Thus the lipophilic channel located in the entrance of the gorge of AChE is proposed as target site for toxic interactions.

Dodecaborate cluster lipids

New dodecaborate cluster lipids were synthesized for application in boron neutron capture therapy of tumors. For the synthesis, a new strategy was designed which allows a facile preparation in relative high product yields, is not very time-consuming and offers the possibility to vary the lipid structure, e.g. the linker or the lipid tails. All boron lipids carry only one single net charge, have a double-tailed lipophilic part and the dodecaborate cluster as head group. They differ in the linker connecting the head group and the lipid backbone, in the length of their lipid tails and the chemical basic structure of the lipophilic part which can compose of a diethanolamine or an *N*-methyl-*p*-bisalkylmethylpyridinium frame. All lipids were characterized in their physical-chemical behaviors, in their ability to form liposomes and in their toxicity *in vitro* and *in vivo*. In addition, each of them was incorporated into pegylated liposomes composed of DSPC, cholesterol and DSPE-PEG_{2000} for the purpose of delivery of boron-containing compounds to tumor tissues.

The linker influences the physical-chemical and toxic properties of the lipids depending on the lipid backbone. Thus a prediction of the linker influence is not possible for a defined boron lipid and consequently no linker can be favored for lipid synthesis in the future.

In general, the length of the lipid tails plays a role in the lipid transition from gel to fluid phase and influences the ability to incorporate the boron lipid into a membrane composed of helper lipids. Longer lipid tails lead to a decrease of toxicity and are consequently recommended for dodecaborate cluster lipids.

After application of liposomes containing dodecaborate cluster lipids in mice a massive and rapid tumoral hemorrhage was observed. This bleeding is associated with extravasated red blood cells in the tumor interstitial space and probably caused by destruction of the tumor blood vessels. The induction of tumor hemorrhage for BNCT is not necessarily a desired effect, especially when accompanied with a non-impressive uptake of boron into the tumor as observed here.

Zusammenfassung

Generelle Aspekte für Dodecaboratecluster-Substanzen

Der Dodecaboratcluster weist Eigenschaften eines Pharmacophors auf und bewirkt dadurch bestimmte pharmakologische Interaktionen. Er ist verantwortlich für die starke Bindung zu Membranoberflächen, welche durch die Interaktionen mit den Kopfgruppen von Phosphatiylcholin-Lipiden zustande kommt. Substanzen, die den Dodecaboratcluster enthalten, übernehmen diese unerwarteten Eigenschaften, die bisher für keine andere ionische Verbindung bekannt ist.

Amphiphile Derivate des Dodecaboratcluster lösen andere pharmakologische Effekte aus als rein ionische Derivate. In Abhängigkeit vom lipophilen Rest können sie als Detergenzien reagieren oder lassen sich in bestehende Membranen inkorporieren, ohne diese zu schädigen.

Substanzen mit einem hohen Molekulargewicht induzieren pharmakologische Effekte, die völlig unerwartet und bisher nicht auf molekularer Ebene verstanden sind.

Ionische Flüssigkeiten

N,N,N-Trialkylammonioundecahydrododecaborate (ABs) sind interessant als Anionen für ionische Flüssigkeiten. Ihre toxikologischen Gefährdungspotentiale wurden für Mensch und Umwelt ermittelt. Die Teststrategie umfasste die Säugetierzellen V79, die Grünalge *Scenedesmus vacuolatus* und das Ezyme Acetylcholinesterase. Qualitative Trends konnten für alle ABs mit *n*-alkyl Ketten etabliert werden und gelten für jedes genannte Testsystem. Das toxische Potential der ABs steigt mit zunehmender Lipophilie, die von der Länge der Alkylketten abhängig ist. Die Kettenlänge beeinflusst drastisch das Verhalten der ABs, so weisen ABs mit längeren Ketten zunehmend Tensid-ähnliche Eigenschaften auf.

Eine quantitative Vorhersage der Toxizität für ABs mit längeren Ketten war nur für die Säugetierzellen möglich. Qualitative Schlussfolgerungen oder quantitative Vorhersagen waren für ABs mit verzweigten Ketten oder einer gemischten Substitution nicht möglich.

Die Zellmembran ist der wahrscheinlichste Ort für toxische Interaktionen. Mit Hilfe von Liposomen (Modell für eine Zellmembran) und daraus erhaltenen Zetapotential- und DSC-Daten konnte ein Bindungsmodell für die ABs entwickelt werden. Wir nehmen an, dass der Dodecaboratcluster mit den Lipidkopfgruppen elektrostatisch wechselwirkt und dass die Ammoniumgruppe mit der tiefer gelegenen Phosphatgruppe interagiert. Die Alkylketten gehen dann hydrophobe Wechselwirkungen mit dem unpolaren Kohlenwasserstoffteil der Membran ein. Die letztgenannten Interaktionen sind eine wichtige treibende Kraft für die Bindung an die Membranoberfläche.

Verschiedene toxische Wirkungsweisen sind für die ABs vorstellbar und können Änderungen des Membranpotentials, eine Permeabilisierung der Membran durch die Ausbildung von Poren oder eine komplette Zerstörung der Membran beinhalten.
Ein Mechanismus für die Hemmung des Enzyms AChE wurde in der Theorie entwickelt anhand von Struktur-Wirkungs-Beziehungen. Als Wirkungszielort wird der lipophile Kanal am Eingang des Enzyms angenommen.

Dodecaboratclusterlipide

Neue Dodecaboratclusterlipide wurden synthetisiert für die Anwendung in der Borneutroneneinfangtherapie (BNCT). Für die Synthese wurde eine neue Strategie entwickelt, die eine leichte Herstellung mit hohen Ausbeuten erlaubt, nicht so aufwendig ist und es ermöglicht, die Lipidstruktur zu variieren, z.B. den Linker oder die Lipidreste. Alle Borlipide sind nur einfach negativ geladen, bestehen aus einem doppelt-schwänzigen Lipidteil und weisen den Dodecaboratcluster als Kopfgruppe auf. Sie unterscheiden sich im Linker, der die Kopfgruppe mit dem Lipidrückgrat verbindet, in der Länge ihrer Lipidschwänze und in der chemischen Grundstruktur des lipophilen Teils, die aus ein Diethanolamin- oder *N*-Methyl-*p*-bisalkylmethylpyridinium-Gerüst bestehen kann. Alle Lipide wurden in ihren physikalisch-chemischen Eigenschaften charakterisiert, in ihrer Fähigkeit Liposomen auszubilden und in ihrer *in vitro* und *in vivo* Toxizität. Außerdem wurde jedes von ihnen in pegylierte Liposomen bestehend aus DSPC, Cholesterin und DSPE-PEG_{2000} integriert für einen möglichen Transport von Borverbindungen zum Tumorgewebe.
In Abhängigkeit vom Lipidrückgrat beeinflußt der Linker die physikalisch-chemischen und toxischen Eigenschaften der Lipide. Eine Vorhersage zum Einfluss des Linkers in einem bestimmten Lipid ist nicht möglich und damit kann kein Linker für eine Lipidsynthese bevorzugt werden.
Die Länge der Lipidschwänze spielt eine generelle Rolle bei den Lipidübergängen von der gelartigen zur fluiden Phase und beeinflusst die Inkorporierung von Borlipiden in eine bestehende Membran aus Helferlipiden. Längere Lipidschwänze führen zu einer Verminderung der Toxizität und sind somit empfehlenswert für Dodecaboratclusterlipide.
Nach der Verabreichung von Liposomen, die Dodecaborateclusterlipide enthalten, an Mäuse wurde eine schnelle und massive Einblutung im Tumor beobachtet. Diese Blutung ist zurückzuführen auf rote Blutkörperchen, die in den interstitiellen Raum gelangt sind, wahrscheinlich ausgelöst durch zerstörte Tumorblutgefäße. Die Einblutung ist nicht unbedingt ein gewünschter Effekt für die Borneutroneneinfangtherapie, speziell dann nicht wenn die Boraufnahme im Tumor relativ gering ist wie in diesem Fall.

INDEX OF CONTENTS

1. Introduction

1.1 Liposomes

Liposomes (Phospholipid vesicles) are first published by Bangham *et al*. (1965) and are described in more detail by Sessa and Weismann (1968). At that time the biological properties of membranes were interpreted in terms of chemistry and physics of lipids. Therefore liposomes are a suitable model to simulate biological membranes and processes on them. Later liposomes are discovered as drug carriers, e.g., for peptides, proteins, DNA plasmids and drugs for a specific therapy or cosmetic application. (Uhlrich, 2002)

Liposomes consist commonly of **phospholipids**. Phospholipids are amphipathic molecules because they contain a hydrophilic head group (e.g., choline, serine, ethanolamine) connected to a hydrophobic lipid backbone. The chemical structure is composed of a glycerol matrix which is esterified on positions 1 and 2 with fatty acids and with phosphate in position 3 (Fig. 1). The fatty acids can vary in their length (C_{10}-C_{18}) and can contain *cis*-configured double bonds.

When phospholipids are dispersed in water, the formation of ordered **bilayers** occurs spontaneously. The driving force is the hydrophobic effect. (Voet *et al*., 2002) Here the fatty acids keep together to avoid the contact with water whereas the head groups form associates with the water, so that a hydrate shell is generated (Fig. 1). The formation of possible micelles is not favorable because the two fatty acid chains are too bulky to fit into the interior of a micelle.

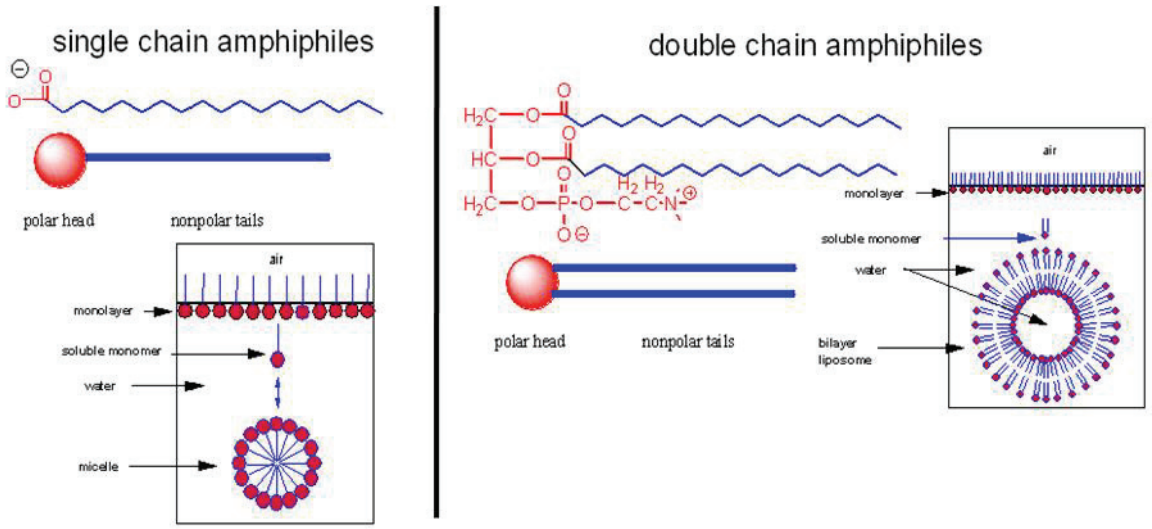

Figure 1: Lipids with single- or double-tailed moiety dispersed in water: formation of micelles or bilayers. (http://employees.csbsju.edu)

Liposomes are tiny vesicles formed by lipid bilayers. A large number of liposome subclasses are known in the literature. A suspension of **multilamellar vesicles** (MLV) is obtained when

the lipids are dissolved in an organic solvent, subsequent drying, and finally hydrating under agitation above the lipid phase transition temperature. (Bangham *et al*., 1965; Ulrich, 2002; Chrai, 2002) The MVLs, however, are less suitable for some studies or to mimic the cell membrane than a bilayer system. (Sessa and Weissmann, 1968) Sonication disrupts MLV to produce **small unilamellar vesicles** (SUV) with radii around 30-60 nm which tend to aggregate and fuse together. (Ulrich, 2002) The most popular method to prepare **large unilamellar vesicles** (LUV) (Fig. 2) is a repeated extrusion of the MLV suspension through a polycarbonate filter of well-defined pore size. (Hope, 1985; Ulrich, 2002) The lamellarity can be controlled better and the trapping efficiencies can be enhanced when the MLV suspension is frozen and thawed prior the extrusion step. (Mayer *et al*., 1985; Mayer *et al*., 1986)

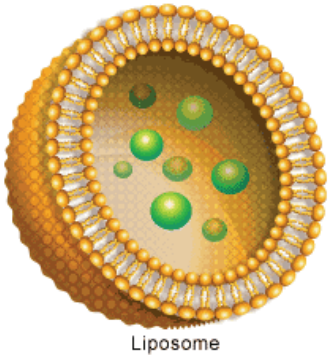

Figure 2: Schematic picture of an unilamellar liposome: the lipid bilayer encloses an inner aqueous core in which drugs can be encapsulated. (http://www.bioteach.ubc.ca)

LUVs prepared from naturally occurring lipids are the best models for simulation of a cell membrane. (Torchilin *et al*., 2003)

Lipids are also able to form other morphologies than the lamellar phases described so far. Lipids with a large head group and a small hydrocarbon cross-section have a cone-like geometry and form spontaneously micelles. Lipids that are cylindrical in shape, having nearly equal head group to hydrocarbon area, favor the formation of bilayers. Finally, lipids with small head groups adopt “inverted” phases such as hexagonal (H_{II}) and cubic phases (Q). In the hexagonal phase the lipid tails are arranged in cylindrical rods wherein the head groups are ordered towards the aqueous core. Cubic phases are made up of bicontinuous surfaces, several channels are formed by lipids which are permeable for water. The lipid **polymorphism** and the different morphologies are shown more in detail in Fig. 3. (Ulrich, 2002)

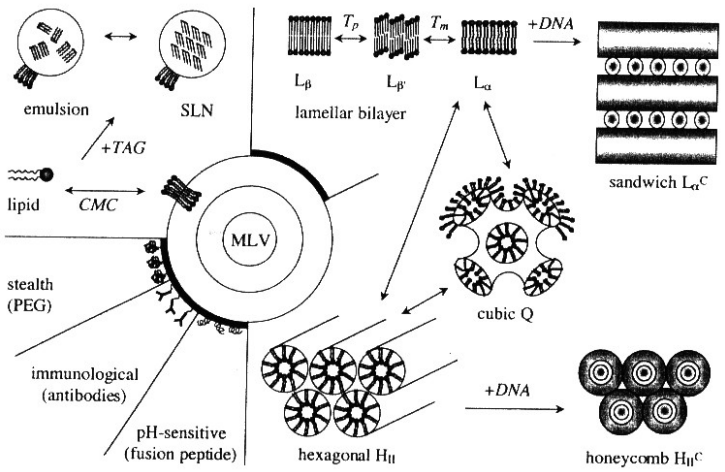

Figure 3: Overview of the lipid phase transitions and polymorphism (Ulrich, 2002)

Depending on the temperature lipid bilayers pass through different phases of fluidity. In the lamellar "solid" gel phase (L_β) the lipid acyl chains are preferentially aligned in an *all-trans* conformation and lateral diffusion is very slow. When the phase transition temperature which is different for each lipid is reached, the membrane passes into the "fluid" liquid crystalline phase (L_α). Here the lipids are disordered and diffuse freely laterally and the acyl chains undergo rapid *trans-gauche* fluctuations. (Ulrich, 2002) Addition of cholesterol decreases the phase transition temperature. The lipid crystallization in the gel phase is hindered when cholesterol is incorporated in the membrane. At 50% cholesterol the membrane is saturated and the lipid phase transition is completely abolished. (Ulrich, 2002)

1.2 Pegylated liposomes

Liposomes are ideal drug carriers being biodegradable and of minimal toxicity. But their short circulation time in blood is a drawback. After their intravenous injection liposomes are rapidly removed primarily by Kupffer cells of the liver and fixed macrophages of the spleen. Therefore modified liposomes are essential to reach long circulation times in the body and to avoid the uptake by the reticuloendothelial system (RES). (Hashizaki *et al*., 2003) Blume and Cecv (1990) observed that the surface charge is the main factor for vesicle uptake. Therefore a steric surface protection should slow down the adsorption of macromolecules. Liposomes coated by long flexible polymer residues have greatly extended times of blood circulation. The polymer residues form a steric barrier which reduces opsonization and protein interactions in general. (Silvander, 2002; Allen *et al*., 2002) Therefore the steric barrier created delays recognition and clearance from the blood stream. (Drummond, 1999)

The most important method for obtaining a polymer-coated liposome is to attach the polymer covalently to one of the components of the membrane. Polyethylene glycol (PEG) lipids are the most commonly used stabilizers for steric stabilization of liposomes. The PEG is here

attached to a lipid, typically a double-tailed phosphatidyl ethanolamine (PE), as anchor in the membrane. Several chain lengths of PEG are in use, such as PEG_{750}, PEG_{2000}, and PEG_{5000}. When considering a liposome containing pegylated lipids, it is believed that the PEG will extend away from the liposome into the solvent as it is not attached to the lipid bilayer.

Depending on the PEG concentration two different regimes of grafted polymer behavior are defined (Fig. 4). If the PEG density is low, the polymer is said to be in the mushroom regime. When the graft density is high the polymers are said to be in the brush regime. (Allen *et al*., 2002) The lateral repulsion at high surface concentration is one reason to affect the structural properties of the liposome and eventually lead to its disruption. (Silvander, 2002) But before the disruption can occur, a maximum on PEG has to incorporate in the liposomal membrane. (Edwards *et al*., 1997)

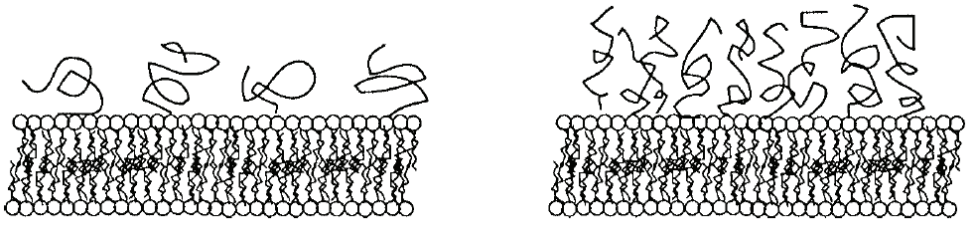

Figure 4: A schematic view of the mushroom regime (left) and the brush regime (right) of polmer coils. (Silvander, 2002)

The incorporation of the PEG lipid in the liposomal membrane leads to changes in the physicochemical properties. Thus the particle size decreases significantly by increasing the amount of PEG. (Sriwongsitanont and Ueno, 2002) Furthermore the formation of liposomes or other structures depends on percentages of PEG (Fig. 5). At low concentrations unilamellar liposomes are obtained. With increasing PEG concentrations the formation of disks are favored and at 20 mol% of PEG-lipid, only a few liposomes are found and relatively small disks are strongly dominating structures. When the PEG content is increased further, it results in the complete disappearance of the liposomes and significant decrease in the disk size. For 50 mol% and 68 mol% of PEG-lipid respectively only spherical micelles are obtained. It was also found that a decrease in phospholipid chain length decreases the amount of PEG lipid needed to induce micelle formation, whereas phospholipid saturation or the presence of cholesterol has little or no effect. (Edward *et al*., 1997; Johnson and Edwards, 2003)

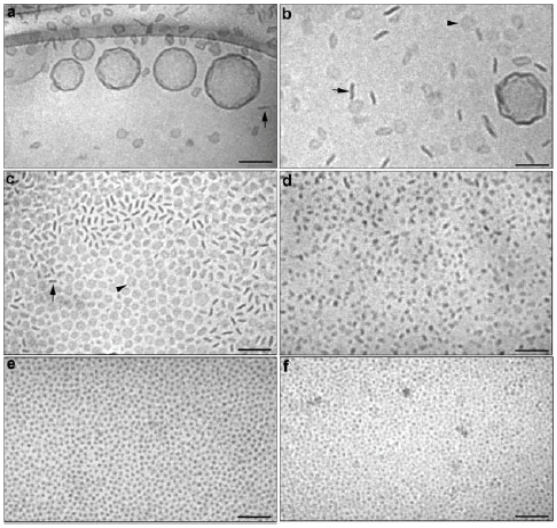

Figure 5: Cryo-TEM images of DPPC dispersions containing DPPE-PEG_{2000} in concentrations of (a) 4.5 mol%, (b) 9.5 mol%, (c) 19.5 mol%, (d) 30.2 mol%, (e) 49.7 mol%, (f) 68 mol%. The arrowheads in b and c denote disks observed edge-on and face-on, respectively. Scale bar: 100 nm (Johnsson and Edwards, 2003)

The phase transition temperature is also affected by incorporation of PEG in the liposomal membrane. Here the transitions are shifted to higher temperature with increasing PEG concentrations. (Hashizaki *et al*., 2003)

1.3 Targeting of liposomes

Liposomes can be tagged with tumor-seeking entities which allow selective accumulation in the tumor tissue. In this case liposomes can transport their content specifically to the tumor. This procedure for ligand liposomes allows generally the combination of various ligand and boron compounds. Therefore the liposomes can be tailored for each tumor model depending on the receptor availability on the cell surface.

There are many possibilities for liposome targeting. **Epidermal growth factor receptors** (EGFRs) are overexpressed in many tumor cells (Chaidarun, 1994) and can be used as a tumor-seeking entity. Bohl Kullberg (2002) developed a method to couple EGF to DSPC/cholesterol/DSPE-PEG liposomes. The first step is the activation of EGF with Traut´s reagent (2-iminothiolane) followed by coupling to maleimide-PEG-DSPE. The conjugated was incorporated into preformed liposomes via the micelle transfer method at 60°C. Higher temperatures lead to leakage of the liposomal contents. Also the amount of PEG in the liposomal membrane plays a role, thus the incorporation efficiency decreases at higher PEG concentrations. Furthermore empty liposomes can be modified better with the EGF-conjugate than loaded ones. The *in vitro* experiments demonstrate that the EGF-liposomes bind specifically to their receptors on the cell surface. (Bohl Kullberg et al, 2002)

The **HER2 protooncogene** and the growth receptor **p185^{HER2}** appear to play a central role in the pathogenesis of many human cancers. The overexpression of the receptor in cancer cells makes it an attractive target for liposome delivery as normal tissues expressed it only in low levels. Park *et al*. (1995) developed immunoliposomes as a tumor-targeting vesicle and showed that these liposomes are internalized into cells via receptor-mediated endocytosis. The liposome uptake is influenced by the amount of PEG, thus higher PEG percentages lead to slower internalization.

Folic acid (FA) is one of the well-studied targeting ligands used for receptor-mediated endocytosis. The folate receptor (FR) is amplified in a variety of human tumors. (Carlsson *et al*., 2003) The FR is a glycosyl-phosphatidylinositol-anchored glycoprotein with high affinity to the FA vitamin. Gabizon *et al*. (2003) coupled the folate group with the outer end of PEG, thus it is located away from the bilayer. DSPE-PEG was used as pegylated component which was then incorporated in the liposomal membrane. Pan *et al*. (2002) have shown that folated liposomes are a suitable delivery system *in vitro* whereas Gabizon *et al*. (2003) detected no higher tumor levels than for non-folated liposomes and a rapid clearance of folated liposomes by the liver. Both investigators found a more selective liposome delivery in the presence of a folate excess since the clearance of folated liposomes is blocked.

Liposomes were also modified with an oligomer of **hyaluronic acid** (HA) which is incorporated in the liposome membrane. Cells are able to internalize these functionalized liposomes when they exhibit the CD44 receptor on their cell surface such as carcinoma, melanoma, lymphoma, breast and lung tumor cells. The *in vitro* studies demonstrate that the uptake of these liposomes is receptor-mediated and higher as for non-modified liposomes. Therefore liposomes functionalized with HA are potent transporters for drug delivery. (Eliaz and Szoka, 2001) But no CD antigens of interest as targets for ligand liposomes have so far been identified on gliomas. (Carlsson *et al*., 2003)

Ishida *et al*. (2001) explored the possibility of using **transferrin** (TF) for liposomal drug delivery. TF is a glycoprotein responsible for the ferric ion transport in the body. It transfers the iron via receptor-mediated endocytosis to the cells. The TF receptor concentrations on tumor cells are much higher than in normal cells and allow specific drug transport to the tumor. To obtain TF-modificated liposomes TF was coupled to the distal terminal of the PEG-chains in pegylated liposomes as follows: DSPE-PEG-COOH is reacted with 1-(3-dimethylaminopropyl)-3-ethylcarbodiimide hydrochloride (EDCI) to an unstable reactive *O*-acylisurea ester. Addition of transferrin leads to the covalently binding of transferrin to the PEG-chain via formation of a stable amide bond. (Ishida *et al*., 2001) Maruyama *et al*. (2004) used the transferrin-PEG liposomes to transfer encapsulated BSH to solid tumors. The study demonstrates that this kind of liposomes achieves a potentially useful boron accumulation in

the tumor in conjunction with an extremely low plasma boron concentration. Thus, TF-PEG liposomes could be useful as a new intracellular targeting carrier in the treatment of cancer.

1.4 Liposome uptake in solid tumors

Many of the drug delivery approaches take advantage of the unique pathophysiology of tumor vasculature. In the growing process of a tumor high amounts of nutrients and oxygen are necessary to ensure the fast dispersion of the tumor. The tumor cells release cytokines and other signaling molecules that recruit new blood vessels to the tumor, in a process called angiogenesis. Thus tumors contain a high density of abnormal blood vessels that are dilated and poorly differentiated, with chaotic architecture and aberrant branching. The vasculature functions are also impaired, such as a higher permeability than normal vessels. The angiogenic blood vessels have gaps as large as 600 to 800 nm between adjacent endothelial cells. Thus drug carriers, e.g., liposomes depending on their size can extravasate through these gaps into the tumor interstitial space (Fig. 6).

This phenomenon is known as concept of enhanced permeability and retention effect which results from the increasing permeability of tumor blood vessels as well as the decreased rate of clearance caused by the lack of functional lymphatic vessels in the tumor. All these facts lead to a higher accumulation of macromolecules (liposomes) in tumors. The passive accumulation leads rather to focal localization than to a homogenous distribution which is not well understood in detail. (Dreher *et al*., 2006; Allen and Cullis, 2004)

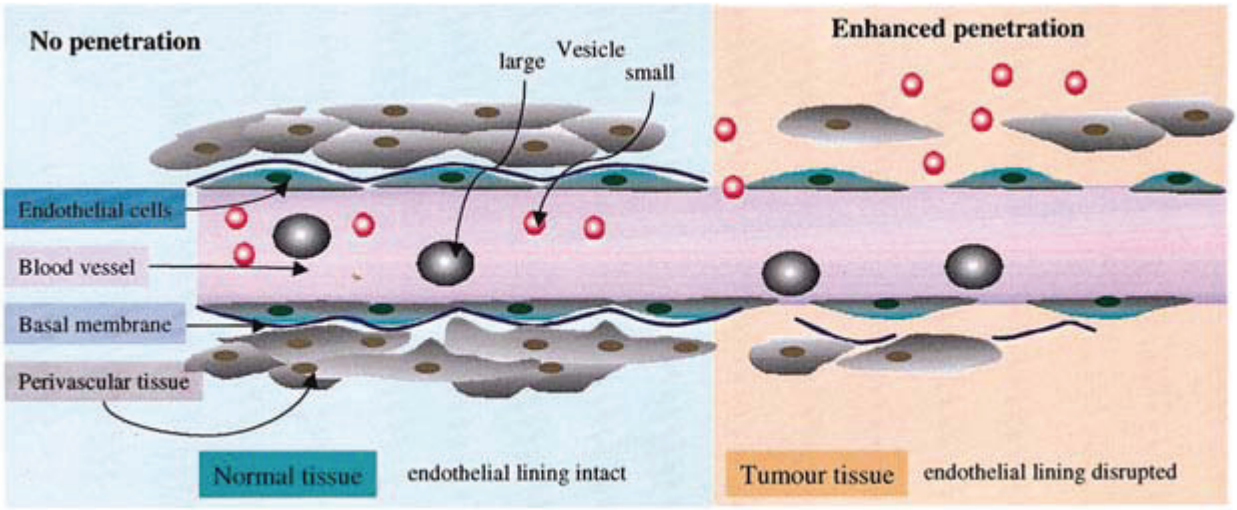

Figure 6: Comparison of normal and tumor blood vessels (http://www.pharmj.com)

In general the level of accumulation depends on the following factors: the size and the charge of the liposome (factors influence the clearance celerity), the circulation half-life of the liposomes (longer life-time leads to higher accumulation), the degree of tumor vascularization

(poorly vascularized tumors take up less liposomes), the degree of angiogenesis (small pre-angiogenic tumors or large necrotic tumors will accumulate liposomes poorly) and the size of the gaps. (Allen and Cullis, 2004; Dreher *et al*., 2006)

The molecular weight influences the permeability for macromolecules. Thus the permeability deceases significantly if the weight increases, which would slow the rate of extravation for larger compounds. Furthermore the weight and the size influence the penetration distance, e.g., large dextrans are highly concentrated only near the vascular surface. But this can lead, to a greater therapeutic effect considering that these cells have a higher proliferation rate compared to those located farther away from the vascular surface. (Dreher *et al*., 2006)

1.5 Liposome-cell interaction

Four different mechanisms for the liposome uptake are known (Fig. 7). (Sandra and Pagano, 1979) The appearance of one of these mechanisms depends on the size, charge, composition, the presence of targeting devices, the cell type and environmental factors. (Torchilin *et al*., 2003)

Adsorption to the cell surface was found for liposomes without targeting devices due to physical attractive forces and for liposomes with targeting which bind specifically to the receptors located on the cell surface. Adsorption seems to be rather a pre-requisite for other interactions, eventually leading to internalization.

1. The model of **contact release** (also named content release) is not clearly understood. It has been suggested that the contact of liposome and cell membrane leads to a higher permeability of the liposomal membrane, so that the content is released and can diffused into the cytoplasm or can act on the cell membrane.
2. The **intermembrane transfer** is an exchange of lipids between the liposomal and the cell membrane. The integrity of the membrane is here not influenced. The common hypopthesis is that the transfer is mediated via an exchange protein. (Sandra and Pagano, 1979)
3. The **endocytosis/phagocytosis** is the major way for cellular uptake *in vivo* and is often receptor-mediated. Liposomes are taken up as sub-cellular vacuoles, termed as phagosomes or endosomes, originating by invagination of the plasma membrane. These vacuoles fuse with lysosomes followed by a lysosomal digestion of the endosomal contents. The resulting fatty acids can either be released from the cell or recycled and reincorporated into cellular phospholipids. The original liposomal

content is then released into the lysosome in which it may be destroyed, leak out or remain sequestered until exocytosis.

4. **Fusion** of the liposome with the cell membrane leads to a complete lipid intermixing and the release of the liposomal contents into the cytoplasm.

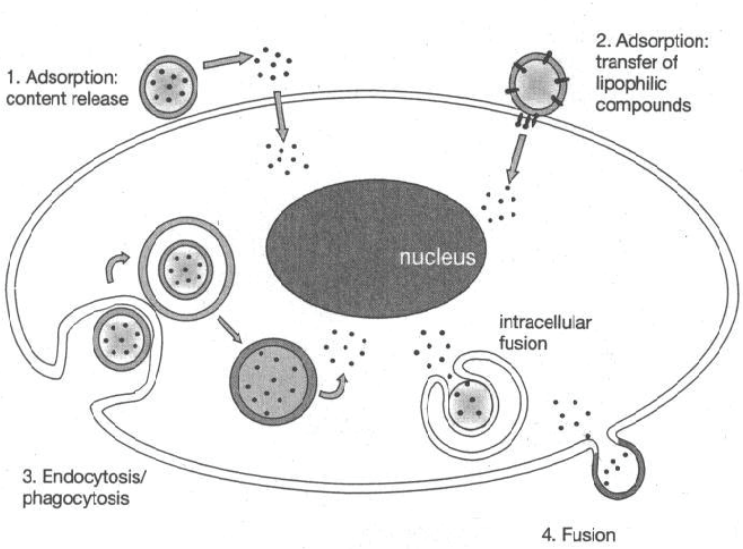

Figure 7: Possible mechanisms of liposome uptake into cells (Torchilin *et al*., 2003)

1.6 Polyhedral boranes and polyhedral boron hydrides

The simplest borane is BH_3 which only appears in the form of a dimere $(BH_3)_2$. The higher boranes result from the clustering of boranes B_mH_{m+2} (m = 1, 2, 3 etc.) which do not exist alone, that means in pure form. In general higher boranes are favorable with the molecular formula B_nH_{n+4} (n = 2, 5, 6, 8, 10, 11, 12, 14, 16, 18) and B_nH_{n+6} (n = 4, 5, 6, 7, 8, 9, 10, 13, 14, 15, 20), but also the boranes B_nH_{n+8} (n = 8, 10, 14, 15, 30) and B_nH_{n+10} (n = 8, 26, 40) exist. In these polyboranes the boron atoms are connected to cage-like structures, polyhedrons, in which each boron atom is located on a polyhedron vertex (Fig. 8). The steric structures can be predicted with the rule of Wade. Thus the *closo*-structure is a polyhedron with n edges and the molecular formula B_nH_{n+2}, the *nido*-structures B_nH_{n+4} result in a polyhedron with n+1 vertices where one vertex is not occupied. In *arachno*-polyhedrons B_nH_{n+6} two vertices are not filled from a total of n+2 and three vertices are not filled in *hypho*-polyhedrons B_nH_{n+8} with n+3 vertices. (Holleman and Wiberg, 1995)

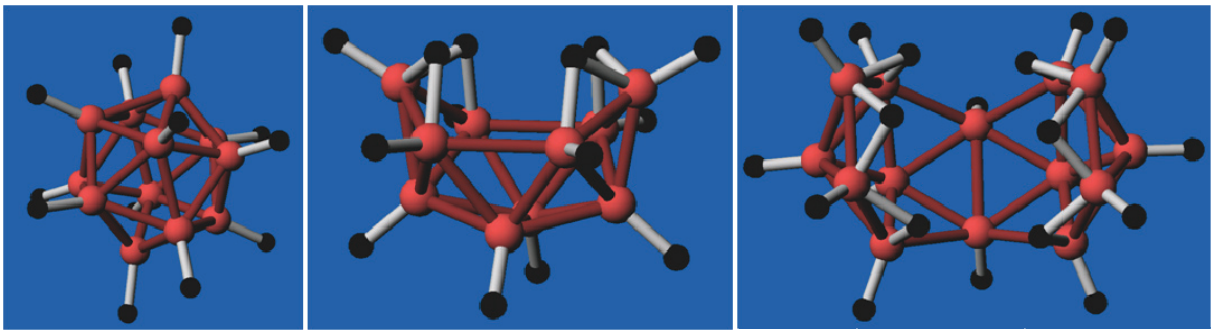

Figure 8: Polyhedrons: *closo*-structure (left), *nido*-structure (central) and *arachno*-structure (right). (http://ruby.chemie.uni-freiburg.de/)

Polyhedral boron hydrides are derived from boranes via proton elimination and exhibit the molecular formluar $B_nH_n^{p-+m-p}$. All boron hydrides are characterized by electron-deficient bonding. This means that some of the valence electrons are involved in three-centered two-electron bonds, which typically result in the formation of trigonal faces and hypercoordination. (Lipscomp, 1963) These hydrides exhibit aromatic properties. Thus were the first examples of non-planar three-dimensional aromatic compounds and resulted in the development of the concept of three-dimensional aromaticity. (King, 2001)

The exchange of a BH unit to a heteroatom is possible, e.g., the substitution of BH versus CH leads to the formation of carboranes (Fig. 9). These offer the possibility of “normal” organic chemistry in view of the C-C-bond formation. Carboranes are extremely lipophilic.

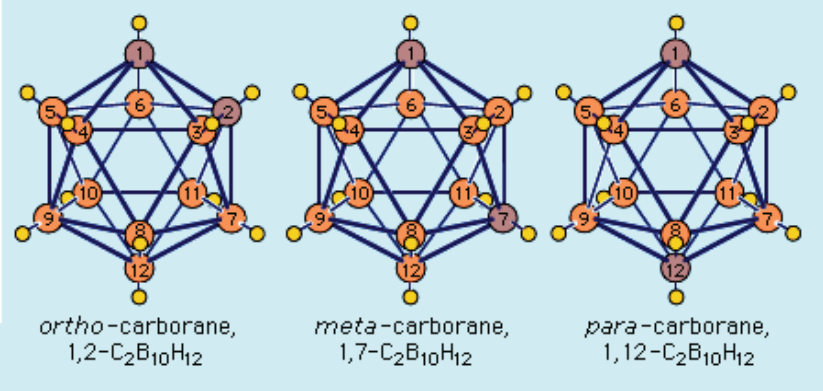

Figure 9: The common structures of carboranes: B atom is located on the orange bubbles, C atoms on the rose balls and the H atoms on the yellow bubbles. (http://media-2.web.britannica.com)

The dodecahydro-*closo*-dodecaborate anion $B_{12}H_{12}^{2-}$ was first synthesized by Pitochelli and Hawthorne in 1960. It is exceptionally stable against acids and bases. Depending on the cation the double negative charge makes it well water-soluble. A derivatization is facile with electrophilic agents. Attacks with nucleophilic reagents are also possible after removal of a hydride. This kind of reaction is explained in more detail under 1.12.

1.7 Ionic liquids

In the last years there has been a great attention for ionic liquids (ILs) in the academic and industrial research fields. ILs are salts which are liquid at low temperatures (<100°C). Their special properties which are negligible vapor pressure, not inflammable, high electric conductivity, wide electrochemical window, tolerance to strong acids, and excellent thermal and chemical stability (Justus *et al.,* 2008; Larsen *et al, 2000*) make them very attractive for different applications. The development of ionic liquids goes back to 1914. Ethylammonium nitrate was the first ionic liquid with a melting point of 12°C. In 1948 chloroaluminate ions were designed by Hurley and Wier (Hurley and Wier, 1951). More than thirty years later systems of chloroaluminate were obtained which melt at room temperature. In the beginning of the eighties chloroaluminate melts were used as non-aqueous, polar solvents for research into transition metal complexes. On the basis of these works ionic liquids come into the focus of the general public. Later acid ionic liquids with chloroaluminate ions were used as effective Friedel-Crafts-catalysts. Ionic liquids containing tetrafluoroborate ions were successfully applied into the hydroformylation of olefins. (Wasserscheid, Keim, 2000) The history of ionic liquids points their multi-faceted applications. They can be new kinds of solvents, can react as chemical catalysts or biocatalysts and can be used in electrochemistry. (Wasserscheid, Keim*,* 2000*;* Welton, 1999*;* Sheldon, 2001; Endres, 2002)

The most established ILs consist of a simple anion (chloride, tetrafluoroborate, hexafluorophosphate) and a cation of following important classes (imidazolium, pyridinium, ammonium, phosphonium) (Fig. 10).

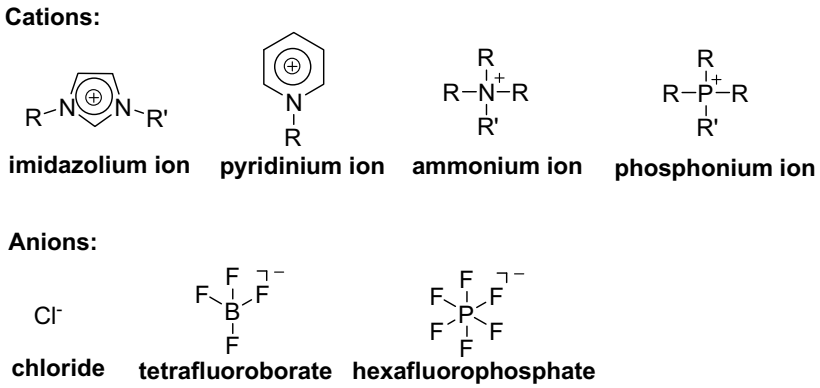

Figure 10: The important kinds of cations and anions in ionic liquids. R and R' can be different alkyl residues.

The size and the structure of the cations and anions in ionic liquids hinder the formation of a strong crystal lattice and thus little energy is enough to overcome the lattice energy and break the lattice structure.

The high possibilities of cation/anion combination (10^{18} combinations) (Wasserscheid and Keim, 2000) and the possibility of specific tuning make the ionic liquids very attractive for

different application. Therefore the properties can be influenced and tailored (designer solvents).

In the recent literature the ionic liquids are discussed as solvents for “clean processes” and as candidates for a “Green Chemistry”, respectively. The efforts are to minimize the consumption of solvents and catalysts in chemical processes. In contrast to volatile, organic solvents the ionic liquids have no measurable vapor pressure and hence a loss of solvent does not occur. The usage of ionic liquids allows the separation of the catalysts from the reaction mixture and hence the recycling of catalysts. The application of ionic liquids leads to environmentally friendly processes in the industry and thus they are often classified as “Green Solvents”. (Wasserscheid and Keim, 2000)

There still exists, however, the demand to new ionic liquids in view of the variety of possible applications. New anions are developed to combine them with common cations. In this field exceptional anions are meltable stannaborate salts (Ronig *et al*., 2002) or carborane anions combinated with alkylpyridinium cations. (Zhu *et al.*, 2003; Larsen *et al*., 2000)

In our group a new kind of ionic liquids was published in which *N*-trialkylammonioundecahydrododecaborates (1-) as anions are combined with simple cations such as potassium, lithium or unsolvated H^+. (Justus *et al.*, 2008) In Fig. 11 the *N,N,N*-trialkylammonioundecahydrododecaborates (1-) consisting of the dodecaborate cluster and trialkylated ammonium group are shown. Derivatives are synthesized with three identical alkyl chains from methyl to hexyl and one derivative with an asymmetric substitution (two ethyl chains and one benzyl group).

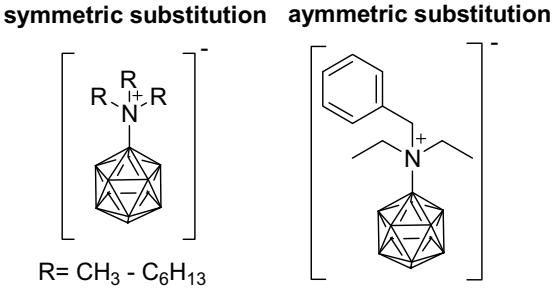

Figure 11: *N,N,N*-trialkylammonioundecahydrododecaborates (1-)

Depending on the cation, these compounds have melting points below 100°C, and some are liquid at room temperature. The *N,N,N*-trialkylammonioundecahydrododecaborates (1-) are prepared with a wide range of cations. Interestingly the potassium and lithium salts give also ionic liquids and thus they are the first examples of a non-corrosive ionic liquid with lithium as cation, and might therefore be used as electrolyte in lithium batteries.

The synthesis of *N,N,N*-trialkylammonioundecahydrododecaborates (1-) (ABs) is based on the *N*-alkylation of ammonioundecahydrododecaborate (B12NH3). (Justus *et al*., 2008) B12NH3 was first described by Hertler and Raasch (1964).

1.8 Boron neutron capture therapy (BNCT)

A therapy for patients with high-grade gliomas, specially glioblastoma multiforme, malignant neoplasms, melanomas and their metastatic manifestations has had only limited success with conventional treatments such as surgery or chemotherapy. (Barth, 2003; Koryakin, 2006; Barth *et al*., 2005) Overall the prognosis of survival is bad for the patients (12 months – 3 years). The boron neutron capture therapy (BNCT) has been focused on the treatment of these types of cancer in the last fifty years.

The therapy is based on the nuclear reaction which occurs when boron-10 is irradiated with thermal neutrons followed by nuclear fission to high energy alpha particles (^{4}He) and lithium (^{7}Li) nuclei with 2.31 million electron volts of energy. (Barth *et al*., 2005) The high energy makes the particles very deadly to the cell in which they originate.

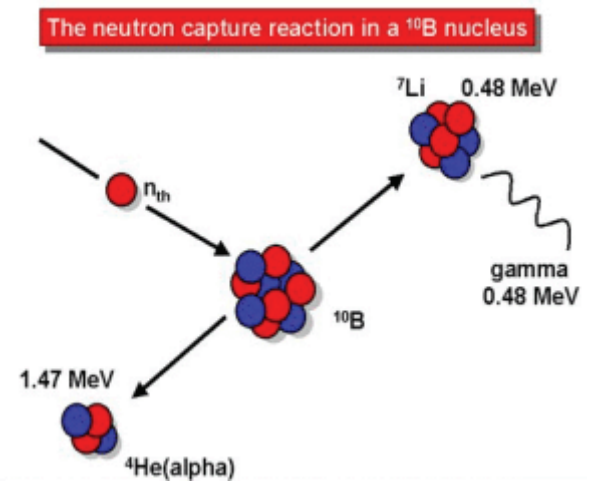

Figure 12: Scheme of boron neutron catpture reaction (http://www.ts.infn.it/uploads/pics/Immagine2_small_01.gif)

These particles only act in a short range (cell diameter) which offers a selective damaging of the cancer cells if the boron-10 is selectively accumulated in the tumor. (Gabel, 1997)

For successful treatment a high amount of boron is necessary (10^{9} B atoms per cell, or 20-30 µg per gram of tumor), enough thermal neutrons must be absorbed by them to obtain a lethal ^{10}B(n,α)^{7}Li capture reaction and more boron should be accumulated in the tumor than in the surrounding healthy tissue.

1.9 Boron compounds

The development of boron delivery agents for BNCT began around 50 years ago and is an ongoing task. The most important requirements for a successful boron delivery agent are as follows:

a) low systemic toxicity and a tumor/healthy tissue ratio greater than 1
b) achieve around 20 µg boron per gram of tumor
c) rapid clearance from blood and normal tissue and persistence in tumor during BNCT

At this time, however, no boron delivery agent fulfills all of these criteria. (Barth *et al*., 2005)

The clinical treatment of tumors with BNCT was started in the 1950s and early 1960s with the usage of sodium borate (e.g., borax, pentaborate) as well as boric acid and its derivatives. The therapy was not successful and patients succumbed from recurrent disease. (Soloway *et al*., 1998) The synthesis of 4-dihydroxyborylphenylalanine (**BPA**) by Snyder and his associates has been furthered the BNCT because the compound has achieved large tumor-to-blood ratios. The discovery of the polyhedral borane anions, $B_{10}H_{10}^{2-}$ and $B_{12}H_{12}^{2-}$, by Hawthorne and collaborators has been made available boron delivery agents with more than one boron atom. (Soloway *et al*., 1998) Mercaptoundecahydro-*closo*-dodecaborate (**BSH**) was first introduced in clinical trials initiated in Japan in the mid-1960s. (Hawthorne and Lee, 2003)
So far BPA and BSH (Fig. 13) are the only compounds used for clinical trials, but they do not reach “ideal” boron concentration in the tumor (Koryakin, 2006) and are hence no optimal boron delivery agents.

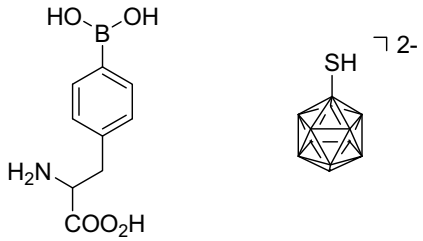

Figure 13: The boron delivery agents BPA (left) and BSH (right)

Low molecular weight boron-containing **nucleosides** and **nucleotides** have been prepared for utilizing the hyperproliferation of malignant cells. The first boronated nucleoside was 5-(dihydroxyboryl)-2’-deoxyuridine (DBDU) (Fig. 14) ccontaining only one boron atom. (Schinazi *et al*., 1985). The insertation of a carboranyl group, having 10 boron atoms, could be advantageous since such nucleosides would have a 10-fold increase of the boron

percentage. One limitation of them is, however, their significant lipophilicity which could influence enzymatic reactivity. (Soloway *et al*., 1998)

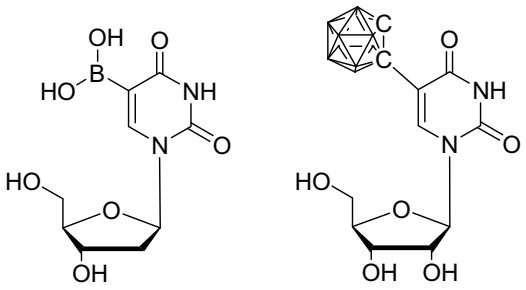

Figure 14: Boron-containing nucleic acid bases: DBDU (left) and a carborane derivative (right)

Many boron-containing **carbohydrates** of glucose, mannose, ribose, gulose, fucose, galactose, maltose and lactose molecules have been synthesized. The idea was to utilize the transporter-mediated uptake of the sugars with increased cell metabolism. But there is no evident that any of the compounds use the active transport system to achieve differential uptake in tumors. (Barth *et al*., 2005; Soloway *et al*., 1998)

Several uptake pathways are possible for **porphyrin** and **phthalocyanine derivatives**, which are determined by its structure, mode of delivery and tumor type. (Osterloh and Vicente, 2002) These uptake ways are not explained here in detail. In general, porphyrin and phthalocyanine derivatives are able to interact with DNA when they reach the cell nucleus. The most widely studied boronated porphyrin is the tetrakis-carboranecarboxylate ester of 2,4-bis-(*α,β*-dihydroxyethyl)deuterioporphyrin IX (BOPP) which is presented in Fig. 15. This compound is toxic at the levels required to obtain useful tumor concentrations. Therefore it is improbable that BOPP will be used in clinical treatments. (Kahl and Koo, 1990; Soloway *et al*., 1998).

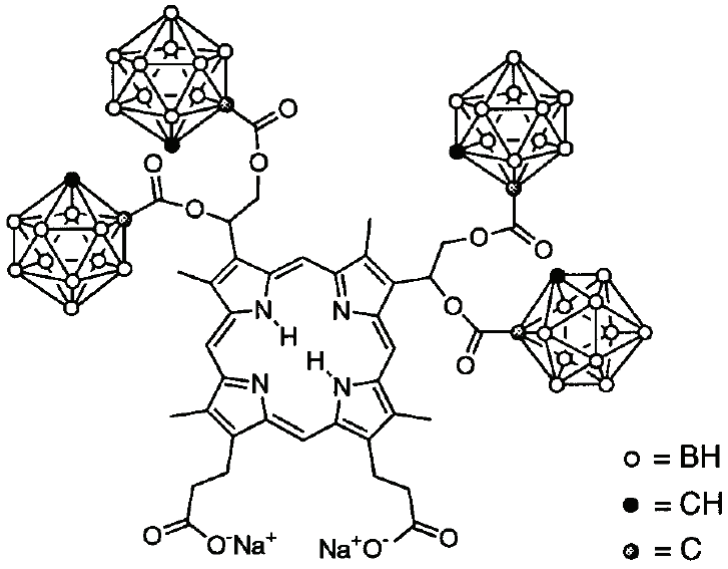

Figure 15: Boron-containing porphyrin (BOPP) (Soloway *et al*., 1998)

But a general toxic effect by boronated porphyrins cannot be proposed, and many other groups are involved in the synthesis of this kind of porphyrins. (Vicente *et al*., 2003; Fronczek *et al*., 2005)

Other researchers have synthesized boron-containing phthalocyanines which are chemically and biologically much more stable than the porphyrins; their decreased water solubility and aggregation are less suitable properties for BNCT.

Another class, however, of boron delivery agents are **DNA-binding molecules**, such as alkylating agents, intercalators, groove binders, and polyamines. But partly these compounds have a high toxicity which limits their application. (Barth *et al*., 2005)

High molecular weight boronated agents, such as **antibodies** and their fragments, are prepared which can recognize a tumor-associated epitope. (Barth *et al*., 1994; Novick *et al*., 2002; Wu *et al*., 2004) But their rapid clearance by the reticuloendothelial system (RES) and the problem to couple enough boron per antibody molecule for successful therapy are disadvantages.

The basis for the development of **growth factors** as boron carriers is that the receptors for these factors are overexpressed in tumor cells and the modification of these factors with boron substituents is first described by Carlsson *et al*. (2003). *In vivo* studies demonstrate, however, that there is a significant extraction and retention by the liver as well as very low boron concentrations in the tumor follows intravenous injection. (Soloway *et al*., 1998)

Some kinds of tumors are strongly hormone-dependent in their proliferation. **Steroid hormones** are important in this context and they have receptors localized in the cell nucleus, the key target for the neutron capture reaction. Therefore several boronated steroid hormones have been synthesized. But the estimated receptor sites available per cell are far less than the number of required to achieve therapeutic levels of boron. (Hawthorne, 1993)

Malignant cells have an increased need of cholesterol and hence of **low-density lipoproteins** (LDLs) to form new membranes. Therefore the receptor for LDLs is overexpressed on the cell surface of tumor cells. To use this advantage of the high LDL uptake the idea was to remove cholesterol from LDL particles and replace it with a boron species which simulate cholesterol. For this strategy different carborane-containing compounds (Fig. 16) have been synthesized. One problem is that some LDL particles show an inability to cross the blood brain barrier (BBB). (Hawthorne and Lee, 2003)

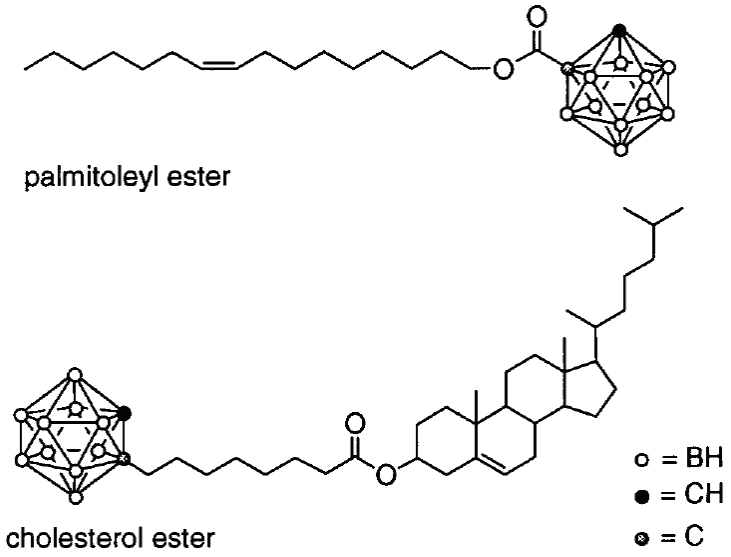

Figure 16: Boronated compounds for LDLs (Soloway *et al*., 1998)

1.10 Liposomes in BNCT

Liposomes show a great promise for boron delivery to the tumor. Hawthorne and his coworkers have carried out extensive studies of unilamellar liposomes for BNCT. (Hawthorne, 1993) Small, water-soluble boron compounds can be encapsulated into the liposomal aqueous core and after administration the liposomes can penetrate the tumor membrane and localize intracellularly. Sodium salts of polyhedral borane anions $B_{10}H_{10}^{2-}$ and 2-$NH_3B_{10}H_9^{1-}$ were encapsulated into unilamellar liposomes. (Hawthorne, 1993; Soloway *et al*., 1998; Shelly *et al*., 1992) The boron compounds in their free form have no affinity for tumors and were rapidly cleared from the body, but boron concentrations in therapeutic ranges could be achieved with liposomes as boron delivery system. (Carlsson *et al*., 2003; Hawthorne, 1993) The encapsulation of BSH into liposomes led to a significant improvement in the circulation time compared to injection of free BSH and still greater therapeutic effects are achieved with pegylation of the liposomes. (Mehta *et al*., 1996)

For an increasing selective boron transport the liposome can be tagged with tumor-seeking entities. For example Maruyama and coworkers (2004) prepared BSH-loaded transferrin-PEG liposomes and reached higher boron concentrations in the tumor.

This encapsulation procedure, however, holds some disadvantages. These include a sometimes low encapsulation efficiency, and leakage upon storage or in contact with serum. Further, it was recently shown that charged boron cluster compounds can profoundly affect the structure of liposomes (Gabel *et al*., 2007). These problems can be avoided by incorporating boron-containing lipids directly into liposomal membranes.

1.11 Boron lipids and cholesterol derivatives

Boron-containing lipids are very interesting building blocks for liposome preparation. They might incorporate into a liposomal membrane or might form liposomes by themselves. Lemmen *et al*. (1995) published the first boron lipid, a carborane-containing ether lipid (B-Et-11-OMe) with a one-tailed moiety. The absence of enzymatically cleavable bonds makes the lipid persistent. A double-tailed nido-carborane ether lipid was synthesized by Nakamura *et al.* (2004). The double-tailed moiety should offer a facile incorporation into the liposome membrane and consequently stable liposomes with a high boron content. Liposomes could be prepared in the presence of the helper lipid DSPC. A very similar ether lipid is described by Li *et al*. (2006) which only differs in the number of methylene groups in the side chain. Liposomes consisting of DSPC, cholesterol and the boronated ether lipid show lethal toxicity in mice (dosages of 6 mg boron per kg body weight). Therefore these *nido*-carborane lipids are not the optimal boron delivery agents for BNCT.

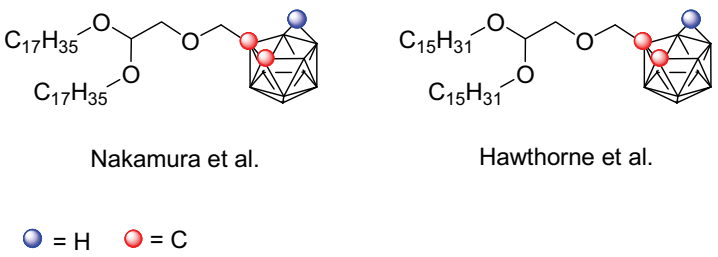

Figure 17: *nido*-Carborane ether lipids

Based on mercapto-undecahydro-*closo*-dodecaborate (BSH) different boron lipids have been synthezised. BSH is clinically used for BNCT and has low toxicity. The boron lipids are expected to show a similar low toxicity. Dodecaborate cluster lipids were described by Lee *et al*. (2007) and Nakamura *et al*. (2007), they form liposomes in the presence of DMPC, cholesterol and polyethyleneglycol-conjugated DSPE (PEG-DSPE). In our group also two new dodecaborate cluster lipids B-6-14 and B-6-16 were synthesized. Both lipids have BSH as head group but differ in the length of their lipid tails. (Justus *et al.*, 2007) The formation of liposomes can be achieved when an equimolar mixture of the boron lipid, DSPC and cholesterol is used for liposome preparation. The *in vitro* studies demonstrate the low toxicity of both lipids. All published dodecaborate cluster lipids are presented in Fig. 18.

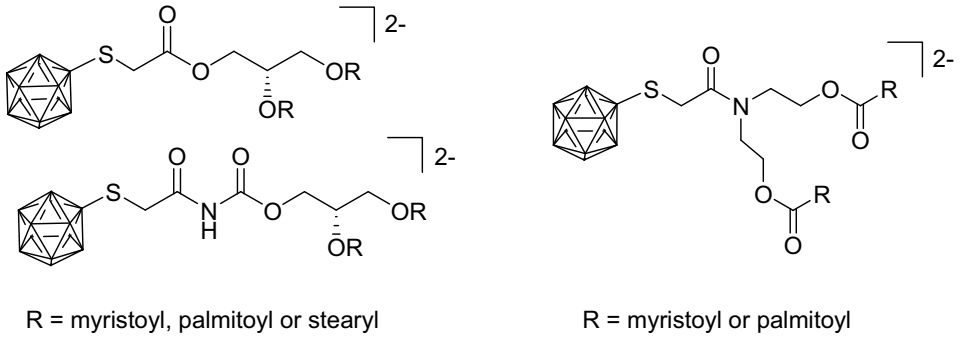

R = myristoyl, palmitoyl or stearyl

R = myristoyl or palmitoyl

Figure 18: *closo*-Dodecaborate cluster lipids synthesized by Nakamura *et al*. and Lee *et al*. (left) as well as by Justus *et al*. (right)

Another possibility to incorporate a boron-containing moiety in the liposomal membrane is to synthesize a suitable cholesterol derivative. *nido*-Carborane cholesterols were prepared by Feakes *et al*. (1999) in which the hydrophilic *nido*-carborane is connected to the cholesterol via ester and ether linkage, respectively. Ji *et al*. (2002) synthesized a cholesterol-carborane conjugate (BCH) which shows low toxicity in cells. BCH in liposomes consisting of DPPC, cholesterol and BCH seems to be effectively taken up and retained in human glioma cells. Cellular concentrations were 10 times higher than required for BNCT. (Peacock *et al*., 2004)

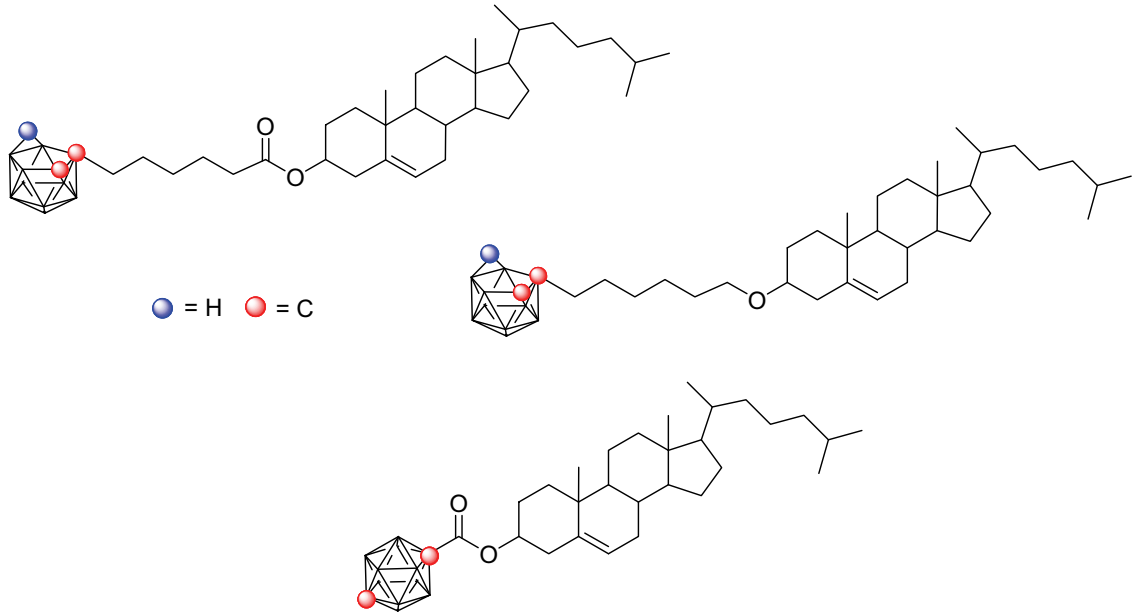

Figure 19: The chemical structure of cholesteryl-6-(1,2-dicarba-*nido*-dodecaboran(12)-1-yl)hexanoate cholesteryl (left, above) and 1-(6-(1,2-dicarba-*nido*-dodecaboran(12)lyl)hexoxy cholesterol (right, above) as well as 1,12-dicarba-*closo*-dodecaborane-1-carboxylate (BCH) (below)

Dodecaborate-conjugated cholesterols have been synthesized by Nakamura and Gabel (2007). The three derivatives based on BSH as hydrophilic part are connected via different linkers to the cholesterol backbone (Fig. 20).

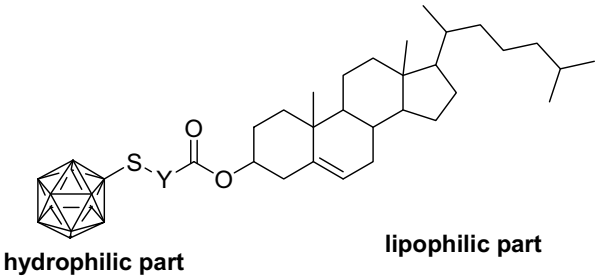

3a: Y = CH_2
3b: CH_2CH_2
3c: $NHCOCH_2$

Figure 20: Structures of the boron cluster-conjugated cholesterols (Nakamura *et al*., 2007)

The cholesterol derivative 3a was investigated in more detail. Liposomes were prepared from DMPC, cholesterol, dodecaborate-conjugated cholesterol 3a and PEG-DSPE (1:0.5:0.5:0.1). Toxicity experiments on cells demonstrate that the cholesterol exhibit a higher toxicity than BSH at the same boron concentrations. The higher toxicity may be due to the higher lipophilicity and higher molecular weight of 3a in comparison to BSH. (Nakamura *et al*., 2007) A new approach is to develop cholesterol mimics which have similar physicochemical properties as cholesterol (Fig. 21). Three carboranyl cholesterol derivatives were synthesized but only one has been analyzed in more detail. Compound I was incorporated in liposomes which do not exhibit differences to common liposomes. No apparent toxicity could be detected.

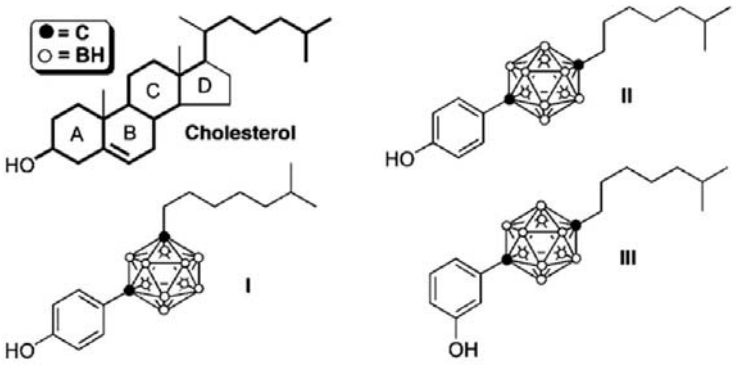

Figure 21: Structures of cholesterol and boronated cholesterol mimics I-III (Thirumamagal *et al*., 2006)

1.12 Cyclic oxonium derivatives of polyhedral boron hydrides

Oxonium derivatives offer a facile introduction of polyhedral boron hydrides into biological relevant molecules. In these oxonium derivatives the boron cage is connected to a cyclic ether system via a covalent B-O^+ bond. At present two different ways are known for the synthesis of oxonium derivatives. The first one is based on the reaction of boron hydrides with ethers in the presence of Lewis or Brønsted acids. This type of reaction is practically unknown in organic chemistry and is explained here in more detail (Fig. 22). The reaction

involves the primary attack of an electrophilic agent on the borane hydride followed by a simultaneous elimination of hydride and electrophile resulting in a carbocation-like center on the boron atom. In the next step a nucleophile attacks this positively charged boron atom to form a covalent bond. This mechanism is called electrophile-induced nucleophilic substitution (EINS). In the absence of strong nucleophilic species even weak nucleophiles, such as ether solvent molecules, attack the boron atom giving the corresponding oxonium derivatives. (Semioshkin *et al*., 2008)

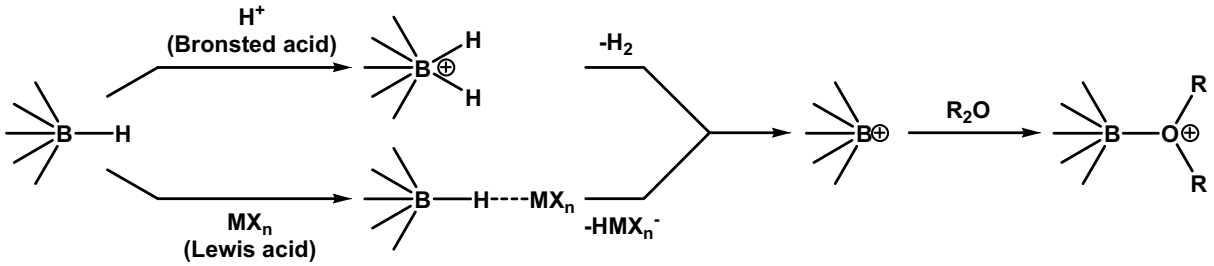

Figure 22: Reaction ways for the synthesis of cyclic oxonium derivatives of polyhedral boron hydrides (Semioshkin *et al*., 2008)

In the presence of a Brønsted acid a hydrogen molecule is eliminated whereas in the case of Lewis acid a simple abstraction of the hydride hydrogen atom by the acid results directly in a quasi-carbocation particle $B_{12}H_{11}^-$. The intermediate $B_{12}H_{11}^-$ is supported by quantum chemical calculations for protonation of the *closo*-dodecaborate anion $B_{12}H_{12}^{2-}$. (Mebel *et al*., 1999)

The first oxonium derivatives were described in 1969. Here the 7,8-dicarba-*nido*-undecaborate anion reacts with $FeCl_3$ in tetrahydrofurane to two isomeric tetramethylene oxonium derivatives. (Young *et al.*, 1969)

A tetrahydropyrane (THP) derivative of the dodecaborate cluster had first been published by Peymann *et al.* (1996) and had prepared by alkylation of hydroxyundecahydro-*closo*-dodecaborate with dibromopentane. This synthesis strategy comprises more reaction steps.

More convenient methods are developed later by Sivaev *et al.* (2000) and summarized in Fig. 23. For both synthesis ways the EINS is used. At first, the synthesis of the THF and dioxane derivative of the cluster respectively was obtained via the reaction of $B_{12}H_{12}^{2-}$ with $BF_3{\cdot}OEt_2$ in the corresponding cyclic ethers. (Sivaev *et al*., 2000) Recently a new synthesis way was proposed by Sivaev *et al*. (2008) in which $B_{12}H_{12}^{2-}$ reacts with hydrogen chloride in 1,4-dioxane in the presence of $NaBF_4$.

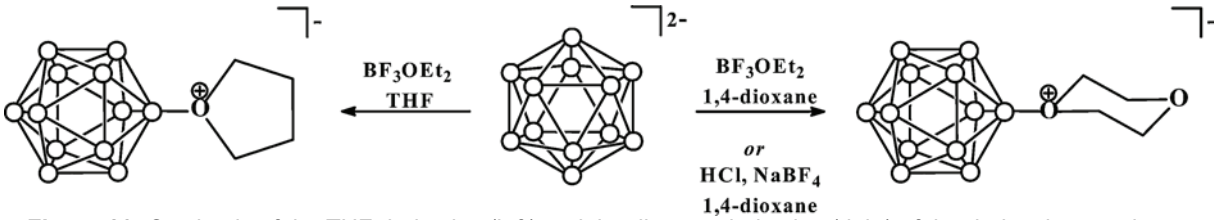

Figure 23: Synthesis of the THF derivative (left) and the dioxane derivative (right) of the dodecaborate cluster (Semioshkin *et al*., 2008)

In 1996 the first nucleophilic ring opening reactions (RORs) are published. Peymann *et al.* (1996) had been opened the tetrahydropyrane ring with hydroxide and fluoride as nucleophile. In 2000 Sivaev *et al*. described also nucleophilic RORs with the cyclic oxonium derivatives (THF and dioxane) and thereby established a facile method for functionalization of a wide range of compounds. Ring opening reactions are possible with oxygen, sulfur, phosphorus, halogens or carbon as nucleophiles. Semioshkin *et al*. (2007) published the reaction of oxonium derivatives with various amines and the preparation of novel B_{12}-containing piperazines and amino acids. The ring opening reactions have a wide range of application, mainly in the preparation of boron compounds for BNCT. They have so far not been used to synthesize boron lipids.

2. Experimental techniques

2.1 Differential scanning calorimetry (DSC)

In general a system will reach higher or lower states of energy depending on the temperature. Thus changes in energy state distribution can occur in a rather dramatic manner if the system undergoes a cooperative change in structure. Biological examples are the thermotropic transitions of lipids, the thermal unfolding of proteins or the temperature-induced melting of DNA. (Biltonen and Lichtenberg, 1993)

Differential scanning calorimetry (DSC) is a technique for measuring the energy necessary to establish a nearly zero temperature difference between a substance and an inert reference. Thus the technique is able to record changes in enthalpy or heat capacity that occur during controlled increase (or decrease) in temperature. (Bhadeshia, 2002)

The DSC machine measures the amount of energy which is necessary to maintain the same temperature in a sample and a reference cell upon increasing the temperature of the whole system at a constant rate. In the moment in which the sample undergoes a thermotropic transition, the applied heat is used for the melting process instead for increase of the temperature and thus the temperature of this cell will tend to lag behind that of the reference cell. Therefore extra heat is applied to the sample cell by an auxiliary heater to maintain a negligible temperature difference. This extra heat is recorded and converted to apparent molar excess heat capacity (kJ $mol^{-1}K^{-1}$). (Biltonen and Lichtenberg, 1993)

2.2 Zeta potential

All particles in suspension exhibit a surface charge or zeta potential. In general the knowledge of this zeta potential allows the prediction of the formulation stability, the verification of product quality or the prediction of interactions in a multi-component system. (http://www.particlescic.com/pdf/an_08.pdf)

The double layer model (Fig. 24) is used to visualize the ionic environment of charged particles. The net charge of the particle affects the ion distribution surrounding the particle. In the case of a positive net charge the negativelyly charged counter-ions are distributed around the particle surface and are firmly bound to it. The layer formed is known as the *Stern layer*.

A negatively charged particle attracts more positively charged ions but these are repelled by the *Stern layer* as well as by other positive ions which approach the negative particle. The formation of the ions results in a *diffuse layer* in which the ion concentration gradually decreases with distance, until equilibrium is reached with the ion concentration in the solution. The ions in the *diffuse layer* are loosely associated.

The concentration of positively charged ions increases with increasing distance to the particle surface because the repulsion forces of the positively charged particle decrease.

The *Stern layer* and the *diffuse layer* are known as the double layer and their thickness depends upon the type and concentration of ions in solution. (http://www.zeta-meter.com/5min.pdf)

When a voltage is applied the particle moves with the ions through solution. But within the diffuse layer a boundary is constructed beyond which the ions do not move with the particle. This boundary of hydrodynamic shear is called slipping plane and the potential at this point is defined as the zeta potential. (http://www.particlescic.com/pdf/an_08.pdf; http://www.zeta-meter.com/5min.pdf)

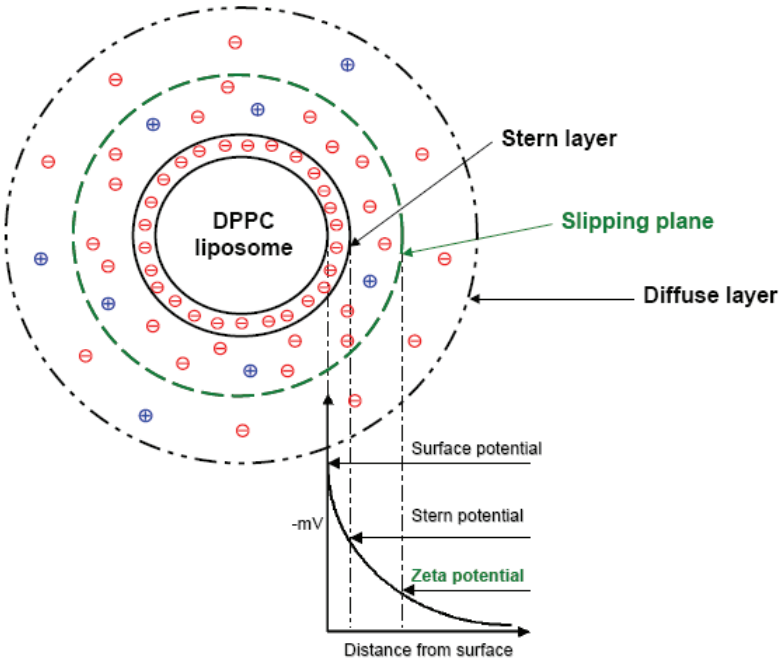

Figure 24: Schematic representation of the ions distribution around a DPPC liposome. (diploma thesis of Jingyu Li, 2008, University of Bremen)

The zeta potential can be calculated from the measured mobility with the following Henry equation:

$$\zeta = \frac{3\eta u}{2\varepsilon_0 \varepsilon_r f(\kappa a)} \qquad (1)$$

in which u is the mobility, η is the viscosity of the medium, ε_0 is the permittivity of free space and ε_r the relative permittivity of the medium. $f(\kappa a)$ is the Henry function in which κa is the product of the Debye parameter (κ) and the liposome radius (a).

The Debye parameter (κ) is given by:

$$\kappa^2 = \frac{2e^2 N 10^3}{\varepsilon_o \varepsilon_r kT} \cdot \mathrm{I} \qquad (2)$$

where *e* is the electronic charge, *k* is the Boltzmann constant, *N* is the Avogadro's constant, *T* is the temperature and I is the ionic strength. The reciprocal Debye parameter is a parameter to predict the thickness of the double layer.

Liposomes have a surface charge and consequently zeta potential depending on the lipid composition and the environment. The zeta potential for liposomes is mostly calculated by the Smoluchowski equation (3).

$$\zeta = \frac{\eta u}{\varepsilon_r \varepsilon_0} \qquad (3)$$

In this simplified approach, the electrostatic driving force is opposed by the frictional force and the other effects are neglected. The error associated with the use of this formula is $< 5\%$ when large particles and high ionic strength is used and the zeta potentials are not too large. (Cohen *et al.*, 2003) At these ion concentrations the double layer is relative small in view of the liposome size. (Jones, 1995)

2.3 Cryo-transmission electron microscopy (Cryo-TEM)

Cryo-TEM is a useful method to image structures formed by amphiphilic molecules in aqueous solution without drying, staining and fixation steps.

In this method the solution which is to be investigated is placed to a microscopy grid in such a way that a very thin aqueous film is formed. Then the grid is plunged into a cooling medium, such as liquid ethane, where the film is very rapidly vitrifies without crystallization. After vitrification the grid is transferred to the microscope, and examined at liquid nitrogen temperature in transmission mode. The preparation and vitrification are performed very fast, so that no dehydration of the sample and reorganization of the structures take place.

The contrast is, however, a limiting factor for visualization. It depends on the difference in electron density between the atoms of the amphiphile and the surrounding water. A dimension of 4-5 nm is the smallest dimension which can be resolved.

On the other extreme, the size of the structure visualized and the thickness of the film is limited to 500 nm. Otherwise the scattering of electrons by water gets too large and the cooling rate during vitrification too slow. (Almgren *et al*., 2000)

In Fig. 25 the preparation of the specimen is illustrated in detail. A drop of the sample is placed on a grid which is modified with a polymer film. By a blotting procedure the sample is thinned and is dispersed on the grid so that a film of the sample is spanned. Then the sample is vitrified in liquid ethane.

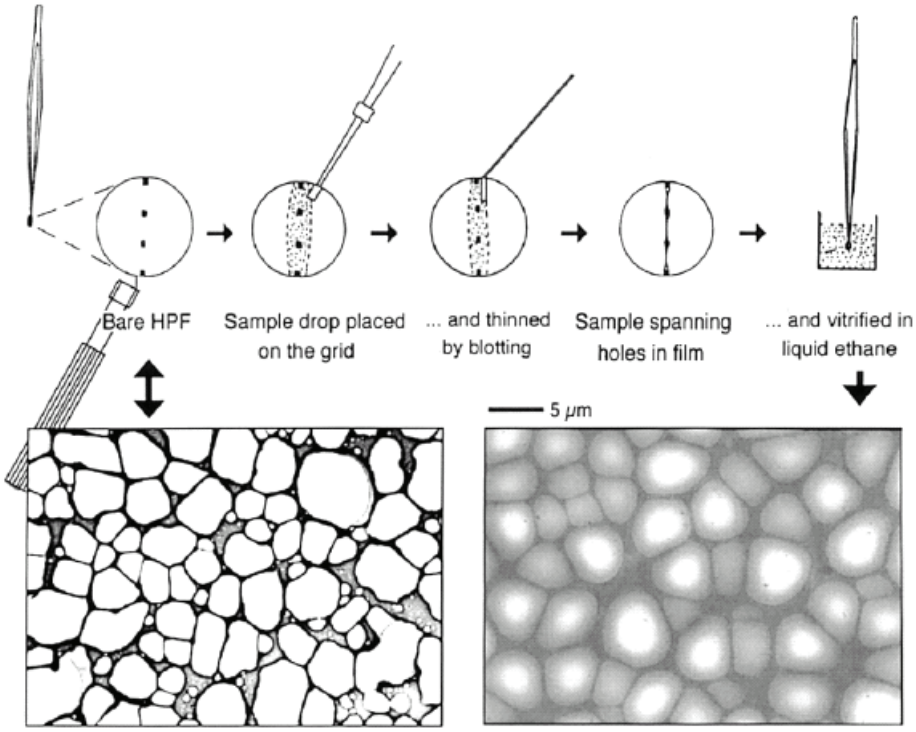

Figure 25: A holey polymer film, empty and after application of sample, blotting and vitrification. (Almgren *et al*., 2000)

For the film preparation a climate chamber in which humidity and temperature can be controlled is essential to avoid evaporation. A controlled environment vitrification system has been designed by Egelhaaf *et al*. (2000) to optimize the blotting procedure.

In Figure 26 the controlled environment vitrification system is shown. The chamber is formed by two Plexiglas tubes (a and b). The thermally isolation from the environment and the adjustment of the temperature is allowed by water circulation of appropriate temperature. Humidity is controlled by a gentle flow of gas which has the desired saturation and temperature.

The samples can be equilibrated inside the chamber using a special holder (c) and then transferred to the specimen support using a pipette tip, which was also equilibrated within the chamber. The specimen support grid is held by tweezers (d), which can be propelled downwards by a pneumatic cylinder. The plunge velocity (3 m s^{-1}) together with the plunge depth (30 mm) and the high cooling rate (of the order of 10^6 K s^{-1}), ensures that the sample reaches the cryogen temperature before it stops.

The vitrification of the sample occurs inside a polystyrene box (h). A constant, dry atmosphere is important inside the box to avoid crystallization of the sample or contamination with water. It is maintained by a continuous flow of cold and dry nitrogen. A resistor (i) heats gently liquid nitrogen to obtain evaporation and consequently nitrogen flow. The liquid nitrogen level is indicated by a wooden stick (k).

The cryogen (ethane) is kept in a small vessel (m), which can be moved vertically and fixed at two heights. During plunging the vessel is in the upper position. After plunging it is slowly lowered, which removes the vitrified specimen from the cryogen while allowing the cryogen to drain off. The whole polystyrene box is then shifted, which positions the grid over a second vessel (n). This vessel is filled with liquid nitrogen and contains a transfer box. Finally, the sample is transferred to the microscope.

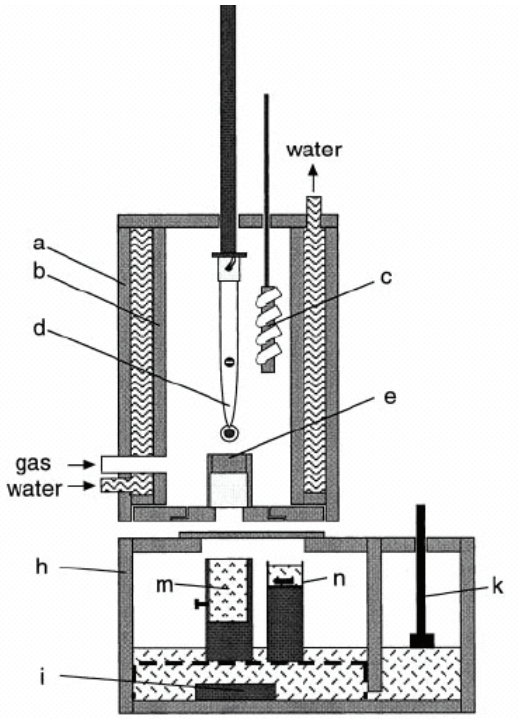

Figure26: Schematic diagram of the climate chamber and cryogen reservoir (Egelhaaf *et al*., 2000)

2.4 Fluorescence resonance energy transfer (FRET)

Membrane fusion occurs in various intra- and intercellular processes, such as exocytosis, endocytosis, membrane genesis, and fertilization. Liposomes are often used as a model for cell membranes and a fusion can be induced here by, e.g., divalent metal ions. The membrane fusion involves the complete intermixing of internal aqueous contents and membrane components of two fusing vesicles. (Müller *et al*., 2003; Rosenberg *et al*., 1983)

The fluorescence resonance energy transfer (FRET) technique is commonly used to visualize the fusion process. Here two different fluorophors are incorporated in the liposomal membrane. One of them is a molecule with high energy absorption, called donor (D), and the other one with lower energy absorption, called acceptor (A). If the emission spectrum of the donor overlaps with the excitation spectrum of the acceptor, energy can be transferred from the excited donor molecule to the acceptor through long-range dipole-dipole interaction. This process results in quenching of the donor, while the acceptor emits fluorescent light.

The energy transfer is only possible by short distances (110 nm) between the two fluorophors. (Szöllősi *et al*., 2002) When fusion takes place between fluorescent-labeled and unlabeled liposomes, the distance between donor and acceptor increases and consequently the energy transfer is disabled. Therefore the emission intensity of the acceptor decreases whereas the emission intensity of the donor increases.

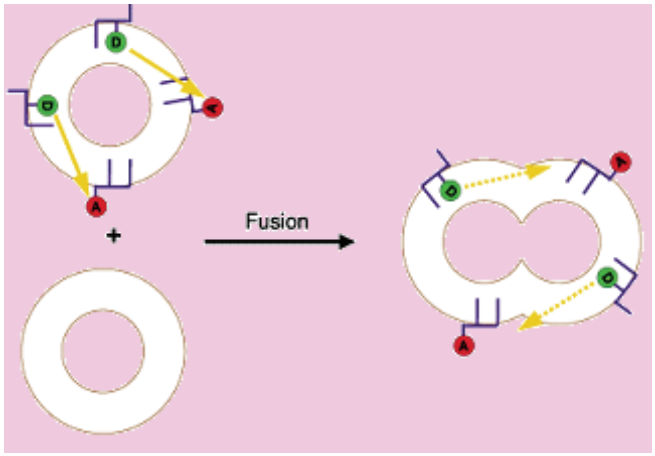

Figure 27: Principle of the lipid mixing assay. (http://www.probes.com/handbook/images/g001811.gif)

One established donor/acceptor system to investigate liposome fusion is 7-nitrobenz-2-oxa-1,3-diazol (NBD) as donor and rhodamine (Rh) as acceptor.

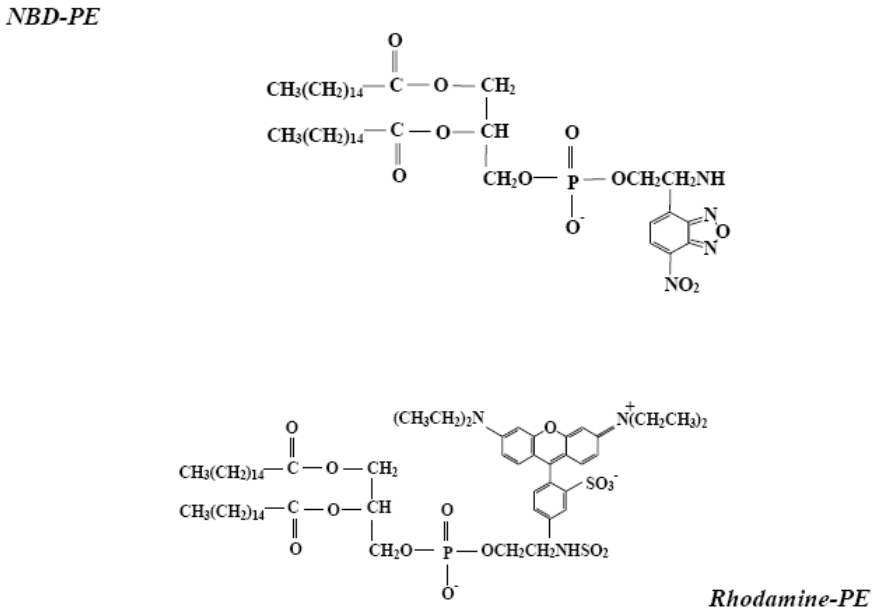

Figure 28: Chemical structures of NBD-PE and rhodamine-PE. (Müller *et al*., 2005)

2.5 Flow cytometry

Flow cytometry is a powerful technique to generate multi-parameter data from particles and cells in the size of 0.5 µm to 40 µm diameter. The technique uses the principle of light

scattering, fluidics, light excitation and emission by fluorescent dyes. By means of fluidics a laminar flow of cells is generated through the equipment so that only one cell passes the laser beam at one time. Upon excitation of the cell with the laser beam, the light scatters in forward and side pattern and the cell or particle emits fluorescence, if fluorescently labeled. Scattered and emitted light from cells or particles is converted to electrical pulses by optical detectors.

The scattered light is detected by photodiodes while the fluorescence is detected by photomultiplier tubes. Therefore a total of three different data points (light scattering in forward (FSC) and side (SSC) pattern as well as fluorescence) can be detected and multidimensional plots can be generated.

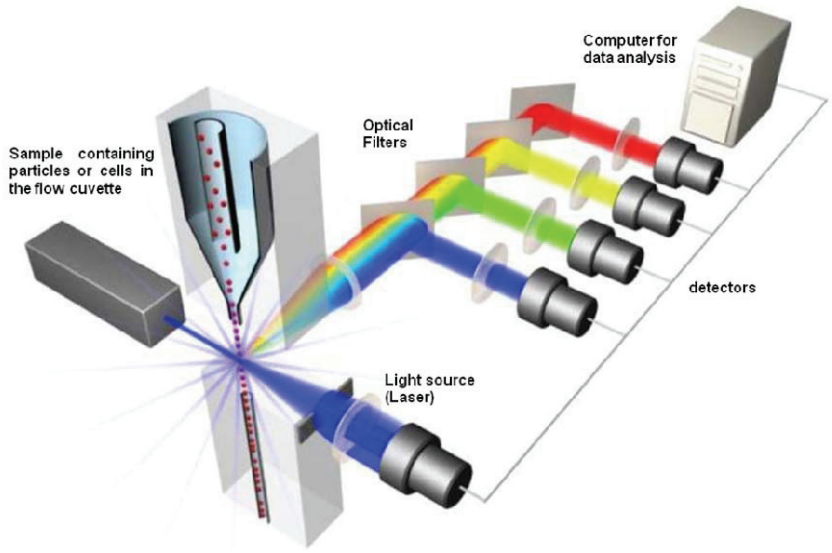

Figure 29: Schematic diagram of a Flow cytometry machine with different detectors. (http://flow.csc.mrc.ac.uk/wp-content/uploads/fcm-fig1-overview1.jpg)

2.6 Assessment of cell toxicity

Tetrazolium salts are used extensively in cell proliferation and cytotoxicity assays. They are metabolically reduced to water-soluble highly colored end products called formazans. (Berridge *et al*., 1996) The dye reduction is proportional to the number of viable cells in exponential growth phase. The tetrazolium salts have generally a positively charged quaternary tetrazole ring core containing four nitrogen atoms. This central structure is surrounded by three aromatic groups that usually involve phenyl moieties. The reduction of these salts leads to the disruption of the tetrazole ring and brightly colored formazan products emerge from colorless salts (Fig. 30). The absorbance of the formazan can be quantified by a scanning multiwell spectrophotometer (ELISA reader). The tetrazolium salt WST-1 (4-[3-(4-iodophenyl)-2-(4-nitrophenyl)-2*H*-5-tetrazolio]-1,3-benzene disulfonate) was here used for the cytotoxicity assay.

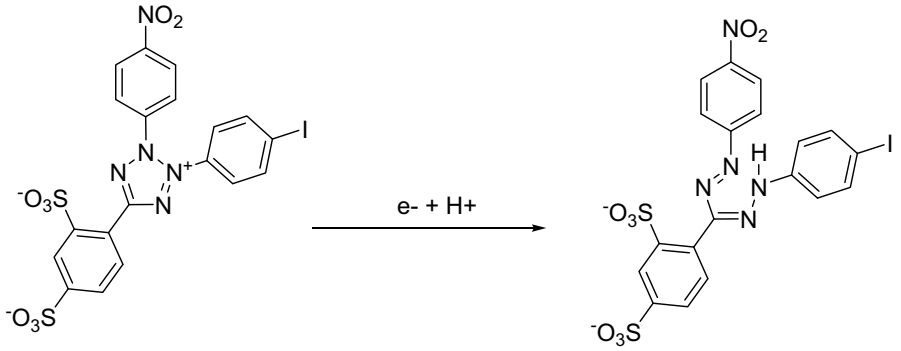

Figure 30: Reduction of WST-1 dye (left) to the formazan (right).

The WST-1 dye contains two sulfonate groups giving it a net charge that would exclude it from cells. Therefore WST-1 is reduced extracellularly, most likely by electron transport across the plasma membrane from intracellular NADH to WST-1 via intermediate electron acceptors (IAs), such as mPMS (1-methoxy-5-methyl-phenazinium methyl sulfate). Therefore one electron is transferred to mPMS to generate a radical which then reduced WST-1. The formazan is obtained after two single electron reduction events.

NADH formed in the mitochondria is an efficient electron donor and it is involved in the electron transport to the membrane. It is transported via the malate/aspartate shuttle in the cytoplasm. The electron of NADH is then transferred to the ubiquinone cycle (complex II in the plasma membrane) which transports the electron to the extracellular side for further WST-1 reduction. (Berridge *et al*., 2005)

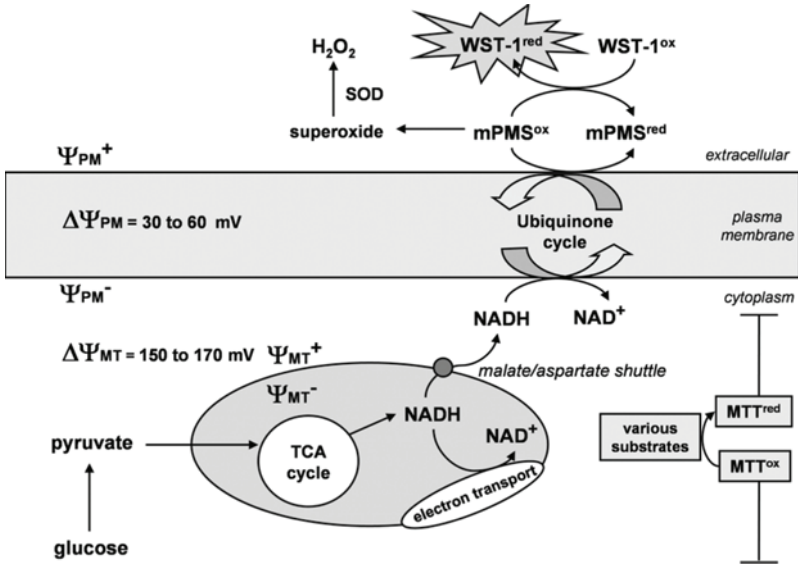

Figure 31: Schematic representation of the proposed mechanism of cellular WST-1. (Berridge *et al*., 2005)

2.7 Acetylcholinesterase (AChE)

Acetylcholinesterase is an enzyme which is found in all higher organisms, including humans. The principal role of the enzyme is the termination of neuronal impulse transmission by rapid

hydrolysis of the neurotransmitter acetylcholine. (Colletier *et al*., 2006) Inhibition leads to disorders in the neuronal system such as heart diseases (influence of the cardiac response to vagal innervation) and myasthenia. (Chemnitius *et al*., 1999; Pope *et al*., 2005)

The enzyme is a relevant target for toxic interaction. (Arning *et al*., 2008) In the case of inhibition an *in vivo* effect cannot be excluded and consequently an exposure to the substances could be a risk factor for higher organism. Therefore knowledge about enzyme inhibition is important.

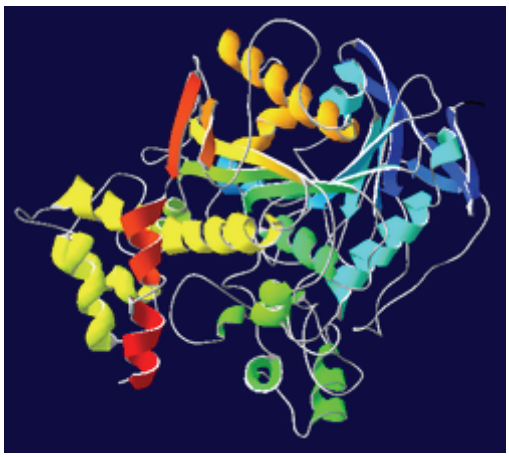

Figure 32: 3D structure of acetylcholinesterase. (http://1.bp.blogspot.com)

The catalytic site of the enzyme and the substrate binding pocket is well studied by X-ray defraction. (Sussman *et al*., 1991) In the catalytic cycle of the acetylcholinesterase three enzyme domains are important: the peripheral anionic site (PAS), a lipophilic channel located in the entrance of the gorge and the esteratic site as the active center. (Bourne *et al*., 2003; Harel *et al*., 1993) The neurotransmitter hydrolysis starts with the attraction between the choline group of the substrate and the negative potential of the PAS which is located near the entrance. The substrate is here orientated to the active center. (Bourne *et al.*, 2003) Then the molecule is subsequently transferred to the active center which is located at the bottom of a narrow gorge and is lined with lipophilic aromatic amino acids. Thus the substrate passes first the lipophilic channel before it binds to the active center via cation-π interactions between the choline group and the tryptophane residue (Harel *et al*., 1993) and simultaneously the acetyl group reaches the esteratic site. The ester bond is hydrolyzed and the choline group leaves the active center through the gorge. The acetate is detached from the acetylated enzyme by a water molecule and passes through a channel which is formed by the lipophilic gorge. (Arning *et al.*, 2008, Bourne *et al.*, 2003)

A look of known enzyme inhibitors indicates that a positively charged quaternary nitrogen atom, certain lipophilicity and an electron-deficient aromatic system are features of compounds which are able to inhibit the enzyme. (Arning *et al*., 2008)

The inhibition of the enzyme is measured using a colorimetric assay based on the reduction of the dye 5,5'-dithio-bis-(2-nitrobenzoic acid) (DTNB) by the enzymatically formed thiocholine moiety from the enzyme substrate acethylcholine iodide. The test system is first described by Ellman *et al*. (1961).

2.8 Reproduction inhibition assay with limnic green algae *Scenedesmus vacuolatus*

The limnic green algae *Scenedesmus vacuolatus* belongs to the group of chlorophyta and can be found in limnic plankton as well as in moist soils. It is a spherical unicellular micro alga with a diameter of around 10 µm. The cell wall consisting of different cellulose layers is extremely stable under mechanical stress. The content of chlorophyll in these algae is high allowing high photosynthesis rates which are comparable to that of higher plants.

The algae have a high reproduction rate in the range of 16-20 h makes them very useful for reproduction screening assays. They are routinely used in bioassays monitoring wastewater qualities.

To determine the cytotoxicity of chemicals the inhibition of reproduction is measured. The algae test system reflects generally the cell viability. Chemicals can also interfere with the photosynthesis system which indicates a further cellular mechanism.

In the assay the algae is incubated with chemicals for 24 h and then the number of cells is determined with the Coulter Z2 Counter (Company Beckmann).

3. Aim of the Work

Previous studies in our group have demonstrated that in contrast to other ionic compounds the low molecular weight compound BSH exhibits special properties and unexpected behavior. Thus following i.v. administration to patients with glioblastoma it binds strongly and persistently to tumor tissues (Otersen *et al.*, 1997) which can probably be attributed to interactions with the head groups of phosphatidylcholine lipids. (Lutz *et al*., 2000) In sections of these glioblastoma multiforme tissues it was found that BSH is strongly associated with extracellular structures, the cell membrane and regions within the nucleus. (Neumann *et al.*, 2002) These data point out that, in contrast to other ionic compounds, BSH is also able to enter the cell membrane. Awad *et al.* (2009) further investigated behavior of BSH in a liposome model and put forward a hypothesis for the interaction of BSH with the liposomal membrane. In this mechanism interactions between BSH and the choline head groups of the lipids are involved.

So far, apart from BSH, no other dodecaborate cluster compounds have been investigated in such detail. For this reason, we decided to study other low molecular weight compounds as well as high molecular weight substances containing the dodecaborate cluster, trying to answer the question whether they exhibit similarly unusual behavior, comparable to that of BSH.

3.1 Ionic liquids

In our group new ionic liquids (ILs) have been synthesized which consist of a new kind of anions combined with simple cations such as lithium, potassium, sodium or proton (see 1.7). These ILs could be applied in many industrial processes, e.g., as electrolytes in batteries. According to the European chemical legislation REACH (registration, evaluation, authorization and restriction of chemicals), however, the manufacturers are responsible for the safety of chemicals and products and the convention applies accordingly “no data, no market”. Therefore the knowledge of toxicological hazard potentials of chemicals, their toxic modes of action and possible target sites respectively is important before an industrial use of the chemicals can be considered.

In view of the last mentioned aspects no data, however, have been available for these new ILs. Thus the new ILs had to be investigated for their toxicity in different biological test systems. The test strategy comprised the mammalian cell line V79 to determine toxic hazards for humans and animals, the limnic green algae *Scenedesmus vacuolatus* as one representative of many plant species, to get a better understanding of possible risks for the environment, and the enzyme acetylcholinesterase which is found in all higher organisms,

including humans. An inhibition of this enzyme leads to disorders in the neuronal system which has fatal consequences for the metabolism of an organism.
In addition we wanted to establish a quantitative correlation for every biological system which allows predicting the toxic potentiality of other ILs with the same chemical basic structure. For this project the physical properties of the ILs have been investigated to determine one of them as key factor for toxicity. The lipophilicity of a compound plays often an important role in toxicity so that a correlation between the lipophilicity and toxicity might permit a quantitative prediction.
In the literature the cell membrane is often discussed as target for toxic interactions of ILs. To test this hypothesis liposomes were investigated which are commonly used as model for biological cell membranes. Leakage experiments would indicate wether events on the membrane are responsible for toxicity and allow to establish a qualitative prediction of the toxic behavior of a compound from simple experiments.
If interactions between the new ILs and the membrane were observed, they should be investigated in more detail for analyzing the mode of toxic actions. Liposomes incubated with different concentrations of the ILs could be investigated for changes in zeta potential, changes in their thermotropic behavior, changes in morphology and lipid mixing to give information about events on the membrane.

3.2 Dodecaborate cluster lipids

Boron neutron capture therapy (BNCT) is focused on the treatment of badly treatable types of cancer. In the past, however, many prospective boron agents have been synthesized, but most of them show disqualifying features.
Liposomes are promising transport systems for boron agents, as they can carry a large amount of boron. Problems which appear by the encapsulation of low molecular boron agents into the liposomal inner core can be avoided by incorporation of boron-containing lipids in the liposomal membrane.
All existing dodecaborate cluster lipids have been prepared by time-consuming methods which is not advantageous for industrial production. One aim of this work is to develop a synthesis strategy which allows a facile preparation in high yield and offers the possibility to vary the lipid structure (head group, linker or lipid tails). The influence of different linkers connecting the dodecaborate cluster and the lipid backbone should be investigated in more detail. In addition all dodecaborate cluster lipids published are doubly negatively charged. Therefore we aimed to on the synthesis of lipids carrying only a single negative net charge and investigated the physical-chemical behavior and toxicity for comparing them with the known lipids.

As noted above, liposomes are delivery systems for boron. Therefore the morphologies formed by pure lipid have to be studied. In addition it should be tested, if an incorporation of the boron lipids into a liposomal membrane consisting of helper lipids is possible.

Before a medical application on patients the *in vitro* and *in viv*o toxicity as well as the distribution of drugs in the body have to be determined. Therefore the boron lipids were tested on mammalian cells and on mice.

4. Results

4.1 Toxicity of *N,N,N*-trialkylammoniododecaborates as new anions of ionic liquids in cellular, liposomal and enzymatic test systems (Appendix I)

The ILs from MeAB to HxAB and an asymmetrically substituted Et2BnAB were tested in different biological test systems and the results obtained are summarized in Table 1.

Table 1: Octanol/water partition coefficients, EC_{50} values in V79 cells and in *S. vacuolatus* algae, and IC_{50} values for AChE for the compounds tested.

compound	Kow	EC_{50} [mM] V79	EC_{50} [mM] algae	IC_{50} [mM] AChE
MeAB	0.04 ± 0.00	9.1	-	21.9
EtAB	0.33 ± 0.03	1.66	-	9.77
PrAB	1.84 ± 0.09	0.48	1.86	2.04
BuAB	3.04 ± 0.17	0.31	0.59	0.51
HxAB	4.73 ± 0.31	0.19	0.016	0.0325
iPnAB	4.03 ± 0.03	0.25	1.4	0.089
Et2BnAB	0.58 ± 0.02	0.72	1.33	1.26

We determined the octanol/water partition coefficient Kow as a parameter for lipophilicity. The lipophilicity increases from MeAB to HxAB as expected. The asymmetrically substituted compound Et2BnAB has a partition coefficient between EtAB and PrAB.

The toxicity in V79 cells increases with longer alkyl chains. The asymmetrically substituted derivative Et2BnAB has a toxic potential between the EtAB and PrAB. The general trend is observed that increasing lipophilicity (determined by the Kow value) leads to increasing toxicity. A linear correlation is found when log Kow is plotted versus log EC_{50}.

The enzyme acetylcholine is inhibited by all ABs tested. The concentration required decrease, however, with increasing chain length. In a log Kow-log EC_{50} plot no simple relation is found. With longer alkyl chains, the inhibitory power increases much more than the lipophilicity. Unexpected from its position in the Kow values, Et2BnAB inhibits more than PrAB.

The reproduction of the algae *Scenedesmus vacuolatus* is not influenced by MeAB and EtAB up to 3 mM. The addition of the other ABs to the algae system leads to inhibition which increases with increasing chain length and lipophilicity. iPnAB with branched chains shows lower inhibition effect than BuAB with *n*-alkane chains. In contrast to EtAB, Et2BnAB is able to induce inhibition.

All ABs tested are able to induce leakage in a dose dependent manner. The leakage kinetic does not follow first order but is rather complex. The initial release is very fast and then slows down. The ABs act differently in the leakage induction. Smaller compound concentrations are required to obtain the same percent of leakage with increasing lipophilicity. Furthermore steric effects influence the capability of leakage induction as iPnAB is less potent as BuAB.

4.2 Interaction of *N,N,N*-trialkylammonioundecahydro-*closo*-dodecaborates with dipalmitoyl phosphatidylcholine liposomes (Appendix II)

The interactions between the *N,N,N*-trialkylammonioundecahydrododecaborates and DPPC liposomes, used as a model for biological membranes, are investigated in more detail. The ILs from MeAB to HxAB are tested in different physical test systems and the results performed are summarized in Table 2.

Table 2: Dissociation constants, limiting zeta potential, results of DSC, FRET and cryo-TEM

Substance	**dissociation constant [mM] derived surface potential**	***c_0 (= log c at inflection point)***	***concentration [mM] from inflection point***	***ratio substance/lipid at inflection point***	***limiting zeta potential z_{min} (mV)***
MeAB	2.9	1.45 ± 0.54	28.2	56	-98 ± 37
EtAB	0.85	0.67 ± 0.6	4.7	9.4	-100 ± 34
PrAB	0.18	-0.18 ± 0.42	0.66	1.3	-94 ± 21
BuAB	0.037	-1.03 ± 0.19	0.093	0.19	-101 ± 13
HxAB	0.008	-1.75 ± 0.06	0.018	0.036	-118 ± 1

Substance	Differential scanning calorimetry (DSC)	Fluorescence resonance energy transfer (FRET)	Cryo-TEM pure substance	Cryo-TEM with liposomes
MeAB	disappearance of pre-transition, shift of main transition	100% lipid mixing with 40 mM	no micelles	large bilayer
EtAB	no measurement	no measurement	no micelles	large bilayer
PrAB	no measurement	no measurement	micelles	disk-shaped bilayer
BuAB	no measurement	no measurement	micelles	open and very small liposomes
HxAB	broadening of transition until disappearance	no measurement	micelles	concentric multilayered liposomes

In the DSC experiment the derivatives MeAB, as a typical example for short alkyl chains, and HxAB, as a typical example for long chain lengths, were incubated with DPPC liposomes. In the presence of MeAB the pre-transition peak disappears completely and the main transition peak shifts slightly to lower temperatures.

With increasing HxAB concentration the transition is broadened and the enthalpy is lowered gradually until the transition disappears completely.

The zeta potential of DPPC liposomes drops down to negative values with increasing AB concentration. As expected compounds like MeAB cause moderately negative zeta potentials. In contrast compounds like HxAB cause drastic changes and reach highly negative values of -100 mV for the limiting zeta potential. Such negative zeta potentials have rarely been observed before for liposomes. Only for particles from pure phosphatidylserine, ζ potentials of –100 mV have been observed at low ionic strength (Ermakov, 1990).

The binding to the liposomal membrane is stronger with increasing alkyl chain length. This fact is demonstrated on the basis of the dissociation constants derived from the surface potential. The concentrations at the inflections point of the zeta potential curves exhibit the same qualitative tendency.

The addition of MeAB results in liposome fusion. Lipid mixing of 100% is obtained at a concentration of 40 mM.

The cryo-TEM pictures demonstrate that MeAB and EtAB, which have comparably high aqueous monomer solubilities, showed no tendency to form micelles. This is in contrast to PrAB, BuAB and HxAB. Drastic changes in the liposome morphology are observed upon incubation of DPPC liposomes with the cluster derivatives. The incubation with MeAB and EtAB leads to large bilayer sheets. In contrast PrAB is able to transform the liposomes into disk-shaped bilayers, BuAB tends to induce the formation of both open and very small liposomes and HxAB promotes the formation of concentric multilayered liposomes with a rather homogeneous spacing of 13 nm.

4.3 Dodecaborate cluster lipids with variable head groups for boron neutron capture therapy: Synthesis, physical-chemical properties and toxicity (Appendix III)

Two new boron-containing lipids with potential use in boron neutron capture therapy of tumors were prepared. The lipids consist of a double-tailed moiety and a dodecaborate cluster as head group, connected with different spacers (Scheme 1). Both lipids are only singly negatively charged.

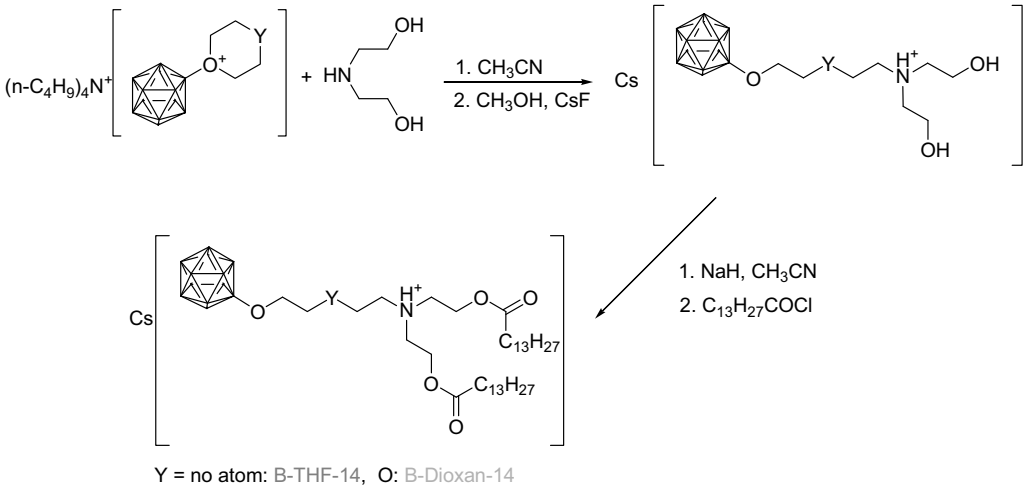

Y = no atom: B-THF-14, O: B-Dioxan-14

Scheme 1: Synthesis of the boron lipids B-THF-14 and B-Dioxan-14.

For connecting the cluster moiety and the lipid backbone nucleophilic ring opening reactions were carried out in which the THF- or dioxane derivative of the cluster reacts with 2 eq. diethanolamine followed by an esterification at the hydroxyl groups with the acid chloride (Scheme 1).

In the DSC experiment B-THF-14 shows a small pre-transition at 46°C and a sharp main transition at 48.9°C. Surprisingly no phase transition temperature could be identified for B-Dioxan-14.

In pure state both lipids show different morphologies in cryo-TEM. B-THF-14 forms predominantly bilayer disks whereas B-Dioxan-14 forms tubular peanut-shaped liposomes. Unilamellar liposomes were obtained for both lipids in the presence of helper lipids.

B-THF-14 inhibits the cell growth by 50% with a concentration of 0.38 mM. In contrast B-Dioxan-14 is less toxic and has an EC_{50} value of 2 mM.

4.4 Pyridinium lipids with the dodecaborate cluster as polar head group: Synthesis, characterization of the physical-chemical behavior and toxicity in cell culture (Appendix IV)

Nine new dodecaborate cluster lipids with potential use in boron neutron capture therapy of tumors have been synthesized. This new generation of boron lipids carries only a single negative net charge. The lipid backbone is pyridinium core with C_{12}, C_{14} and C_{16} chains and is connected through the nitrogen atom via different linkers to the oxygen atom on the dodecaborate cluster as head group. The linkers are butylene, pentylene or ethyleneoxyethylene chains (Scheme 2). The chemical structure has the advantage of the absence of enzymatically cleavable bonds (esters, amides) and thereby might allow longer retention in the body because of reduced degradation.

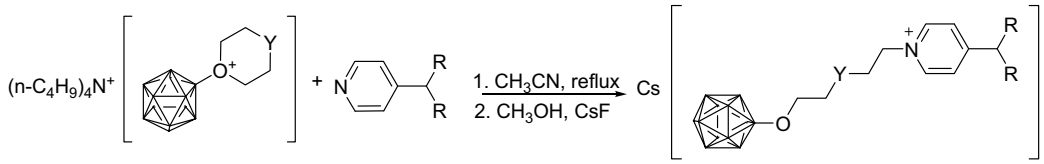

Y= no atom: THF-SAINT-12 (R= $C_{12}H_{25}$)
THF-SAINT-14 (R= $C_{14}H_{29}$)
THF-SAINT-16 (R= $C_{16}H_{33}$)

O: Dioxan-SAINT-12 (R= $C_{12}H_{25}$)
Dioxan-SAINT-14 (R= $C_{14}H_{29}$)
Dioxan-SAINT-16 (R= $C_{16}H_{33}$)

CH_2: Pyran-SAINT-12 (R= $C_{12}H_{25}$)
Pyran-SAINT-14 (R= $C_{14}H_{29}$)
Pyran-SAINT-16 (R= $C_{16}H_{33}$)

Scheme 2: Synthesis of the boron lipids via ring opening reactions between 4-(bisalkylmethyl)pyridine and the THF, dioxane and THP derivative of the dodecaborate cluster respectively.

The lipids were obtained by nucleophilic attack of 4-(bisalkylmethyl)pyridine on the tetrahydrofurane, the dioxane and a newly prepared tetrahydropyrane derivative, respectively, of *closo*-dodecaborate (Scheme 2).

Morphologies formed by pure boron lipid are quite different. The lipids with dodecyl chains produce a mixture of liposomes and some open structures. In the case of Pyran-SAINT-12 some inverted structures were observed. Closed structures were found in greatest abundance for all the three derivatives with 14-carbon chains. For the longer 16-carbon chains, the structures formed appear to be almost exclusively open.

In the presence of helper lipids the formation of liposomes is influenced by the chain length of the tails in the SAINTs. With mixtures containing the short-chain derivatives, an increased tendency to form open structures can be seen.

In the DSC measurements no phase transition could be detected for any of the three SAINT-12 derivatives. All SAINT-14 derivatives show a broad transition which indicates the heterogeneity of the liposome composition. The following main transitions were identified: 13.8°C and 16.8°C for THF-SAINT-14, 12.3°C for Dioxan-SAINT-14, and 8.5°C and 12.4°C for Pyran-SAINT-14. The thermotropic behavior was found to be increasingly complex and polymorphic for all SAINT-16 and a classification of transition was not possible.

Except for two lipids Dioxan-SAINT-12 and Dioxan-SAINT-14, all lipids have low *in vitro* toxicity, and longer alkyl chains lead to a significant decrease in toxicity.

4.5 Cell association of boron-containing liposomes (unpublished results)

Othmann (2008) showed in his master thesis that a remarkable increase in liposome association is obtained upon incorporation of B-6-16 in pegylated liposomes. In this study the cell lines V79 (Chinese hamster cells), IPC-81 (rat leukaemic cells) and CT26 (colon

carcinoma cells) are used. Liposomes containing B-6-16 produce a higher uptake as liposome with targeting devices.

In cooperation with Prof. Peschka-Süss and Prof. Schubert from the University of Freiburg (Breisgau) the cell association (adsorption and endocytosis) of the SAINT lipids is investigated. Here different kinds of boron-containing liposomes labeled with fluorescent markers were prepared and incubated with Kelly cells (human neuroblastoma cell line). For differentiation of passive adsorption and active uptake (which can occur by fusion, endocytosis or intermembrane transfer) the liposome incubation occurred at 4°C and 37°C. The liposomes were not actively targeted with tumor-seeking entities.

The cell association was determined quantitatively using flow cytometry with fluorescence detection.

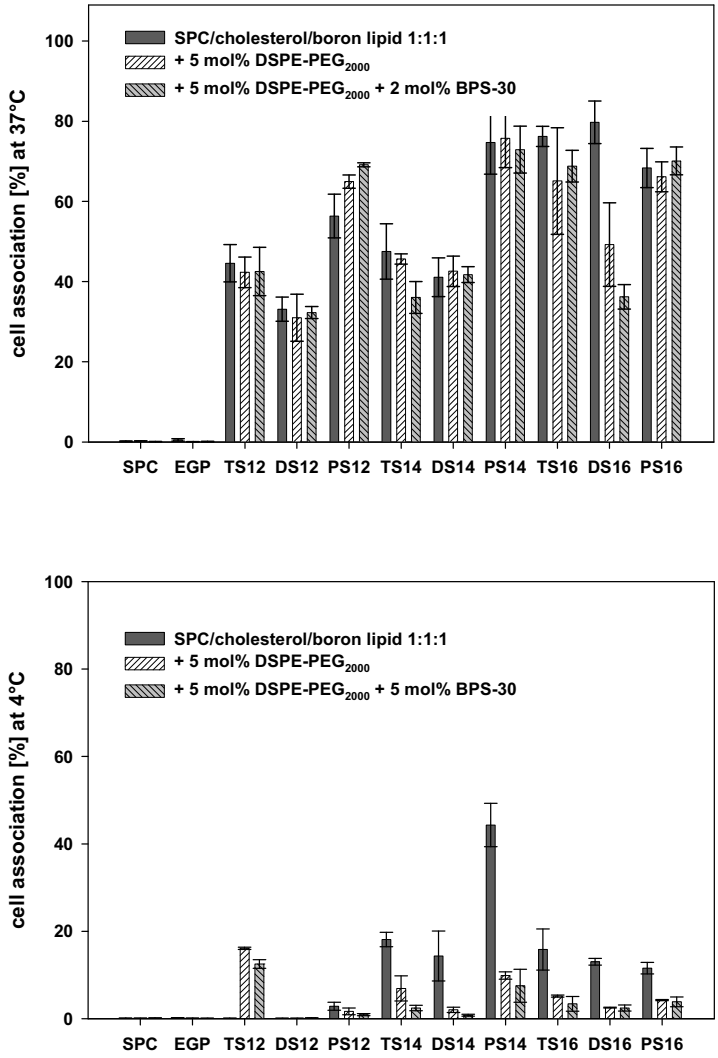

Figure 33: Cell association of different liposome compositions at different temperatures: 4°C for passive adsorption (below) and 37°C for an active cell uptake (above). The reference are SPC (SPC/cholesterol 2:1) and EPG (SPC/cholesterol/EPG 1:1:1) liposomes. SPC is soy phosphatidyl choline, EPG is egg phosphatidyl glycerol and BPS-30 is a pegylated egg sterol.

As can be seen in Fig. 33 the reference sample without boron lipid shows no cell association at both temperatures. In contrast, liposomes containing boron lipid exhibit an increasing cell association which is not influenced drastically by additional pegylation. The charge of the lipids alone cannot be responsible for the high association because liposomes containing the charged egg phosphatidyl glycerol show no tendency for association with cells.

At 4°C all liposomes containing boron lipids show slight adsorption on the cell membrane. At 37°C an active transfer into the cell occurs.

4.6 Tumoral hemorrhage induced by dodecaborate-containing lipids (Appendix V)

The following dodecaborate-containing lipids were tested in an *in vivo* experiment in tumor bearing mice: B-THF-14, B-6-14, THF-SAINT-12 and THF-SAINT-16. One lipid, B-THF-14, led to death of two animals within 5 minutes after the injection. The other three lipids, given in the same concentrations, were well tolerated by the animals.

Two different tumor types were investigated. In whole-body cryosectioning of the animals and in histology, massive bleeding is observed in the tumor after application of the boron lipids B-6-14, THF-SAINT-12 and THF-SAINT-16. Hemorrhage occurred rapidly, and was visible in the tumor *in situ* within about one hour (Fig. 34).

Neutron capture radiography shows that boron was taken up much in liver and spleen (despite the fact that the liposomes were pegylated). The concentration in the tumor was about as the concentration in blood (Fig. 34).

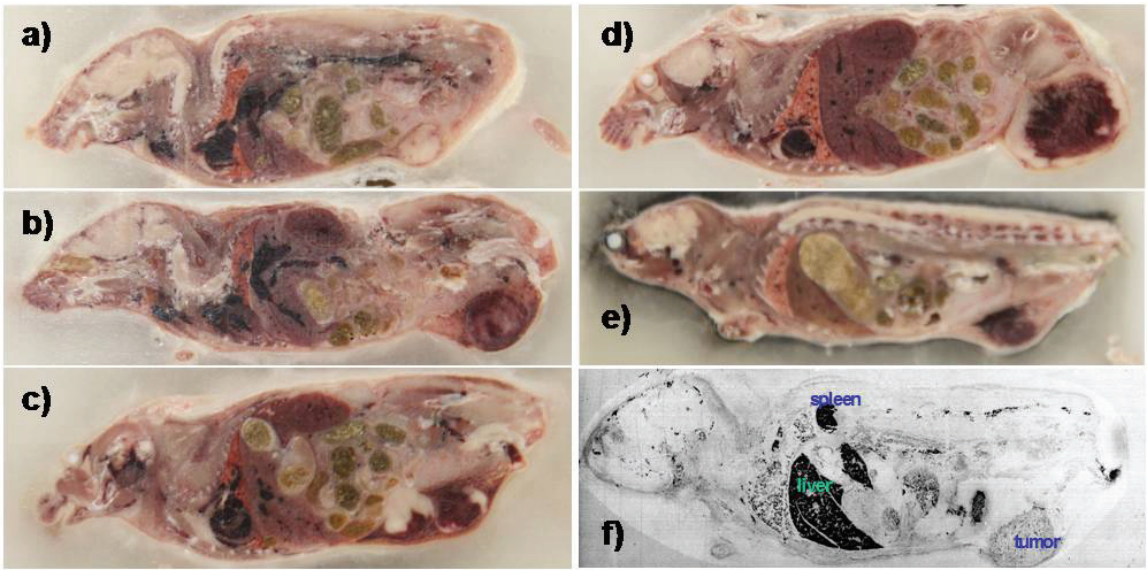

Figure 34: Photographs of mice embedded in CMC during cryo-sectioning: Balb/c without treatment (a), Balb/c THF-SAINT-12 3 h post injection (b), Balb/c THF-SAINT-16 22 h post injection (c), Balb/c B-6-14 20 h post injection (d), C3H THF-SAINT-12 4 h post injection (e). In each animal, the tumor is located at the right lower edge. With no treatment (a), the tumor is lighter in color than muscle. Neutron capture radiogram of a section of an animal having received THF-SAINT-12 four hours before sacrifice (f). Tumor, spleen and liver are labelled. High boron concentrations are indicated by darker color

5. Discussion

5.1 Toxicity of *N,N,N*-trialkylammoniododecaborates as new anions of ionic liquids in cellular, liposomal and enzymatic test systems (Appendix I)

The screening of the toxicity demonstrates that in all biological test systems the ionic liquids are increasingly toxic with increasing chain length and consequently with increasing lipophilicity. This qualitative trend is also observed for other ILs. Here the cations are more toxic with longer side chains. Examples are substituted quinolium and pyridinium rings.

Thus the lipophilicity influenced by the chain length of the ILs is definitely one key factor for toxic interactions. (Ranke *et al.*, 2007; Stolte et al., 2007)

HxAB is the most toxic substance in this compund series and has a hazard potential for Man and environment, and the exposure to this substance might lead to inhibition of the enzyme acetylcholinesterase (AChE) which would be a fatal intervention in the metabolism of higher organisms.

With regard to structural aspects the alkyl chains are probably responsible for the toxicity of the ILs. The dodecaborate cluster unit alone ($B_{12}H_{12}^{2-}$) or the unsubstituted ammonioundecahydro-*closo*-dodecaborate ($B_{12}H_{11}NH_3^-$) are not really toxic (EC_{50} values not yet published). The length of the chains plays an important role in toxicity.

A valid quantitative structure-toxicity-correlation can only be establish for mammalian cells which allows the prediction of EC_{50} values for ABs with longer alkyl chains. A linear regression is obtained when log Kow is plotted versus log EC_{50}.

For the other test systems, an equally good quantitative prediction as for the effect on mammalian cells is not possible. For acetylcholinesterase, the relationship in the log-log plot is complex and extrapolation to longer alkyl chains is difficult. The complexity allows the following different conclusions for the inhibition effect:

1. The enzyme inhibition is influenced by the lipophilicity and other unknown factors.
2. A minimum of lipophilicity is necessary for enzyme inhibition.

It cannot be deduced from the available data, however, which of the both conclusions is true.

For algae, a definite predictive relationship cannot be established; for this, more data points for longer alkyl chains are necessary.

The correlation between mammalian cells and algae is poor which indicates that, e.g., a compound can be toxic for aqueous environments but is not necessarily toxic for higher organisms. Therefore all substances must be tested in both systems for assessment of the toxic potential for Man and environment. The reason why no correlation exists might be the different composition of the cell membrane in mammalian and algal cells.

Liposomes are used as simple model of a cell membrane. The leakage induction by all ABs classifies the cell membrane as potential target site for toxic interactions in mammalian cells or algae. The membrane is discussed in the literature as target site for ionic liquids. (Stolte *et al*., 2007; Ranke *et al*., 2004) In this case the mode of action includes mostly lipophilic interactions. In view of this fact the increasing toxic potential from MeAB to HxAB is not surprising because of the increasing lipophilicity. For understanding the events on the liposomal membrane in detail, further investigations should be performed. The leakage experiment only allows the prediction of qualitative trends with regard to toxicity in cells, e.g., compounds should be more toxic with increasing lipophilicity, but no quantitative prediction of EC_{50} values is possible.

In the case of enzyme inhibition, it is surprising that an anion should inhibit an enzyme whose regular substrate carries a positive charge. The enzyme has three distinct sites where molecular interactions can take place: the peripheral anionic site (PAS), a lipophilic channel located in the entrance of the gorge and the hydrolytic site as the active center (see 2.7). Hydrophobic interactions between the ABs and the amino acid residues lining the channel appear to be the most probable way of inhibition. If MeAB and EtAB react in the same manner is not clear (see explanation above).

One derivative (iPnAB) containing branched instead of linear chains was tested in the biological systems. A qualitative prediction of the behavior in a test system, however, cannot be proposed. Thus iPnAB follows the common trend in the assay with mammalian cells and the enzyme but it is less toxic for algae than BuAB and differs in the capacity to induce leakage. To achieve a valid analysis about the role of branched chains versus linear chains in different test systems more compounds with *i*-alkyl chains should be tested.

The Et2BnAB as one representative of a compound with mixed substitution takes a position between EtAB and PrAB in the compound series in view of lipophilic properties, toxicity in V79 cells and leakage. In the algae assay the EC_{50} of Et2BnAB lies between the values of PrAB and BuAB but it should be noted that the standard deviation is quite high so that a valid grading in the compound series is not possible. In the inhibition of AChE Et2BnAB is definitely classified between PrAB and BuAB which might be explained with additional π-π interactions of the aromatic ring of the benzyl group.

5.2 Interaction of *N,N,N*-trialkylammonioundecahydro-*closo*-dodecaborates with dipalmitoyl phosphatidylcholine liposomes (Appendix II)

The results of the zeta potential measurements indicate that the compounds bind to the liposomal surface, as drastic changes of the surface potential occur upon addition of the

compounds. The binding to the hydrophobic part of the membrane becomes energetically more favorable with increasing chain length, shown by the dissociation constants of the ABs. From the compound/lipid concentrations ratio of BuAB and HxAB, it appears that a single lipid head group does not represent one binding site for a cluster molecule, but rather that each binding site comprises several lipid molecules. In case of BuAB and HxAB, and perhaps also PrAB, it is fair to say that the alkylated substance behaves like a conventional surfactant and are hence able to interact with the lipophilic core of the membrane. (Paternostre *et al*., 1995) In contrast, MeAB and EtAB show no surfactant-like behavior.

The isotherms obtained from plotting zeta potential versus the root of compound concentrations indicate that the binding of further molecules is influenced by the already bound molecules through electrostatic repulsion forces and consequently the association affinity is reduced.

Within the Poisson-Boltzmann theory the surface potential is proportional to the surface charge density at low concentration (Debye-Hückel approximation). This range can be described by a binding constant. The calculated dissociation constants of the substances from the surface potential reflect the previous qualitative observations.

The limiting zeta potential of around -100 mV measured for HxAB and calculated from fitted curves for the other ABs is a rarely negative potential for liposomes. Liposomes incubated with BSH (Awad *et al*., 2009) do not exhibit such negative potentials and the incorporation of negatively charged arsonolipids (Fatourus *et al*., 2005) or dodecaborate cluster lipids (Justus *et al*., 2007) leads only to potentials of -50 mV and -67 mV, respectively. Only liposomes consisting of pure phosphytidylserine exhibit zeta potentials around -100 mV. A more detailed molecular simulation of interactions between the ABs and liposomes is required to explain the low potentials. It might be speculated that the water layer around the liposome surface is affected so that the slipping plane, where the zeta potential is detected, is shifted closer to the liposomal surface and consequently the shielding of the negative charges is decreased.

In the case of MeAB, the complete loss of the pre-transition temperature in the DSC profile indicates that it interacts with the choline head groups of DPPC but no interference with the lipid tails occurs. In contrast, HxAB acts more as a detergent and causes a complete disappearance of the peak representing the gel-to-liquid crystalline phase transition. It seems that it penetrates and incorporates into the liposomal membrane similar to TRITON-100 and perfluorinated drugs (PFOS) so that the anionic part is most likely located at the lipid-water interface whereas the alkyl chains interfere with the palmitoyl chains of DPPC which cause significant disruption of the packing of the lipid tails of DPPC. (Goňi *et al*., 1986; Lehmler and Bummer, 2004; Lehmler *et al*., 2006)

On the basis of the existing data the following hypothesis for the compound binding to the liposomal surface is proposed: All ABs interact with their doubly negatively charged dodecaborate cluster with the positively charged choline head groups, and the positively charged ammonium group is probably in contact with the deeper-laying negatively charged phosphate. ABs with short alkyl chains only exhibit interactions in the head group region which are probably electrostatic in nature. Additional effects affecting the water layer cannot be excluded.

As the length of the alkyl chains increases, additional interferences with the lipid tails are involved. Thus the interactions are electrostatic and additionally lipophilic.

From this hypothesis is not evident how deep the ABs protrude into the lipid bilayer and hence the binding model shown in Fig. 35 is only qualitative in its nature.

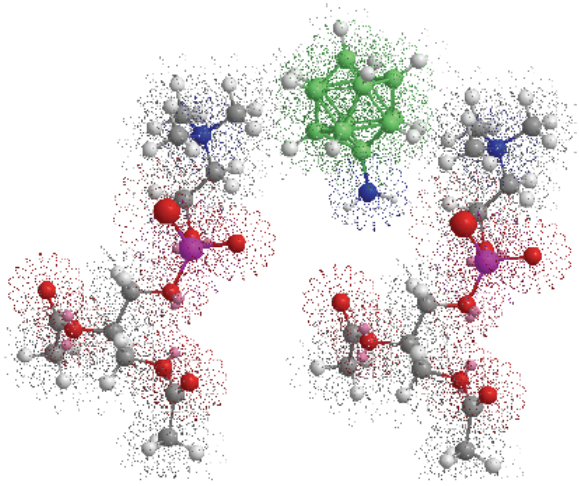

Figure 35: Binding model for ABs to the liposomal surface. The lipids and the ABs are presented in the ball-and-stick model and additionally the van der Waals radii for all atoms are shown.

The compound/lipid ratio used in cryo-TEM induces drastic changes in the morphology. Thus the influence of MeAB and EtAB leads to large bilayer sheets which are stable after heating up to 37°C and storage for one week. The other ABs differ as they are able to form micelles by themselves. This fact suggests that they share important properties with conventional ionic micelle-forming surfactants which are well known to insert into liposomal membranes, and may, at sub-solubilizing concentrations, induce a range of structural transformations of the liposomes. The insertion of surfactants into the outer lipid leaflet of the membrane frequently also leads to a process in which small liposomes are budded off from the original liposome. (Heerklotz, 2008) Thus the transformations occurring after addition of PrAB and BuAB are not surprising.

In the case of HxAB the formed concentric multilayered liposomes with a rather homogeneous spacing of 13 nm are more difficult to understand. So far these onion ring-like structures are only known for pegylated liposomes, liposomes incubated with DNA (Clement

et al., 2005; Letrou-Bonneval *et al*., 2008) or for miniemulsion polymerization with lanthanide complexes (Ramírez *et al*., 2006). For HxAB, it can only be speculated that a compound layer around the liposome prevents a closer approach of the membranes.

MeAB initiates a fusion process at smaller concentrations compared to BSH. (Awad *et al*., 2009) Therefore it seems that the change of the SH-group to the $N(CH_3)_3$-group makes the substances more effective in view of lipid mixing. It should be noted, however, that both compounds have different net charges and that the fusion mediated by BSH was tested on DMPC liposomes which have a lower phase transition temperature as DPPC liposomes. Thus DMPC liposomes are in the fluid phase during fusion whereas DPPC liposomes remain in the gel phase.

The fusion process was not indeed tested for EtAB. The bilayers in cryo-TEM are, however, obviously the product of fusion and consequently this process is highly probable also for this compound.

The leakage induced by ABs is probably not caused by fusion based on the fact that the time scale of both processes is different. In addition the fusion process depends on the lipid concentration; the concentration is quite high in the lipid mixing experiment, but quite low in the leakage experiment. In addition we have shown before that leakage from DPPC liposomes occurs also when fusion processes are prevented by the incorporation of PEG chains into the liposomal membrane. (Gabel *et al*., 2007) The complex leakage kinetics, which is not first order, might rather indicate the formation of transient defects or holes. The peptide melittin, which is known to form pores, shows similar leakage kinetics. In addition the pore formation depends on the peptide concentration; an increasing concentration leads to faster leakage. (Schwarz *et al*., 1992) The same tendency is observed for all ABs.

The data of this study indicate that interactions of ABs with other membranes (e.g., cell membranes) must be assumed. The different toxic modes of actions are feasible: the binding of ABs to the cell membrane will result in a higher membrane potential followed by a change of cell behavior. In addition the ability of the ABs to induce leakage by pore formation might affect the permeability of the cell membrane and consequently influence the cell function. A complete disruption of the cell membrane cannot be excluded in the case of BuAB and HxAB with their detergent-like behavior.

5.3 Dodecaborate cluster lipids with variable head groups for boron neutron capture therapy: Synthesis, physical-chemical properties and toxicity (Appendix III)

Two new boron lipids, B-THF-14 and B-Dioxan-14, have been synthesized which differ from the lipid B-6-14 previously described by Justus *et al*. (2007) (see 1.11) by carrying only one

negative net charge and additionally in the linker connecting the dodecaborate cluster as head group with the lipid backbone. The synthesis method is not very time-consuming and gives relative high yields. In addition the method allows very facile to vary the linker and consequently to investigate the different behavior influenced by the linker.

The thermotropic profile of the B-THF-14 is not comparable with that of other known lipids. Therefore DMPC containing the same hydrophobic part shows a much lower transition. Even B-6-14 differing only in the linker to the cluster unit exhibits a different thermotropic behavior. By changing the butylene to the ethyleneoxyethylene linker the profile in the DSC is again completely different. In the latter case no transition can be detected. We suggest that the membrane packing is disturbed due to the more hydrophilic and flexible nature of the linker. It is assumed that lipid transitions are not only influenced by the head group and lipid tails but also by the linker.

The observed bilayer discs formed by pure B-THF-14, rather than the closed vesicles found for other lipids are not so surprising. The anionic lipid egg DMPG (dimyristoylphosphatidylglycerol) forms large and small bilayer sheets at low ionic strength. Repulsion forces between the head groups lead to a limitation of the vesicle curvature so that small discs or sometimes larger sheets are the preferred energetic morphologies. (Epand and Hui, 1986) Surprisingly B-Dioxan-14 in pure state forms predominantly tubular peanut-shaped liposomes. Here it seems that the repulsion forces between the head groups are less pronounced so that closed vesicles are the energetically preferred formation. How the membrane packing for B-THF-14 and B-Dioxan-14 looks in detail on a molecular level is not deducible from the existing data. For this, molecular dynamic simulations are required.

The different forms observed in cryo-TEM for the different lipids indicate definitely that the linker has a strong influence on the morphology.

In comparison to the ionic liquids (ABs) with long alkyl chains, such as BuAB or HxAB, the boron lipids here do not form micelles. Therefore the carbon matrix connected to the dodecaborate cluster influences strongly the morphologies and the connection with a lipid moiety allows the formation of disks or liposomes.

In the case of B-THF-14, no correlation between the DSC profile and cryo-TEM data exists. Normally discs show a broadening of the transition in contrast to vesicles which has a sharp transition. The broadening in the case of discs can be attributed to a loss in cooperativity. (Shaw *et al*., 2004) B-THF-14, however, displays a sharp transition while discs are found in cryo-TEM. An explanation for this discrepancy might be that closed vesicles will be formed at higher temperature. This hypothesis, however, cannot be proven because cryo-TEM is not manageable at temperatures of 47 or more degree. In contrast both DSC and cryo-TEM measurements indicate a disturbance of the membrane packing in the case of B-Dioxan-14.

In contrast to the ABs both lipids do not disturb the liposomal formation; rather they can incorporate into the liposomal membrane formed by helper lipids. Therefore the lipid moiety linked to the dodecaborate cluster leads to other compound properties compared to ABs and prevents a detergent-like behavior. The reason of the different behavior is that ABs exhibit a cone-like geometry which normally leads to micelles. The boron lipids are cylindrical in shape, having nearly equal head group to hydrocarbon area, and hence favor the formation of bilayers.

The *in vitro* toxicity as well as the *in vivo* toxicity are again influenced by the linker. Thus the introduction of an ether function in the linker decreases the toxic potential. No data, however, exist about the toxic mode of action of these lipids. It is possible that the boron lipids are incorporated into the cell membrane through a fusion process or a lipid exchange which could result in a decrease of the membrane potential followed by a dysfunction of membrane channels as well as the change of membrane fluidity.

In summary it seems that the choice of the linker plays an important role which behavior a lipid exhibits.

With a view to medical application B-Dioxan-14 might represent a suitable boron carrier for boron neutron capture therapy with its low toxicity and the formation of liposomes in pure state compatible with intravenous injection.

5.4 Pyridinium lipids with the dodecaborate cluster as polar head group: Synthesis, characterization of the physical-chemical behavior and toxicity in cell culture (Appendix IV)

Nine new dodecaborate lipids, the SAINT derivatives, with a net charge of minus one have been synthesized. The basic structure of these lipids is completely different to other known boron lipids. The SAINTs prepared here carry a bisalkylmethyl group on the *p*-position of a pyridine, which is *N*-alkylated with a linker carrying the dodecaborate cluster as polar head group. This basic structure has the advantage of the absence of enzymatically cleavable bonds (esters, amides) and thereby might allow longer retention in the body because of reduced degradation.

For the synthesis the nucleophilic ring opening reactions (RORs) are again used which make the synthesis strategy straightforward, not very time-consuming and proceeds with good yields; in addition it offers the possibility of varying the length of the alkyl chains and the linker between the pyridinium and the boron cluster.

In this study a new linker, pentylene, is established. For the first time the tetrahydropyrane derivative (THP) of the dodecaborate cluster is used in RORs with pyridine-containing structures. So far RORs for THP are only known with very simple nucleophilics, such as

fluoride, chloride or hydroxide. (Peymann *et al*., 1997) Normally the most commonly used oxonium derivatives for RORs are tetrahyrofurane (THF) and dioxane. (Semioshkin *et al*., 2007; Semioshkin *et al*., 2008)

The THP derivative had first been published by Peymann *et al*. (1996) and had been prepared by alkylation of hydroxyundecahydro-*closo*-dodecaborate with dibromopentane, which requires two synthesis steps from the dodecaborate cluster to the THP derivative. We developed a reaction procedure which leads to the THP derivative from the unsubstituted dodecaborate cluster in one step and in good yields. This synthesis strategy makes the THP derivative accessible faster than the old one.

The introduction of THP in RORs offers the possibility to compare linkers which only differ in their length but not in their chemical behavior. Therefore it can be determined whether the length of linker influences the properties of a lipid.

The cryo-TEM data demonstrate that it is possible to prepare closed vesicles (liposomes) in addition to some open bilayers from pure boron lipid when the temperature of preparation is above the main phase transition. For the SAINT derivatives with long tails temperatures above 50°C should be chosen. The liposomes are stable when stored at 4°C, although both the SAINT-14 and SAINT-16 derivatives are in the gel phase; under these conditions the boron lipid B-6-14 forms large bilayer sheets. (Justus *et al*., 2007) Interestingly the choice of the linker plays no major role for the liposome formation in contrast to B-THF-14 and B-Dioxan-14. It can be noted that the influence of a linker depends on the lipid backbone and thus is more or less pronounced.

In comparison to the ABs (introduced above) again the lipid backbone connected on the dodecaborate cluster prevents micelle formation and makes available liposomes formed by dodecaborate cluster-containing compounds.

The incorporation of the SAINT derivatives in a liposomal membrane consisting of helper lipids also leads to liposomes. No drastic morphological changes are observed, again different from the addition of the ABs. Therefore if the carbon matrix connected on the cluster is long enough and is cylindrical in shape, the surfactant behavior is eliminated.

It should be pointed out that the choice of the helper lipid influences the formation of liposomes. Thus the helper and boron lipids should not differ significantly in their tail lengths. For DSPC and the SAINT-12 derivatives this was the case.

The DSC data of the SAINT-12 and SAINT-14 derivatives are in line with the literature as well as the cryo-TEM micrographs. The heterogeneity in vesicle size and shape of the SAINT-14 samples causes a broadening of the transition and the splitting into two main transitions.

All SAINT-16 lipids display a rich polymorphism in their DSC profiles. An exact classification of all transitions is not possible with the existing data and molecular dynamics simulations would certainly be required for SAINT-16 lipids to answer precisely the question of lipid packing. Such polymorphism, however, is known for methylated pyridinium cores depending on the counter ion. A tilted smetic phase is described by Sudhölter *et al*. (1982) for 1-methyl-4-(dihexadecylmethyl)pyridinium iodide. There the iodide anion is located between the pyridinium cores and the overlap of the lipids with each other is minimized. A similar arrangement of the SAINT lipids might be suggested; here, however, the negatively charged cluster unit takes the places between the pyridinium cores. The voids which would be generated in the hydrophic region of the bilayer might be filled by lipids of the opposite monolayer. In consequence the bilayer would adopt an interdigitated conformation. (Garidel *et al*., 2008) It should be noted once more that we have no evidence for this hypothesis.

The choice of the linker has again no influence of the thermotropic behavior of the lipids which is in contrast to B-THF-14 and B-Dioxan-14.

With the exception of Dioxan-SAINT-12 and Dioxan-SAINT-14 the SAINT lipids have low toxicity. It seems that the choice of the linker influences the toxicity in the case of short alkyl chains. The dioxane linker leads to a higher toxic effect compared to the THF or THP linker. This is the opposite effect as for the boron lipids B-THF-14 and B-Dioxan-14 where the introduction of an ether function in the hydrocarbon spacer leads to a decrease of toxicity.

A general trend can be established for boron lipids: longer alkyl chains lead to a decrease of toxicity. This is observed forthe SAINT lipids as well as for B-6-14 and B-6-16.

In summary it can be noted that the linker influence the thermotropic behavior of a lipid, the morphologies formed by pure lipid and the lipid toxicity depending on the lipid moiety. The length of the lipid tails also influences the common properties of a lipid.

5.5 Cell association of boron-containing liposomes (unpublished results)

All liposomes containing B-6-16 or the SAINT lipids show an exceptional cell association. Without any targeting 40% till 80% of the cells show an uptake of the boronated liposomes. Pegylation of the liposomes does not markedly influence the cell association neither in the case of SAINT lipids nor in the case of B-6-16.

In fact, such an effect is not known for commonly available lipids, and so far the cell association is not investigated for other published dodecaborate cluster lipids.

The high cell association cannot be exclusively explained with the charge of the lipids. On the one hand the SAINT lipids carry only a single negative charge whereas B-6-16 is doubly negatively charged, and on the other hand liposomes containing the negatively charged lipid EPG (egg phosphatidylglycerol) show no uptake. In addition the lipid moiety connected on

the dodecaborate cluster has also no influence because all tested dodecaborate cluster lipids show this exceptional cell association.

It seems that the dodecaborate cluster as head group with its double negative charges is the important structure element leading to the cell association.

BSH ($B_{12}H_{11}SH^{2-}$) is found in glioblastoma tissue intracellularly and associated with membranes, following its administration to patients prior to surgery (Otersen *et al*., 1997; Neumann *et al*., 2002). The membranes of glioblastoma tissue are rich in choline (Ott *et al*., 1993), and interactions between BSH and the head groups of the phosphatidylcholine lipids are suggested. (Awad *et al*., 2009) These interactions are supported by the fact that most of the tetraalkylammonium salts (e.g., tetramethylammonium, tetrabutylammonium) of $B_{12}H_{12}^{2-}$ derivatives, including BSH, are insoluble in water (Gabel *et al*., 1993), so that the quaternary ammonium group of choline is probably involved. (Gabel *et al*., 2007)

The dodecaborate cluster unit of all tested ABs is also able to interact with the choline head groups despite the fact that they have a different substitution as BSH.

Therefore it might be speculated that the cell membranes are rich in phosphatidylcholine lipids and that the dodecaborate cluster lipids interact with the lipid headgroups leading to an adsorption to the cell surface.

The exceptional cell association is, however, mediated by active processes at higher temperatures and not only by passive cell adsorption. The active uptake, however, can include fusion, an endocytotic-mediated pathway or an intermembrane transfer.

This exceptional cell association mediated by the dodecaborate cluster lipids is not necessarily a desirable process because it is not target-orientated. *In vivo* this kind of liposomes could interact with all choline-rich membranes which are not necessarily located in the tumor tissue.

5.6 Tumoral hemorrhage induced by dodecaborate-containing lipids (Appendix V)

Massive tumoral hemorrhage is observed after injection of liposomes containing dodecaborate cluster lipids. Interestingly, all tested dodecaborate cluster lipids induce this effect despite the fact that they differ in net charge and lipid moiety. The boron lipids have in common only the doubly negatively charged dodecaborate cluster as head group.

Neutron capture radiography demonstrates that spleen and liver take up most of the boronated liposomes. This fact is not surprising, as several studies report that pegylated liposomes are accumulated in these organs. (Blume and Cecv, 1990; Gabizon and Papahadjopoulos, 1988) The boron concentration in the tumor is similar to that in blood but

not very high which indicates that small boron amounts already provoke this massive hemorrhage.

The bleeding is probably associated with extravasated red blood cells caused by destruction of the tumoral blood vessels. Such a selective destruction has been observed before by combinations of tumor necrosis factor α (TNFα) in combination with melphalan (Hoving *et al*., 2006), by multiple doses of doxorubicin-containing liposomes (Zhou *et al*., 2006), and by a combination of galactosamine and endotoxin. (Ito *et al*., 2006) All these studies deal with the hypothesis that the hemorrhage is initiated by gap formations. The process is, however, not clarified in detail.

Normally the angiogenic blood vessels show abnormal permeability caused by gaps (0.6-0.8 µm) located between adjacent endothelial cells through which liposomes can extravasate. Red blood cells, however, are oversized with a diameter of around 7 µm. Therefore the diameter of existing gaps would have to be increased following the exposure to boronated liposomes, or new gaps would have to be generated.

It might be speculated that dodecaborate cluster lipids incorporated into the liposomes are able to interact with the endothelial cells. In view of the fact that dodecaborate cluster lipids are responsible for extreme cell association this scenario is entirely feasible. If the boron lipids enter the endothelial membrane by an active uptake process or a lipid exchange between both membranes, the cell-cell contacts might be influenced by which new gaps could be generated or the diameter of the existing gaps could increase in size.

The induction of tumor hemorrhage for BNCT is not necessarily a desired effect, especially when accompanied, as observed here, with a non-impressive uptake of boron into the tumor. Thus strategies should be developed to prevent this effect.

6. Conclusion and outlook

6.1 Ionic liquids

The toxicological hazard potentials of different ABs are determined for Man and environment. Qualitative trends of toxicity are established for all ABs with *n*-alkyl chains, a quantitative prediction is, however, only successful for mammalian cells. Therefore more substances should be screened for the algae and enzyme system.

A number of additional compounds, in which the substituents should be varied in a more systematic and comprehensive way, would have to be investigated before any qualitative conclusions or quantitative predictions for asymmetrically or branched side chains can be drawn.

The cell membrane is proposed as target site for toxic interactions for mammalian cells and algae. A model for the binding of the compound to the membrane is devised on the basis of zeta potentials and DSC data. Molecular dynamics simulations can be additionally carried out to check the proposed model and to clarify possible deformations on the water layer around the membrane. In addition, the pore formation by which leakage is probably induced should be investigated in more detail. Therefore fluorescent dyes of different molecular sizes (e.g., carboxyfluorescein, FTIC-dextran) could be encapsulated into the liposome to get an idea about the pore sizes. (Rex, 1996) Another method would be to encapsulate radioactively labeled carbohydrates of different molecular weights. (Schubert *et al*., 1986)

Different toxic modes of action are feasible for the ABs and might concern changes in the membrane potential of cells, permeabilization of the membrane by pore formation or the complete disruption of the membrane. Alterations in the membrane potentials of cells could be detected by staining with the anionic oxonol dye bis-(1,3-dibutylbarbituric acid) trimethine oxonol DiBAC as described by Nuccitelli *et al*. (2006). The integrity of the membrane could be detected, e.g., with the neutral red test.

A potential mechanism for AChE inhibition is theoretically developed for ABs with *n*-alkyl chains on the basis of thinking in terms of structure activity relationships. Thus the lipophilic channel located in the entrance of the gorge of AChE is proposed as target site for toxic interactions. More thorough investigations of the AB interactions with the enzyme would be required to evidence this model. In addition, ABs with short alkyl chains should be investigated in more detail, if they really inhibit the enzyme in the same manner as ABs with longer alkyl chains.

In general, the melting points of the ABs decrease with longer alkyl chains, but the hazard potential increases. Therefore a functionalization of the chains, e.g., with ether functions or introduction of hydroxyl groups, should be considered to possibly reduce the toxic potential.

The ABs are derivatives from B12NH3 (ammonioundecahydro-*closo*-dodecaborate) and are obtained by alkylation. It should be noted that BSH can also be alkylated with one or two alkyl chains so far; however, these compounds have not been investigated whether they exhibit an ionic liquid-like behavior or whether their toxicity or toxic mode of actions differ from that of the ABs.

6.2 Dodecaborate cluster lipids

A synthesis strategy is designed which allows a facile preparation in relative high product yields, is not very time-consuming and offers the possibility to vary the lipid structure (linker, lipid tails). The influence of the linker as well as the lipid tails are investigated in more detail. All prepared dodecaborate cluster lipids carry only one negative charge and are characterized with respect to their physical-chemical behavior, their ability to form liposomes and their toxicity *in vitro* and *in vivo*.

Some aspects should be investigated in more detail in the future. The membrane packing formed from pure lipids should be clarified with molecular dynamic simulations in the case of B-THF-14, B-Dioxan-14 and the SAINT-16 derivatives.

In general, the toxic potential of the boron lipids decreases with increasing chain length. Therefore the synthesis of B-THF-16 with palmitoyl chains might also reduce its toxicity. Another idea is to prepare lipids with unsaturated lipid tails which might influence the toxicity and certainly the physical-chemical behaviors.

The cellular uptake of the dodecaborate cluster lipids should be investigated in more detail. On the one hand it will be important to check, if their exceptional cell uptake can be also reached in other cells line and especially in cells which show low transfection tendency, e.g., HSMC (human smooth muscle cells) or HAEC (human aortic endothelial cells). Additionally the way by which the uptake is mediated should be clarified. Endocytosis, fusion and intermembrane transfer (lipid exchange) come into considerations as uptake possibilities. Therefore inhibitors of the endocytosis could be used to point out changes in the cell association. A fusion process could be detected with fluorescent-labeled helper lipids which would enter the cell membrane. For the lipid exchange from the liposomal to the cell membrane the boron lipids would have to be labeled fluorescently to detect them in the cell membrane. In addition, the cellular distribution of the dodecaborate cluster lipids should be investigated in detail.

Furthermore the toxic mode of actions of these lipids should be clarified. If the boron lipids are exclusively located in the cell membrane, the membrane potential will be influenced. A possible detection method is described by Nuccitelli *et al*. (2006). The membrane fluidity could also be changed. These kinds of alterations could be assessed by measuring the

fluorescence polarization with the fluorescent dye 1,6-diphenyl-1,3,5-hexatriene (DPH). (Tang *et al*., 2008)

The phenomenon of bleeding after application of dodecaborate cluster lipids should be investigated in more detail. On the one hand smaller concentrations could be tested to determine a limiting concentration which does no longer induce hemorrhage. In addition, the integrity of the cell-cell contacts should be controlled. For this purpose, a layer of MDCK cells ((epithelial) Madin-Darby canine kidney cells) could be grown on a polycarbonate membrane and loss of junctions could be detected by a decrease of the transepithelial electrical resistance. The transport of substances out of the cell mediated by the P-glycoprotein could determine if the cell function is influenced by the presence of dodecaborate cluster lipids. Thus a decreased or increased transport of the radioactively labeled substrate ^{3}H-Digoxin of the P-glycoprotein gives information about this fact.

In view of the massive hemorrhage induced by the dodecaborate cluster lipids we also intend to prepare boron-containing lipids with no net charge, or a net charge of +1, to see whether such lipids also cause hemorrhage. For this intention other linkers would be advantageous which offer the possibility for alkylation and bring positive charges for the compensation of the negative ones near to the cluster unit. To use the newly designed synthesis strategy as tool for easily accessible boron lipids it will be helpful to try the ring opening reactions with the following dodecaborate cluster derivatives:

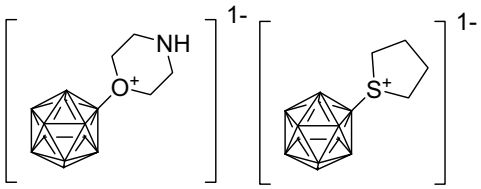

Scheme 3: Possible compounds for new ring opening reactions

If the hemorrhage would occur with these newly prepared dodecaborate cluster lipids despite different net charges, other head groups should be applied to hopefully prevent this undesirable effect. The ring opening reactions could be carried out with the following compounds to get new head groups:

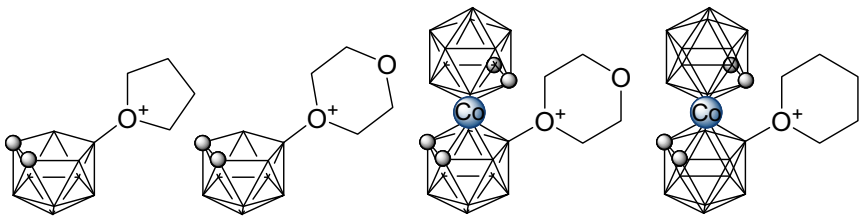

Scheme 4: Oxonium derivatives of 7,8-dicarba-nido-undecaborate and of cobalt bis(dicarbollide)

6.3 General conclusions for dodecaborate cluster compounds

In this study derivatives of the dodecaborate cluster were investigated which have no similarities at the first glance. Some general conclusion could be nevertheless drawn for compounds containing the cluster unit.

The existing results indicate that the dodecaborate cluster unit $B_{12}H_{12}^{2-}$ is a pharmacophor on its own and consequently responsible for certain pharmacologic interactions. Thus it is able to interact electrostatically with the head groups of phosphatidylcholine lipids which are located in liposomal or cellular membranes. These interactions lead to a firm binding to membrane surfaces.

A substitution of the cluster with a sulfhydryl group or N-alkylammonium group as well as a connection to a lipid moiety does not influence the interactions between the cluster unit and the choline head groups. Thus, when compounds contain the dodecaborate cluster unit, they also exhibit this pharmacologic behavior.

It cannot, however, be deduced from the data to which extent derivatization influences the molecular binding of the cluster compounds to the membrane. For the ABs, a binding model is postulated which need not to be necessarily correct for all other low molecular weight compounds containing the dodecaborate cluster. Thus, e.g., the sulfhydryl group of BSH could point toward the hydrophobic part of the membrane or could protrude into the surrounding water phase when the dodecaborate cluster interacts with the choline head groups.

The implications of these pharmacologic interactions are, however, not predictable for a given dodecaborate cluster compound. Thus BSH is probably able to enter the cell membrane due to these interactions, but no high toxic hazard is involved. Amphiphilic compounds, containing of the hydrophilic dodecaborate cluster in combination with a hydrophobic part, cause a different pharmacologic effect than pure ionic substances. They are able to interact additionally with the lipophilic part of the cell membrane which could lead to disturbances within the membrane or to a complete disruption. In dependence of the compound geometry these amphiphilic compounds exhibit a detergent-like behavior or could be incorporate into the membrane.

Thus, e.g., the substitution with the N-alkylammonium group leads to toxicity according to the length of alkyl chains. Here the cluster unit probably enables the ABs to interact with the membrane; the cone-like geometry, and thereby the detergent-like behavior, of the alkyl residue is, however, responsible for the high toxicity. In the case of the boron lipids, the dodecaborate cluster as head group causes a pronounced adsorption to the membrane surface followed by an active uptake into the cell at higher temperatures (37°C). In addition it seems that the cluster unit is responsible for the massive hemorrhage in tumors which is a

completely different pharmacologic effect from that of BSH. High molecular weight compounds cause pharmacologic effects which are unexpected and so far not understood in molecular detail.

Prospective studies, which deal with amphiphilic compounds of the dodecaborate cluster, should consider these general conclusions. It might be helpful to prevent some pharmacological effects.

7. References

Allen, C.; Dos Santos, N.; Gallagher, R.; Chiu, G. N. C.; Shu, Y.; Li, W. M.; Johnstone, S. A.; Janoff, A. S.; Mayer, L. D.; Webb, M. S. and Bally, M. B. (2002) Controlling the physical behavior and biological performance of liposome formulations through use of surface grafted poly(ethylene glycol). *Biosci. Rep.* 22, 225-250.

Allen, T. M. and Cullis, P. R. (2004) Drug delivery systems: Entering the mainstream. *Science.* 303, 1818-1822.

Almgren, M.; Edwards, K. and Karlsson, G. (2000) Cryo transmission electron microscopy of liposomes and related structures. *Colloids Surf., A* 174, 3-21.

Arning, J.; Stolte, S.; Böschen, A.; Stock, F.; Pitner, W. R.; Welz-Biermann, U.; Jastorff, B. and Ranke, J. (2008) Qualitative and quantitative structure activity relationships for the inhibitory eccets of cationic head groups, functionalized side chains and anions of ionic liquids on acetylcholinesterase. *Green Chem.* 10, 47-58.

Awad, D.; Damian, L.; Winterhalter, M.; Karlsson, G.; Edwards, K. and Gabel, D. (2009) Interactions of $Na_2B_{12}H_{11}SH$ with dimyristoyl phosphytidylcholine liposomes. *Chem. Phys. Lipids* 157, 78-85.

Bangham, A. D.; Standish, M. M. and Watkins, J. C. (1965) Diffusion of univalent ions across the lamellae of swollen phospholipids. *J. Mol. Biol.* 13, 238-52.

Barth, R. F. (2003) A critical assessment of boron neutron capture therapy: an overview. *J neurooncol.* 62, 1-5.

Barth, R. F.; Coderre, J. A.; Vicente, M. H. G. and Blue T. E. (2005) Boron neutron capture therapy of cancer: Current status and future prospects. *Clin. Cancer Res.* 11, 3987-4002.

Berridge, M. V.; Tan, A. S. and Herst, P. M. (2005) Tetrazolium dyes as tools in cell biology: new insights into their cellular reduction. *Biotechnol. Annu. Rev.* 11, 127-152.

Berridge, M. V.; Tan, A. S.; McCoy, K. D. and Wang, R. (1996) The biochemical and cellular basis of cell proliferation assays that use tetrazolium salts. *Biochemica* 4, 14-19.

Bhadeshia, H. K. D. H. (2002) Differential scanning calorimetry. *Teaching materials, Materials Science & Metallurgy, University of Cambridge*. (http://www.msm.cam.ac.uk/phasetrans/2002/Thermal2.pdf)

Biltonen, R. L. and Lichtenberg, D. (1993) The use of differential scanning calorimetry as a tool to characterize liposome preparations. *Chem. Phys. Lipids* 64, 129-142.

Blume, G. and Cevc, G. (1990) Liposomes for the sustained drug release in vivo. *Biochim. Biophys. Acta.* 1029, 91-97.

Bohl Kullberg, E.; Bergstrand, N.; Carlsson, J.; Edwards, K.; Johnsson, M.; Sjöberg, S. and Gedda, L. (2002) Development of EGF-conjugated liposomes for targeted delivery of boronated DNA-binding agents. *Bioconjugate Chem.* 13, 737-743.

Bourne, Y.; Taylor, P.; Radic, Z. and Marchot, P. (2003) Structural insights into ligand interactions at the acetylcholinesterase peripheral anionic site. *EMBO J.* 22, 1-12.

Carlsson, J.; Bohl Kullberg, E.; Capala, J.; Sjöberg, S.; Edwards, K. and Gedda, L. (2003) Ligand liposomes and boron neutron capture therapy. *J neurooncol.* 62, 47-59.

Chaidarun, S. S.; Eggo, M. C.; Sheppard, M. C. and Stewart, P. M. (1994) Expression of epidermal growth factor (EGF), its receptor, and related oncoprotein (erbB-2) in human pituitary tumors and response to EGF in vitro. *Endocrinology.* 135, 2012-2021.

Chemnitius, J. M.; Sadowski, R.; Winkel, H. and Zech, R. (1999) Organophosphate inhibition of human heart muscle cholinesterase isoenzymes. *Chem.-Biol. Interact.* 120, 183-192.

Chrai, S. S.; Murari, R. and Ahmad, I. (2002) Liposomes: a review, part I: manufacturing issues. *Pharm. Technol.*, 28-34.

Clement, J.; Kiefer, K.; Kimpfler, A.; Garidel, P. and Peschka-Süss, P. (2005) Large-scale production of lipoplexes with long shelf-life. *Eur. J. Pharm. Biopharm.* 59, 35-43.

Cohen, J. A.; Gabriel, B.; Teissie, J. and Winterhalter, M. (2003) Transmembrane voltage sensor. In *Planar Lipid Bilayers and their applications* by Tien, T Ti, Ottova-Leitmannova, A. pp. 847-886, Elsevier, New York.

Colletier, J. P.; Fournier, D.; Greenblatt, H. M.; Stojan, J.; Sussman, J. L.; Zaccai, G.; Silman, I. and Weik, M. (2006) Structural insights into substrate traffic and inhibition in acetylcholinesterase. *EMBO J.* 25, 2746-2756.

Dreher, M. R.; Liu, W.; Michelich, C. R.; Dewhirst, M. W.; Fan, Y. and Chilkoti, A. (2006) Tumor vascular permeability, accumulation, and penetration of macromolecular drug carriers. *J. Natl. Cancer Inst.* 98, 335-344.

Drummond, D. C.; Meyer, O.; Hong, K.; Kirpotin, D. B. and Papahadjopoulos, D. (1999) Optimizing liposomes for delivery of chemotherapeutic agents to solid tumors. *Pharmacol. Rev.* 51, 691-743

Edwards, K.; Johnsson, M.; Karlsson, G. and Silvander, M. (1997) Effect of polyethyleneglycol-phospholipids on aggregate structure in preparations of small unilamellar liposomes. *Biophys J.* 73, 258-266.

Ehelhaaf, S. U.; Schurtenberger, P. and Müller, M. (2000) New controlled environment vitrification system for cryo-transmission electron microscopy: design and application to surfactant solutions. *J. Microsc.* 200, 128-139.

Eliaz, R. E. and Szoka, F. C. Jr. (2001) Liposome-encapsulated doxorubicin targeted to CD44: a strategy to kill CD44-overexpressing tumor cells. *Cancer Res.* 61, 2592-2601.

Ellman, G. L.; Courtney, K. D.; Andres, V. Jr. and Featherstone, R. M. (1961) A new and rapid colorimetric determination of acetylcholinesterase activity. *Biochem. Pharmacol.* 7, 88-95.

Endres, F. (2002) Ionic liquids: Solvents for the electrodeposition of metals and semiconductors. *ChemPhysChem* 3, 144-154.

Epand, R. M. and Hui, S.-W. (1986) Effect of electrostatic repulsion on the morphology and thermotropic transitions of anionic phospholipids. *FEBS Lett.* 209, 257-260.

Ermakov, Y. A. (1990) The determination of binding site density and association constants for monovalent cation adsorption onto liposomes made from mixtures of zwitterionic and charged lipids. *Biochim. Biophys. Acta* 1023, 91-97.

Fatourus, D. G.; Klepetsanisa, P.; Ioannou, P. V. and Antimisiaris, S. G. (2005) The effect of pH on the electrophoretic behavior of a new class of liposomes: arsonoliposomes. *Int. J. Pharm.* 288, 151-156.

Feakes, D. A.; Spinier, J. K. and Harris, F. R. (1999) Synthesis of boron-containing cholesterol derivatives for incorporation into unilamellar liposomes and evaluation as potential agents for BNCT. *Tetrahedron* 55, 11177-11186.

Fronczek, F. R. and Vicente, M. G. H. (2005) Synthesis and cellular studies of an octa-anionic 5,10,15,20-tetra[3,5(*nido*-carboranyl-methyl)-phenyl]porphyrin (H_2OCP) for application in BNCT. *Bioorg. Med. Chem.* 13, 1633-1640.

Gabel, D.; Moller, D.; Harfst, S.; Rösler, J. and Hetz, H. (1993) Synthesis of S-alkyl and S-acyl derivatives of mercaptoundecahydrododecaborate, a possible boron carrier for neutron capture therapy. *Inorg. Chem.* 32, 2276-2278.

Gabel, D. (1997) Bor-Neutroneneinfangtherapie von Tumoren. *Chem. unserer Zeit* 5, 235-240.

Gabel, D.; Awad, D.; Schaffran, T.; Radovan, D.; Daraban, D.; Damian, L.; Winterhalter, M.; Karlsson, G. and Edwards, K. (2007) The anionic boron cluster $(B_{12}H_{11}SH)^{2-}$ as a means to trigger release of liposome contents. *ChemMedChem* 2, 51-53.

Gabizon, A. and Papahadjopoulos, D. (1988) Liposome formulations woth prolonged circulation time in blood and enhanced uptake by tumors. *Proc. Natl. Acad. Sci. USA* 85, 6949-6953.

Gabizon, A.; Horowitz, A. T.; Goren, D.; Tzemach, D.; Shmeeda, H. and Zalipsky, S. (2003) In vivo fate of folate-targeted polyethylene-glycol liposomes in tumor-bearing mice. *Clin. Cancer Res.* 9, 6551-6559.

Garidel, P.; Howe, J.; Milkereit, G.; Rössle, M.; Linser, S.; Gerber, S.; Willumeit, R.; Gutsmann, T.; Vill, V. and Brandenburg, K. (2008) Structural polymorphism of hydrated ether-linked dimyristyl maltoside and melibioside. *Chem. Phys. Lipids* 151, 18-29.

Goňi, F. M.; Urbaneja, M.-A.; Arrondo, J. L. R.; Alonso, A.; Durrani, A. A. and Chapman, D. (1986) The interaction of phosphatidylcholine bilayers with Triton X-100. *Eur. J. Biochem*. 160, 659-665.

Harel, M.; Schalk, I.; Ehret-Sabatier, L.; Bouet, F.; Goeldner, M.; Hirth, C.; Axelsen, P. H.; Silman, I. and Sussman, J. L. (1993) Quaternary ligand binding to aromatic residues in the active-site gorge of acetylcholinesterase. *Proc. Natl. Acad. Sci. USA.* 90, 9031-9035.

Hashizaki, K.; Taguchi, H.; Itoh, C.; Sakai, H.; Abe, M.; Saito, Y. and Ogawa, N. (2003) Effects of poly(ethylene glycol) (PEG) chain length of PEG-lipid on the permeability of liposomal bilayer membranes. *Chem. Pharm. Bull.* 51, 815-820.

Hawthorne, M. F. and Lee, M. W. (2003) A critical assessment of boron target compounds for boron neutron capture therapy. *J neurooncol.* 62, 33-45.

Hawthorne, M. F. (1993) The role of chemistry in the developement of boron neutron capture therapy of cancer. *Angew. Chem. Int. Ed. Engl.* 32, 950-984.

Heerklotz, H. (2008) Interactions of surfactants with lipid membranes. *Q. Rev. Biophys.* 41, 205-264.

Hertler, W. R. and Raasch, M. S. (1964) Chemistry of boranes. XIV. Amination of $B_{10}H_{10}^{2-}$ and $B_{12}H_{12}^{2-}$ with hydroxylamine-O-sulfonic acid. *J. Am. Chem. Soc.* 86, 3661-3668.

Holleman, A. F. and Wiberg, N. (1995) „Lehrbuch der anorganischen Chemie“ 101. verb. und erw. Auflage, *Walter de Gruyter.*

Hope, M. J., Bally, M. B., Webb, G. and Cullis, P. R. (1985) Production of large unimellar vesicles by a rapid extrusion procedure. Characterization of size distribution, trapped volume and ability to maintain a membrane potential. *Biochim. Biophys. Acta.* 812, 55-65.

Hoving, S.; Seynhaeve, A. L. B.; van Tiel, S. T.; aan de Wiel-Ambagtsheer, G.; de Bruijn, E. A.; Eggermont, A. M. M. and ten Hagen, T. L. M. (2006) Early destruction of tumor vasculature in tumor necrosis factor-[alpha]-based isolated limb perfusion is responsible for tumor response. *Anti-Cancer Drugs* 17, 949-959.

Hurley, F. H. and Wier, T. P. Jr. (1951) The electrodeposition of aluminum from nonaqueous solutions at room temperature. *J. Electrochem. Soc.* 98, 207-212.

Ishida, O.; Maruyama, K.; Tanahashi, K.; Iwatsuru, M.; Sasaki, K.; Eriguchi, M. and Yanagie, M. (2001) Liposomes bearing polyethyleneglycol-coupled transferrin with intracellular targeting property to the solid tumors *in vivo. Pharm. Res.* 18, 1042-1048.

Ito, Y.; Abril, E. R.; Bethea, N. W., McCuskey, M. K.; Cover, C.; Jaeschke, H. and McCuskey, R. S. (2006) Mechanisms and pathophysiological implications of sinusoidal endothelial cell gap formation following treatment with galactosamine/endotoxin in mice. *Am. J. Physiol. Gastrointest. Liver Physiol.* 291, 211-218.

Ji, B.; Peacock, G. and Lu, D. R. (2002) Synthesis of cholesterol-carborane conjugate for targeted drug delivery. *Bioorg. Med. Chem. Lett.* 12, 2455-2458.

Johnsson, M. and Edwards, K. (2003) Liposomes, disks, and spherical micelles: aggregate structure in mixtures of gel phase phosphatidylcholines and poly(ethylene glycol)-phospholipids. *Biophys J.* 85, 3839-3847.

Jones, M. (1995) The surface properties of phospholipid liposome systems and their characterization. *Adv. Colloid Interface Sci.* 54, 93-128.

Justus, E., Rischka, K., Wishart, J. F., Werner, K. and Gabel, D. (2008) Trialkylammoniododecaborates: Anions for ionic liquids with potassium, lithium and protons as cations. *Chem. Eur. J.* 14, 1918-1923.

Justus, E.; Awad, D.; Hohnholt, M.; Schaffran, T.; Edwards, K.; Karlsson, G.; Damian, L. and Gabel, D. (2007) Synthesis, liposomal preparation, and *in vitro* toxicity of two novel dodecaborate cluster lipids for boron neutron capture therapy. *Bioconjugate Chem.* 18, 1287-1293.

Justus, E.; Vöge, A. and Gabel D. (2008) *N*-Alkylation of ammonioundecahydro-*closo*-dodecaborate(1-) for the preparation of Anions for ionic liquids. *Eur. J. Inorg. Chem.* 33, 5245-5250.

Kahl, S. B. and Koo, M.-S. (1990) Synthesis of tetrakis-carborane-carboxylate esters of 2,4-bis-(a,β-dihydroxyethyl)-deuteroporphyrin IX. *J. Chem. Soc., Chem. Commun.,* 1769-1771.

King, R. B. (2001) Three-Dimensional Aromaticity in Polyhedral Boranes and Related Molecules. *Chem. Rev.* 101, 1119-1152.

Koryakin, S. N. (2006) Molecular-biological problems of drug design and mechanism of drug action. *Pharm. Chem. J.* 40, 583-587.

Larsen, A. S.; Holbrey, J. D.; Tham, F. S. and Reed, C. A. (2000) Designing ionic liquids: Imidazolium melts with inert carborane anions. *J. Am. Chem. Soc.* 122, 7264-7272.

Lee, J-D.; Ueno, M.; Miyajima, Y. and Nakamura, H. (2006) Synthesis of boron cluster lipids: *closo*-dodecaborate as an alternatve hydrophilic function of boronated liposomes for neutron capture therapy. *Organic Lett.* 9, 323-326.

Lehmler, H.-J. and Bummer, P. M. (2004) Mixing of perfluorinated carboxylic acids with dipalmitoylphosphatidylcholine. *Biochim. Biophys. Acta.* 1664, 141-149.

Lehmler, H.-J.; Xie, W.; Bothun, G. D.; Bummer, P. M. and Knutson, B. L. (2006) Mixing of perfluorooctanesulfonic acid (PFOS) potassium salt with dipalmitoyl phosphatidylcholine (DPPC). *Colloids Surf. B*, 51, 25-29.

Lemmen, P.; Weißfloch, L.; Auberger, T. and Probst, T. (1995) Uptake and distribution of the boron-containing ether lipid B-Et-11-OMe in tumor-bearing mice. *Anticancer Drugs* 6, 744-748.

Letrou-Bonneval, E.*;* Chèver, R.; Lambert, O.; Costet, P.; André, C.; Tellier, C. and Pitard, B. (2008) Galactosylated multimodular lipoplexes for specific gene transfer into primary hepatocytes. *J. Gene Med.* 10, 1198-1209.

Li, T.; Hamdi, J. and Hawthorne, M. F. (2006) Unilamellar liposomes with enhanced boron content. *Bioconjugate Chem.* 17, 15-20.

Lipscomb, W. N. (1963) Boron Hydrides. *W. A. Benjamin Inc., New York.*

Lutz, S.; Neumann, M.; Bellmann, D. and Gabel, D. (2000) The interaction of $Na_2B_{12}H_{11}SH$ (BSH) with liposomes; relevance to cellular BSH uptake. *Program and abstracts 9th International Symposium on Neutron Capture Therapy*, p.p. 69-70.

Maruyama, K.; Ishida, O.; Kasaoka, S.; Takizawa, T.; Utoguchi, N.; Shinohara, A.; Chiba, M.; Kobayashi, H.; Eriguchi, M. and Yanagie, H. (2004) Intracellular targeting of sodium mercaptoundecahydrododecaborate (BSH) to solid tumors by transferrin-PEG liposomes, for boron neutron-capture therapy (BNCT). *J. Controlled Release* 98, 195-207.

Mayer, L. D.; Hope, M. J. and Cullis, P. R. (1986) Vesicles of variable sizes produced by a rapid extrusion procedure. *Biochim. Biophys. Acta.* 858, 161-168.

Mayer, L. D.; Hope, M. J.; Cullis, P. R. and Janoff, A. S. (1985) Solute distributions and trapping efficiencies observed in freeze-thawed multilamellar vesicles. *Biochim. Biophys. Acta.* 817, 193-196.

Mebel, A. M.; Najafian, K.; Charkin, O. P. and Schleyer, P. V. (1999) An ab initio study of protonation of $B_{12}H_{12}^{2-}$. Structure and non-rigidity of $B_{12}H_{13}^{-}$ and formation of $B_{12}H_{11}^{-}$ and B_{23}^{3-}. *THEOCHEM* 461, 187-202.

Mehta, S. C.; Lai, J. C. and Lu, D. R. (1996) Liposomal formulations containing sodium mercaptoundecahydrododecaborate (BSH) for boron neutron capture therapy. *J. Microencapsul.* 13, 269-279.

Müller, M.; Zschörnig, S.; Ohki, S. and Arnold, K. (2003) Fusion, leakage and surface hydrophobicity of vesicles containing phosphoinositides: Influence of steric and electrostatic effects. *J. Membrane Biol.* 192, 33-43.

Müller, M.; Zschörnig, O. and Arnold, K. (2005) Cation-induced membrane fusion detected by fluorescence spectroscopy (MF). *Biophysics internship, Medical physics & biophysics, University of Leipzig.* (http://www.uni-leipzig.de/~pwm/kas/praktikum/MF06.pdf)

Nakamura, H.; Lee, J.-D.; Ueno, M.; Miyajima, Y. and Ban, H. S. (2007) Synthesis of *closo*-dodecaboryl lipids and their liposomal lormation for boron neutron capture therapy. *Nanobiotechnol.* 3, 135-145.

Nakamura, H.; Miyajima, Y.; Takei, T.; Kasaoka, S. and Maruyama, K. (2004) Synthesis and vesicle formation of a *nido*-carborane cluster lipid for boron neutron capture therapy. *Chem. Commun*, 1910-1911.

Nakamura, H.; Ueno, M.; Lee, J.-D.; Ban, H.-S.; Justus, E.; Fan, P. and Gabel, D. (2007) Synthesis of dodecaborate-conjugated cholesterols for efficient boron delivery in neutron capture therapy. *Tetrahedron Lett.* 48, 3151-3154.

Neumann, M.; Kunz, U.; Lehmann, H. and Gabel, D. (2002) Determination of the subcellular distribution of mercaptoundecahydro-*closo*-dodecaborate (BSH) in human glioblastoma multiforme by electron microscopy. *J. Neuro-Oncol.* 57, 97-104.

Novick, S.; Quastel, M. R.; Marcus, S.; Chipman, D.; Shani, G.; Barth, R. F. and Soloway, A. H. (2002) Linkage of boronated polylysine to glycoside moieties of polyclonal antibody; Boronated antibodies as potential delivery agents for neutron capture therapy. *Nucl. Med. Biol.* 29, 159-167.

Nuccitelli, S.; Cerella, C.; Cordisco, S.; Albertini, M. C.; Accorsi, A.; De Nicola, M.; Radogna, F.; Magrini, A.; Bergamaschi, A. and Ghibelli, L. (2006) Hyperpolarization of plasma

membrane of tumor cells sensitive to antiapoptotic effects magentic fields. *Ann. New York Acad. Sci.* 1090, 217-225.

Osterloh, J. and Vicente, M. G. H. (2002) Mechanisms of porphyrinoid localization in tumors. *J. Porphyrins Phthalocyanines* 6, 305-324.

Otersen, B.; Haritz, D.; Grochulla, F.; Bergmann, M.; Sierralta, W. and Gabel, D. (1997) Binding and distribution of $Na_2B_{12}H_{11}SH$ on cellular and subcellular level in tumor tissue of glioma patients in boron neutron capture therapy. *J. neurooncol.* 33, 131-139.

Othman, A. (2008) Quantitative study of the cellular interactions of B-6-16 boron containing liposomes. *Master thesis*, University of Bremen.

Ott, D.; Hennig, J. and Ernst, T. (1993) Human brain tumors: assessment with in vivo proton MR spectroscopy. *Radiology* 186, 745-752.

Pan, X. Q.; Wang, H.; Shukla, S.; Sekido, M.; Adams, D. M.; Tjarks, W.; Barth, R. F. and Lee, R. J. (2002) Boron-containing folate receptor-targeted liposomes as potential delivery agents for neutron capture therapy. *Bioconjugate Chem.* 13, 435-442.

Park, J. W.; Hong, K.; Carter, P.; Asgari, H.; Guo, L. Y.; Keller, G. A.; Wirth, C.; Shalaby, R.; Kotts, C.; Wood, W. I.; Papahadjopoulos D. and Benz. C. (1995) Development of anti-p185HER2 immunoliposomes for cancer therapy. *Proc Natl. Acad. Sci. USA* 92, 1327-1331.

Paternostre, M.; Meyer, O.; Grabielle-Madelmont, C.; Lesieur, S.; Ghanam, M. and Ollivon, M. (1995) Partition coefficient of a surfactant between aggregates and solution: Application to the micelle-vesicle transition of egg phosphatidylcholine and octyl β-D-glucopyranoside. *Biophys. J.* 69, 2476-2488.

Peacock, G.; Sidwell, R.; Pan, G.; Øie, S. and Lu, D. R. (2004) In vitro uptake of a new cholesteryl carborane ester compound by human glioma cell lines. *J. Pharm. Sci.* 93, 13-19.

Peymann, T.; Lork, E. and Gabel, D. (1996) Hydroxoundecahydro-closo-dodecaborate (2-) as a nucleophile. Preparation and structural characterization of O-acyl derivatives of hydroxoundecahydro-closo-dodecaborate (2-). *Inorg. Chem.* 35, 1355-1360.

Peymann, T.; Kück, K. and Gabel, D. (1997) Ring opening of tetrahydropyran attached to undecahydro-*closo*-dodecaborate (1-) by nucleophilics. *Inorg. Chem.* 36, 5138-5139.

Pitochelli, R. A. and Hawthorne, F. M. (1960) The isolation of the icosahedral $B_{12}H_{12}^{2-}$ ion. *J. Am. Chem. Soc.* 82, 3228-3229.

Pope, C.; Karanth, S. and Liu, J. (2005) Pharmacology and toxicology of cholinesterase inhibitors: uses and misuses of a common mechanism of action. *Environ. Toxicol. Pharmacol.* 19, 433-446.

Ramírez, L. P.; Antonietti, M. and Landfester, K. (2006) Formation of novel layered nanostructures from lanthanide-complexes by secondary interactions with ligating monomers in miniemulsion droplets. *Macromol. Chem. Phys.* 207, 160-165.

Ranke, J.; Mölter, K.; Stock, F.; Bottin-Weber, U.; Poczobutt, J.; Hoffmann, J.; Ondruschka, B.; Filser, J. and Jastorff, B. (2004) Biological effects of imidazolium ionic liquids with varying chain lengths in acute *Vibrio fischeri* and WST-1 cell viability assays. *Ecotoxicol. Environ. Saf.* 58, 396-404.

Ranke, J.; Müller, A.; Bottin-Weber, U.; Stock, F.; Stolte, S.; Arning, J. and Jastorff, B. (2007) Lipophilicity parameters for ionic liquid cations and their correlation to in vitro cytotoxicity. *Ecotoxicol. Environ. Saf.* 67, 430-438.

Rex, S. (1996) Pore formation induced by the peptide melittin in different lipid vesicle membranes. *Biophys. Chem.* 58, 75-85.

Ronig, B., Pantenburg, I. and Wesemann, L. (2002) Meltable stannaborate salts. *Eur. J. Inorg. Chem.*, 319-322.

Rosenberg, J.; Düzgüneş, N. and Kayalar, Ç. (1983) Comparison of two liposome fusion assays monitoring the intermixing of aqueous contents and of membrane components. *Biochim. Biophys. Acta* 735, 173-180.

Sandra, A. and Pagano, R. E. (1979) Liposome-cell interactions. Studies of lipid transfer using isotopically asymmetric vesicles. *J. Biol. Chem.* 254, 2244-2249.

Schinazi, R. F. and Prusoff, W. H. (1985) Synthesis of 5-(dihydroxyboryl)-2´-deoxyuridine and related boron-containing pyrimidines. *J. Org. Chem.* 50, 841-847.

Schubert, R.; Beyer, K.; Wolburg, H. and Schmidt, K.-H. (1986) Structural changes in membranes of large unilamellar vesicles after binding of sodium cholate. *Biochemistry 25*, 5263-5269.

Schwarz, G.; Zong, R.-T. and Popescu, T. (1992) Kinetics of melittin induced pore formation in the membrane of lipid vesicles. *Biochim Biophys Acta.*, 1110, 97-104.

Semioshkin, A.; Nizhnik E.; Godovikov, I.; Starikova, Z. and Bregadze, V. (2007) Reactions of oxonium derivatives of $[B_{12}H_{12}]^{2-}$ with amines: Synthesis and structure of novel B12-based ammonium salts and amino acids. *J. Organomet. Chem.* 692, 4020-4028.

Semioshkin, A. A.; Sivaev, I. B. and Bregadze, V. I. (2008) Cyclic oxonium derivatives of polyhedral boron hydrides and their synthetic applications. *Dalton Trans.*, 977-992.

Sessa, G. and Weissmann, G. (1968) Phospholipid spherules (liposomes) as a model for biological membranes. *J. Lipid Res.* 9, 310-318.

Shaw, A. W.; McLean, M. A. and Sligar, S. G. (2004) Phospholipid phase transitions in homogenous nanometer scale bilayer discs. *FEBS Lett.* 556, 260-264.

Sheldon, R. (2001) Catalytic reactions in ionic liquids. *Chem. Commun*., 2399-2407.

Shelly, K.; Feakes, D. A.; Hawthorne, M. F.; Schmidt, P. G.; Kirsch, T. A. and Bauer, W. F. (1992) Model studies directed toward the boron neutron capture therapy of cancer: Boron delivery to murine tumors with liposomes. *Proc. Natl. Acad. Sci. USA* 89, 9039-9043.

Silvander, M. (2002) Steric stabilization of liposomes - a review. *Progr Colloid Polym Sci.* 120, 35-40.

Sivaev, I. B.; Kulikova, N. Y.; Nizhnik, E. A.; Vichuzhanin, M. V.; Starikova, Z. A.; Semioshkin, A. A. and Bregadze, V. I. (2008) Practical synthesis of 1,4-dioxane derivative of the *closo*-dodecaborate anion and its ring opening with acetylenic alkoxides. *J. Organomet. Chem.* 693, 519-525.

Sivaev, I. B.; Semioshkin, A. A.; Brellochs, B.; Sjöberg, S. and Bregadze, V. I. (2000) Synthesis of oxonium derivatives of the dodecahydro-*closo*-dodecaborate anion $[B_{12}H_{12}]^{2-}$. Tetramethylene oxonium derivative of $[B_{12}H_{12}]^{2-}$ as a convenient precursor for the synthesis of functional compounds for boron nutron captre therapy. *Polyhedron* 19, 627-632.

Soloway, A. H.; Tjarks, W.; Barnum, B. A.; Rong, F.-G.; Barth, R. F.; Codogni, I. M. and Wilson, J. G. (1998) The chemistry of neutron capture therapy. *Chem. Rev.* 98, 1515-1562.

Sriwongsitanont, S. and Ueno, M. (2002) Physicochemical properties of PEG-grafted liposomes. *Chem. Pharm. Bull.* 50, 1238-1244.

Stolte, S.; Matzhe, M.; Arning, J.; Böschen, A.; Pitner, W.-R.; Welz-Biermann, U.; Jastorff, B. and Ranke, J. (2007) Effects of different head groups and functionalised side chains on the aquatic toxicity of ionic liquids. *Green Chem.* 9, 1170-1179.

Sudhölter, E. J. R.; Engberts, J. B. F. N. and de Jeu, W. H. (1982) Thermotropic liquid-crystalline behavior of some single- and double chained pyridinium amphiphiles. *J. Phys. Chem.* 86, 1908-1913.

Sussman, J. L.; Harel, M.; Frolow, F.; Oefner, C.; Goldman, A.; Toker, L. and Silman, I. (1991) Atomic structure of acetylcholinesterase from torpedo cal fornica: A prototypic acetylcholine-binding protein. *Science* 253, 872-879.

Szöllőssi, J.; Nagy, P.; Sebestyén, Z.; Damjanovich, S.; Park, J. W. and Mátyus, L. (2002) Applications of fluorescence resonance energy transfer for mapping biological membranes. *Rev. Mol. Biotechnol.* 82, 215-266.

Tang, W.; Liu, Q.; Wang, X; Mi, N.; Wang, P. and Zhang, J. (2008) Membrane fluidity altering and enzyme inactivating in sarcoma 180 cells post the exposure to sonoactivated hematoporphyrin *in vitro*. *Ultrasonics* 48, 66-73.

Thirumamagal, B. T. S.; Zhao, X. B.; Bandyopadhyaya, A. K.; Narayanasamy, S.; Johnsamuel, J.; Tiwari, R.; Golightly, D. W.; Patel, V.; Jehning, B. T.; Backer, M. V.; Barth, R. F.; Lee, R. J.; Backer, J. M. and Tjarks, W. (2006) Receptor-targeted liposomal delivery of boron-containing cholesterol mimics for boron neutron capture therapy (BNCT). *Bioconjugate Chem*. 17, 1141-1150.

Torchilin, V. and Weissig, V. (2003) Liposomes: a practical approach. 2. Auflage, *Oxford University Press.*

Uhlrich, A. S. (2002) Biophysical aspects of using liposomes as delivery vehicles. *Biosci. Rep.* 22, 129-147.

Vicente, M. G. H.; Wickramasighe, A.; Nurco, D. J.; Wang, H. J. H.; Nawrocky, M. M.; Makar, M. S. and Miura, M. (2003) Syntheses, toxicity and biodistribution of two 5,15-di[3,5-(*nido*carboranylmethyl)phenyl]porphyrin in EMT-6 tumor bearing mice. *Bioorg. Med. Chem.* 11, 3101-3108.

Voet, D.; Voet, J. G. and Pratt, C. W. (2002) Lehrbuch der Biochemie. *Wiley-VCH*

Wasserscheid, P. and Keim, W. (2000) Ionische Flüssigkeiten – neue „Lösungen“ für die Übergangmetallkatalyse. *Angew. Chem.* 112, 3926-3945

Welton, T. (1999) Room-temperature ionic liquids. Solvents for synthesis and catalysis. *Chem Rev*. 99, 2071-2084.

Wu, G.; Barth, R. F.; Yang, W.; Chatterjee, M.; Tjarks, W.; Cielsielski, M. J. and Fenstermaker, R. A. (2004) Site-specific conjugation of boron containing dendrimers of anti-EGF receptor monoclonal antibody cetuximab (IMC-C225) and its evaluation as a potential delivery agent for neutron capture therapy. *Bioconjugate Chem.* 15, 185-194.

Young, D. C., Howe, D. V. and Hawthorne, M. F. (1969) Ligand derivatives of (3)-1,2-dicarbadodecahydroundecaborate(-1). *J. Am. Chem. Soc.* 91, 859-862.

Zhou, R.; Mazurchuk, R. and Straubinger, R. M. (2006) Antivasculature effects of doxorubicin-containing liposomes in an intracranial rat brain tumor model. *Cancer Res.* 62, 2561-2566.

Zhu, Y.; Ching, C.; Carpenter, K.; Xu, R.; Selvaratnam, S.; Hosmane, N. S. and Maguire, J. A. (2003) Synthesis of the novel ionic liquid [*N*-pentylpyridinium]$^+$ [*closo*-$CB_{11}H_{12}$]$^-$ and its usage as a reaction medium in catalytic dehalogenation of aromatic halides. *Appl. Organometal. Chem.* 17, 346-350.

8. Appendices

I

Toxicity of *N,N,N*-trialkylammoniododecaborates as new anions of ionic liquids in cellular, liposomal and enzymatic test systems

in press by Green Chemistry

Toxicity of *N,N,N*-trialkylammoniododecaborates as new anions of ionic liquids in cellular, liposomal and enzymatic test systems

Tanja Schaffran[a], Eugen Justus[a], Maike Elfert[a], Tina Chen[a], Detlef Gabel[a]

[a]Department of Chemistry, University of Bremen, D-28357 Bremen, Germany

Graphical abstract:

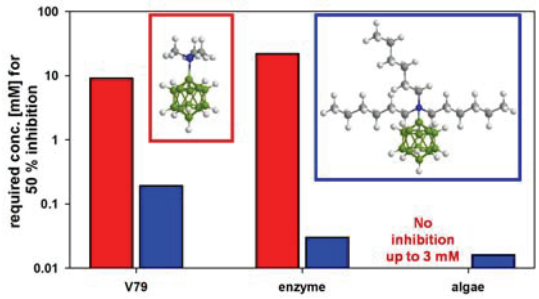

N,N,N-trialkylammoniododecaborates, anions of a new class of ionic liquids, were tested for their hazard potential in various biological test systems. The data demonstrate that increasing hydrophobicity leads to higher toxicity for straight alkyl chains. Compared to commonly used ILs this new class has a comparable toxicity in biological systems and carries no more risks than the established ones.

Summary

Representatives of *N,N,N*-trialkylammoniododecaborates, which are anions in a new class of ionic liquids, were tested for their hazard potential. As biological test systems, toxicity against V79 mammalian cells, reproduction inhibition of *Scenedesmus vacuolatus* algae, and inhibition of acetylcholineesterase were studied. EC_{50} values for the toxicity against V79 cells range between 9.1 mM for the trimethylammonio derivative and 0.19 mM for the trihexyl derivative. Reproduction inhibition of *S. vacuolatus* range between over 3 mM for the trimethylammonio derivative down to 0.016 mM for the trihexyl derivative. Fifty percent inhibition of acetylcholinesterase was caused by 21.9 mM of the trimethylammonio derivative, as compared to 0.03 mM for the hexyl derivative The data demonstrate that increasing hydrophobicity leads to higher toxicity and inhibition for straight alkyl chains. All tested ABs are able to induce leakage in liposomes and the capability for triggering strongly increases with the length of the alkyl chain and consequently with lipophilicity. The leakage experiments could be an indicator for toxic tendencies *in vitro* but they allow no quantitative prediction of EC_{50} values. For branched chains and for derivatives with mixed substitution a prediction of the toxic potential is not simple. The new class of ionic liquids is in general no more toxic than the ionic liquids presently in industrial applications.

Introduction

Research of ionic liquids (ILs) is one of the most rapidly growing fields in the last years. ILs are salts with melting points below 100°C. Their properties differ from those of molecular solvents. They have very low vapor pressure, are not flammable, have high electric conductivity, show tolerance to strong acids and have high thermal and chemical stability. They are also able to solubilize different materials.[1-2] Various

applications for ILs are noted as e.g. solvents, chemical catalysts, biocatalysts or in electrochemistry.[3-6]

The most established ILs consist of a simple anion (chloride, tetrafluoroborate, hexafluorophosphate) and a cation of one of the following classes: tetraalkylammonium, tetraalkylphosphonium, *N*-alkylpyridinium, *N*-methyl-*N'*-alkylimidazolium. Uncommon ILs are e.g. meltable stannaborate salts[7] or alkylpyridinium combined with carborane anions.[8]

Recently we published a new kind of ionic liquids.[1] In Fig. 1 the *N,N,N*-trialkylammonioundecahydrododecaborates (1-) are shown: they consist of the dodecaborate cluster substituted with one *N*-trialkylated ammonium group. We investigated derivatives with three identical alkyl chains from methyl to hexyl and one derivative with an asymmetric substitution (two ethyl chains and one benzyl group). Depending on the cation, these compounds have melting points below 100°C, and some are liquid at room temperature. We prepared the *N,N,N*-trialkylammonioundecahydrododecaborates (1-) with a wide range of cations. Interestingly the potassium and lithium salts give also ionic liquids.

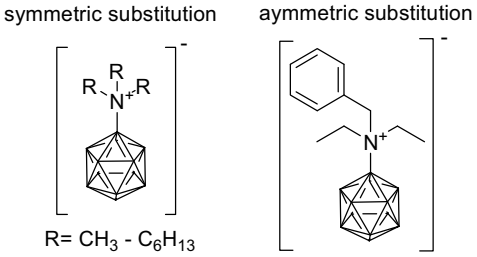

Fig. 1: *N,N,N*-trialkylammonioundecahydrododecaborates (-)

These ILs exhibit high chemical and physical stability and thus are attractive for different applications. They are the first example of a non-corrosive IL with lithium as cation, and might therefore be used as electrolyte in lithium batteries. With the new European legislation on chemicals REACH (registration, evaluation, authorization and restriction of chemicals), the knowledge about toxicological risk potentials of chemicals for organism, plants and environment increases in importance. Before technical applications can be started, the hazards should be identified.

In this study, we tested the potassium salts of the trialkylammonio derivatives of the recently discovered ILs in various biological test systems. We determined the cytotoxicity of these compounds for one animal cell line, for estimating the effect on Man and animals. In order to assess possible risks for the aquatic environment, we also studied the influence of the ILs on the limnic green algae *Scenedesmus vacuolatus*. Inhibition of acetylcholinesterase (AChE) as an enzyme found in all higher organisms was also investigated. An inhibition of this enzyme leads to disorders in the neuronal system such as heart diseases (influence of the cardiac response to vagal innervation) and myasthenia.[9-10]

In order to approach possible mechanisms of the toxic actions on cells, we investigated the action of the ILs on several simpler models. Liposomes were used as a model for cell membranes.[11]

We measured the octanol/water partition coefficient (Kow), which is the most commonly used parameter to determine the hydrophilic or lipophilic behaviors of a

substance,[12] in order to investigate how well a simple physical-chemical parameter could be used as predictor for toxic action.

The following ILs were used (with their abbreviations in parentheses): *N,N,N*-trimethylammonio-undecahydro-*closo*-dodecaborate (-) (MeAB), *N,N,N*-triethylammonio-undecahydro-*closo*-dodecaborate (-) (EtAB), *N,N,N*-tripropylammonio-undecahydro-*closo*-dodecaborate (-) (PrAB), *N,N,N*-tributylammonio-undecahydro-*closo*-dodecaborate (-) (BuAB), *N,N,N*-triisopentylammonio-undecahydro-*closo*-dodecaborate (-) (iPnAB), *N,N,N*-trihexylammonio-undecahydro-*closo*-dodecaborate (-) (HxAB), *N,N*-diethyl-*N*-benzylammonio-undecahydro-*closo*-dodecaborate (-) (Et2BnAB).

Results

The results of all measurements performed are found in Table 1. In the following, we present and comment these results in detail for each type of assay.

Table 1: Octanol/water partition coefficients EC_{50} values in V79 cells and in *S. vacuolatus* algae, and IC_{50} values for AChE for the compounds tested

compound	**Kow**	**log EC_{50} ± SD**	**EC_{50} [mM]**	**log EC_{50} ± SD**	**EC_{50} [mM]**	**log IC_{50} ± SD**	**IC_{50} [mM]**
test system		V79	V79	algae	algae	AChE	AChE
MeAB	0.04 ± 0.00	0.96 ± 0.01	9.1	no inhibition at 3 mM	-	1.34 ± 0.02	21.9
EtAB	0.33 ± 0.03	0.22 ± 0.06	1.66	no inhibition at 3 mM	-	0.99 ± 0.03	9.77
PrAB	1.84 ± 0.09	-0.32 ± 0.01	0.48	0.27 ± 0.04	1.86	0.31 ± 0.01	2.04
BuAB	3.04 ± 0.17	-0.51 ± 0.08	0.31	-0.23 ± 0.07	0.59	-0.29 ± 0.02	0.51
HxAB	4.73 ± 0.31	-0.72 ± 0.01	0.19	-1.79 ± 0.03	0.016	-1.49 ± 0.023	0.0325
iPnAB	4.03 ± 0.03	-0.61 ± 0.02	0.25	0.14 ± 0.15	1.4	-1.05 ± 0.01	0.089
Et2BnAB	0.58 ± 0.02	-0.14 ± 0.01	0.72	0.1 ± 0.1	1.33	0.102 ± 0.010	1.26

Octanol-water partition coefficient

We determined the octanol/water partition coefficient Kow as a parameter for lipophilicity. The results are shown in Table 1, column 2.

Lipophilicity of the compounds increases from MeAB to HxAB as expected. The MeAB derivative has a small partition coefficient of 0.04 and distributes almost exclusively into the water phase, compared to the HxAB derivative with a value of 4.73, which is found mostly in the octanol phase. The substances from PrAB to HxAB form white interphases between water and octanol, therefore neither water nor octanol appear to be the optimal solvents for these compounds. iPnAB with its branched alkyl chains follows the common trend and its Kow value lays between BuAB and HxAB. The asymmetric substituted Et2BnAB exhibits lipophilicity between that of EtAB and PrAB.

Ammonioundecahydrododecaborate $B_{12}H_{12}NH_3$(1-) (B12NH3) which is identical in structure to the ILs tested, but is not alkylated, has a partition coefficient of 0.103± 0.032 and distributes also predominantly into the water phase. It has a slightly higher solubility in octanol than the trimethylated derivative MeAB.

Cytotoxicity in V79 cells

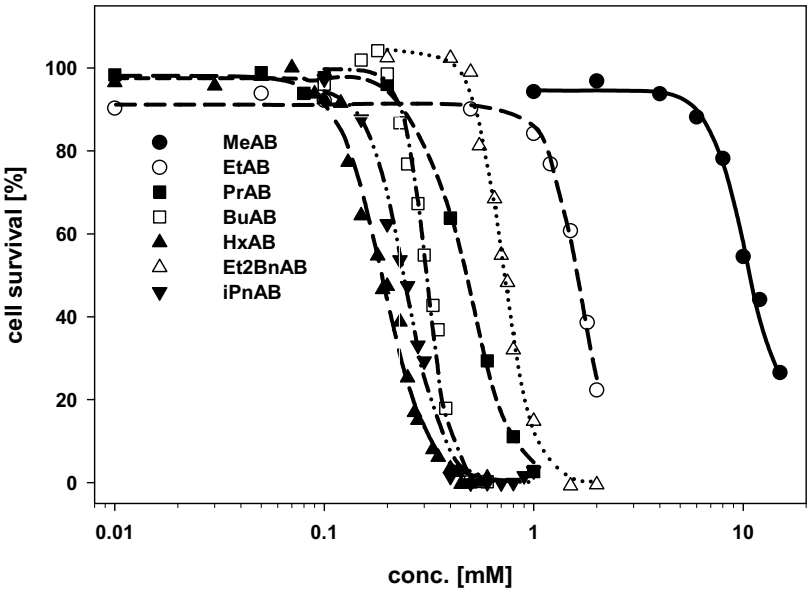

Fig. 2: Toxicity in V79 cells for *N,N,N*-trialkylammonioundecahydrododecaborates (1-) with alkyl chains. The points are the measured values and the lines are the curves fitted with equation 2.

As can be seen from Fig. 2, the cytotoxicity for V79 cells increases with longer alkyl chain length. IC_{50} values range from 9.1 mM for MeAB to 0.19 mM for HxAB. The asymmetrically substituted derivative Et2BnAB has a toxic potential between the EtAB and PrAB derivatives. All IC_{50} values are shown in Table 1.

B12NH3 was also tested and found to have an IC_{50} value of 45 mM. Thus the structure of the ammoniododecaborate alone is not very toxic in itself, and it seems that the alkyl chains are responsible for the toxicity increase.

In Figure 3 we compare the toxicity against V79 cells with the Kow partition coefficient. We observe the general trend that increasing lipophilicity (as measured by the Kow value) leads to increasing toxicity. The correlation is not, however, linear; only when plotted in a log-log plot, a regression line with a slope of –0.77 is obtained.

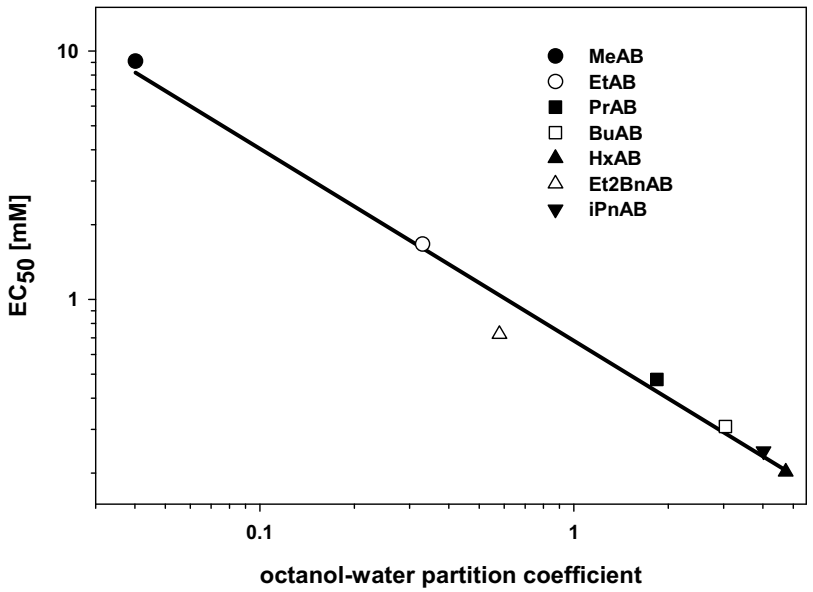

Fig. 3: Correlation between lipophilicity (log Kow) and cytotoxicity in V79 cells (log EC_{50}). The regression line shown has a slope of -0.77 (r^2 =0.98).

Leakage

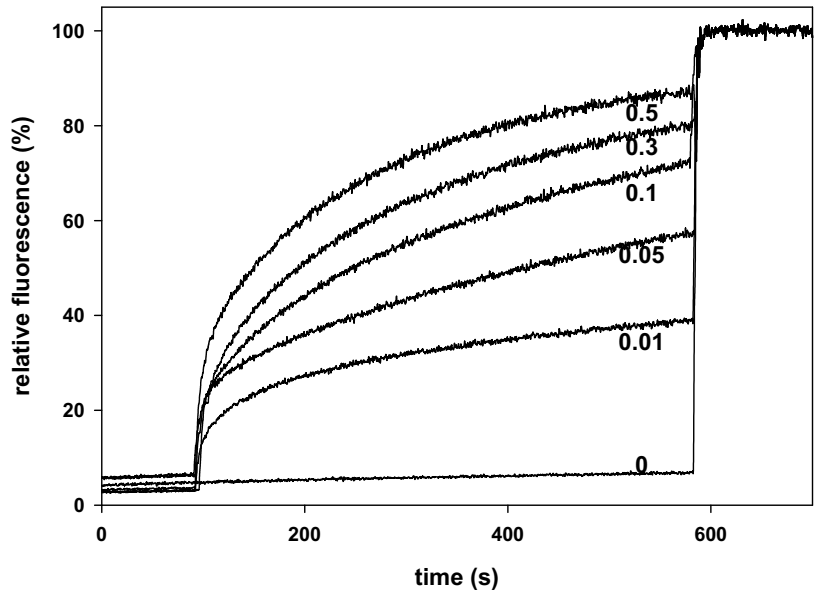

Fig. 4: Leakage of CF triggered by BuAB derivative at 37 °C. Lines from bottom are for 0, 0.01, 0.05, 0.1, 0.3 and 0.5 mM, respectively.

All trialkylammonio derivatives are able to induce release of liposome contents, in contrast to the unsubstituted B12NH3. In Fig. 4, the results for the leakage induced by the BuAB derivative at different concentrations are shown as representative for the different compounds.

The velocity of the leakage depends on the dose of the IL. After addition of 0.5 mM BuAB, the release is nearly complete after 580 seconds, while with 0.01 mM, only 38% is set free in this time period.

After addition of the compound, the initial release of liposomal content is very fast and then slows down. Leakage does not follow simple first order kinetics. At small concentrations of BuAB of around 0.01 mM, the kinetics appears to be biphasic, with the emergence of transient holes which lead to the observed rapid leakage in the first 20-30 seconds. Leakage has been observed for high concentrations of *N*-methyl-*N'*-alkylimidazolium salts, but only at very much higher concentrations of around 100 mM.[13] Also there, more complex kinetic behavior was found.

The concentrations required to induce around 80% leakage after 8 minutes decrease with increasing hydrophobicity, from 10 mM for MeAB, and 0.5 mM for BuAB, to 0.05 mM for HxAB. The data demonstrate that the capability to induce leakage strongly increases with the length of the alkyl chain. In contrast, BNH_3 without any alkyl chains is not able to induce leakage even at 100 mM. iPnAB requires more than ten times higher concentrations for 80 % leakage than HxAB, and also more than BuAB, indicating that additional factors, such as steric effects, might be required to explain the action of compounds with iso-alkyl chains. A leakage of 80 % is obtained with 5mM Et2BnAB which is expected on the basis of its Kow value.

AChE inhibition

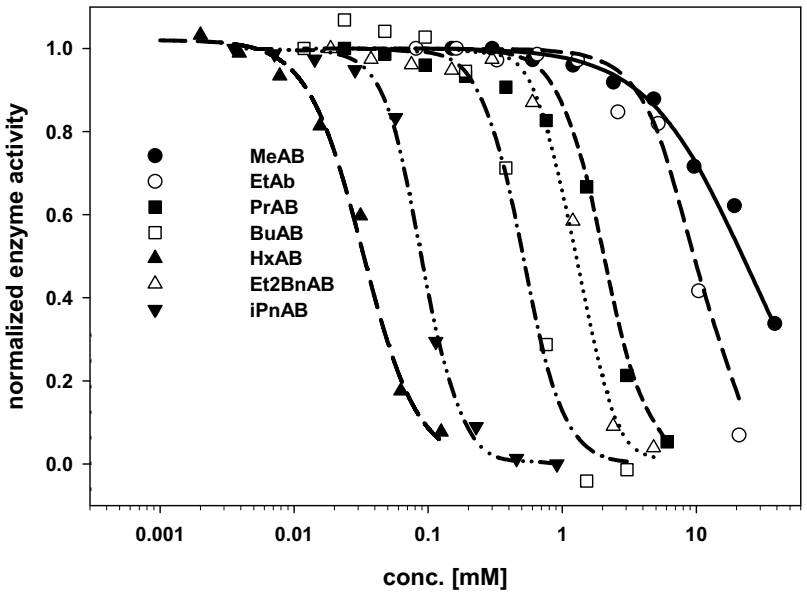

Fig.5: Response curves for AChE inhibition for the tested compounds. Curves were fitted with equation 2.

The compounds inhibit the enzyme AChE. The measured enzyme activities and curves fitted to the measurements are shown in Fig. 5 and the IC_{50} values are presented in Table 1. The enzyme inhibition increases with increasing alkyl chain length. The MeAB derivative inhibits to 50 % at a concentration of 21.9 mM; in comparison only 32.5 µM of HxAB are required for 50 % inhibition. Interestingly, Et2BnAB inhibits more than PrAB, which is unexpected from its position in the Kow values, and from its effect on V79 cells.

In Fig. 6, we compared the Kow value with the IC_{50} value for enzyme inhibition. Although there is a trend for increasing enzyme inhibition with increasing Kow values,

this relation is not simple. With longer alkyl chains, the inhibitory power increases much more than the lipophilicity. Et2BnAB does not fit into this trend; its enzyme inhibitory power is larger than expected from its Kow value.

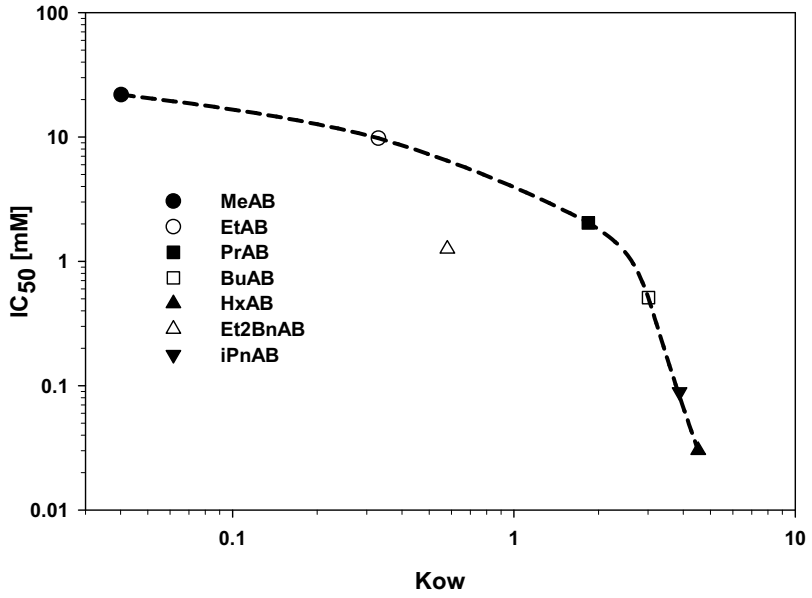

Fig. 6: Correlation between (log Kow) and (log IC_{50}) for enzyme inhibition. The dashed line is only intended as guide to the eye.

Reproduction inhibition of *S. vacuolatus*

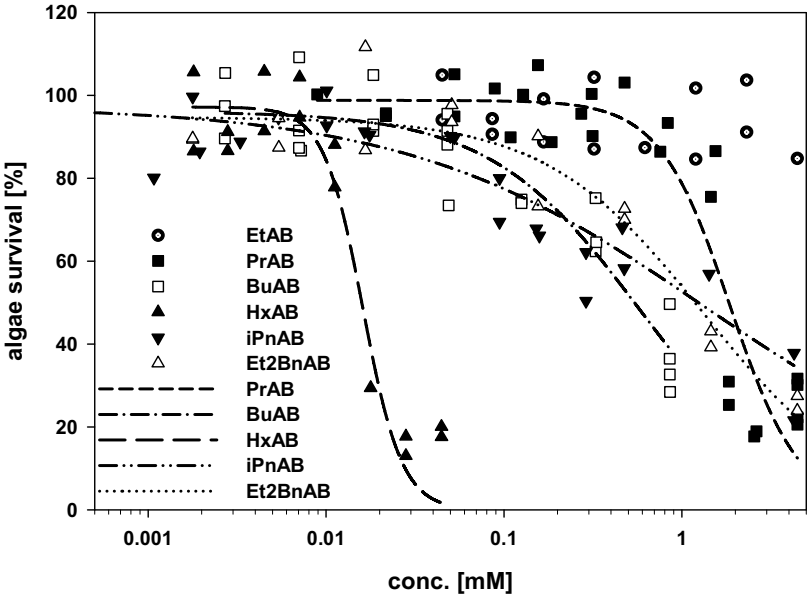

Fig. 7: Reproduction inhibition of *S. vacuolatus* in the presence of EtAB, PrAB, BuAB, HxAB, iPnAB and Et2BnAB. The lines are the curves fitted with equation 2. The squared correlation coefficient r^2 are 0.88 for PrAB and BuAB, 0.93 for HxAB, 0.81 for iPnAB and 0.93 for Et2BnAB. The hollow circles are the data points for EtAB, for which no line is shown.

MeAB and EtAB have no inhibitory effect on the algae reproduction up to a concentration of 3 mM. In Fig. 7, the individual data from EtAB are shown as one representative; those of MeAB are similar, but are omitted for clarity. When replacing one ethyl group by a benzyl group to Et2BnAB, 50% inhibition is observed at 1.33 mM. As can be seen in Fig. 7, PrAB inhibits the reproduction by 50 % at a concentration of 1.86 mM. BuAB and HxAB are more effective, and 16 µM of HxAB leads to 50 % reproduction inhibition. iPnAB with branched chains shows again lower inhibition effect than BuAB with n-alkane chains.

The data demonstrate that the inhibition increases with increasing lipophilicity of the compounds containing straight alkyl chains. This common trend is observed for toxicity and enzyme inhibition as well, although the quantitative dependence differs between the test systems.

Discussion

Several recent studies deal with cytotoxic effects of ILs. Kumar et al. (2008)[14] have looked at a few examples each of pyrrolidinium, piperidinium, and pyridinium ILs. In mammalian cells, they found that toxicity increased with increasing alkyl chain length, but toxicity was also influenced by the anion present. Cho et al. (2007)[15] found the same tendency on phytoplancton for the four alkylmethylimidazolium ILs investigated. Ranke (2007)[16] has assessed the hydrophobicity of a great number of representatives from different classes of ILs by chromatography. They found a general correlation between the degree of hydrophobicity, as measured by chromatography, with toxicity against a mammalian cell line.

In general, we found that the concentrations of the ABs required to effect mammalian cells, algae, AChE, and liposomes decreased with increasing octanol/water partition coefficient Kow. Thus, our study falls qualitatively in line with data from the literature, despite the fact that we have investigated anions of different hydrophobicity, whereas the ILs referenced above all have cations of different hydrophobicity.

We found that the Kow value had the best predictive power for toxicity on V79 cells. In general, increasing hydrophobicity leads to increased toxicity in V79 cells, in about the same way as observed by Ranke (2007)[16] for other mammalian cells. Plotting log EC_{50} values versus log Kow a linear correlation is obtained similar as by Ranke (2007)[16].

For the other test systems used, an equally good quantitative prediction as for the effect on V79 cells is not possible. For acetylcholinesterase, the lipophilicity/toxicity correlation is not linear, which in contrast to the relationship found by Arning (2008)[17]. The correlation in our case is more complex, and extrapolation to longer alkyl chains is difficult.

For algae, a definite predictive relationship cannot be established; for this, more data points for longer alkyl chains are necessary. Stolte (2007)[18] has found a good correlation between hydrophobicity and effect, but they investigated only straight-chain ILs of a different structure.

In our investigation, the effects of two compounds, iPnAB and Et2BnAB, were more difficult to predict from their Kow values. iPnAB has three identical, but branched alkyl chains, and Et2BnAB has two different side chains, one of which being aromatic. A number of additional compounds, in which the substituents should be varied in a

more systematic and comprehensive way, would have to be investigated before any general conclusions about asymmetrically or branched side chains can be drawn.

The influence of some ILs on aquatic organisms has been reviewed by Kulacki et al. (2007).[19] Data for various algae (*Oocystis submarina*, *Cyclotella meneghiniana, Pseudokirchneriella subcapitata)* have been presented by Latala *et al*. (2005)[20] and Wells *et al*. (2006)[21], and for the algae *S. vacuolatus,* by Matzke *et al.* (2007)[22] and Stolte *et al.* (2007)[18]. The response of the algae, when exposured to ionic liquids, is slightly different depending on the species; this has been attributed to differences in the cell wall composition. For imidazolium salts (side chain: ethyl to octadecyl) the observed EC_{50} values range from micromolar to nanomolar depending on the side chain; longer alkyl side chains lead to higher lipophilicity and concomitantly higher toxicity. When compared to the imidazolium salts, the ABs with short chains are less toxic, the first substance for which toxicity in the micromolar concentration range is found is BuAB.

The correlation between toxicity in V79 cells and in *S. vacuolatus* is poor. In the algae, the most hydrophobic HxAB is by far the most toxic of the compounds tested, being about 100 times more toxic than PrAB. In V79 cells, HxAB is only about 2.5 times more toxic than PrAB. For the same algae, a similar trend was observed for methylimidazolium ILs.[22] These differences might be a result of the different structures of mammalian and algal cells.

For moderately lipophilic ABs, we did not find marked enzyme inhibition. In contrast, the more lipophilic ABs iPnAB and HxAB were potent inhibitors. At a first glance, it is surprising that an anion should inhibit an enzyme whose regular substrate carries a positive charge. The enzyme has three distinct sites where molecular interactions can take place: the peripheral anionic site (PAS), a lipophilic channel located in the entrance of the gorge and the hydrolytic site as the active center.[23-24,17]

Arning (2008)[17] interpretated the enzyme inhibition by ILs with the (positively charged) imidazolium and pyridinium structures as electrostatic interactions between the positively charged cation with negatively charged amino acids in the PAS. The ABs investigated by us contain also a positively charged nitrogen which might interact with the PAS. In view of the negative net charge of the compounds, binding to the PAS might, however, be considered less probable. Also cation-π-interaction formed by the ILs and a tryptophane residue in the hydrolytic site might lead to inhibition.[17] This might, in principle, also be possible for the ABs. The third site of inhibition includes the channel of the narrow gorge, where hydrophobic interactions between the ILs and the amino acid residues lining the channel are important.[17] As the inhibitory power of the ABs increases with increasing n-alkyl chain length and accordingly increasing lipophilic properties, this kind of inhibition appears to be the most probable of the three possibilities mentioned here.

Liposomes have frequently been used as a model for cell membranes.[11] Disturbance of the liposome membrane or disordering of the bilayer lead to leakage of the liposomal content. This model can help to identify the cell membrane as one target of toxic interactions. We found that the addition of hydrophobic ABs leads to leakage of the liposome contents. The capability to induce leakage increases with the length of the alkyl chains and hence with lipophilicity. This qualitative tendency is in line with

the results we obtained for the other biological systems. A more thorough investigation of membrane defects through which leakage occurs, or a detailed analysis of the kinetics of leakage, such as described by Schubert (1986)[25], possibly together with molecular dynamics simulations, would be needed to fully understand the events on the liposomal membrane. Leakage of liposomal contents triggered by ILs has first been described by Evans (2006)[13], who investigated *N*-methyl-*N'*-alkylimidazolium cations. For methyl-*N'*-octylimidazolium chloride, around 100 mM were needed to induce 50 % leakage in liposomes after 250 sec. In contrast, *N*-methyl-*N'*-octylimidazolium chloride had an EC_{50} value of about 0.1 mM.[16] As pointed out by Evans (2006)[13], the possibility of micelle formation of the alkylimidazolium cations cannot be excluded at the high concentrations required for leakage, and thus, the effective compound concentration for leakage induction is not known. Smaller concentration as 100 mM had not been tested in the experiment. On the basis of the existing data, no correlation between toxicity and leakage exists for ILs containing imidazolium cations because relative higher concentrations are necessary to trigger leakage as for a toxic effect. Thus it seems that leakage effects play no major role in view of toxicity in cells in the case of imidazolium ILs.

For the similarly toxic HxAB (EC_{50} = 0.19 mM), concentrations of 0.05 mM, well below its EC_{50} value, are required for nearly complete leakage of the liposomal content within minutes. Therefore the leakage experiment does not allow a quantitative prediction of EC_{50} values for the V79 cells. In contrast to Evans (2006)[13], we found, however, that both leakage and toxicity increased with increasing lipophilicity. This might indicate that effects on the membrane might partially be responsible for toxic actions. Ranke (2007)[16] and Stolte (2007)[18] also explained the observed toxic effects in mammalian cells and algae by the assumption that the ILs adsorb or intercalate into the membrane resulting in membrane perturbation.

Conclusion

The ILs investigated here have toxicity values similar to those of other, more widespread ILs based on organic cations with simple inorganic anions. Trends can be seen insofar as more hydrophobic ILs tend to be more toxic. For safe handling of ILs of this class, the data presented here give hints about possible risks associated with manufacturing, use, and disposal.

Materials and Methods

Materials

DPPC was a gift from Lipoid, Ludwigshafen (Germany). CF was from Kodak. WST-1 dye was from Roche Diagnostics (Mannheim, Germany). Bovine serum albumin was from Sigma–Aldrich (Steinheim, Germany) and acetylthiocholine iodide from Fluka (Buchs, Switzerland). Acetylcholinesterase (AChE, EC 3.1.1.7) from the electric organ of the electric eel (*Electrophorus electricus*) type VI-S was purchased from Sigma–Aldrich (Steinheim, Germany). The activity was determined to be 463 U per mg protein.

5,5´-Dithio-bis-(2-nitrobenzoic acid) (DTNB) was from Sigma (Steinheim, Deutschland). Alga *S. vacuolatus* (strain 211-15, SAG culture collection of algae) was from the University of Göttingen, Germany.[18,22]

Compounds
The dodecaborate cluster was synthesized according to Komura *et al.* (1987)[26] or purchased from BASF (Ludwigshafen, Germany). $B_{12}H_{11}NH_3^-$ ($B12NH_3$) was prepared from $B_{12}H_{12}^{2-}$ with hydroxylamine-*O*-sulfonic acid.[27] Trialkylated products were prepared as described by Justus *et al.* (2008).[1]

Liposome preparation
Dipalmitoylphosphatidylcholine (DPPC) was dissolved in chloroform/methanol (2:1) and a lipid film was obtained after evaporation and drying in vacuum. Then the lipid film was hydrated and dispersed by vortexing in 100 mM carboxyfluorescein (CF) solution (100 mM CF dissolved in HEPES (4-(2-hydroxyethyl)-1-piperazineethanesulfonic acid) buffer (10 mM), pH 7.4). The resulting suspension was extruded 21 times through a polycarbonate membrane with a pore diameter of 100 nm (Avestin, Mannheim, Germany) at a temperature of 54 °C.[28-29] Free CF was removed by size exclusion chromatography on a pre-packed Sephadex G-25 M column (GE Healthcare Bio-Sciences, Uppsala, Sweden). The equilibration and elution buffer was HEPES buffered saline, pH 7.4 (150 mM NaCl, 10 mM HEPES). The lipid concentration was determined with the Stewart assay.[30]

Leakage experiments
CF was encapsulated passively in a self-quenched concentration (100 mM) into liposomes. Leakage was determined through an increase of fluorescence after compound addition, where CF leaked out and was diluted to a fluorescent concentration (excitation 490 nm, emission 515 nm). To obtain a 100 % fluorescence value TRITON X-100 (final concentration: 0.1%) was added at the end of measurement.

The fluorescence of CF was quenched by the MeAB and Et2BnAB derivatives, therefore the curves were corrected with the following equation:

$$F_t = F_0 + (F - F_0) \cdot f_{compound} \qquad \text{(equation 1)}$$

where F_t is the corrected fluorescence without any quenching effects, F_0 is the start fluorescence and F is the fluorescence at a defined time point in the experiment. $f_{compound}$ is a correction factor and comprises the following ratio: $\frac{100\%}{\text{end fluorescence [\%]}}$.
Here the end fluorescence is defined by the fluorescence reached after addition of the test compound (MeAB or Et2BnAB). The end fluorescence is calculated in percent by the following formula: $\frac{\text{end fluorescence} \cdot 100\%}{\text{fluorescence after TRITON addition}}$ in which the fluorescence after TRITION addition describes the maximum of reachable fluorescence and is consequently the 100 % value.

Partition coefficient octanol/water (Kow)
Partition coefficients were determined using the shaking-flask method (SFM)[31]. Fourier transform infrared (FTIR) spectroscopy was used for determination of boron content in water and octanol phase, respectively. This simple and rapid method has been described for BSH by Kageji *et al.* (1998)[32].

A stock solution of each boron compound was prepared in a volume mixture of water/octanol (equal volume). The compound concentration was 80 mM in this

mixture. The solutions were vortexed for some minutes. After the phase separation the boron concentration was determined in each phase.

For the FTIR detection we used a Bio Rad FTS 155 spectrometer with a Mid-IR DTGS detector at a resolution of 16 cm^{-1}. For each measurement 256 scans were collected. To determine the boron concentrations in solution, a variable path length demountable SL-2 cell kit from International Crystal Laboratories (Garfield, New Jersey, United States) with calcium fluoride windows was used, with a path length of 0.5 mm for octanol and 0.1 mm for water. The background was recorded as single-beam spectrum of the solvents and then subtracted from the test spectrum. Each spectrum was baseline corrected before the boron level was quantified.

A calibration curve was established to determine the boron concentration in the water and octanol phase. For this, samples with defined boron concentrations were prepared. For the water phase, $Na_2B_{12}H_{11}SH$ and $Na_2B_{12}H_{12}$ respectively were used and for the octanol phase, the tetrabutylammonium salt of $B_{12}H_{11}SH(2-)$. The position of the maximal B-H absorption was picked. In water the absorption was in the wave number range of 2485 – 2500 cm^{-1} and in octanol, at 2500 cm^{-1}. Finally the boron concentrations were plotted against the absorption values. The values obtained from linear regression were used to determine compound concentrations in each phase; their ratio was calculated to give the partition coefficient.

Toxicity in animal cell culture

Cell survival was detected by the enzymatic reduction of the WST-1 dye from living cells to a yellow formazan salt whose absorbance could be measured.[33]

The cell line V79 (lung fibroblasts of Chinese hamster) was used and cultivated with Ham´s F10 medium and 10 % newborn calf serum at 37 °C and 5 % CO_2. Cells (11,000) per well were seeded into 96-well plates and grown for 24 h. Then the cells were incubated with different concentrations of compounds for 24 h. The cell survival was determined with the WST-1 test system. The supernatant was removed and the wells were filled with 100 µl each of a WST-1 stock solution (1:4 diluted with phosphate buffered saline (PBS) and additionally 1:10 with medium). After 4-6 h at 37°C the absorbance at 450 nm was measured.[29]

The cell survival values were obtained by fitting a sigmoidal curve with the following equation:

$$f = \frac{a}{(1+e^{-(x-xo)/b})} \qquad \text{(equation 2)}$$

in which *f* is the percentage survival of cells*, a* the highest point of response, *x* the concentration of the tested substance, *b* the slope of the response curve, and *xo* the concentration of the tested substance that provokes 50% cell death. Fitting was performed using the non-linear fitting module of Sigmaplot 2001 (SPSS, Erkrath, Germany).

Enzyme inhibition

The test system to determine the acetylcholine inhibition is based on a reduction of the dye 5,5´-dithio-bis-(2-nitrobenzoic acid) (DTNB) by the enzymatically formed thio-choline moiety from the AchE substrate acetylthiocholine iodide. The reduction can be followed colorimetrically.

The modified assay as described in detail in Stock *et al.* (2004)[34] was used. Different dilutions of the tested compound were prepared in a 96-well plate with phosphate buffer (0.02 M, pH 8.0) and 0.75 % DMSO. DTNB (2 mM, 0.185 mg/mL $NaHCO_3$ in phosphate buffer pH 8.0) and the enzyme (0.26 U/mL, plus 0.25 mg/mL bovine serum albumin in phosphate buffer pH 8.0) were added to each well. The reaction was started with the addition of 25 µl acetylthiocholine iodide (2 mM in phosphate buffer).

The end concentration of DNTB was 0.5 mM, of acetylthiocholine iodide 0.5 mM, and of AChE 0.0512 mM.

The changes of optical density (∆OD) at 405 nm were measured in a microplate-reader (MRX Dynatech). The first measurement was taken after a time delay of 150 seconds and then every 30 seconds for a total time period of 5 minutes. A linear regression line through all data points gave ∆OD min^{-1}.

The inhibition value was obtained by fitting, with Sigmaplot 2001, a sigmoidal curve with the same equation (equation 2) as for toxicity determinations.

Reproduction inhibition assay with the limnic green alga *S. vacuolatus*

The synchronized unicellular limnic green algae *S. vacuolatus* was used as test system. The algae was cultivated under photoautotrophical conditions at 28 °C in an inorganic, sterilized medium (pH 6.4) according to Faust *et al.* (1992)[35] with white light (intensity of 22 to 33 kilolux, Lumilux Daylight L 36 W-11 and Lumilux Interna L 36 W-41, Osram, Berlin, Germany) and 1.5 vol% CO_2. For the synchronization, a day-and-night cycle of 14 h and 10 h was used. The stock culture was diluted every day to a density of $5*10^5$ cells/mL. The methods for stock culturing and testing are described in detail by Faust *et al.* (1992)[35].

The protocol for the assay described by Altenburger *et al*. (1990)[36] was used, but in a modified procedure. For the start of the test, autospores were collected and were incubated with the test compounds for 24 h. The tested substances were dissolved in medium with 0.1 % DMSO. For the whole time period the algae were stirred and cultivated under the same conditions as for synchronization except for the CO_2 source, where instead 150 µl $NaHCO_3$ solution (1.5 M) was added to the test system. The assay was performed in sterilized glass tubes (20 mL Pyrex tubes sealed with caps containing a gas tight Teflon membrane).

The cell number of treated samples after 24 h was counted with a Coulter Counter Z2 (Beckmann, Nürnberg, Germany) and compared to the cell number of controls (untreated samples) the ratio gave the reproduction inhibition.

The inhibition value was obtained by fitting a sigmoidal curve with equation 2.

Fluctuations of the algae growth were found between the measurement days and they are responsible for the scatter of the data points. Data sets of three different measurements were chosen for the graphs and for the fitting of the curves.

Acknowledgment

The authors gratefully thank Dr. Johannes Ranke, Dr. Marianne Matzke and the UFT institute of the University of Bremen for making the enzyme and algae test systems available. We thank Jennifer Bergemann for help with the FTIR measurements and Thaddeus Gbem for help with V79 cell experiments.

References

1 E. Justus, K. Rischka, J. F. Wishart, K. Werner and D. Gabel, *Chem. Eur. J.*, 2008, **14**, 1918-1923.

2 A. S. Larsen, J. D. Holbrey, F. S. Tham and C. A. Reed, *J. Am. Chem. Soc.*, 2000, **122**, 7264-7272.

3 P. Wasserscheid and W. Keim, *Angew. Chem.*, 2000, **112**, 3926-3945.

4 T. Welton, *Chem Rev*., 1999, **99**(8), 2071-2084.

5 R. Sheldon, *Chem. Commun*., 2001, **23**, 2399-2407.

6 F. Endres, *ChemPhysChem*, 2002, **3**(2), 144-154.

7 B. Ronig, I. Pantenburg, L. Wesemann, *Eur. J. Inorg. Chem.*, 2002, 319-322.

8 Y. Zhu, C. Ching, K. Carpenter, R. Xu, S. Selvaratnam, N.S. Hosmane and J. A. Maguire, *Appl. Organometal. Chem.*, 2003, **17**, 346-350.

9 J. M. Chemnitius, R. Sadowski, H. Winkel and R. Zech, *Chem.-Biol. Interact.*, 1999, **120**, 183-192.

10 C. Pope, S. Karanth and J. Liu, *Environ. Toxicol. Pharmacol.*, 2005, **19**(3), 433-446.

11 G. Sessa and G. Weissmann, *J. Lipid Res.*, 1968, **9**, 310-318.

12 A. T. Fisk, B. Rosenberg, C. D. Cymbalisty, G. A. Stern and D. C. G. Muir, *Chemosphere,* 1999, **39**(14), 2549-2562.

13 K. O. Evans, *Colloids Surf., A,* 2006, **274**, 11-17.

14 R. A. Kumar, N. Papaïconomou, J.-M. Lee, J. Salminen, D. S. Clark and J. M. Prausnitz, *Environ. Toxicol*., 2008, DOI 10.1002/tox.

15 C. W. Cho, T. P. T. Pham, Y.-C. Jeon, K. Vijayaraghavan, W.-S. Choe and Y. S. Yun, 2007, *Chemosphere*, **69**, 1003-1007.

16 J. Ranke, A. Müller, U. Bottin-Weber, F. Stock, S. Stolte, J. Arning, R. Störmann and B. Jastorff, *Ecotoxicol. Environ. Saf.*, 2007, **67**, 430-438.

17 J. Arning, S. Stolte, A. Böschen, F. Stock, W. R. Pitner, U. Welz-Biermann, B. Jastorff and J. Ranke, *Green Chem.*, 2008, **10**, 47-58.

18 S. Stolte, M. Matzke, J. Arning, A. Böschen, W. R. Pitner, U. Welz-Biermann, B. Jastorff and J. Ranke, *Green Chem.*, 2007, **9**, 1170-1179.

19 K. J. Kulacki, D. T. Chaloner, D. M. Costello, K. M. Docherty, J. H. Larson, R. J. Bernot, M. A. Brueseke, C. F. Kulpa Jr. and G. A. Lamberti, 2007, *Chim. Oggi*, **25**(6), 32-36.

20 A. Latala, P. Stepnowski, M. Nedzi and W. Mrozik, *Aquat. Toxicol.*, 2005, **73**(1), 91-98.

21 A. S. Wells and V. T. Coombe, *Org. Process Res. Dev.*, 2006, **10**(4), 794-798.

22 M. Matzke, S. Stolte, K. Thiele, T. Juffernholz, J. Ranke, U. Welz-Biermann and B. Jastorff, *Green Chem.*, 2007, **9**, 1198-1207.

23 Y. Bourne, P. Taylor, Z. Radic and P. Marchot, *The EMBO J.*, 2003, **22**(1), 1-12.

24 M. Harel, I. Schalk, L. Ehret-Sabatier, F. Bouet, M. Goeldner, C. Hirth, P. H. Axelsen, I. Silman and J. L. Sussman, *Proc. Natl. Acad. Sci. U. S. A.*, 1993, **90**(19), 9031-9035.

25 R.Schubert, K. Beyer, H. Wolburg and K. H. Schmidt, *Biochemistry,* 1986, **25**, 5263-5269.

26 M. Komura, K. Aono, K. Nagasawa and S. Sumimoto, *Chem. Expr.*, 1987, **2**, 173-176.

27 W. R. Hertler and M. S. Raasch, *J. Am. Chem. Soc.*, 1963, **85**, 3661-3668.

28 S. A. Abraham, K. Edwards, G. Karlsson, S. MacIntosh, L. D. Mayer, C. McKenzie and M. B. Bally, *Biochim. Biophys. Acta*, 2002, **1565**, 41-54.

29 D.Gabel, D. Awad, T. Schaffran, D. Radovan, D. Daraban, L. Damian, M. Winterhalter, G. Karlsson and K. Edwards, *ChemMedChem*, 2007, **2**, 51-53.

30 J. C. Stewart, *Anal. Biochem.*, 1980, **104**, 10-14.

31 A. Finizio, M. Vighi and D. Sandroni, *Chemosphere*, 1997***,*** **34**(1), 131-161.

32 T. Kageji, B. Oterson, D. Gabel, R. Huiskamp, Y. Nakagawa and K. Matsumoto, *Biochim. Biophys. Acta,* 1998, **1391**, 377-383.

33 M. V. Berridge, A. S. Tan and P. M. Herst, *Biotechnol. Annu. Rev*., 2005, **11**, 127-152.

34 F. Stock, J. Hoffmann, J. Ranke, R. Störmann, B. Ondruschka and B. Jastorff, *Green Chem.*, 2004, **6**(6), 286–290.

35 M. Faust, R. Altenburger, W. Boedecker and L. H. Grimme, *Schriftenr. Ver. Wasser Boden Lufthyg.*, 1992, **89**, 311-321.

36 R. Altenburger, W. Boedecker, M. Faust and L. H. Grimme, *Ecotoxicol. Environ. Saf.*, 1990, **20**(1), 98-114.

II

Interaction of *N,N,N*-trialkylammonioundecahydro-*closo*-dodecaborates with dipalmitoyl phosphatidylcholine liposomes

under revision in Chemistry and Physics of Lipids

Interaction of *N,N,N*-trialkylammonioundecahydro-*closo*-dodecaborates with dipalmitoyl phosphatidylcholine liposomes

Tanja Schaffran[a,1], Jingyu Li[a], Göran Karlsson[b], Katarina Edwards[b], Mathias Winterhalter[c], Detlef Gabel[a]

[a] *Department of Chemistry, University of Bremen, PO Box 330440, D-28334 Bremen, Germany*

[b] *Department of Physical and Analytical Chemistry, University of Uppsala, S-751 23 Uppsala, Sweden*

[c] *School of Science and Engineering, Jacobs University Bremen, Campus Ring 1, D-28759 Bremen, Germany*

Keywords: liposomes, ionic liquids, cryo-TEM, differential scanning calorimetry, fusion, leakage

Abstract:

N,N,N-trialkylammonioundecahydrododecaborates (1-), a novel class of compounds of interest for use as anions in ionic liquids, interact with DPPC liposomes. Increasing compound concentration cause an increasing negative ζ potential. Dissociation constants demonstrate that the binding capacity increases strongly with longer chain length. *N,N,N*-trialkylammonioundecahydrododecaborates with longer alkyl chains show a detergent like behavior: the compounds incorporate into the liposome membrane and differential scanning calorimetric experiment show already low concentrations cause a complete disappearance of the peak representing the gel-to-liquid crystalline phase transition. In contrast, compounds with shorter alkyl chains only interact with the head groups of the lipids. Investigations by means of cryo TEM revel that all derivatives induce significant morphological changes of the liposomes. *N,N,N*-trialkylammonioundecahydrododecaborates with short alkyl chains produce large bilayer sheets, whereas those with longer alkyl chains tend to induce the formation of open or multi-layered liposomes. We propose that the binding of *N,N,N*-trialkylammonioundecahydrododecaborates is mainly due to electrostatic interactions between the doubly negatively charged cluster unit and the positively charged choline headgroup; the positively charged ammonium group might be in contact with the deeper-lying negatively charged phosphate. For *N,N,N*-trialkylammonioundecahydrododecaborates with longer alkyl chains hydrophobic interactions with the non-polar hydrocarbon part of the membrane constitute an additional important driving force for the association of the compounds to the lipid bilayer.

Introduction

In the last years ionic liquids (ILs) have attracted great attention in the academic and industrial research fields. ILs are salts with melting points below 100 °C. Their special properties, including negligible vapor pressure, high electrical conductivity, wide electrochemical window, tolerance to strong acids, excellent thermal and chemical stability, and the fact that they are not inflammable (Justus et al. 2008; Larsen et al., 2000), make

Abbreviations: AB, N,N,N-trialkylammonioundecahydrododecaborate; BSH, $Na_2B_{12}H_{11}SH$; C_p, specific heat capacity; DPPC, dipalmitoylphosphatidylcholine; DSC, differential scanning calorimetry; FRET, fluorescence resonance energy transfer; HBS, HEPES buffers saline; HEPES, 2-[4-(2-Hydroxyethyl)-1-piperazine]ethanesulfonic acid; Ils, ionic liquids; NBD-PE, N-(7-nitrobenz-2-oxa-1,3-diazol(-4-yl)-1,2-di-hexadecanoyl-sn-glycero-3-phospho-ethanolamine, triethylammonium salt; Rh-PE, rhodamine B 1,2-dihexadecanoyl-sn-glycero-3-phospho-ethanolamine,trimethylammonium salt; TEM, transmission electron microscopy.

* Corresponding author. Tel.: +49 421 21863252; fax: +49 421 21863259. *E-mail address:* ta_sc2@uni-bremen.de (T. Schaffran).

them very attractive for different applications. ILs can be employed as a new kind of solvents, can function as chemical catalysts or biocatalysts and can be used in the electrochemistry (Wasserscheid, Keim, 2000; Welton, 1999; Sheldon, 2001; Endres, 2002).
ILs can be tuned for the application of interest. Different molecular structures can be combined and therefore the properties can be influenced and tailored, which has led to their designation as “designer solvents“ (Stolte et al., 2006).
The most established ILs consist of a simple anion (chloride, tetrafluoroborate, hexafluorophosphate) and a cation of following important classes (tetraalkylammonium, tetraalkylphosphonium, *N*-alkylpyridinium, *N*-methyl-*N´*alkylimidazolium). More uncommon ILs are e.g. meltable stannaborate salts (Ronig et al., 2002) or alkylpyridinium combined with carborane anions (Zhu et al., 2003). The anion repertoire is, however, very limited for tuning the ILs properties.
Recently we published a new kind of ionic liquids in which N-trialkylammonioundecahydrododecaborates (1-) as anions are combined with simple cations such as potassium, lithium or unsolvated H^+ (Justus et al. 2008). In Fig. 1 the *N,N,N*-trialkylammonioundecahydrododecaborates (1-) are shown, in which the dodecaborate cluster is substituted with a trialkylated ammonium group. We investigated derivatives with three identical alkyl chains ranging in length from methyl to hexyl.

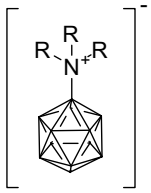

R= CH_3 - C_6H_{13}

Fig. 1: *N,N,N*-trialkylammonioundecahydrododecaborates (1-)

This new kind of anions for ILs allows additional technical applications, e.g. in batteries, because of the possibility to combine these anions with a wide range of simple cations such as potassium or lithium. Before these ILs are to be used in technical applications an analysis of interactions with biological systems is desirable.
We have previously tested the *N,N,N*-trialkylammonioundecahydrododecaborates (1-) for their hazard potential in different biological systems (mammalian cells, algae and, as an enzyme test system, acetylcholinesterase). This new class of ILs has a toxicity in biological systems comparable to that of commonly used ILs, and thus conveys no additional risks when replacing conventional ILs. The hydrophobicity of the substances, and also their *in vitro* toxicity, increases, however, from MeAB to HxAB. It is in this context interesting to note that the *N,N,N*-trialkylammonioundecahydrododecaborates (1-) are able to induce leakage from DPPC liposomes. The capability for leakage induction strongly increases with the length of the alkyl chain (Schaffran et al., 2009).
In this study we investigate in more detail the interactions between the *N,N,N*-trialkylammonioundecahydrododecaborates and liposomes, using the latter as a model for biological membranes. In order to focus on the interaction we have selected the well understood DPPC as phospholipid (El Maghraby et al., 2005) The use of pure DPPC, rather than for instance a more biologically relevant cholesterol containing lipid mixture, allowed important information to be collected by DSC. In addition, comparisons between the previous leakage data and the results from this study are possible.
We have used different methods for determination of the interactions between the clusters and the lipid membrane. With differential scanning calorimetric (DSC) changes in the thermotropic behavior caused by the interaction of molecules such as cholesterol, surfactants and drugs with lipid membranes can be studied (El Maghraby et al, 2005). ζ potential measurements allow identifying changes in the surface charge of the liposomes. With cryo-transmission electron microscopy (cryo-TEM) morphological changes in liposome

shape and structure can be visualized. Liposome fusion can be followed by monitoring the fluorescence resonance energy transfer (FRET) between two fluorescent lipid probes embedded in the lipid membrane (Rosenberg et al., 1983; Vanderwerf, Ullmann, 1980).
The following ILs were tested as potassium salts (with their abbreviations in parentheses): *N,N,N*-trimethylammonio-undecahydro-*closo*-dodecaborate (1-) (MeAB, *N,N,N*-triethylammonio-undecahydro-*closo*-dodecaborate (1-) (EtAB). *N,N,N*-tripropylammonio-undecahydro-*closo*-dodecaborate (1-) (PrAB), *N,N,N*-tributylammonio-undecahydro-*closo*-dodecaborate (1-) (BuAB), *N,N,N*-triisopentylammonio-undecahydro-*closo*-dodecaborate (1-) (iPnAB), *N,N,N*-trihexylammonio-undecahydro-*closo*-dodecaborate (1-) (HxAB).

Materials and Methods

Materials

DPPC was from Lipoid, Ludwigshafen (Germany). NBD-PE (N-(7-nitrobenz-2-oxa-1,3-diazol(-4-yl)-1,2-di-hexadecanoyl-sn-glycero-3-phospho-ethanolamine, triethylammonium salt) and Rh-PE (rhodamine B 1,2-dihexadecanoyl-sn-glycero-3-phospho-ethanolamine,trimethylammonium salt) were from Avanti Polar Lipids, Inc., (Alabaster, Alabama, USA).

Preparation of compounds

The trialkylated cluster derivatives were prepared as described.(Justus et al., 2008).

For the incubation with liposomes, the compounds were first dissolved in buffer or in buffer containing DMSO (PrAB, BuAB, HxAB) and were then added to the liposome suspension; the final concentration of DMSO was 3% for PrAB, BuAB and HxAB. *N,N,N*-trialkylammonioundecahydrododecaborates with long alkyl chains are poorly water-soluble and therefore DMSO was used as solubilizer.

Liposome preparation

DPPC was dissolved in chloroform/methanol (2:1) and a lipid film was obtained after evaporation and drying in vacuum. Then the lipid film was hydrated and dispersed by vortexing in 10 mM HEPES buffer saline, pH 7.4 (150 mM NaCl, 10 mM HEPES). The resulting suspension was frozen and thawed in 10 cycles followed by extrusion (21 times) through a polycarbonate membrane with a pore diameter of 100 nm (Avestin, Mannheim, Germany) at a temperature of 54 °C. (Abraham, 2002) Lipid content was measured by the Stewart assay (Stewart, 1980), using appropriate standard curves for the individual lipids.

Cryo-transmission electron microscopy (cryo-TEM)

The liposomal suspension (lipid concentration 4 mM) was placed on a copper grid coated with a perforated polymer film. Excess solution was thereafter removed by means of blotting with a filter paper. This procedure was performed in a custom-built environmental chamber under controlled humidity and temperature. Immediately after film preparation, the grid was plunged into liquid ethane held at a temperature just above its freezing point. The vitrified sample was mounted and examined in a Zeiss EM 902 A electron microscope (Oberkochen, Germany), operating at an accelerating voltage of 80 keV in filtered bright field image mode at ΔE = 0 eV. The temperature was kept below 108K and images were recorded at defocus settings between 1 and 3µm. A more detailed description of the cryo-TEM procedure can be found elsewhere (Almgren et al., 2000).

Differential scanning calorimetry (DSC)

The phase transition measurements were carried out on a VP-DSC MicroCalorimeter with MicroCal Origin 5.0 as the software for technical graphics and data analysis. HBS (10 mM HEPES / 150 mM NaCl, pH 7.4) was used as buffer system.

DPPC liposomes (final concentration 10 mM) incubated without and with different concentrations of boron cluster compounds (MeAB: 5, 30, 50 and 70 mM, HxAB: 0.5, 1, 2, 3 and 5 mM) at RT for 2 hours were injected in the sample cell, and buffer solution was loaded in the reference cell. Before injection, both incubation mixture and buffer solution were degassed.

Upscans were performed from 20 °C to 60 °C at a scan rate of 90 °C/h, while downscans were performed from 60 °C to 20 °C at a scan rate of 60 °C/h. Four to ten scans were collected with a filtering period of 2 s. A background scan collected with buffer in both cells was subtracted from each scan.

Lipid mixing

For lipid mixing measurements HBS (10 mM HEPES / 150 mM NaCl, pH 7.4) was used as buffer system. Two kinds of DPPC liposomes were prepared separately: Liposomes from DPPC labelled with both NBD- and Rh- labels were prepared from a mixture of 1 mol% of fluorescence energy transfer donor lipid NBD-PE, 1 mol% of acceptor lipid Rh-PE and 98 mol% DPPC lipid. Unlabelled DPPC liposomes were prepared from pure DPPC.

For measurement of lipid mixing, the NBD- and Rh- labeled DPPC liposomes (final concentration 2.4 mM) were mixed with the unlabeled DPPC liposomes (final concentration 16.8 mM). The mixtures were incubated in the absence and presence of different concentrations of MeAB overnight at room temperature.

The fluorescence measurements were carried out with a Perkin-Elmer LS 50B luminescence spectrometer. FL WinLab was used as the control software. Before the fluorescence measurements, 40 µl of each of the above incubation mixtures was diluted with 2 ml buffer. The fluorescence was measured by exciting NBD at 467 nm and recording the fluorescence emission of both NBD and Rh in emission spectra ranging from 490 to 700 nm. Then 20 µl of 10% (v/v) Triton X-100 were added so that the maximum fluorescence intensity of NBD could be measured.

Lipid mixing (%) was calculated using the following formula:

$$\text{Lipid mixing (\%)} = \frac{F_t - F_0}{F_{\max} - F_0} \times 100 \qquad \text{(eq. 1)}$$

F_t: NBD fluorescence intensity with a certain concentration of boron cluster compounds; F_0: NBD fluorescence intensity without boron cluster compounds; F_{max}: NBD fluorescence intensity after the addition of triton.

ζ potential

The current availability of easy to use instruments to measure zeta (ζ) potentials suggests to quantify binding of charged compounds to neutral liposomes by measuring changes in the ζ potential. The ζ potential is caused by the surface charge density; the general relationship is, however, rather complex (Bähr et al. 1998; Cohen et al. 2003). Here we restrict ourselves to low charge densities in the range of where the binding isotherm is almost independent on the already bound molecules.

At low surface charge densities the potential drop will be sufficiently low and the Poisson-Boltzmann equation can be linearized. Within the so-called Debye-Hückel approximation the surface potential Ψ is caused by a charge density σ according to

$$\Psi = \frac{\sigma}{\varepsilon_w \varepsilon_0} \lambda_{Debye} \qquad \textit{(eq. 2)}$$

The surface charge density can be expressed by the ratio bound compound per lipid molecule $\sigma = \frac{c_{bound}}{c_{lipid}} a_{lipid} ze$ where a_{Lipid} = 0.64 nm^2 is the area per lipid and z the valency of the drug. The binding constant of the drug to the lipid defined by

$K = \frac{c_{bound}}{c_{free} c_{lipid}}$ and the mass conservation $c_{total} = c_{bound} + c_{free}$

gives $c_{free} = \frac{c_{total}}{1 + Kc_{lipid}}$ and subsequently for the charge density

$$\sigma = a_{lipid} ze \frac{Kc_{total}}{1 + Kc_{lipid}} \qquad \textit{(eq. 3)}$$

Electrostatic interactions are characterized by the Debye length

$$\lambda_{Debye} = \sqrt{\frac{\varepsilon_w \varepsilon_0 kT}{2 n_0 z^2 e^2}} = \frac{1}{\sqrt{c_{free}}} \sqrt{\frac{\varepsilon_w \varepsilon_0 kT}{2000 N_A z^2 e^2}} \qquad \textit{(eq. 4)}$$

where ε_w =80 is the dielectric constant of the aqueous phase, ε_0=8.85·10^{-12} As/Vm the permittivity of the empty space, kT= 4·10^{-21} VAs the Boltzmann factor at room temperature, n_0 the number of ions, e =1.6·10^{-19} As the elemental charge, N_A the Avogadro number and c_{free} the ion concentration in solution which is in our experiment mainly the free drug.
Accounting for the bound drug the Debye length is

$$\lambda_{Debye} = \frac{1}{\sqrt{\frac{c_{total}}{1 + Kc_{lipid}}}} \sqrt{\frac{\varepsilon_w \varepsilon_0 kT}{2000 N_A z_2 e^2}} = \left(\frac{c_{total}}{1 + Kc_{lipid}} \right)^{-\frac{1}{2}} \sqrt{\frac{\varepsilon_w \varepsilon_0 kT}{2000 N_A z^2 e^2}} \qquad \textit{(eq. 5)}$$

From this it follows for the surface potential Ψ

$$\Psi = K \frac{c_{total}}{1 + Kc_{lipid}} a_{lipid} e \frac{1}{\varepsilon_w \varepsilon_0} \left(\frac{c_{total}}{1 + Kc_{lipid}} \right)^{-\frac{1}{2}} \sqrt{\frac{\varepsilon_w \varepsilon_0 kT}{2000 N_A e^2}}$$

$$\Psi = K \sqrt{\left(\frac{1}{1 + Kc_{lipid}} \right)} \sqrt{c_{total}}\, a_{lipid} \sqrt{\frac{kT}{2000 N_A \varepsilon_w \varepsilon_0}} \qquad \textit{(eq. 6)}$$

According to equation 6 the surface potential Ψ is proportional to $K \sqrt{\left(\frac{1}{1 + Kc_{lipid}} \right)} \sqrt{c_{total}}$.

It should be noted that the ζ potential does not necessarily correspond to the actual surface potential but is somewhat screened due to immobile charges. The surface potential Ψ is related to the ζ potential by an exponential decay with λ_{Debye} as decay length. The shear plane is empirically located at a distance x= 2 Å from the surface (Cohen et al. 2003).

$$\Psi = \zeta \exp(-x / \lambda_{Debye}) \qquad \text{(eq. 7)}$$

In addition, a purely empirical fit of a sigmoidal function to estimate the binding affinity of the ABs was applied (Macdonald, Seelig, 1988), as sigmoidal curves of the measured ζ

potentials *versus* total concentration of the ABs were found. A four-parameter exponential was fitted to the data (using Sigmaplot 2001):

$$\zeta = \zeta_{min} + \frac{a}{1 + e^{\frac{-(c - c_o)}{b}}} \qquad \text{(eq. 8)}$$

where ζ is the ζ potential, a the difference between minimum and maximum of the ζ potential (max.y – min.y), c the logarithm of the concentration of the tested substance, b the slope of the curve at the inflection point, c_0 the logarithm of the concentration of the tested substance at the inflection point, and ζ_{min} the negative maximum of the zeta potential (min.y).

For zeta potential measurements, liposomes (final concentration 0.5 mM) were incubated with different concentrations of the boron cluster anions overnight at room temperature. The buffer system was HEPES (1 mM, pH 7.4). ζ potential measurements were performed with a Malvern Zetasizer Nano ZS. For instrument control and data analysis, the software DTS (Nano) 5.0 was used.

Results

DSC

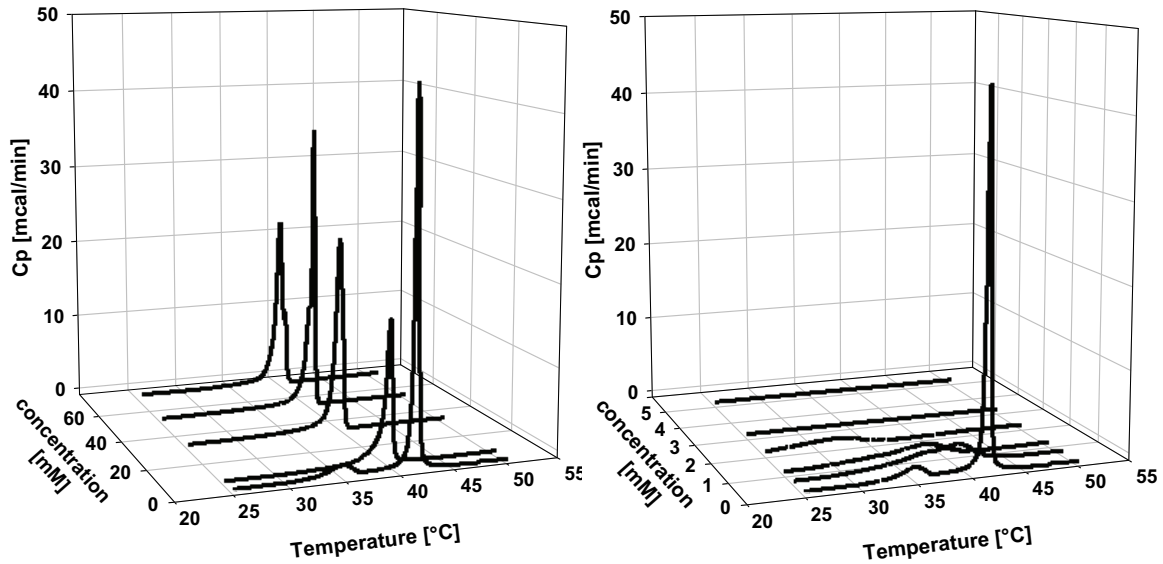

Fig. 2: left: DSC scans with and without MeAB; right: DSC scans with and without HxAB. The lipid concentration is 10 mM.

DSC measurements were performed on samples containing DPPC liposomes alone and following addition of the different cluster compounds. Fig. 2 shows the first heating curves for MeAB as a typical example for short alkyl chains, and for HxAB as a typical example for long chain lengths. In the absence of clusters, DPPC shows a pre-transistion peak at 34.8 °C and a sharp main transition peak at 41.5 °C (see also Gabel et al., 2007). By addition of 5 mM MeAB the pre-transition peak disappears completely and the main transition peak shifts to 39.5 °C. With further increase in MeAB concentration, the temperature of the main transition decreases slightly and gradually.

After incubation with HxAB, the main transition is markedly affected already at a HxAB to lipid molar ratio corresponding to 0.05. The transition is broadened and the enthalpy is lowered gradually until the transition can no longer be detected.

Zeta potential

In Fig. 3 we show the concentration dependence of the ζ potential for various compounds. Due to the charge neutrality of DPPC, the ζ potential in the absence of clusters is close to 0 mV. Compounds like MeAB cause moderately negative ζ potentials. In contrast, compounds like HxAB cause drastic changes and result in highly negative values of –100 mV for the limiting ζ potential at concentrations of 0.3 mM of the compounds. Obviously the interactions with the liposomal membrane increase with longer alkyl chain length.

Fifty percent of the total change of the ζ potential has occurred when the HxAB concentration is only 7% of that of the available headgroups. The amount actually bound might be still lower. For shorter alkyl chains, the solutions contain more of the ABs at half-maximal effect.

Table 1: Concentrations from the inflection pointwith standard error for each compound, the limiting zeta potential, the slope and the ratio substance/lipid derived from the ζ potential curves.

Substance	*c_0 (= log c at inflection point)*	*concentration [mM] from inflection point*	*limiting zeta potential ζ_{min} (mV)*	*b (slope at inflection point)*	*ratio substance/lipid at inflection point*
MeAB	*1.45 ± 0.54*	*28.2*	*-98 ± 37*	*-0.70 ± 0.18*	*56*
EtAB	*0.67 ± 0.6*	*4.7*	*-100 ± 34*	*-0.83 ± 0.32*	*9.4*
PrAB	*-0.18 ± 0.42*	*0.66*	*-94 ± 21*	*-0.93 ± 0.3*	*1.3*
BuAB	*-1.03 ± 0.19*	*0.093*	*-101 ± 13*	*-0.86 ± 0.28*	*0.19*
HxAB	*-1.75 ± 0.06*	*0.018*	*-118 ± 1*	*-0.65 ± 0.05*	*0.036*

We interpret the inflection points of the ζ potential curves as points where 50% of the maximally achievable binding of the clusters has occurred, noting that the concentration at this point does not correspond to the intrinsic association constant (see derivation of eq. 5 above). A numerically larger value means a less strong binding.

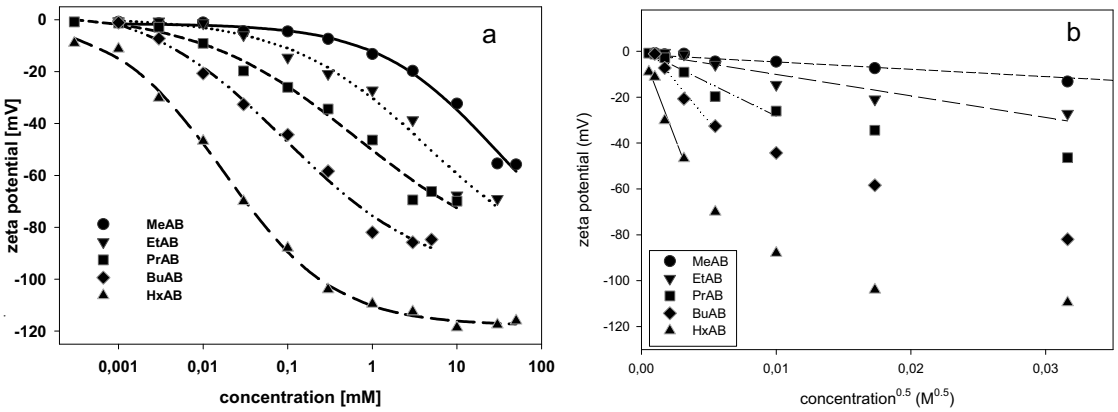

Fig. 3. a (left): ζ potentials of DPPC liposomes incubated with the substances MeAB, EtAB, PrAB, BuAB and HxAB. The lines are the regression curves according to eq. 8. The squared correlation coefficients r^2 for the regression are 0.99 for each curve. The liposome concentration was 0.5 mM. The measurement was carried out at room temperature. b (right): Analysis of the binding constant at low concentration of the compounds. Here the interaction of bound molecules can be neglected.

We have calculated association and dissociation constants from eq. 6. At low concentrations the electrostatic interaction between the individual compounds can be neglected. For this case we can calculate an association constant. At higher concentrations the already bound

molecules reduce the affinity for further binding by electrostatic repulsion and the concept of a binding isotherm must be applied. In Fig. 3b we have applied a linear fit to the data with smaller ζ potentials; from the slope, the association constant is obtained. The association constant K was converted, by inversion, to a dissociation constant K^{-1}; the latter data are summarized in Table 2.

Table 2: Dissociation constants obtained from eq. 6 and eq. 8.

Substance	Slope from plotting ζ potential versus $\sqrt{c_{total}}$ (eq. 6) (see Fig. 3b)	squared correlation coefficient r^2 from the linear fitting (eq. 6) (see Fig. 3b)	Dissociation constant from eq. 6 (K^{-1}) [mM]	Concentration [mM] at inflection point (eq. 8)
MeAB	-319.2	0.99	2.9	28.2
EtAB	-936.7	0.92	0.85	4.7
PrAB	-2888.8	0.95	0.18	0.66
BuAB	-7058.2	0.98	0.037	0.093
HxAB	-15244.4	0.97	0.008	0.018

The calculated dissociation constants using eq. 6 are qualitatively in line with the values obtained from the fits using eq. 8. The calculated dissociation constants from eq. 6 are generally smaller than the concentrations at the inflection point.

Lipid mixing

Lipid mixing was investigated for MeAB (Fig. 4). The mixing increases with increasing compound concentration. For complete mixing, 40 mM is needed. For the derivatives with longer alkyl chains, lipid mixing was not investigated, as the cryo-TEM results show that large sheets are obtained.

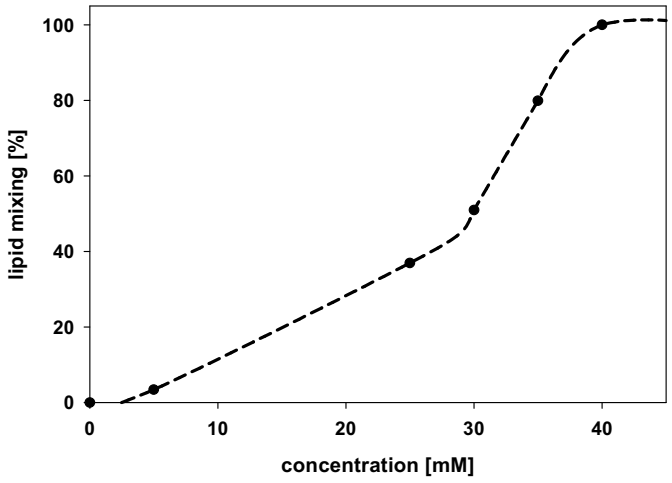

Fig. 4: Lipid mixing in percent for MeAB. Incubation was overnight at room temperature. Lipid concentration 19.2 mM. The line is for guidance only.

Cryo-TEM

Fig. 5 shows a cryo-TEM image of the liposome suspension in the absence of alkylated subtances The majority of the liposomes are unilamellar and show the angular, or facetted, morphology typical for PC liposomes at temperatures below the phase transition temperature.

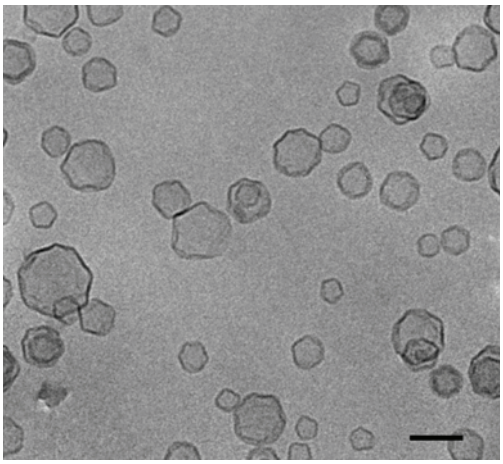

Fig. 5. DPPC liposomes in the presence of 3% DMSO at 25°C, Scale bar = 100 nm

As shown in Fig. 6, PrAB and HxAB were at concentrations corresponding to 64 mM found to self-associate into small globular micelle-like aggregates. Similar structures were formed also by BuAB (results not shown). MeAB and EtAB, which have comparably high aqueous monomer solubilities (Schaffran et al., 2009), showed no tendency for micelle formation.

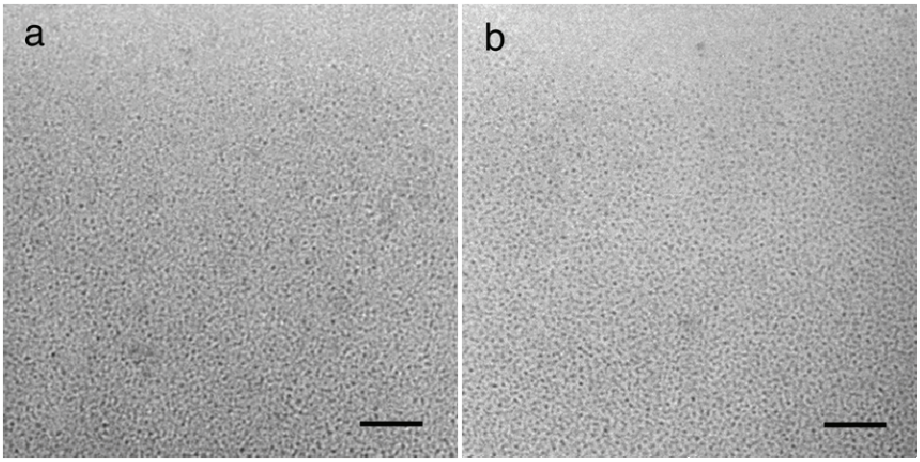

Fig. 6. Micelles formed by PrAB (a) and HxAB (b). Scale bar 100 nm.

Drastic changes in the sample morphology were observed upon incubation of the DPPC liposomes with the cluster derivatives. As shown in Fig. 7a, very few closed liposomes were observed after incubation with 64 mM MeAB at 25 °C, and the majority of the lipid material was instead found in bilayer disks or sheets of different sizes. Upon increasing the incubation temperature to 37 °C, the average size of the bilayer structures increased (Fig. 7b).

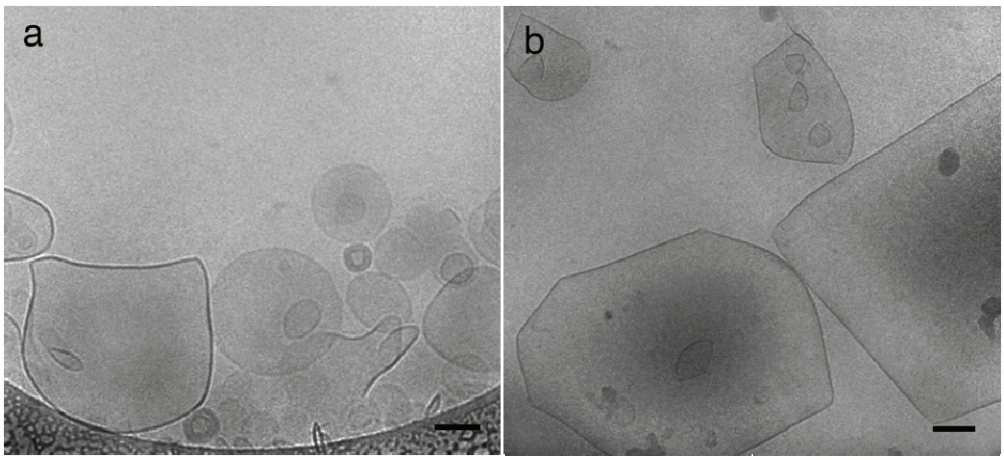

Fig. 7: Liposomes (4 mM) are incubated with MeAB (64 mM) at 25 °C (a) and at 37 °C (b). Scale bar 100 nm.

Liposome samples incubated with 64 mM EtAB were dominated by large, and often folded, bilayer sheets (Fig. 8a). Upon storage at 4 °C for 1 week the bilayers tended to grow larger (Fig. 8b).

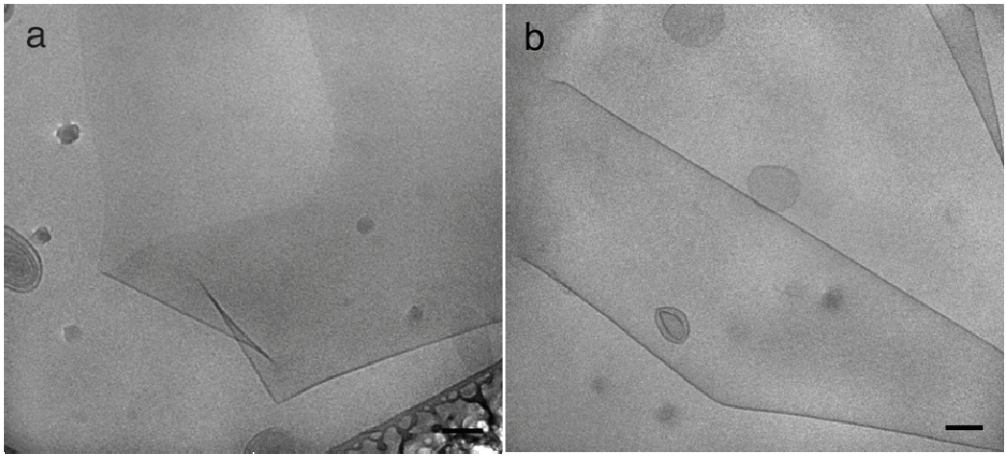

Fig. 8: DPPC liposomes (4 mM) and EtAB (64 mM) at 25 °C (c) and after sample storage for 1 week at 4 °C (d). cryo-TEM measurement at 25 °C. Scale bar 100 nm.

Liposome samples incubated with the PrAB formed the structures shown in Fig. 9. Flat, or partly folded, bilayer disks made up the majority of structures in samples containing 32 mM PrAB (Fig. 8a), which are smaller than those found for MeAB and EtAB. In contrast, samples incubated with 64 mM PrAB displayed mainly globular micelles (Fig. 8b).

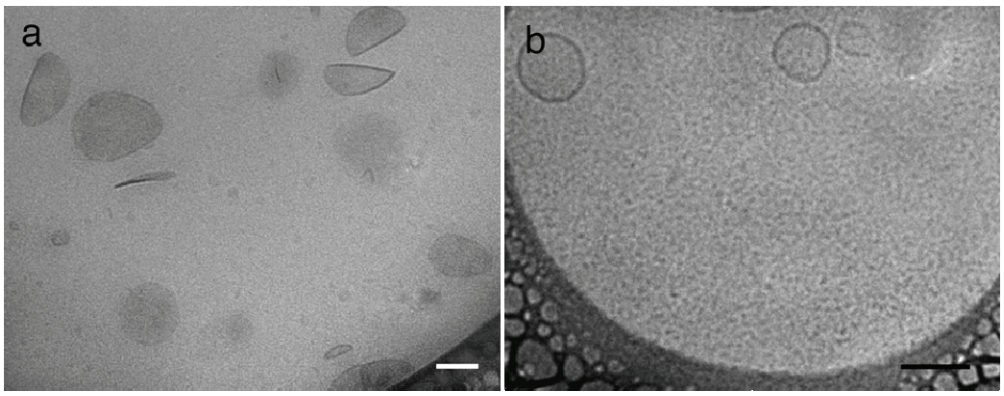

Fig. 9: DPPC liposomes (4 mM) after incubation with 32 mM (a) and 64 mM (b) of PrAB at 25 °C. Scale bar 100 nm.

In case of BuAB, micelles were detected already in samples containing 32 mM of the derivative (Fig. 10a). In addition to micelles many very small liposomes, as well as partly unclosed liposome structures, were seen in the micrographs. Liposomes encapsulating several smaller liposomes were frequently observed. Remarkably, the liposomes did not display the angular appearance observed for pure DPPC samples (Fig. 5) but exhibited the type of smooth surface normally found above the gel-to-liquid crystalline phase transition temperature. BSH has the same effect on DPPC liposomes. (Gabel et al., 2007)Upon increasing the BuAB concentration to 64 mM, the number of micelles increased and in addition to liposomes also large bilayer sheets could be found in the samples (Fig. 10b).

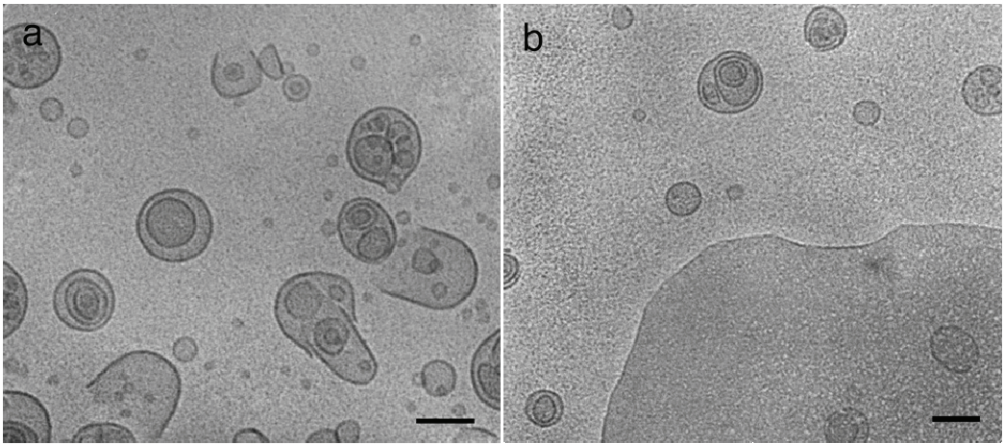

Fig. 10: DPPC liposomes (4 mM) incubated with 32 mM (a) and 64 mM (b) of BuAB at 25 °C. Scale bar 100 nm.

Upon addition of HxAB the majority of the liposomes transformed into distinct multilayered structures (Fig. 11a). Some of the structures were very concentric and the layers evenly spaced (~ 13 nm), making them look like “onion rings”. As seen in Fig. 11 a, some of the outermost layers in the multilayered structures appeared to be incompletely closed (marked by arrow in Fig. 11a). Similar to the case with BuAB and PrAB, globular micelles coexisted with the bilayer structures. As seen in Fig. 11b, the sample structure remained essentially the same when the incubation temperature was increased to 37 °C.

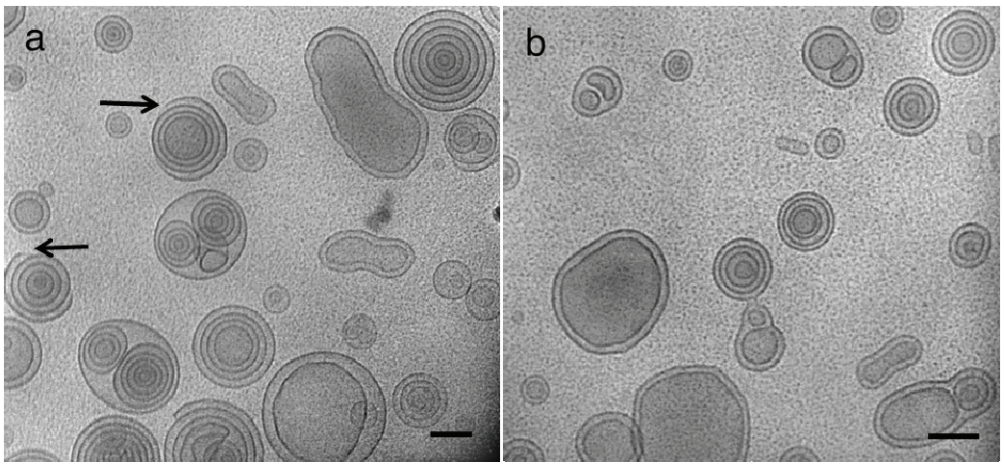

Fig. 11: DPPC liposomes (4 mM) incubated with HxAB derivative (64 mM) at 25°C (a) and 37 °C (b).

Discussion

In this study we have investigated the interactions between the new ILs anions and liposomal DPPC membranes. In the cryo-TEM experiments, compound/lipid ratios of 16:1 (64 mM compound) were tested for every substance and 8:1 (32 mM compound) for PrAB and BuAB. In the pictures large bilayers can be observed after addition of MeAB and EtAB. They are stable after one week storage at 4°C and heating to 37°C. PrAB, BuAB and HxAB, on the other hand, do not display the same tendency to convert the liposomes into large bilayer sheets; the derivatives with the longer alkyl chains differ from the two ones with shorter chains also in their ability to form micelles. The fact that PrAB, BuAB and HxAB assemble into micelles suggest that they share important properties with conventional ionic micelle-forming surfactants. These are well known to insert into liposomal membranes, and may, at sub-solubilizing concentrations, induce a range of structural transformations of the liposomes. Commonly the surfactants act as “edge-actants” and stabilize open membrane structures (Almgen et al., 2000; Johansson et al., 2008). The insertion of surfactants into the outer lipid leaflet of the membrane frequently also leads to a process in which small liposomes are budded off from the original liposome (Heerklotz, 2008). It thus comes as no surprise that PrAB is able to transform the liposomes into disk-shaped bilayers (Fig, 8a), or that BuAB tends to induce the formation of both open and very small liposomes (Fig. 9a).

It is, however, more difficult to see why HxAB promotes the formation of concentric multilayered liposomes with a rather homogeneous spacing of 13 nm. This distance is much larger than the size of the small cluster (having dimensions of around 4Å (Azev et al., 2004). Similar structures are known to form when liposomes are incubated with DNA under certain conditions (Clement et al., 2005; Letrou-Bonneval et al., 2008) but have, to our knowledge, not been detected after incubation of liposomes with small molecules. Pegylated multilayered liposomes also exhibit a constant distance between the lipid layers as a result of the PEG-polymer chains which stick out from the lipid bilayer. Landfester et al. (2006) reported the formation of onion-like nanostructures after miniemulsion polymerization in the presence of lanthanide complexes. For explaining the identical distances between the polymer films they suggest that a homogenous lanthanide-complex layer has been formed between films. It can be hypothesized that, at high concentrations, HxAB forms a similar compound layer around a liposome and that repulsion forces might prevent a closer approach of the liposomal membranes.

The results of the ζ potential measurements indicate that the compounds bind to the liposomal surface, as drastic changes of the surface potential occur upon addition of the compounds. Qualitative tendencies can be noted from the ζ potential curves (see Fig. 3a).

For MeAB a large excess of the compound over the lipid is necessary to achieve 50 % changes in the ζ potential. Association of MeAB to the liposome surface is energetically not favorable, and consequently most of the compound remains free in solution. It should be noted that liposomes do not exist at compound/lipid ratios greater than 16:1; rather, bilayer sheets are formed (see cryo-TEM results). As shown in the literature (Cohen et al. 2003) the ζ potential for liposomes does not depend much on shape and size of the particle. When, however, the particles have grossly different sizes, and especially when large open membranes coexist with smaller structures (as found for MeAB and EtAB, see Figs. 7 and 8), the measured ζ potential might be affected. With increasing alkyl chain length, the binding to the hydrophobic part of the membrane becomes energetically more favorable. For HxAB, 50 % change in the ζ potential is observed when its concentration is around 7% of that of the accessible lipid headgroups. From the concentration ratio, it appears that a single lipid headgroup does not represent one binding site for a cluster molecule, but rather that each binding site comprises several lipid molecules. In case of BuAB and HxAB, and perhaps also PrAB, it is fair to say that the alkylated substances behave like conventional surfactants in the sense that they partition between the lipid and aqueous phase rather than bind to a specific binding site (Paternostre et al., 1995).

The compound concentrations at the inflection point of the ζ potential curves are, however, no direct measure for the binding affinity because different aspects are not considered here. Electrostatic interactions are fairly nonlinear. Within the Poisson-Boltzmann theory the surface potential is proportional to the surface charge density at low concentration (Debye-Hückel approximation). This range can be described by a binding constant. At higher densities a logarithmic dependency is predicted. The isotherms in Fig. 3b demonstrate this fact. The compound binding to the liposomal surface is influenced by the molecules already bound and hence the association affinity is reduced by the electrostatic repulsion forces between the molecules.

The calculated dissociation constants of the substances from eq. 6 reflect the previous qualitative observations. The obtained values indicate a better surface binding than what can be expected from the concentrations at the inflection point. This simple model deals with some simplifications but it makes a quantification of a binding affinity accessible. A number of more detailed models have been suggested to better determine the binding strength. They take into account finite size of the ions, ion-ion interaction, solvent effects, hydration etc. (Cevc, 1990). Data of the ABs for these parameters are, however, not available, preventing the use of more refined models.

The limiting zeta potentials ζ_{min} of around –100 mV is reached for HxAB from a concentration of 0.3 mM. Such negative ζ potentials have rarely been observed before for liposomes. For example, previously DMPC liposomes have been incubated with the doubly negatively charged boron cluster BSH ($B_{12}H_{11}SH^{2-}$), which differs from the clusters investigated here inasfar as the trialkylammonio group has been replaced by a sulfhydryl group, and ζ potentials of -35 mV were observed (Awad et al., 2009). Thus the limiting potentials found here for high concentrations of the alkylated substances were quite surprising. For negatively charged liposomes prepared from arsonolipids, ζ potentials of about -50 mV have been observed at pH 7.0 (Fatourus et al., 2005), and liposomes made from lipids containing the dodecaborate cluster as headgroup (Justus et al., 2007) show a ζ potential of -67 mV, also these considerably less negative than the values here. Only for particles from pure phosphatidylserine, ζ potentials of –100 mV have been observed at low ionic strength (Ermakov, 1990).

The limiting zeta potentials ζ_{min} of the other compounds are only obtained from the curve fitting procedure, and are not actually measured. The limiting zeta potential ζ_{min} would be reached at compound/lipid ratios exceeding 16:1, which is the ratio used in cryo-TEM. At such ratios, mixtures of smaller structures and large bilayer sheets are present.

An explanation for the low ζ potential is not obvious, but would rather require a more detailed molecular modeling of potential ways of interaction between the clusters and the lipid surface.

The DSC profile is an excellent indicator to identify and analyze interactions with liposomal membranes in more detail. Normally the pre-transition gives rise to a broad endothermic peak. For the main transition a sharp, intense endothermic peak is expected. The transition passes different states from a highly ordered gel state ($L_ß$) to a so called rippled gel phase and finally to a non-ordered liquid crystalline phase ($L_α$) (Koynova, Caffrey, 1998). A compound that interacts with the headgroups will affect the pre-transition. The main transition is a consequence of the chain melting (Biruss et al., 2007).

In the case of MeAB the pre-transition disappears completely already at concentrations which are sub-stoichiometric with respect to the number of available headgroups. The main transition is only slightly shifted to lower temperatures, but this indicates that the fluid state ($L_α$) is somewhat favored thermodynamically in the presence of MeAB. The main transition peak decreases in size and slightly broadens. The broadening may indicate the presence of liposomes of different sizes and lamellarity, in co-existence with bilayers (Biltonen and Lichtenberg, 1993). In regard to these data we suggest that the singly negatively charged MeAB derivative interacts only with the positively charged choline headgroups of the DPPC and does not interfere with the lipid tails.

After incubation with the HxAB the enthalpy of the main transition observed is greatly reduced and the temperature interval is broadened at small HxAB concentrations and disappears completely at higher HxAB concentrations.

Many different classes of compounds are known to influence the thermotropic behavior of lipid bilayers. Steroid hormones and their analogs tend to shift the the pre-transition and the main transition to lower values. A broadening of the main transition peak is commonly observed but the transition does not disappear completely (Biruss et al., 2007; Korkmaz, Severcan, 2005). In contrast, Triton X-100, as an example for a detergent, causes with increasing concentration a gradual broadening and finally a complete loss of the transition peaks.. The width of the transition peak is considered to reflect the cooperativity of the transition (Chapman, 1975) and a broadening of the peak suggests a reduction in cooperativity (Goňi et al., 1986). Perfluorinated drugs (PFOS) also show the same effect on DPPC liposomes (Lehmler, Bummer, 2004; Lehmler et al., 2006). Triton X-100 and PFOS penetrate and incorporate into the bilayer. For the PFOS is suggested that the anionic part is most likely located at the lipid-water interface whereas the perfluorinated tails interfere with the palmitoyl chains of DPPC which cause to a significant disruption of the packing of the tails of DPPC and reduces van der Waals interactions. HxAB appears to act as a powerful detergent, somewhat similar to Triton X-100 and PFOS.

The existing data allow the following hypothesis for the interaction between the N-trialkylammonioundecahydrododecaborates and the liposome membrane. In general, the doubly negatively charged dodecaborate cluster unit interacts with the positively charged choline headgroups and the positively charged ammonium group might be in contact with the deeper-laying negatively charged phosphate. In the case of short alkyl chains, e.g. MeAB, no interferences with the lipid tails are involved and the interaction might be predominantly electrostatic in its nature. Additional effects, such as a possible change in the water layer immediately around the surface, cannot be excluded.

As the length of the alkyl chains increases, the N-trialkylammonioundecahydrododecaborates can interact not only with the head group region, but also with the deeper lying hydrophobic part of the membrane. Thus, electrostatic, as well as lipophilic interactions, between the substance and the membrane now become possible.

This hypothesis is in line with the results of the DSC measurements. In addition, the gradient of the dissociation constant can also be explained, thus additional lipophilic interactions for ABs with longer alkyl chains makes the binding to the liposome surface more favorable.

The lipid mixing experiment demonstrates that MeAB induces a fusion process that involves intermixing of the membrane components (Rosenberg et al., 1983). In order to induce 100% lipid mixing 40 mM of MeAB was required in a sample with a total lipid concentration corresponding to 19.2 mM. Previously we have shown that BSH induces lipid mixing in samples containing DMPC liposomes only at concentrations of over 50 mM, and that this process occurred to roughly the same extent in the temperature range 15-41°C, and only slightly less at 5°C (Awad et al., 2009). It should be noted that BSH carries two negative charges, and MeAB only one. Also the phase transition temperature of the lipid used here is higher than that of DMPC which was used before.

The bilayers which are seen in the cryo-TEM pictures are obviously the product of a fusion process, as the concentration of MeAB in this experiment was sufficient to induce 100 % lipid mixing. EtAB was not tested in the fusion experiment, but the formation of bilayers, as revealed by cryoTEM, makes this process highly probable also for these compounds.

Recently we reported that the N-trialkylammonioundecahydrododecaborates are able to induce leakage from liposomes. Also with respect to leakage, substances with longer alkyl chains are more effective, just as the apparent binding constant increases with increasing alkyl chain length (Schaffran et al., 2009).

We have shown before that leakage from DPPC liposomes occurs also when fusion processes are prevented by the incorporation of PEG chains into the liposomal membrane (Gabel et al., 2007). Fusion and leakage thus appear to be independent processes, and the latter might be the result of transient defects and holes (Schaffran et al., 2009). This has also been suggested for the nonionic surfactant octyl-*β*-D-glucopyranoside (Lesieur et al., 2003).

We observe that with increasing chain length the binding to the liposome surface is more favored and at the same time the concentrations required for leakage decrease (Schaffran et al., 2009). Surface binding and leakage correlate: ABs with longer alkyl chains are more powerful in the leakage induction; at the same time, they bind more strongly to the liposome surface.

Conclusion

This study demonstrates that *N,N,N*-trialkylammonioundecahydrododecaborates are able to interact with the liposomes. The association to the liposomal membrane becomes stronger with increasing alkyl chain length. In case of MeAB and EtAB the binding is most likely brought about by electrostatic interactions between the doubly negatively charged cluster unit and the positively charged choline headgroup; and the positively charged ammonium group might be in contact with the deeper-lying negatively charged phosphate. We propose that *N,N,N*-trialkylammonioundecahydrododecaborates with longer alkyl chains, such as HxAB and BuAB, are able to interact, in addition to the electrostatic component, with the membrane through their hydrophobic tails. The binding of the alkylated substances leads at high compound concentration to dramatic changes in the morphology. ILs with short alkyl chains produce large bilayer sheets, whereas those with longer alkyl chains tend to induce the formation of open or multi-layered liposomes.

There is no correlation between leakage and lipid mixing. Both processes are independent from each other. Leakage is most probably induced by pore formation, based on its kinetics Leakage and the dissociation constants correlate qualitatively, thus higher affinity to the liposomal surface leads to a decrease of concentration required for leakage induction.

Data of the present study show that interactions between ABs and the liposomal membrane exist and consequently interactions with other membranes (e.g. cell membranes) must be

assumed. Therefore the cell membrane might be the place for toxic interactions of the ABs. Different modes of toxic actions, however, are feasible. On the one hand the binding of ABs to the cellular membrane will result in a higher negative membrane potential. The polarity of the plasma membrane controls the extracellular/intracellular exchange of information, and changes should lead to a different cell behavior. It is known, e.g., that the function of ion channels located in the cell membrane depends on the membrane potential and therefore the influx/efflux of ions will be affected by changes in the potential. These alterations, however, must not necessarily be toxic when the integrity of the membrane is retained (de Nicola et al., 2008; White et al., 2000). On the other hand, the ability of the ABs to induce leakage by pore formation might affect the permeability of the cell membrane and consequently influence the cell function. As an example, the peptide BTM-P1 also forms pores and thereby influences the affected cells (Arias et al., 2009). In addition, ABs with long alkyl chains, such as BuAB and HxAB, show a detergent-like behavior. Therefore a complete disruption of the cell membrane after addition of these ABs cannot be excluded. All these effects can explain the cellular toxicity of the ABs which we found in a previous study (Schaffran et al., 2009).

Acknowledgment

The authors thank Dr. Denise Ferreira for providing some of the cryo-TEM pictures. We are also grateful for the gift of lipids from Lipoid GmbH, Ludwigshafen, Germany. D.G. acknowledges support from the German Research Foundation DFG and the German Academic Exchange Service DAAD. K.E. gratefully acknowledges financial support from the Swedish Research Council, the Swedish Cancer Society, and the Swedish Foundation for International Cooperation in Research and Higher Education STINT.

References

Abraham, S.A., Edwards, K., Karlsson, G., MacIntosh, S., Mayer, L.D., McKenzie, C., Bally, M.B., 2002. Formation of transition metal-doxorubicin complexes inside liposomes. Biochim. Biophys. Acta.1565, 41–54.

Almgren, M., Edwards, K., Karlsson, G., 2000. Cryo transmission electron microscopy of liposomes and related structures. Colloids Surf., A 174, 3-21.

Arias, M., Orduz, S., Lemeshko, V.V., 2009. Potential-dependent permeabilization of plasma membrane by the peptide BTM-P1 derived from the Cry11Bb1 protoxin. Biochim. Biophys. Acta. Biomembr. 1788, 532-537.

Awad, D., Damian, L., Winterhalter, M., Karlsson, G., Edwards, K., Gabel, D., 2009. Interaction of $Na_2B_{12}H_{11}SH$ with dimyristoyl phosphatidylcholine liposomes. Chem. Phys. Lipids 157, 78-85.

Azev, Y.A., Lork, E., Duelcks, T., Gabel, D., 2004. New possibilities of 1,2,4-triazines functionalization: first examples of synthesis and structure of boron-containing 1,2,4-triazines. Tetrahedron Lett. *45*, 3249-3252.

Bähr G, Diederich A, Vergères G, Winterhalter M., 1998. Interaction of peptides corresponding to the effector domain of MARCKS and MRP with different model membrane systems. Biochemistry 37, 16252-16261.

Biltonen, R.L., Lichtenberg, D.,1993. The use of differential scanning calorimetry as a tool to characterize liposome preparations. Chem. Phys. Lipids 64, 129-142.

Biruss, B., Dietl, R., Valenta, C., 2007. The influence of selected steroid hormones on the physicochemical behaviour of DPPC liposomes. Chem. Phys. Lipids 148, 84-90.

Cevc, G., 1990. Membrane electrostatics. Biochim. Biophys. Acta 1031, 311-382.

Chapman, D., 1975. Phase transitions and fluidity characteristics of lipids and cell membranes. Q. Rev. Biophys. 8, 185-235.

Clement, J., Kiefer, K., Kimpfler, A., Garidel, P., Peschka-Süss, P., 2005. Large-scale production of lipoplexes with long shelf-life. Eur. J. Pharm. Biopharm. 59, 35-43.

Cohen, J.A., Gabriel B, Teissie J, Winterhalter M. 2003. Transmembrane voltage sensor. In *Planar Lipid Bilayers and their applications* by Tien, T Ti, Ottova-Leitmannova, A. pp. 847-886, Elsevier, New York.

De Nicola, M., Bellucci, S., Traversa, E., De Bellis, G., Micciulla, F., Ghibelli, L., 2008.Carbon nanotubes on Jurkat cells: effects on cell viability and plasma membrane potential. J. Phys. Condens. Matter 20, 474204-474212.

Endres, F., 2002. Ionic liquids: Solvents for the electrodeposition of metals and semiconductors. ChemPhysChem 3, 144-154.

Ermakov, Y.A., 1990. The determination of binding site density and association constants for monovalent cation adsorption onto liposomes made from mixtures of zwitterionic and charged lipids. Biochim. Biophys. Acta 1023, 91-97.

Fatourus, D.G, Klepetsanisa, P., Ioannou P.V., Antimisiaris S.G., 2005. The effect of pH on the electrophoretic behavior of a new class of liposomes: arsonoliposomes. Int. J. Pharm. 288, 151-156.

Gabel, D., Awad, D., Schaffran, T., Radovan, D., Daraban, D., Damian, L., Winterhalter, M., Karlsson G., Edwards K., 2007. The anionic boron cluster $(B_{12}H_{11}SH)^{2-}$ as a means to trigger release of liposome contents. ChemMedChem 2, 51-53.

Goňi, F.M., Urbaneja, M.-A., Arrondo, J.L.R., Alonso, A., Durrani, A.A., Chapman, D., 1986. The interaction of phosphatidylcholine bilayers with Triton X-100. Eur. J. Biochem. 160, 659-665.

Heerklotz, H., 2008. Interactions of surfactants with lipid membranes. Q. Rev. Biophys. 41, 205-264.

Johansson, E., Sandström, M.C., Bergström, M., Edwards, K., 2008. On the formation of versus threadlike micelles in dilute aqueous surfactant/lipid systems. Langmuir 24, 1731-1739.

Justus E., Rischka, K., Wishart, J.F, Werner, K., Gabel, D., 2008. Trialkylammoniododecaborates: Anions for ionic liquids with potassium, lithium and protons as cations. Chem. Eur. J. 14, 1918-1923.

Koynova, R., Caffrey, M., 1998. Phases and phase transitions of the phosphatidylcholines. Biochim. Biophys. Acta. 1376, 91-145.

Korkmaz, F., Severcan, F., 2005. Effect of progesterone on DPPC membrane: Evidence for lateral phase separation and inverse action in lipid dynamics. Arch. Biochem. Biophys. 440, 141-147.

Larsen, A.S., Holbrey, J.D., Tham, F.S., Reed, C.A., 2000. Designing ionic liquids: Imidazolium melts with inert carborane anions. J. Am. Chem. Soc. 122, 7264-7272.

Lehmler, H.-J., Bummer, P.M., 2004. Mixing of perfluorinated carboxylic acids with dipalmitoylphosphatidylcholine. Biochim. Biophys. Acta. 1664, 141-149.

Lehmler, H.-J., Xie, W., Bothun, G.D., Bummer, P.M., Knutson, B.L., 2006. Mixing of perfluorooctanesulfonic acid (PFOS) potassium salt with dipalmitoyl phosphatidylcholine (DPPC). Colloids Surf., B, 51, 25-29.

Lesieur, S., Grabielle-Madelmont, C., Ménager, C., Cabuil, V., Dadhi, D., Pierrot, P. and Edwards, K., 2003. Evidence of surfactant-induced formation of transient pores in lipid bilayers by using magnetic-fluid-loaded liposomes. J. Am. Chem. Soc. 125, 5266-5267.

Letrou-Bonneval, E., Chèver,R., Lambert, O., Costet, P., André, C., Tellier, C. and Pitard, B. (2008) Galactosylated multimodular lipoplexes for specific gene transfer into primary hepatocytes. J. Gene Med. 10, 1198-1209.

Macdonald, P.M. and Seelig, J., 1988. Anion binding to neutral and positively charged lipid membranes. Biochemistry 27, 6769-6775.

Paternostre, M., Meyer, O., Grabielle-Madelmont, C., Lesieur, S., Ghanam, M., Ollivon, M., 1995. Partition coefficient of a surfactant between aggregates and solution: Application to the micelle-vesicle transition of egg phosphatidylcholine and octyl β-D-Glucopyranoside. Biophys. J. 69, 2476-2488.

Ramírez, L.P., Antonietti, M., Landfester, K., 2006. Formation of novel layered nanostructures from lanthanide-complexes by secondary interactions with ligating monomers in miniemulsion droplets. Macromol. Chem. Phys. 207, 160-165.

Ronig, B., Pantenburg, I., Wesemann, L., 2002. Meltable Stannaborate Salts. Eur. J. Inorg. Chem., 319-322.

Rosenberg, J., Düzgünes, N., Kayalar, C., 1983. Comparison of two liposome fusion assays monitoring the intermixing of aqueous contents and of membrane components. Biochim. Biophys. Acta. 735, 173-180.

Schaffran, T., Justus, E.; Elfert, M., Chen, T., Gabel, D., 2009. Toxic actions in biological by *N,N,N*-trialkylammoniododecaborates as new anions of ionic liquid. Green Chem., doi: 10.1039/b906165g (in the press)

Sheldon, R., 2001. Catalytic reactions in ionic liquids. *Chem. Commun*. 23, 2399-2407.

Stewart, J.C., 1980. Colorimetric determination of phospholipids with ammonium ferrothiocyanate. Anal. Biochem. 104, 10-14.

Stolte, S., Arning, J., Bottin-Weber, U., Matzke, M., Stock, F., Thiele, K., Uerdingen, M., Welz-Biermann, U., Jastorff, B. , Ranke, J., 2006. Anion effects on the cytotoxicity of ionic liquids. Green Chem. 8, 621-629.

Vanderwerf, P., Ullman, E.F., 1980. Monitoring of phospholipid vesicle fusion by fluorescence energy transfer between membrane-bound dye labels. Biochim. Biophys. Acta. 596, 302-314.

Wasserscheid, P., Keim, W., 2000. Ionic liquids – New “solutions“ for transition metal catalysis. Angew. Chem. Int. Ed. 39, 3772-3789.

Welton, T., 1999. Room-temperature ionic liquids. Solvents for synthesis and catalysis Chem Rev. 99, 2071-2084.

White, P.J., Piñeros, M., Tester, M., Ridout, M.S., 2000. Cation permeability and selectivity of a root plasma membrane calcium channel. J. Membrane Biol. 174, 71-83.

Zhu, Y., Ching, C., Carpenter, K., Xu, R., Selvaratnam, S., Hosmane, N.S., Maguire, J.A., 2003. Synthesis of the novel ionic liquid [*N*-pentylpyridinium]$^{+}$ [*closo*-$CB_{11}H_{12}$]$^{-}$ and its usage as a reaction medium in catalytic dehalogenation of aromatic halides. Appl. Organometal. Chem. 17, 346-350.

III

Dodecaborate cluster lipids with variable head groups for boron neutron capture therapy: Synthesis, physical-chemical properties and toxicity

published in Journal of Organometallic Chemistry

Journal of Organometallic Chemistry 694 (2009) 1708–1712

Contents lists available at ScienceDirect

Journal of Organometallic Chemistry

journal homepage: www.elsevier.com/locate/jorganchem

Dodecaborate cluster lipids with variable headgroups for boron neutron capture therapy: Synthesis, physical–chemical properties and toxicity

Tanja Schaffran [a,*], Franziska Lissel [a], Brighton Samatanga [b], Göran Karlsson [c], Alexander Burghardt [d], Katarina Edwards [c], Mathias Winterhalter [b], Regine Peschka-Süss [d], Rolf Schubert [d], Detlef Gabel [a]

[a] Department of Chemistry, University of Bremen, Leobener Str. NW2 C3020, D-28357 Bremen, Germany
[b] School of Science and Engineering, Jacobs University Bremen, D-28725 Bremen, Germany
[c] Institute of Physical and Analytical Chemistry, Uppsala University, S-75123 Uppsala, Sweden
[d] Institute of Pharmaceutical Sciences, Department of Pharmaceutical Technology and Biopharmacy, University of Freiburg, D-79104 Freiburg, Germany

ARTICLE INFO

Article history:
Received 31 October 2008
Received in revised form 17 December 2008
Accepted 18 December 2008
Available online 25 December 2008

Keywords:
Boron neutron capture therapy
Boron cluster
Lipid
Liposome
Toxicity

ABSTRACT

We have prepared two new boron-containing lipids with potential use in boron neutron capture therapy of tumors. These lipids consist of a diethanolamine frame with two myristoyl chains bonded as esters, and a butylene or ethyleneoxyethylene unit linking the doubly negatively charged dodecaborate cluster to the amino function of the frame, obtained by nucleophilic attack of the amino on the tetrahydrofurane and dioxane derivatives, respectively, of *closo*-dodecaborate. The latter cluster lipid can form liposomes at 25 °C whereas the former lipid at this temperature assembles into bilayer disks. Both lipids form stable liposomes when mixed with suitable helper lipids. The thermotropic behavior was found to be different for the two lipids, with the butylene lipid showing sharp melting transitions at surprisingly high temperatures. Toxicity *in vitro* and *in vivo* varies greatly, with the butylene derivative being more toxic than the ethyleneoxyethylene derivative.

1. Introduction

Boron neutron capture therapy (BNCT) is a radiation therapy for cancer treatment. The short ranged charged particles which are generated in the nuclear reaction between the nontoxic species ^{10}B and thermal neutrons have a great biological effect within the cancer cell. For successful treatment a high amount of boron (approx. 20–30 μg of boron-10 per gram of tumor) and a sufficiently selective accumulation is necessary. Several strategies have been investigated for the boron transfer system, e.g., antibodies [1], nucleic acid precursors [2] and porphyrin derivatives [3].

Liposomes show selective localization in tumors [4] and might be useful vehicles for boron transfer. In general it is possible to encapsulate low-molecular boron substances in the aqueous core of the liposomes or to incorporate boron-containing lipids in the liposomal membrane. The encapsulation method has been described in the literature [5], but this procedure holds some disadvantages. These include a sometimes low encapsulation efficiency, and leakage upon storage or in contact with serum. Further, it was recently shown that charged boron cluster compounds can profoundly affect the structure of liposomes [6]. These problems can be avoided by incorporating boron-containing lipids directly into liposomal membranes.

Only a few boron lipids are described in the literature. Lemmen et al. [7] reported a carborane-containing ether lipid which showed neither tumor selectivity nor retention in tumor tissue. Nakamura et al. [8] described a nido-carborane cluster lipid with a double tailed moiety which was tolerated well in mice [9]. A very similar lipid had been published later by Li et al. [10] but it turned out to be very toxic in mice.

The first dodecaborate ether lipid was described by Lee et al. [11]. Based on mercapto-undecahydro-*closo*-dodecaborate (BSH) different boron lipids have been synthezised. BSH is clinically used for BNCT and has a low toxicity. The boron lipids are expected to show a similar low toxicity. In 2007 Nakamura et al. [12] published a *closo*-dodecaborate-containing lipid. The boron lipids form liposomes in the presence of helper lipids. Recently we described two novel dodecaborate lipids [13]. Both lipids could be formulated into liposomes by use of the helper lipids DSPC (distearoylphosphatidylcholine) and cholesterol. One of the lipids, B-6-14, was shown to form liposomes also in the absence of helper lipids. The lipids were found to be nontoxic *in vitro*.

The existing dodecaborate lipids have a double negative charge. In this study we focused on lipids carrying only a single negative net charge; furthermore, we investigated the effect of different linkers between the dodecaborate cluster head group and the lipid

* Corresponding author.
E-mail address: t.schaffran@web.de (T. Schaffran).

0022-328X/$ - see front matter © 2009 Elsevier B.V. All rights reserved.
doi:10.1016/j.jorganchem.2008.12.044

backbone. These lipids differ from the lipid B-6-14 previously described by us [13] with respect to the net charge, the linker between the cluster and the hydrophobic moiety.

2. Experimental

2.1. General

A Bruker Esquire spectrometer was used for electrospray mass spectrometry. For boron-containing compounds the peak with the highest mass is declared. To identify the charge of the compound isotope satellite peaks are used. NMR spectra were recorded on a Bruker DPX 200 spectrometer. IR spectra were collected on a BioRad FTS 155 using KBr pellet. Melting points were measured on a Büchi 512 melting point apparatus.

3. Chemistry

3.1. 1-Tetramethylene-(3-oxa)-oxonium-closo-undecahydrododecaborate (-1), tetrabutylammonium salt (1a)

The convenient method recently described was used, in which *closo*-dodecaborate was reacted with hydrogen chloride in 1,4-dioxane in the presence of $NaBF_4$ [14].

3.2. 1-Tetramethyleneoxonium-closo-undecahydrododecaborate (-1), tetrabutylammonium salt (1b)

The method as for **1a** was used, but replacing hydrogen chloride with *p*-toluenesulfonic acid.

3.3. 4-(N,N-bis(2-hydroxyethyl)-N-ethoxy-ammonium)-ethoxy-undecahydro-closo-dodecaborate (-1), cesium salt (2a)

Compound **1a** (0.5 g, 1.05 mmol) and diethanolamine (2 equiv., 0.22 g, 2.1 mmol) were dissolved in dry acetonitrile and then heated to 82 °C for 4 days. The solvent was evaporated and the residue dissolved in methanol. After addition of cesium fluoride (1.5 equiv., 0.24 g, 1.58 mmol) which was dissolved in methanol a white precipitate was formed and filtrated. The product was dried in oil pump vacuum. Yield 0.465 g (95%), m.p. above 245 °C. MS (ESI, acetonitrile, *m/z*) negative 332.1 [A^--H_2], 355.8 [A^--H^++Na^+], 466 [A^--H^++Cs^+]; positive 132.8 [Cs^+], 467.2 [A^-+Cs^++H^+], 600.1 [A^-+2 Cs^+]. NMR measurements were not very easy for **2a**, due to the formation of micelles.

^{1}H NMR (200 MHz, ([D_3] CD_3CN, 25 °C, TMS): δ = 3.3 (m, 6H, –O–CH_2–CH_2–O–CH_2–), δ = 3.63 (m, 4H, –CH_2–O–), δ = 3.86 (m, 6H, –N^+–(CH_2)$_3$), δ = 4.19 (m, 1H, –NH^+–). ^{13}C NMR (200 MHz, [D_6] DMSO, 25°C, TMS): δ = 52.84, 55,76, 67.67, 71.34. ^{11}B NMR (200 MHz, [D_6] DMSO, 25 °C): –22.9 (1B), –17.91 (5B), –16.65 (5B), 7.01 (1B). IR (KBr): ν = 3404 (–O–H), 2869 (C–H), 2484 (B–H), 1623 (–N–H), 1460 (C–H), 1163 (–C–N–), 1066 (–C–O–C–; –B–O–C–).

3.4. 4-(N,N-bis(2-hydroxyethyl)ammonium)-butoxy-undecahydro-closo-dodecaborate (-1), cesium salt (2b)

Similar to **2a**. Yield 0.45 g (94%), m.p. above 245 °C. MS (ESI, acetonitrile, *m/z*) negative 318.0 [A^-]; positive 132.9 [Cs^+]. Also for **2b**, NMR measurements were not very, due to the formation of micelles.

^{1}H NMR (200 MHz, [D2] D2O, 25 °C, TMS): δ = 1.41–1.79 (m, 6 H, –O–CH_2–CH_2 –CH_2–), 3.20–3.36 (m, 6 H, –N^+–(CH_2)$_3$), 3.48 (m, 1H, –NH^+–), 3.88 (m, 4H, –CH_2–O–). ^{13}C NMR (200 MHz, [D6] DMSO, 25 °C, TMS): δ = 24.59, 30.85, 55.24, 56.56, 58.50, 69.00. ^{11}B NMR (200 MHz, [D_6] DMSO, 25 °C): –22.52 (1B), –17.74–(–16.83) (10B), 6.60 (1B).

IR (KBr): ν = 3404 (–O–H), 2940 (C–H), 2865 (C–H), 2482 (B–H), 1631 (–NH–), 1464 (C–H), 1150 (–C–N–), 1059 (–B–O–C–).

3.5. 4-(N,N-bis(2-myristoyloxyethyl)-N-ethoxy-ammonium)-ethoxy-undecahydro-closo-dodecaborate (-1), cesium salt (B-Dioxan-14)

Compound **2a** (0.3 g, 0.643 mmol) was suspended in dry acetonitrile and a 60% suspension of NaH (3.5 equiv., 0.09 g, 2.25 mmol) was added under N_2 atmosphere. The mixture was heated to 70 °C and stirred for 2 h. After cooling, myristoyl chloride (3 equiv., 0.476 g, 1.93 mmol) was added and stirred for 24 h. A precipitate was removed by filtration, followed by evaporation of the solvent. The residue was dissolved in hot methanol. The product **3a** precipitated upon cooling, was filtrated and dried in oil pump vacuum. Yield 0.228 g (40%) MS (ESI, acetonitrile, *m/z*) negative 752.6 [A^-–H_2], 776.6 [A^-–H^++Na^+], 792.6 [A^-–H^++K^+], 886.5 [A^-–H^++Cs^+]; positive 132.9 [Cs^+], 596.6 [A^-–$B_{12}H_{11}O$]. $^{1H\ NMR}$ (200 MHz, [D_1] $CDCl_3$, 25 °C, TMS): 0.89 (m, 6H, –CH_3), 1.26 (m, 44 H, –(CH_2)$_{11}$–CH_3), 1.59 (m, 6H, B–O–CH_2–, –CH_2–C=O), 2.36 (m, 4H, –CH_2–O–C=O), 3.61–3.95 (m, 7H, –CH_2–O–CH_2–, –CH_2–N^+–), 4.57 (m, 4H, –NH^+–, –CH_2–N^+–). ^{13}C NMR (200 MHz, ([D_1] $CDCl_3$, 25 °C, TMS): δ = 14.78, 23.76, 25.87, 30.75, 33.03, 34.96, 52.96, 53.89, 64.19, 70.51, 70.96, 174.19. ^{11}B NMR (200 MHz, ([D_6] DMSO, 25 °C): –21.85 (1B), –17.00 (10B), 6.49 (1B). IR (KBr): ν = 2920 (C–H), 2851 (C–H), 2482 (B–H), 1741 (–C=O), 1645 (–NH–), 1469 (C–H), 1170 (–C–N–), 1028 (–C–O–C–; –B–O–C–).

3.6. 4-(N,N-bis(2-myristoyloxyethyl)ammonium)-butoxy-undecahydro-closo-dodecaborate (-1), cesium salt (B-THF-14)

Prepared as described for **B-Dioxan-14.** Yield 0.196 g (35%) MS (ESI, acetonitrile, *m/z*) negative 737.7 [A^-]; positive 132.9 [Cs^+], 580.6 [A^-–$B_{12}H_{11}O$], 1004 [A^-+2Cs^+].

1H NMR (200 MHz, [D_6] DMSO, 25 °C, TMS): δ = 0.86 (m, 6H, –CH_3), 1.24 (m, 48H, –(CH_2)$_{11}$–CH_3, –CH_2–CH_2–), 1.48 (m, 6H, B–O–CH_2–, –CH_2–C=O), 2.18 (t, 4H, –CH_2–O–C=O), 2.80–3.80 (m, 6H, –CH_2–N^+–), 4.40 (m, 1H, –NH^+–). ^{13}C NMR (200 MHz, ([D_1] $CDCl_3$, 25 °C, TMS): 14.78, 23.79, 25.98, 30.58, 33.03, 34.54, 53.35, 55.23, 59.92, 69.97, 72.67, 175.57. ^{11}B NMR (200 MHz, [D_6] DMSO, 25 °C): –23.11 (1B), –18.15 to –16.62 (10B), 6.87 (1B). IR (KBr): ν = 2917 (C–H), 2850 (C–H), 2483 (B–H), 1850–1705 (–C=O), 1468 (C–H), 1306 (–C–N–), 1172 (–C–N–), 1056 (–B–O–C–).

4. Preparation of liposome samples

The boron-containing lipids were either used in pure form or mixed with equal molar amounts of DPPC and cholesterol. The lipid, or lipid mixture (DPPC/cholesterol/boron lipid (1:1:1)), was dissolved in chloroform and dried to a thin lipid film in a round-bottom flask. Then the lipid film was hydrated and dispersed by vortexing in 10 mM HEPES buffer saline, pH 7.4 (150 mM NaCl, 10 mM HEPES). The resulting suspension was frozen and thawed in 10 cycles followed by extrusion (21 times) through a polycarbonate membrane with a pore diameter of 100 nm (Avestin, Mannheim, Germany) at a temperature of 64 °C.

Final lipid concentration was 10 mM. Lipid content was measured by the Stewart assay [15], using appropriate standard curves for the individual lipids.

For DSC measurements, the pure lipids were dispersed from a lipid film (obtained as described above) by hydration with 10 mM HEPES 100 mM NaCl, pH 7.4, through ten freeze–thaw cycles and stored at 4 °C prior to measurement.

4.1. Cryotransmission electron microscopy (cryo-TEM)

A small amount (~1 μl) of the liposome suspension (final lipid concentration 5 mM) was transferred to a polymer-coated copper grid and shock-frozen from 25 °C by injection into liquid ethane. The vitrified sample was examined in Zeiss EM 902 A electron microscopes, operating at an accelerating voltage of 80 keV in filtered bright field image mode at $\Delta E = 0$ eV. The stage temperature was kept below 108 K, and images were recorded at defocus settings between 1 and 3 μm. Images were recorded by a slow scan charge-coupled device (SSCCD) camera using the minimal dose focusing device. To assess the reproducibility of the results several images were recorded in different areas of the specimen.

4.2. Differential scanning calorimetry measurements

Differential scanning calorimetry (DSC) measurements were carried out on a VP-DSC microcalorimeter from Microcal (Northhampton, MA), using the pure boron lipid (final lipid concentration 5 mM). The samples were degassed under vacuum prior to the measurement. For the up- and downscans a scan rate of 60 °C/h and a filtering period of 2 s were used. From each scan a buffer background scan was subtracted. For data analysis, the software package ORIGIN (Microcal) was used. The buffer system for this measurement was 10 mM HEPES with 100 mM sodium chloride.

4.3. Cytotoxicity assay

The cell line V79 (lung fibroblasts of Chinese hamster) was used and cultivated with Hams F10 medium and 10% newborn calf serum at 37 °C and 5% CO_2. 11.000 cells per well were seeded into 96-well plates and grown for 24 h. Then the cells were incubated with different concentrations of boron-containing liposomes for 24 h. Liposomal formulation of DPPC/cholesterol/boron lipid (1:1:1) was used. The cell survival was determined with the WST-1 test system. The supernatant was removed and 100 μl of a WST-1 stock solution (1:4 diluted with PBS and further 1:10 with medium) per well were filled. After 4–6 h the absorbance was measured at 450 nm.

The IC_{50} values were obtained by fitting a sigmoidal curve with the following equation:

$$f = \frac{a}{(1 + e^{-(x - IC_{50})/b})}$$

in which f corresponds to the percentage survival of cells, a corresponds to the highest point of response, x to the concentration of the tested substance, b to the slope of the response curve, and IC_{50} to the concentration of the tested substance that provokes 50% cell death.

4.4. Animal experiments

Animal experiments were carried out with Balb/c mice bred specifically for scientific purposes, following the legally required permission by the government of the Free Hanseatic City of Bremen. Animals were housed in cages with ample access to water and food.

Liposomes (100 μl) were injected into the tail vein of female Balb/c mice. The animals were observed for acute toxicity for 24 h.

5. Results and discussion

In this work, two new lipids were synthesized which differ from the lipid B-6-14 previously described by us [13] by carrying only one negative net charge. The lipids consist of a double-tailed moiety and a dodecaborate cluster as head group, connected with different spacers. The synthesis requires the connection between a derivative of the $B_{12}H_{12}^{2-}$ cluster and a lipid backbone. We used nucleophilic ring opening reactions between the tetrahydrofurane (THF) and dioxane derivatives of the cluster and the secondary amine diethanolamine (Scheme 1).

Semioshkin et al. [16] recently reported reactions of oxonium derivatives with amines, but under different conditions and not applied to boron lipids. The lipid moiety prepared here is similar to that of the recently published lipids B-6-14 and B-6-16 [13].

For the ring opening reactions the THF- or dioxane derivative of the cluster reacts with 2 equiv. diethanolamine followed by an esterification at the hydroxyl groups with the acid chloride (Scheme 1) The first reaction step proceeds with a yield of 94–95% and the esterification, with 35–40%. Both new dodecaborate cluster lipids contain the same lipid backbone and the same head groups, but varying linkers between them.

The phase transition temperature of the pure B-THF-14 lipid was determined with differential scanning calorimetric measurements (DSC) (Fig. 1) A sharp peak at 48.9 °C and a small pre-transition peak at 46 °C is observed. These temperatures are not comparable to other lipids containing the same hydrophobic part. Dimyristoylphosphatidylcholine (DMPC) with the same alkyl chain length has a transition temperature of 24.3 °C. The dodecaborate lipid B-6-14 with two myristoyl chains (recently described by us [13]) on the same diethanolamine frame (differing only in the linker to the cluster) does not exhibit a pre-transition peak and the main transition is at 18.8 °C, in the same temperature region as DMPC.

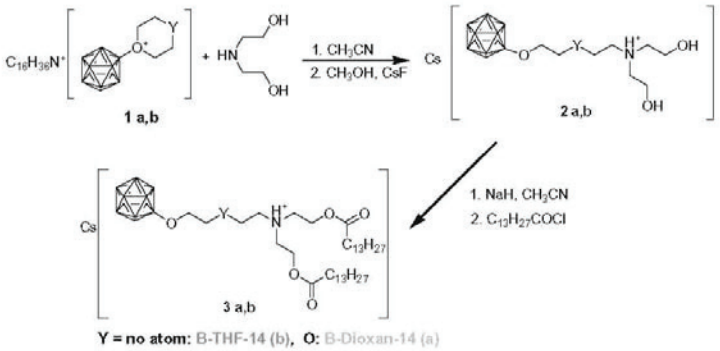

Scheme 1. Synthesis of boron lipids.

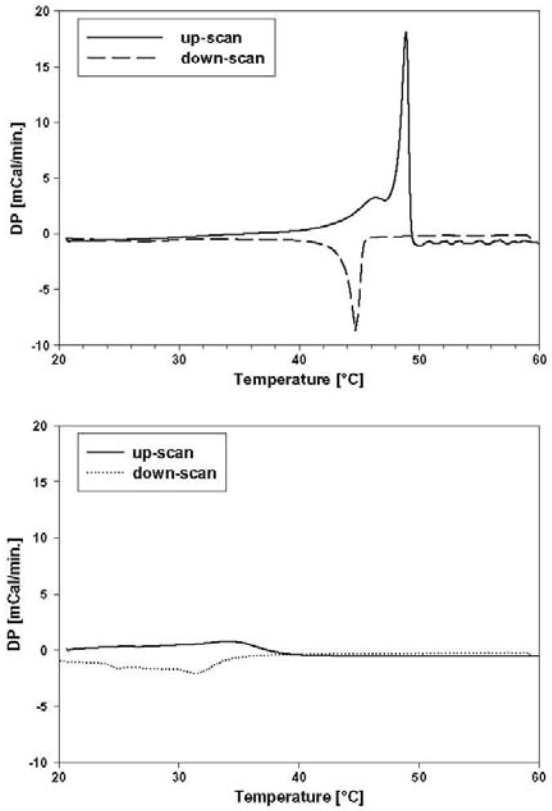

Fig. 1. DSC of pure films of B-THF-14 (above) and B-Dioxan-14 (below) (the first up-scan and the first down-scan are shown). Lipid concentration 5 mM.

The temperature difference between the transition peaks in the up- and down scan (approx. 4°C) is remarkable; such strong hysteresis effect has not been described for other lipids.

For B-Dioxan-14 a phase transition temperature could not be identified. A very broad transition between 20 and 40 °C with minimal endothermic demand is observed. Broad transitions are normally found for lipid species that are not able to form ordered, gel-phase, structures.

The transition temperature depends on both the nature of the headgroup and on the alkyl chain length. Thus DMPC with choline as headgroup has a transition at 24 °C whereas the transition temperature of DMPE with an ethanolamine headgroup lays at 57 °C [17]. B-THF-14 and B-Dioxan-14 share the same polar headgroup, i.e., the dodecaborate cluster. The transition temperature is well known to increase with longer alkyl chain length e.g., DMPC (dimyristoyl-phosphatidylcholine) (24 °C) to DSPC (distearoyl-phosphatidylcholine) (54 °C). The phase transition temperatures are different, however, for B-THF-14 and B-Dioxan-14 despite the fact that they have the same fatty acid chains. The DSC data from pure B-THF-14 and B-Dioxan-14 thus indicate that the phase transition depends also on the linker between the cluster head group and the lipid backbone.

B-Dioxan-14 displays no characteristic gel- to liquid crystalline phase transition and behaves more like a detergent in the DSC. We therefore suspect that the membrane packing is disturbed in this case, possibly due to the more hydrophilic and flexible nature of the linker.

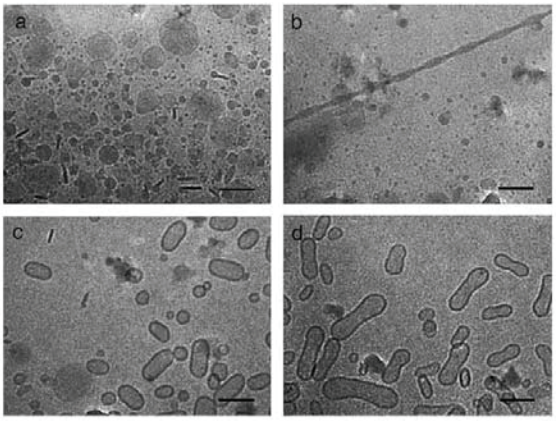

Fig. 2. Cryo-TEM pictures from pure boron lipids: (a) and (b) B-THF-14; (c) and (d) B-Dioxan-14. Scale bar 100 nm.

Cryo-TEM was used to investigate the structures formed from the pure boron lipids (Fig. 2).

B-THF-14 forms predominantly bilayer disks as can be seen in Fig. 2a. The structures are heterogeneous in size; some of them are smaller than 100 nm which is the diameter of the extrusion membrane pores. Long twisted bilayer bands are also found (Fig. 2b), but no closed vesicles could be observed. At the temperature of observation (25 °C), B-THF-14 is in the gel phase, which is less prone to allow the presence of liposomes. For comparison, samples prepared from the lipids B-6-14 and B-6-16 displayed very large bilayer sheets below the phase transition temperatures [13].

In contrast B-Dioxan-14 forms closed liposomes. Some spherical structures are observed, but most of the material is found in tubular peanut-shaped liposomes. The long axis of the tubular structures is very heterogeneous in length. Some of the tubular structures are larger than 200 nm. A few bilayer disks were found in coexistence with the liposomes.

The difference in morphology between the preparations of B-Dioxan-14 and B-THF-14 are striking. The only chemical difference between them is in the spacer linking the negatively charged cluster to the positively charged central nitrogen atom; that of B-Dioxan-14 contains an additional oxygen atom. This should increase the hydrophilicity, as well as the flexibility, of the spacer in comparison to that of B-THF-14. As the class of lipids is, however, new, a detailed molecular picture of the structure would require a molecular dynamics simulation.

Cryo-transmission electron microscopy was employed also to visualize the structure in samples where the boron-containing lipids had been mixed with helper lipids. For liposomal preparations, DPPC/cholesterol/boron-containing lipid in the molar ratio of 1:1:1 were used. DPPC is a commonly used structural component in the formulation of unilamellar liposomes. It consists of a zwitterionic choline-based headgroup and a double-tailed lipid moiety. The physical similarity between DPPC and the boron lipids makes a facile incorporation into the bilayer probable.

As shown in Fig. 3, most of the material forms unilamellar, closed vesicles which exhibit a tolerable size distribution. In the case of B-THF-14 a few multilamellar structures can be observed.

The cryo-TEM pictures demonstrate the possibility to prepare spherical and unilamellar liposomes from the present dodecaborate cluster lipids in the presence of helper lipids. By means of this liposome formulation a high amount of boron can be transferred to the cancer cells. For successful BNCT 10–30 ppm boron is required which corresponds to approx. $(1–3) \times 10^9$ boron atoms for an

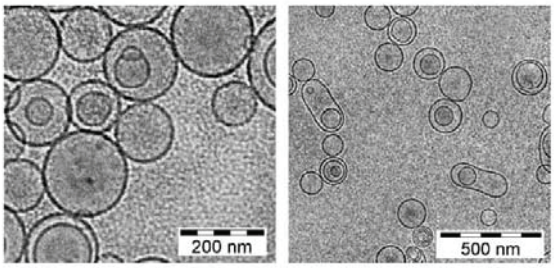

Fig. 3. Cryo-TEM pictures of DPPC/cholesterol/B-THF-14 liposomes (left) and DPPC/cholesterol/B-Dioxan-14 liposomes (right). Scale as indicated.

average mammalian cell [18]. Justus et al. [13] calculated that a 100 nm liposome with an equimolar ratio of DSPC, cholesterol and boron lipid is capable of transferring approx. 6.5×10^5 boron atoms. Only half of that number of boron atoms (3.8×10^5) can be encapsulated in 100 nm liposomes at a dodecaborate cluster concentration of 0.1 M (assuming a volume per liposome of 5.2×10^6 nm^3).

The liposomes prepared here can most probably be tagged with tumor-seeking entities [19] and thereby a selective tumor accumulation should be possible.

In an *in vitro* experiment the toxicity of B-THF-14 and B-Dioxan-14 was determined. We found that B-THF-14 inhibits the cell growth by 50% at a concentration of 0.38 mM. B-Dioxan-14 is less toxic and has an IC_{50} value of 2 mM (Fig. 4).

The liposomal formulation with boron-containing lipid/DSPC/cholesterol (molar ratio 1:1:1) and 2 mol% DSPE-PEG_{2000} was tested for toxicity in mice (0.43 mg boron in 100 μl). The liposomes were injected intravenously into the tail vein of female Balb/c mice. For B-Dioxan-14 no acute toxicity was found but B-THF-14 was lethal after a few minutes. As a consequence, the choice of the linker is an important factor for toxicity. In this case, the introduction of an ether function in the hydrocarbon spacer leads to a decrease of toxicity.

We have previously found that the *in vitro* toxicity of the dodecaborate cluster lipids B-6-14 and B-6-16 [13] decreases with increasing alkyl chain length. The preparation of the lipids B-THF-16 and B-Dioxan-16 with palmitoyl instead of myristoyl chains is in progress. Possibly, the toxicity decreases similarly.

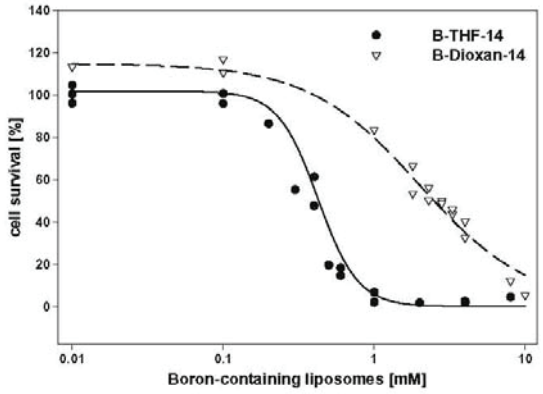

Fig. 4. Survival of V79 Chinese hamster cells exposed to B-THF-14 (circles) and B-Dioxan-14 (triangles), respectively. The solid and the dashed lines are the fitted curves from which the IC_{50} value was calculated.

We have to date no explanation for the high toxicity of B-THF-14. The mechanism by which the boron-containing lipids interact with the cells is not known in any detail. It is possible that the boron-containing liposomes are completely internalized into the cells but an exchange of boron-containing lipid between liposome and cell membrane likely also occur. In this case the membrane potential would decrease because of the negative lipid charge and a dysfunction of the membrane channels would be possible. Alternatively, the membrane fluidity could be changed by incorporation of the lipid into the membranes of cells (including blood cells).

In general the high boron carrying capacity make dodecaborate cluster lipids attractive agents as boron delivery systems for BNCT. B-THF-14 and B-Dioxan-14 form different, but small stable structures (100–200 nm when extruded through a 100-nm filter) when used in pure form. They represent the first dodecaborate-containing lipids which can form structures compatible with intravenous injection without helper lipids which are stable even upon storage at 4 °C. B-Dioxan-14 with its low toxicity might represent a suitable boron carrier for boron neutron capture therapy.

Acknowledgments

We would like to thank Lipoid GmbH for generous gifts of lipids. This work has been financially supported by the German Research Council DFG through a joint grant to D.G., R.S., and R.P.S., the DAAD German Academic Exchange Service and STINT, and the Swedish Research Council and the Swedish Cancer Society to K.E.

Appendix A. Supplementary material

Supplementary data associated with this article can be found, in the online version, at doi:10.1016/j.jorganchem.2008.12.044.

References

[1] F. Alam, R.F. Barth, A.H. Soloway, Antibody Immunoconjug. Radiopharm. 2 (1989) 145.
[2] R.F. Schinazi, W.H. Prusoff, Tetrahedron Lett. 50 (1978) 4981.
[3] (a) M. Miura, D. Gabel, R.G. Fairchild, B.H. Laster, L.S. Warkentien, Strahlenther. Onkol. 165 (1989) 131;
(b) Kahl, M.-S. Koo, Chem. Commun. (1990) 1769.
[4] (a) A.P. Pathak, D. Artemov, B.D. Ward, D.G. Jackson, M. Neeman, Z.M. Bhujwalla, Cancer Res. 65 (2005) 1425;
(b) M.R. Dreher, W. Liu, C.R. Michelich, M.W. Dewhirst, F. Yuan, A. Chilkoti, J. Natl.Cancer Inst. 98 (2006) 335.
[5] (a) S.C. Mehta, J.C. Lai, D.R. Lu, J. Microencapsul. 13 (1996) 269;
(b) M. Johnsson, N. Bergstrand, K. Edwards, J. Liposome Res. 9 (1999) 53;
(c) K. Maruyama, O. Ishida, S. Kasaoka, T. Takizawa, N. Utoguchi, A. Shinohara, M. Chiba, H. Kobayashi, M. Eriguchi, H.J. Yanagie, Control Release 98 (2004) 195.
[6] D. Gabel, D. Awad, T. Schaffran, D. Radovan, D. Daraban, L. Damian, M. Winterhalter, G. Karlsson, K. Edwards, ChemMedChem 2 (2007) 51.
[7] P. Lemmen, L. Weißfloch, T. Auberger, T. Probst, Anticancer Drugs 6 (1995) 744.
[8] H. Nakamura, Y. Miyajima, T. Takei, S. Kasaoka, K. Maruyama, Chem. Commun. (2004) 1910.
[9] Y. Miyajima, H. Nakamura, Y. Kuwata, J.D. Lee, S. Masunaga, K. Ono, K. Maruyama, Bioconjug. Chem. 17 (2006) 1314.
[10] T. Li, J. Hamdi, M.F. Hawthorne, Bioconjug. Chem. 17 (2006) 15.
[11] J.-D. Lee, M. Ueno, M.Y. Miyajima, H. Nakamura, Org. Lett. 9 (2006) 323.
[12] H. Nakamura, J.D. Lee, M. Ueno, Y. Miyajima, H.S. Ban, Nanobiotechnology 3 (2007) 135.
[13] E. Justus, D. Awad, M. Hohnholt, T. Schaffran, K. Edwards, G. Karlsson, L. Damian, D. Gabel, Bioconjug. Chem. 18 (2007) 1287.
[14] I.B. Sivaev, N.Yu. Kulikova, E.N. Nizhnik, M.V. Vichuzhanin, Z.A. Starikova, A.A. Semioshkin, V.I. Bregadze, J. Organomet. Chem. 693 (2008) 519.
[15] J.C. Stewart, Anal. Biochem. 104 (1980) 10.
[16] A. Semioshkin, E. Nizhnik, I. Godovikov, Z. Starikova, V. Bregadze, J. Organomet. Chem. 692 (2007) 4020.
[17] J.R. Silvius, Biochim. Biophys. Acta 857 (1986) 217.
[18] J.H. Ipsen, O.G. Mouritsen, M. Bloom, Biophys. J. 57 (1990) 405.
[19] O. Ishida, K. Maruyama, H. Tanahashi, M. Iwatsuru, K. Sasaki, M. Eriguchi, H. Yanagie, Pharm. Res. 18 (2001) 831.

IV

Pyridinium lipids with the dodecaborate cluster as polar head group: Synthesis, characterization of the physical-chemical behavior and toxicity in cell culture

under revision in Bioconjugate Chemistry

Pyridinium lipids with the dodecaborate cluster as polar head group: Synthesis, characterization of the physical-chemical behavior and toxicity in cell culture

Tanja Schaffran,[2,3] Alexander Burghardt,[4] Sabine Barnert,[4] Regine Peschka-Süss,[4] Rolf Schubert,[4] Mathias Winterhalter,[5] Detlef Gabel[3]

Department of Chemistry, University of Bremen, PO Box 330440, D-28357 Bremen, Institute of Pharmaceutical Sciences, Department of Pharmaceutical Technology and Biopharmacy, University of Freiburg, D-79104 Freiburg and School of Science and Engineering, Jacobs University Bremen, PO Box 750561, D-28725 Bremen.

Running title: Pyridinium-based dodecaborate cluster lipids

Abstract

We have prepared nine new dodecaborate cluster lipids with potential use in boron neutron capture therapy of tumors. This new generation of boron lipids is only singly negatively charged and consists of a pyridinium core with C_{12}, C_{14} and C_{16} chains as lipid backbone, connected through the nitrogen atom via a butylene, pentylene or ethyleneoxyethylene linker to the oxygen atom on the dodecaborate cluster as headgroup. The lipids were obtained by nucleophilic attack of 4-(bisalkylmethyl)pyridine on the tetrahydrofurane, the dioxane and a newly prepared tetrahydropyrane derivative, respectively, of *closo*-dodecaborate. All of these boron lipids are able to form closed vesicles in addition to some bilayers in pure state and in the presence of helper lipids. The thermotropic behavior was found to be increasingly complex and polymorphic with increasing alkyl chain length. Except for two lipids, all lipids have low *in vitro* toxicity, and longer alkyl chains lead to a significant decrease in toxicity. The choice of the linker plays no major role with respect to their ability to form liposomes and their thermotropic properties, but the toxicity is influenced by the linkers in the case of short alkyl chains.

Keywords: boron neutron capture therapy, boron cluster lipid, liposome, differential scanning calorimetry, toxicity

Introduction

Therapy for patients with malignant neoplasms, especially high-grade gliomas, melanomas and their metastatic manifestations has been only marginally successful with conventional treatments such as surgery or chemotherapy *(1, 2, 3)*. Boron neutron capture therapy (BNCT) is focused on the treatment of these types of cancer. The therapy is based on the nuclear reaction which occurs when boron-10 is irradiated with thermal neutrons followed by nuclear fission to high energy alpha particles and lithium-7 nuclei. These products only act in a short range (cell diameter) which offers a selective damaging of the cancer cells if the boron-10 is selectively accumulated in the tumor and not in the surrounding healthy tissue. For successful treatment a high amount of boron is necessary (10^9 B atoms per cell, or 20-30 µg per gram of tumor).

[2] T.Schaffran@web.de. Phone +49 421 21863252, fax +49 421 21863259.
[3] Department of Chemistry, University of Bremen.
[4] Department of Pharmaceutical Technology and Biopharmacy, University of Freiburg.
[5] School of Science and Engineering, Jacobs University Bremen.

[1]Abbreviations: HEPES, 4-(2-hydroxyethyl)-1-piperazineethanesulfonic acid; BNCT, boron neutron capture therapy; DSPC, distearoylphosphatidylcholine; BSH, $Na_2B_{12}H_{11}SH$; DSC, differential scanning calorimetry; DPPC, dipalmitoylphosphatidylcholine; TEM, transmission electron microscopy; ATP, adenosine triphosphate; BPA, boronphenylalanine; EGF, epidermal growth factor; SAINT, *s*ynthetic *a*mphiphiles for *i*nterdisciplinary *n*ucleic acid *t*herapy; ESI, electrospray ionization; ICP-MS, inductively-coupled-plasma mass-spectrometry; DSPE, distearoylphosphatidylethanolamine.

Only two substances are in clinical trials, boronophenylalanine (BPA) and mercaptododecaborate (BSH), but they do not reach “ideal” boron concentration in the tumor *(2)* and are hence no optimal boron delivery agents.

In the past many prospective boron agents have been synthesized, but most of them show disqualifying features *(4)*. Low molecular weight boron-containing nucleosides and nucleotides have been prepared for targeting hyperproliferating malignant cells *(5, 6)*. Sugar derivatives are synthesized for cell uptake via specific transporters into cells with increased metabolism *(7)*. Another strategy is to obtain boron-containing agents for which target receptors are present in the plasma membrane of the tumor cell, possibly followed by translocation into the cell *(4)*. Porphyrin and phthalocyanine derivatives *(8, 9, 10, 11, 12)* are a part of this category; they often exhibit high toxicity, however. High molecular weight boronated agents, such as antibodies and their fragments, have been prepared which can recognize tumor-associated epitopes *(13, 14, 15)*. Their rapid clearance by the reticuloendothelial system and the necessity to couple enough boron to an antibody molecule for successful therapy are, however, disadvantageous.

Liposomes are promising transport systems for boron agents, as they can carry a large amount of boron. In addition, targeting with tumor-seeking entities e.g., folate *(16)*, EGF *(17)* or transferrin *(18)*, makes selective transfer possible. The encapsulation of low molecular boron agents into the inner liposomal core has been studied in a variety of experimental systems *(19, 20)*. For effective delivery of boron, low encapsulation efficiency, leakage upon storage or in contact with serum and the effect of the liposome structure in the presence of charged boron clusters *(21)* are disadvantages.

These problems can be avoided by incorporating boron-containing lipids directly into liposomal membranes.

The first dodecaborate ether lipid has been described by Lee *et al. (22)*. The subsequently published dodecaborate lipids have BSH as headgroup *(23, 24)*. These lipids show similarly low toxicity as BSH. All these boron lipids are doubly negatively charged.

Recently we published the first dodecaborate cluster lipids with only one negative charge *(25)*.

The chemical structure of these boron lipids are shown in Scheme 1.

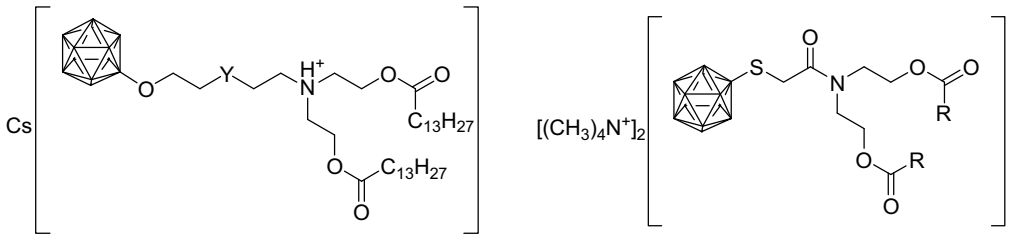

Y = no atom: **B-THF-14**, O: **B-Dioxan-14**

B-6-14: R =$C_{13}H_{27}$
B-6-16: R = $C_{15}H_{31}$

Scheme 1: Structures of the boron lipids: B-THF-14 and B-Dioxan-14 (left) (25) as well as B-6-14 and B-6-16 (right) (24). In the icosahedral structures, each unsubstituted corner represents a B-H unit, and the substituted corner, a B atom. The cluster carries two negative charges which are omitted for clarity.

The new boron lipids in this study also have a single negative charge. We used ring opening reactions of different oxonium derivatives of the dodecaborate cluster with p-bisalkylmethylpyridine as nucleophile. This allows facile preparation and the possibility to vary the structure of the hydrophobic part of the lipid. The lipids prepared have the advantage that no enzymatically cleavable bonds (esters, amides) are present. Commonly *N*-methyl-*p*-bisalkylmethylpyridinium is applied in lipoplexes (so-called SAINTs (*s*ynthetic

*a*mphiphiles for *i*nterdisciplinary *n*ucleic acid *t*herapy)) for gene therapy *(26, 27, 28)*. We adapted this basic structure for the first time for boron lipids with potential use in BNCT.

Experimental procedures

General. A Bruker Esquire spectrometer was used for electrospray mass spectrometry. For boron-containing compounds the peak with the highest intensity is given. To identify the charge of the compound isotope satellite peaks were used. NMR spectra were recorded on a Bruker DPX 200 spectrometer. IR spectra were collected on a BioRad FTS 155 using KBr pellet. Melting points were measured on a Büchi 512 melting point apparatus. Purity of the compounds was assessed by ESI mass spectrometry and ^{1}H-, ^{13}C- and ^{11}B NMR spectroscopy, as it is known that the elemental analysis of dodecaborate containing compounds is not reliable *(29, 30)*.

Chemistry. *1-Tetramethylene-(3-oxa)-oxonium-closo-undecahydrododecaborate (-1), tetrabutylammonium salt (**1a**).* The convenient method recently described was used, in which closo-dodecaborate was reacted with hydrogen chloride in 1,4-dioxane in the presence of $NaBF_4$ *(31)*.

*1-Tetramethyleneoxonium-closo-undecahydrododecaborate (-1), tetrabutylammonium salt (**1b**).* The method as for 1a was used, but replacing hydrogen chloride with p-toluenesulfonic acid (2 equiv.) and tetrahydrofurane as solvent. The compound was identical to that described by Sivaev et al. *(32)*.

*1-Pentamethyleneoxonium-closo-undecahydrododecaborate (-1), tetrabutylammonium salt (**1c**).* The method as for 1b was used, but the solvent was tetrahydropyrane instead of tetrahydrofurane. Yield 70 %, mp. 159°C (lit. mp. 159°C (*33*). MS (ESI, acetonitrile, m/z) negative 227.1 [A^-], 695.6 [2 A^- + $N(n\text{-}C_4H_9)_4^+$], 141.1 [$B_{12}H_{11}^-$]; positive 242.4 [$N(n\text{-}C_4H_9)_4^+$]. ^{1}H NMR (200 MHz, [D3] CD_3CN, 25°C, TMS): δ= 1.32 (t, 12 H, -C*H*$_3$), 1.54 (m, 10 H, N^+-CH_2-CH_2-C*H*$_2$-, -O^+-CH_2-CH_2-C*H*$_2$-), 1.59 (m, 8 H, -N^+-CH_2-C*H*$_2$-), 1.64 (m, 8 H, -O^+-CH_2-C*H*$_2$-), 3.07 (m, 8 H, -N^+-C*H*$_2$-), 4.50 (t, 4 H, -O^+-C*H*$_2$-). ^{13}C NMR (200 MHz, [D3] CD_3CN, 25°C, TMS): δ= 13.25, 19.76, 20.70, 23.74, 25.07, 58.76, 82.54. 11B NMR (200 MHz, [D3] CD_3CN, 25°C): -19.79 (1B), -17.00 (10 B), 8.86 (1 B). IR (KBr): ν= 2962 (-C-H), 2873 (-C-H), 2492 (B-H), 1469 (-C-H), 1045 (-C-O-C-).

*4-(Bisdodecylmethyl)pyridine (**2a**)*, *4-(bistetradecylmethyl)pyridine (**2b**)*, and *4-(bishexadecylmethyl)pyridine (**2c**)* were synthesized as described by Meekel *et al. (34)*.

General method for preparation of dodecaborate derivatives of SAINT lipids. **2** (0.42 g, 1 mmol) was suspended in 30 ml of dry acetonitrile and **1** (0.66 mmol) was added. The reaction mixture was refluxed for 4 days. The solvent was evaporated and the residue dissolved in methanol. After addition of cesium fluoride (0.15 g, 1 mmol) dissolved in methanol a white precipitate as product was formed and filtered off. It was dried in oil pump vacuum.

4-(Bisdodecylmethyl)pyridinio-N-butoxy-undecahydro-closo-dodecaborate (-1), cesium salt (THF-SAINT-12). **2a** and **1b** were used. Yield 0.33 g (65 %). MS (ESI, acetonitrile, m/z) negative 642.5 [A^-]; positive 132.8 [Cs^+]. ^{1}H NMR (200 MHz, [D6] DMSO, 25°C, TMS): δ= 0.82 (t, 6H, -C*H*$_3$), 1.19 (m, 42 H, -$(CH_2)_{10}CH_3$, -O-CH_2-C*H*$_2$-), 1.62 (m, 6H, -C*H*$_2$-$(CH_2)_{10}CH_3$, -O-C*H*$_2$-), 1.91 (m, 2H, -C*H*$_2$-CH_2-N^+-), 2.86 (m, 1H, -C*H*-), 4.67 (m, 2H, -C*H*$_2$-N^+-), 7.93 (d, 2H, -C=C*H*-), 9.01 (d, 2H, -N^+=CH-). ^{13}C NMR (200 MHz, [D6] DMSO, 25°C, TMS): δ= 14.84, 22.99, 27.56, 29.86, 30.79, 32.17, 35.65, 45.78, 60.25, 68.83, 127.39, 145.59, 166.68. ^{11}B NMR (200 MHz, [D6] DMSO, 25°C): -23.28 (1B), -17.24 (10 B), 6.62 (1 B). IR (KBr): ν= 2925 (-C-H), 2854 (-C-H), 2477 (-B-H), 1641 (-C=C-), 1468 (-C-H), 1159 (-C-N-), 1056 (-B-O-C-), 721 (=C-H).

4-(Bisdodecylmethyl)pyridinio-N-ethoxy-ethoxy-undecahydro-closo-dodecaborate (-1), cesium salt (Dioxan-SAINT-12). ***2a** and* **1a** were used. Yield 70 %. MS (ESI, acetonitrile, m/z)

negative 658.6 [A^-]; positive 132.9 [Cs^+]. ^{1}H NMR (200 MHz, [D6] DMSO, 25°C, TMS): δ= 0.82 (t, 6H, -C*H*$_3$), 1.19 (m, 40H, -(C*H*$_2$)$_{10}$-CH$_3$), 1.61 (m, 4H, -C*H*$_2$-(CH$_2$)$_{10}$-CH$_3$), 2.86 (1 H, -C*H*-), 3.41 (m, 2H, B-O-C*H*$_2$-), 3.53 (m, 2H, -CH$_2$-C*H*$_2$-O-), 3.84 (m, 2H,-O-C*H*$_2$-CH$_2$-N^+-), 4.73 (m, 2H,-C*H*$_2$-N^+-), 7.92 (d, 2H, -C=C*H*-), 9.09 (d, 2H, -N^+=CH-). ^{13}C NMR (200 MHz, [D6] DMSO, 25°C, TMS): δ= 13.96, 22.10, 26.70, 29.00, 31.28, 34.76, 44.90, 59.52, 67.27, 68.73, 72.63, 126.26, 143.35, 165.76. ^{11}B NMR (200 MHz, [D6] DMSO, 25°C): -22.96 (1B), -17.42 (10 B), 6.63 (1 B). IR (KBr): ν= 2919 (-C-H), 2852 (-C-H), 2478 (-B-H), 1643 (-C=C-), 1471 (-C-H), 1059 (-B-O-C-, -C-O-C-), 719 (=C-H).

4-(Bisdodecylmethyl)pyridinio-N-pentoxy-undecahydro-closo-dodecaborate (-1), cesium salt (Pyran-SAINT-12). ***2a*** *and* **1c** were used. Yield: 50 %. MS (ESI, acetonitrile, m/z) negative 656.6 [A^-]; positive 132.8 [Cs^+]. ^{1}H NMR (200 MHz, [D6] DMSO, 25°C, TMS): δ= 0.82 (t, 6H, -C*H*$_3$), 1.19-1.38 (m, 44H, -(C*H*$_2$)$_{10}$-CH$_3$, -O-CH$_2$-(C*H*$_2$)$_2$-), 1.61 (m, 6H, -C*H*$_2$-(CH$_2$)$_{10}$-CH$_3$, -C*H*$_2$-CH$_2$-N^+-), 1.89 (m, 2H, -O-C*H*$_2$-), 2.85 (m, 1H, -C*H*-), 4.53 (m, 2H, -CH$_2$-C*H*$_2$-N^+-), 7.97 (d, 2H, -C=C*H*-), 9.00 (d, 2H, -N^+=CH-). ^{13}C NMR (200 MHz, [D6] DMSO, 25°C, TMS): δ= 14.10, 22.24, 26.76, 29.12, 30.61, 31.42, 34.87, 45.04, 60.03, 67,55, 126.88, 144.45, 166.04. ^{11}B NMR (200 MHz, [D6] DMSO, 25°C): -22.99 (1B), -17.42 (10 B), 6.60 (1 B). IR (KBr): ν= 3056 (=C-H), 2942 (-C-H), 2854 (-C-H), 2473 (-B-H), 1642 (-C=C-), 1468 (-C-H), 1160 (-C-N-), 1055 (-B-O-C-), 722 (=C-H).

4-(Bistetradecylmethyl)pyridinio-N-butoxy-undecahydro-closo-dodecaborate (-1), cesium salt (THF-SAINT-14). **2b** and **1b** were used. Yield 60 %. MS (ESI, acetonitrile, m/z) negative 698.8 [A^-]; positive 132.9 [Cs^+]. ^{1}H NMR (200 MHz, [D6] DMSO, 25°C, TMS): δ= 0.82 (t, 6H, -C*H*$_3$), 1.20 (m, 50 H, -(C*H*$_2$)$_{12}$CH$_3$, -O-CH$_2$-C*H*$_2$-), 1.61 (m, 6H, -C*H*$_2$-(CH$_2$)$_{12}$CH$_3$, -O-C*H*$_2$-), 1.91 (m, 2H, -C*H*$_2$-CH$_2$-N^+-), 2.86 (m, 1H, -C*H*-), 4.67 (m, 2H, -C*H*$_2$-N^+-), 7.93 (d, 2H, -C=C*H*-), 9.01 (d, 2H, -N^+=CH-). ^{13}C NMR (200 MHz, [D6] DMSO, 25°C, TMS): δ= 13.93, 22.10, 26.65, 29.03, 29.93, 31.31, 34.73, 44.87, 59.30, 67.92, 126.46, 144.73, 165.76. ^{11}B NMR (200 MHz, [D6] DMSO, 25°C): -22.52 (1B), -17.86 – (-16.83) (10 B), 6.66 (1 B). IR (KBr): ν= 2924 (-C-H), 2854 (-C-H), 2477 (-B-H), 1642 (-C=C-), 1468 (-C-H), 1157 (-C-N-), 1056 (-B-O-C-), 721 (=C-H).

4-(Bistetradecylmethyl)pyridinio-N-ethoxy-ethoxy-undecahydro-closo-dodecaborate (-1), cesium salt (Dioxan-SAINT-14). **1a** and **2b** were used. Yield 60 %. MS (ESI, acetonitrile, m/z) negative 714.8 [A^-]; positive 132.9 [Cs+]. ^{1}H NMR (200 MHz, [D6] DMSO, 25°C, TMS): δ= 0.82 (t, 6H, -C*H*$_3$), 1.2 (m, 48H, -(C*H*$_2$)$_{12}$-CH$_3$), 1.61 (m, 4H, -C*H*$_2$-(CH$_2$)$_{12}$-CH$_3$), 2.86 (1 H, -C*H*-), 3.40 (m, 2H, B-O-C*H*$_2$-), 3.54 (m, 2H, -CH$_2$-C*H*$_2$-O-), 3.84 (m, 2H,-O-C*H*$_2$-CH$_2$-N^+-), 4.73 (m, 2H,-C*H*$_2$-N^+-), 7.91 (d, 2H, -C=C*H*-), 9.10 (d, 2H, -N^+=CH-). ^{13}C NMR (200 MHz, [D6] DMSO, 25°C, TMS): δ= 14.82, 22.99, 27.56, 29.9, 32.19, 35.59, 45.73, 60.41, 68.16, 69.65, 73.52, 127.15, 146.24, 166.62. ^{11}B NMR (200 MHz, [D6] DMSO, 25°C): -22.67 (1B), -17.65- (-16.68) (10 B), 6.93 (1 B). IR (KBr): ν= 3059 (=C-H), 2924 (-C-H), 2853 (-C-H), 2473 (-B-H), 1643 (-C=C-), 1468 (-C-H), 1167 and 1109 (-C-N-), 1057 and 1027 (-B-O-C-, -C-O-C-), 722 (=C-H).

4-(Bistetradecylmethyl)pyridinio-N-pentoxy-undecahydro-closo-dodecaborate (-1), cesium salt (Pyran-SAINT-14). **1c** and **2b** were used. Yield 45 %. MS (ESI, acetonitrile, m/z) negative 712.9 [A^-]; positive 132.8 [Cs^+]. ^{1}H NMR (200 MHz, [D6] DMSO, 25°C, TMS): δ= 0.84 (t, 6H, -C*H*$_3$), 1.20-1.40 (m, 52H, -(C*H*$_2$)$_{12}$-CH$_3$, -O-CH$_2$-(C*H*$_2$)$_2$-), 1.63 (m, 6H, -C*H*$_2$-(CH$_2$)$_{12}$-CH$_3$, -C*H*$_2$-CH$_2$-N^+-), 1.91 (m, 2H, -O-C*H*$_2$-), 2.86 (m, 1H, -C*H*-), 4.55 (m, 2H, -C*H*$_2$-N^+-), 7.96 (d, 2H, -C=C*H*-), 9.02 (d, 2H, -N^+=CH-). ^{13}C NMR (200 MHz, [D6] DMSO, 25°C, TMS): δ= 14.10, 22.24, 26.70, 29.15, 30.63, 31.45, 34.79, 44.98, 60.03, 67,55, 126.88, 144.45, 166.04. ^{11}B NMR (200 MHz, [D6] DMSO, 25°C): -22.67 (1B), -17.65- (-16.68) (10 B), 6.93 (1 B). IR (KBr): ν= 3056 (=C-H), 2942 (-C-H), 2854 (-C-H), 2473 (-B-H), 1642 (-C=C-), 1468 (-C-H), 1160 (-C-N-), 1055 (-B-O-C-), 722 (=C-H).

4-(Bishexadecylmethyl)pyridinio-N-butoxy-undecahydro-closo-dodecaborate (-1), cesium salt (THF-SAINT-16). **2c** and **1b** were used. Yield 50 %. MS (ESI, acetonitrile, m/z) negative 754.9 [A^-]; positive 132.8 [Cs^+]. ^{1}H NMR (200 MHz, [D6] DMSO, 25°C, TMS): δ= 0.82 (t, 6H, -CH_3), 1.20 (m, 58H, -$(CH_2)_{14}$-CH_3, -O-CH_2-CH_2-), 1.62 (m, 6H, -CH_2-$(CH_2)_{14}CH_3$, -O-CH_2-), 1.92 (m, 2H, -CH_2-CH_2-N^+-), 2.86 (m, 1H, -C*H*-), 4.68 (m, 2H, -CH_2-N^+-), 7.92 (d, 2H, -C=C*H*-), 9.01 (d, 2H, -N^+=CH-). ^{13}C NMR (200 MHz, [D1] $CDCl_3$, 25°C, TMS): δ= 13.98, 22.13, 26.65, 29.03, 30.72, 31.31, 34.73, 44.84, 59.35, 67.95, 126.46, 144.46, 149.34. ^{11}B NMR (200 MHz, [D6] DMSO, 25°C): -19.82 (1B), -17.00 (10 B), 7.13 (1 B). IR (KBr): ν= 2920 (-C-H), 2853 (-C-H), 2475 (-B-H), 1641 (-C=C-), 1468 (-C-H), 1160 (-C-N-), 1059 (-B-O-C-), 720 (=C-H).

4-(Bishexadecylmethyl)pyridinio-N-ethoxy-ethoxy-undecahydro-closo-dodecaborate (-1), cesium salt (Dioxan-SAINT-16). **1a** and **2c** were used. Yield. 60 % MS (ESI, acetonitrile, m/z) negative 770.9 [A^-]; positive 132.9 [Cs+]. ^{1}H NMR (200 MHz, [D6] DMSO, 25°C, TMS): δ= 0.82 (t, 6H, -CH_3), 1.20 (m, 56H, -$(CH_2)_{14}$-CH_3), 1.61 (m, 4H, -CH_2-$(CH_2)_{14}$-CH_3), 2.86 (1 H, -C*H*-), 3.40 (m, 2H, B-O-CH_2-), 3.54 (m, 2H, -CH_2-CH_2-O-), 3.84 (m, 2H,-O-CH_2-CH_2-N^{+-}), 4.73 (m, 2H,-CH_2-N^+-), 7.91 (d, 2H, -C=C*H*-), 9.10 (d, 2H, -N^+=CH-). ^{13}C NMR (200 MHz, [D6] DMSO, 25°C, TMS): δ= 13.93, 22.10, 26.65, 29.03, 30.66, 34.68, 44.81, 59.52, 67.30, 68.76, 72.66, 126.23, 145.38, 165.73. ^{11}B NMR (200 MHz, [D6] DMSO, 25°C): -23.46 (1B), -17.24 (10 B), 6.66 (1 B). IR (KBr): ν= 2922 (-C-H), 2853 (-C-H), 2476 (-B-H), 1642 (-C=C-), 1468 (-C-H), 1171 (-C-N-), 721 (=C-H).

4-(Bishexadecylmethyl)pyridinio-N-pentoxy-undecahydro-closo-dodecaborate (-1), cesium salt (Pyran-SAINT-16). **1c** and **2c** were used. Yield 40 %. MS (ESI, acetonitrile, m/z) negative 769.8[A^-]; positive 132.9 [Cs^+]. ^{1}H NMR (200 MHz, [D6] DMSO, 25°C, TMS): δ= 0.85 (t, 6H, -CH_3), 1.22-1.41 (m, 60H, -$(CH_2)_{14}$-CH_3, -O-CH_2-$(CH_2)_2$-), 1.63 (m, 6H, -CH_2-$(CH_2)_{14}$-CH_3, -CH_2-CH_2-N^+-), 1.92 (m, 2H, -O-CH_2-), 2.85 (m, 1H, -C*H*-), 4.55 (m, 2H, -CH_2-CH_2-N^+-), 7.96 (d, 2H, -C=C*H*-), 8.99 (d, 2H, -N^+=CH-). ^{13}C NMR (200 MHz, [D6] DMSO, 25°C, TMS): δ= 14.10, 22.24, 26.76, 29.12, 30.61, 31.42, 34.87, 45.04, 60.03, 67,55, 126.88, 144.45, 166.04. ^{11}B NMR (200 MHz, [D6] DMSO, 25°C): -23.69 (1B), -17.30 (10 B), 7.13 (1 B). IR (KBr): ν= 2923 (-C-H), 2853 (-C-H), 2475 (-B-H), 1641 (-C=C-), 1466 (-C-H), 1159 (-C-N-), 1056 (-B-O-C-), 722 (=C-H).

N-Methyl-4-(dihexydecylmethyl)pyridinium iodide (Me-SAINT-16). The compound was synthesized according to Sudhölter et al. (1982) *(35)* and Meekel et al. *(34)*.

Preparation of liposomes. The boron-containing lipids were either used in pure form or mixed with equal molar amounts of DSPC and cholesterol plus 2 mol% DSPE-PEG_{2000}. The lipid, or lipid mixture, was dissolved in chloroform and dried to a thin lipid film in a round-bottom flask. The lipid film was hydrated and dispersed by vortexing in 10 mM HEPES buffer saline, pH 7.4 (150 mM NaCl, 10 mM HEPES). The resulting suspension was frozen and thawed in 10 cycles followed by extrusion (21 times) through a polycarbonate membrane with a pore diameter of 100 nm (Avestin, Mannheim, Germany) at a temperature of 50°C. Final lipid concentration was 10 mM. Lipid content was measured by the Stewart assay *(36)*, using appropriate standard curves for the individual lipids, and ICP-MS measurements.

Liposomes could not be prepared from Dioxan-SAINT-12; the suspension obtained after hydration of the lipid film yielded larger particles, which could not be extruded even after ultrasound treatment.

For DSC measurements, the pure lipids were dispersed from a lipid film (obtained as described above) by hydration with 10 mM Hepes 100 mM NaCl, pH 7.4, through ten freeze-thaw cycles and stored at 4°C prior to measurement.

Inductively-coupled-plasma mass-spectrometry (ICP-MS). ICP-MS was used to quantify boron in liposome preparations. The analysis was carried out in a ThermoElectron

Element 2 ICP-MS apparatus, by measuring the signal for the boron-11 nuclide. The samples were treated with concentrated nitric acid (HNO_3) in the first dilution step and further diluted with water to concentration ranges appropriate for the sensitivity of the apparatus. The water produced by a Milli-Q system was used. The boron concentrations were determined by a calibration curve obtained from samples with known boron content. Indium was added as internal standard.

Cryotransmission electron microscopy (cryo-TEM). A small amount (~1 µl) of the liposome suspension (final lipid concentration 5 mM) was transferred to a polymer-coated copper grid and shock-frozen from 25°C by injection into liquid ethane. The vitrified samples were examined in a Zeiss EM LEO 912Ω electron microscope, operating at an accelerating voltage of 80 keV in filtered bright field image mode at ΔE = 0 eV. The stage temperature was kept below 108K, and images were recorded at defocus settings between 1 and 3 µm. Images were recorded by a slow scan charge-coupled device (SSCCD) camera using the minimal dose focusing device. To assess the reproducibility of the results several images were recorded in different areas of the specimen.

Differential scanning calorimetry measurements. Differential scanning calorimetry (DSC) measurements were carried out on a VP-DSC microcalorimeter from Microcal (Northhampton, MA), using the pure boron lipid (final lipid concentration 10 mM). The samples were degassed under vacuum prior to the measurement. For the up- and downscans a scan rate of 60°C/h and a filtering period of 2s were used. From each scan a buffer background scan was subtracted. For data analysis, the software package ORIGIN (Microcal) was used. The buffer system for this measurement was 10 mM HEPES with 100 mM sodium chloride, pH=7.4.

Viability assay

The cell viability was determined with the CellTiter-Glo assay (Promega GmbH, Mannheim, Germany), which is based on the quantification of ATP which is in turn proportional to the number of metabolically active cells.

The cell line V79 (lung fibroblasts of Chinese hamster) was cultivated with Ham´s F10 medium and 10 % fetal calf serum at 37°C and 5 % CO_2. Cells (20,000 per well) were seeded into 48-well plates and grown for 24 h. Then the cells were incubated with different concentrations of boron-containing liposomes (DSPC/cholesterol/boron lipid (1:1:1 molar ratio) plus 2 mol% DSPE-PEG_{2000}) for 24 h. Then 300 µl CellTiter-Glo reagent were added and the luminescence was measured after few minutes (Microlumat Plus LB 96, EG & Bertold, Bad Wildbad, Germany).

The average of two wells was compared with the average of eight untreated samples (n=2).

The IC_{50} values were obtained by fitting a sigmoidal curve with the following equation:

$$f = \frac{a}{(1+e^{-(x-IC_{50})/b})}$$

in which *f* corresponds to the percentage survival of cells*, a* corresponds to the response without inhibition, *x* to the concentration of the tested substance, *b* to the slope of the response curve at c=IC_{50}, and IC_{50} to the concentration of the tested substance that provokes 50% reduction of cell viability.

Results

Chemistry. In this study, nine different dodecaborate cluster lipids were synthesized. All of them carry only one negative net charge. Recently we published *(25)* the first boron lipids with a net charge of minus one, but with a completely different basic structure. The lipids prepared here carry a bisalkylmethyl group on the *p*-position of a pyridine, which is *N*-alkylated with a linker carrying the dodecaborate cluster as polar headgroup. The lipids differ both in the alkyl chain length of the tails and in the linkers. For the connection of the

dodecaborate cluster with the lipid backbone nucleophilic ring opening reactions of tetrahydrofurane (THF), dioxane and tetrahydropyrane (THP) derivatives of the cluster with the alkylpyridinium compound (**2a,b,c**) were used (Scheme 2).

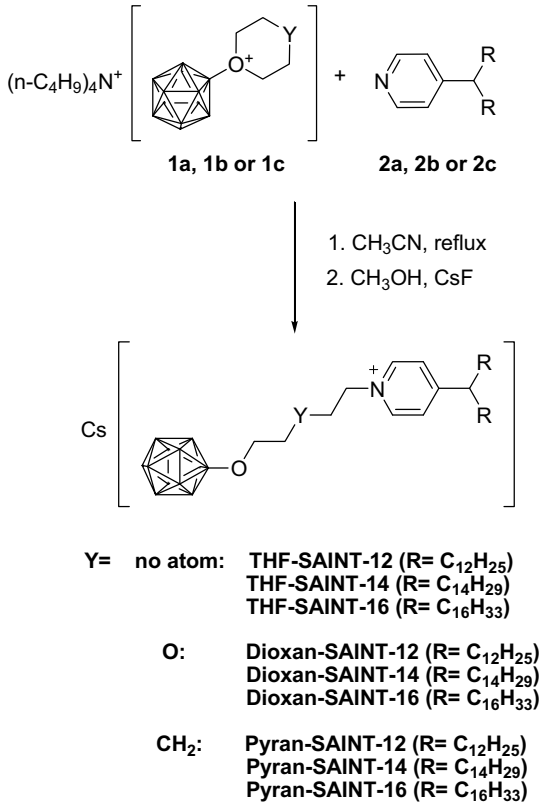

Y= no atom: **THF-SAINT-12 (R= $C_{12}H_{25}$)**
THF-SAINT-14 (R= $C_{14}H_{29}$)
THF-SAINT-16 (R= $C_{16}H_{33}$)

O: **Dioxan-SAINT-12 (R= $C_{12}H_{25}$)**
Dioxan-SAINT-14 (R= $C_{14}H_{29}$)
Dioxan-SAINT-16 (R= $C_{16}H_{33}$)

CH_2: **Pyran-SAINT-12 (R= $C_{12}H_{25}$)**
Pyran-SAINT-14 (R= $C_{14}H_{29}$)
Pyran-SAINT-16 (R= $C_{16}H_{33}$)

Scheme 2. Synthesis of the boron lipids via ring opening reactions between the alkylpyridnium compound (**2a,b,c**) and the THF, dioxane and THP derivative of the dodecaborate cluster respectively.

Semioshkin et al. *(37)* recently reported reactions of oxonium derivatives (THF and dioxane) with amines (also pyridine), but under different conditions and not applied to boron lipids. For the first time we accomplished ring opening reaction with the THP derivative of the cluster. The THP derivative had first been published by Peymann et al. *(33)* and had been prepared by alkylation of hydroxyundecahydro-*closo*-dodecaborate with dibromopentane, which requires two synthesis steps from the dodecaborate cluster to the THP derivative. We developed a reaction procedure which leads to the THP derivative from the unsubstituted cluster in one step and in good yields (Scheme 3).

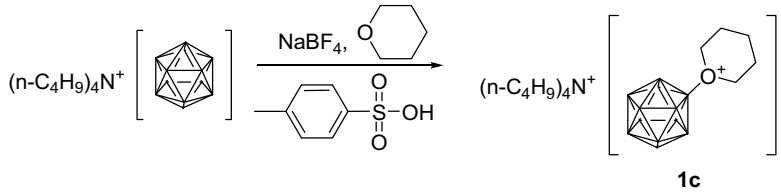

Scheme 3: Synthesis of the tetrahydropyrane (THP) derivative of the dodecaborate cluster.

The dodecaborate cluster is suspended in tetrahydropyrane and 2 equiv. *p*-toluenesulfonic acid and 5 equiv. $NaBF_4$ are added. The product is obtained with a yield of 70 %.

The synthesis of the alkylpyridinium compounds followed the work of Meekel et al. *(34)*. The ring opening reactions are carried out with the THF, dioxane or THP derivatives of the cluster and 1.5 equiv. alkylpyridinium compound (**2a,b,c**) in acetonitrile. The reaction yields are 50-

70 % for the THF and dioxane derivatives, and 40-50 % for the THP derivative, slightly depending on the length of the alkyl chain of the pyridine unit.

Physical characterization and liposome preparation. The lipid film hydration and extrusion method at 50°C was used to prepare liposomes from pure boron lipid. The structures formed were investigated by cryo-TEM (Fig. 1).

The shortest chains with 12 carbons produce a mixture of liposomes and some open structures. THF-SAINT-12 (Fig. 1a) forms predominantly closed vesicles but also some thick bilayer. The closed structures are heterogeneous in size, some of them are smaller than 100 nm which is the diameter of the extrusion membrane pores. Pyran-SAINT-12 (Fig. 1f) is able to form liposomes and inverted structures are observed.

Closed structures are found in greatest abundance for all the three derivatives with 14-carbon chains. Only for THF-SAINT-14 and Dioxan-SAINT-14 some bilayer are observed. Interestingly some of the liposomes show invagination.

For the longer 16-carbon chains, the structures formed appear to be almost exclusively open. Several bilayers have edges bent upward, giving at the first glance an impression of closed structures.

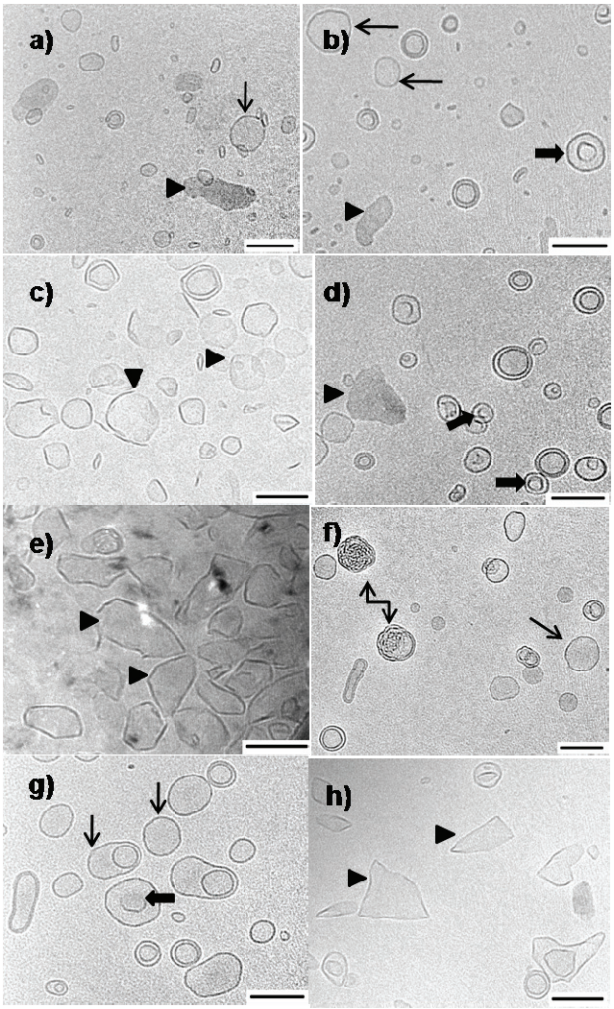

Figure 1. Cryo-TEM pictures from pure boron lipids: a) THF-SAINT-12, b) THF-SAINT-14, c) THF-SAINT-16, d) Dioxan-SAINT-14, e) Dioxan-SAINT-16, f) Pyran-SAINT-12, g) Pyran-SAINT-14, h) Pyran-SAINT-16. Scale bar 200 nm. Regular liposomes are indicated by ←, open structures by ▶, invaginated structures by ➡ , and inverted structures by ↰↳.

At the temperature of extrusion (50°C) and preparation for cryo-TEM (25°C), SAINT-16 derivatives are in the gel phase (see DSC data below), which is less favourable for the formation of liposomes. Extrusion at 65°C and subsequent storage at 4°C produces bilayer disks as well as closed liposomes (Fig. 2a and b) in the case of THF-SAINT-16 and Dioxan-SAINT-16. This behaviour is different from that of the lipid B-6-14, which forms very large bilayer sheets from liposomes below the phase transition temperature *(24)*.

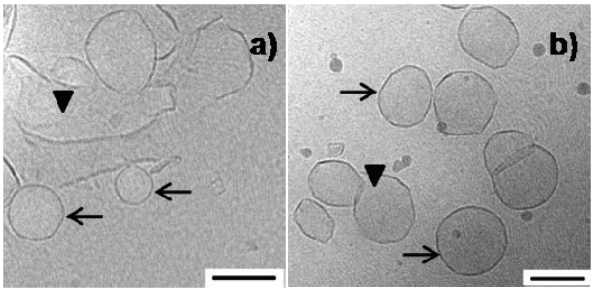

Figure 2: Samples from THF-SAINT-16 (a) and Dioxan-SAINT-16 (b) extruded at 65°C and stored at 4°C. Scale bar 200 nm. Regular liposomes are indicated by ←, open structures by ▶.

Interestingly the choice of the spacer has no drastic influence of the morphology of the liposomes. Recently we found drastic changes in the vesicle shape between the boron lipids B-THF-14 and B-Dioxan-14 *(25)* with change of the linker.

Cryo-TEM was employed also to visualize the structures formed when the boron-containing lipids had been mixed with helper lipids. For liposomal preparations, DSPC, cholesterol, and boron-containing lipid in the molar ratio of 1:1:1 plus 2 mol% DSPE-PEG_{2000} were used. THF-SAINT-12 (Fig. 3a), THFSAINT-14 (Fig. 3b) and THF-SAINT-16 (Fig. 3c) form liposomes in heterogeneous size. The liposome diameters differ from 100 nm, which is the pore size of the extrusion membrane, to 300 nm.

For Dioxan-SAINT-12 (Fig. 3d), Dioxan-SAINT-14 (Fig. 3e) and Dioxan-SAINT-16 (Fig. 3f) also liposomes can be observed in different sizes. By adding helper lipids liposomal vesicles are also found for Pyran-SAINT-12 (Fig. 3g), Pyran-SAINT-14 (Fig. 3h) and Pyran-SAINT-16 (Fig. 3i) with a size distribution. In general the formation of liposomes is influenced by the chain length of the tails in the SAINTs. With mixtures containing the short-chain derivatives, an increased tendency to form open structures can be seen.

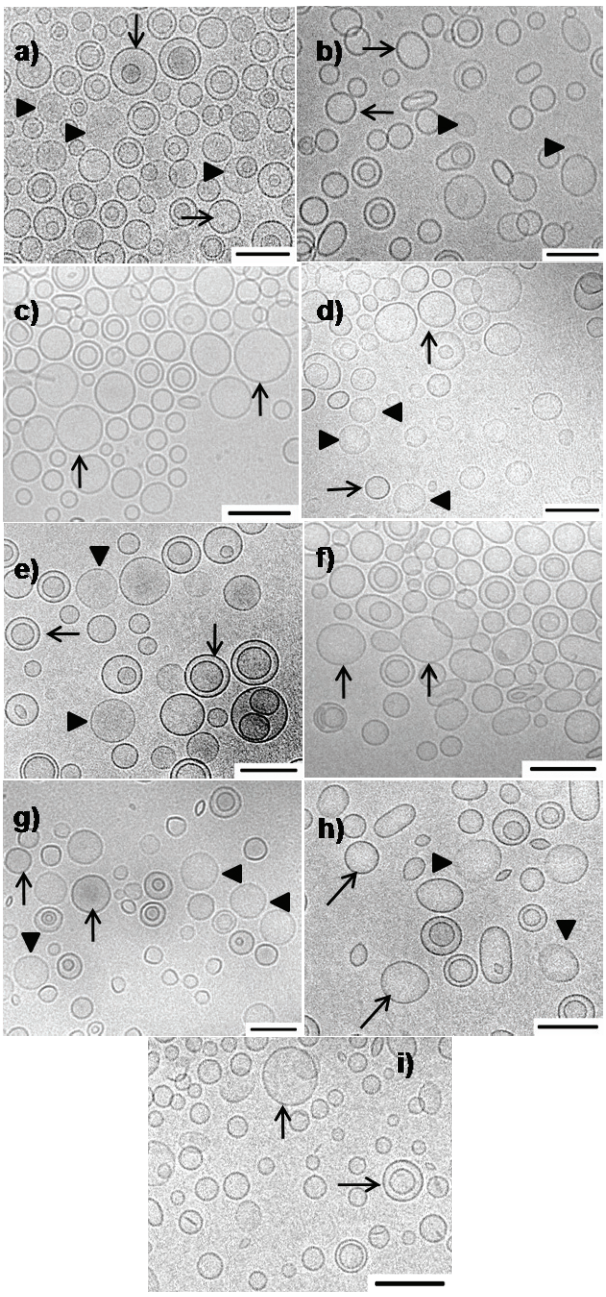

Figure 3. Cryo-TEM pictures of the liposomal preparations with helper lipids: DSPC/cholesterol/boron lipid (1:1:1) plus 2 mol% DSPE-PEG_{2000}: a) THF-SAINT-12, b) THF-SAINT-14, c) THF-SAINT-16, d) Dioxan-SAINT-12, e) Dioxan-SAINT-14, f) Dioxan-SAINT-16, g) Pyran-SAINT-12, h) Pyran-SAINT-14, i) Pyran-SAINT-16. Scale bar 200 nm. Regular liposomes are indicated by ←, open structures by ▶.

In the DSC measurements no phase transition could be detected for any of the three SAINT-12 derivatives. This fact is, however, not surprising because Me-SAINT-12 (*1-methyl-4-(bisdodecylmethyl)pyridinium chloride)* has a phase transition at 0°C *(34)* which is outside the range accessible by the DSC used.

The DSC profile of pure THF-SAINT-14 is shown in Fig. 4a. From 4°C to 20°C a broad peak with complex shape can be seen which consists of two transitions at 13.8°C and 16.8°C. Both transitions change only insignificantly between the first and the second upscan. The two transitions might arise from the heterogeneity of the vesicle shapes and sizes (see Fig. 1b). In the literature it is known that small unilamellar vesicles (SUVs) give rise to a main

transition different from that of multilamellar (MLVs) or large unilamellar vesicles (LUVs) *(38)*. Interestingly in the first upscan two further transitions at 33.0°C and 66.5°C can be observed which disappear in the following upscans. Metastable subtransitions are described e.g., for DPPC (dipalmitoylphosphatidylcholine) bilayers in gel phase *(39, 40)* which are reversible after storage at low temperatures for few days. The transitions for THF-SAINT-14 are surprisingly in the liquid phase and we have no evidence about the reversibility or explanation for structural changes in these phases. In cryo-TEM no changes in the vesicle shape was found after heating (pictures not shown here).

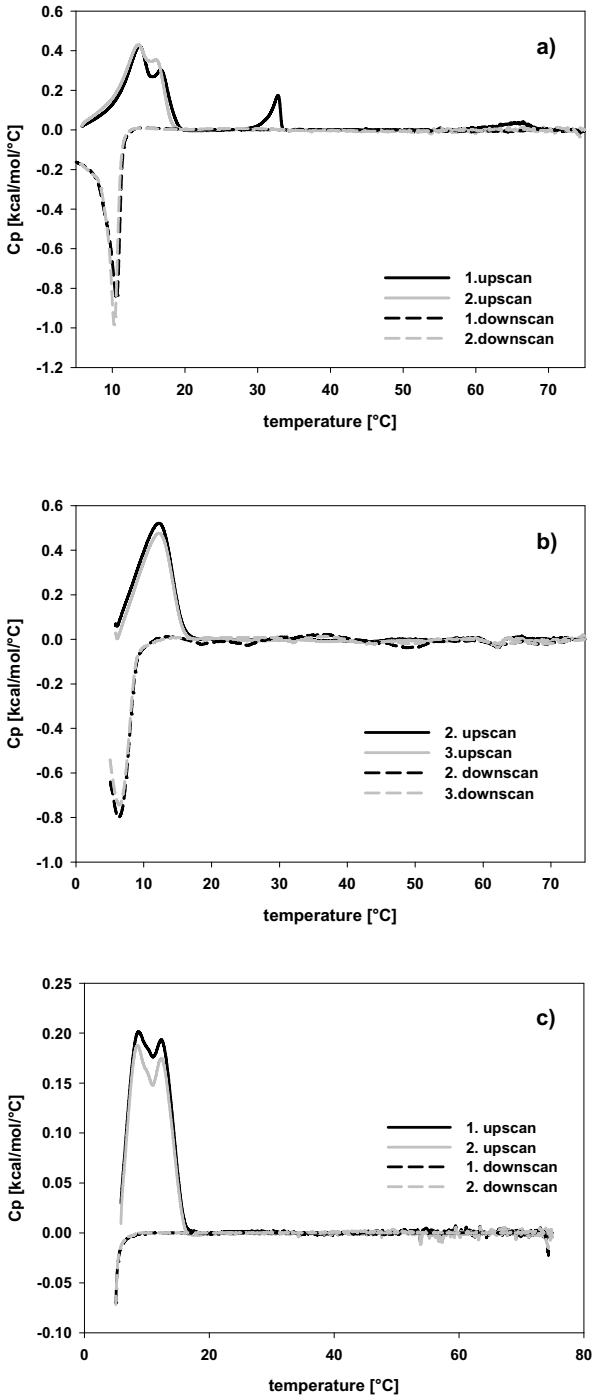

Figure 4: DSC of pure films of THF-SAINT-14 (a), Dioxan-SAINT-14 (b) and Pyran-SAINT-14 (c). Lipid concentration 5 mM.

The temperature difference (approx. 4°C) of the transition peaks between the up and downscans is remarkable; such strong hysteresis has only been described for the boron lipid B-THF-14 *(25)*. Furthermore, it seems that the transitions in the downscan do not end at 4°C and perhaps more transitions might follow. In contrast Dioxan-SAINT-14 (Fig. 4b) has a broad peak with a maximum at 12.3°C. The broadness indicates that the liposome composition is heterogeneous, as can also be observed in cryo-TEM (see Fig. 3d). The temperature difference (approx. 4°C) of the transition peaks between the up and downscans is again remarkable. The transition does not end at 4°C in the downscan. The DSC profile of Pyran-SAINT-14 (Fig. 4c) shows a broad peak from 4°C to 18°C, similar to THF-SAINT-14. The maxima are located at 8.5°C and 12.4°C and are probably the main transitions. Meekel et al. *(34)* recorded a main transition of Me-SAINT-14 (*1-Methyl-4-(ditetradecylmethyl)pyridinium chloride)* at approx. 16°C. We again attribute the two transitions to the heterogeneity of vesicle formation and size. No transitions in the downscan can be observed which indicate that they are located outside of the temperature range in which the measurements were performed.

The DSC profile is more complex for all SAINT-16 derivatives (Fig. 5). All of them show multiple transitions, which occur at similar temperatures; the transitions recur during all up- and downscans. THF-SAINT-16 (Fig. 5a) has a main transition at 56.0°C. Sudhölter et al. *(35)* reported a main transition for Me-SAINT-16 (*1-Methyl-4-(dihexadecylmethyl)pyridinium chloride*) at 64°C and we also detected it, although at 58°C (data not shown here). THF-SAINT-16 passes through three further transitions at 24.9°C, 39.0°C and 62.8°C. A rich polymorphism in the DSC is known for *N*-methylated pyridinium cores depending on the counterion, with solid-solid transitions and transitions between smectic phases *(35)*. Therefore solid-solid and liquid-liquid transitions are not very special for this boronated pyridinium lipid.
A tilted smectic phase is described by Sudhölter et al. *(35)* for Me-SAINT-16 iodide. Molecular dynamics simulation would certainly be required for THF-SAINT-16 to answer precisely the question of lipid packing.
In the downscan only two transitions are visible. As can be seen in Fig. 5b Dioxan-SAINT-16 has also four transitions which are located at 26.8°C, 39.9°C, 55.2°C and 62.8°C. Two solid-solid transitions can be noted and a main transition at 55.2°C as well as a liquid-liquid transition at 62.8°C which is comparable to THF-SAINT-16. Again only two peaks in the downscan can be observed.

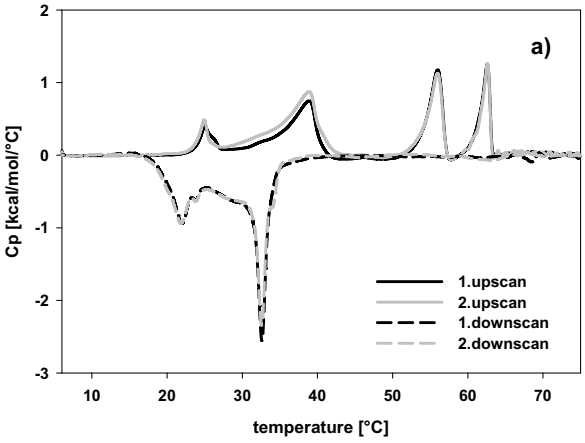

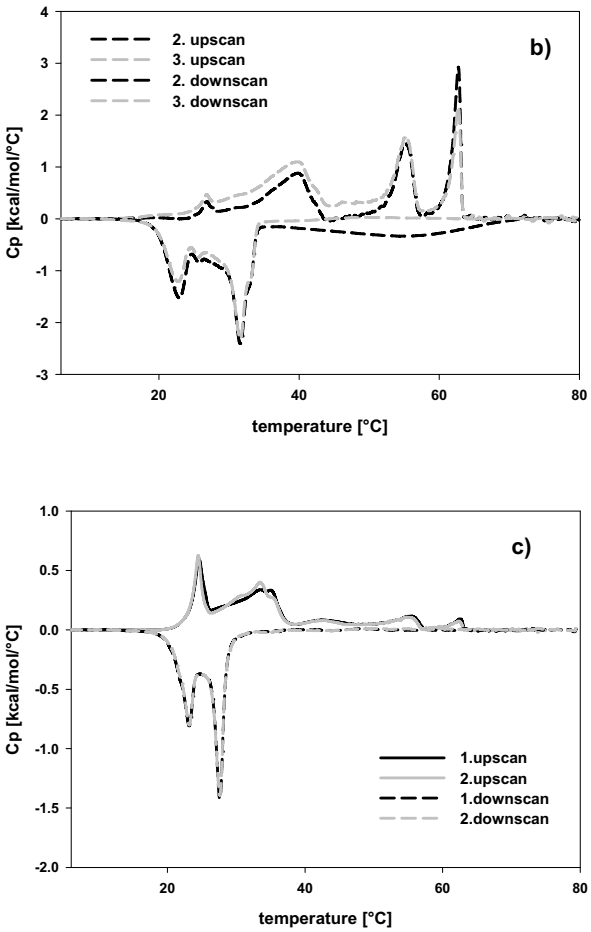

Figure 5: DSC of pure films of THF-SAINT-16 (a), Dioxan-SAINT-16 (b) and Pyran-SAINT-16 (c). Lipid concentration 10 mM.

Pyran-SAINT-16 shows transitions in the same temperature region (24.4°C, 33.6°C, 55.1°C and 62.4°C) as THF-SAINT-16 and Dioxan-SAINT-16, but for Pyran-SAINT-16, the transitions at higher temperatures have very small enthalpies. We have no explanation for this, but it might be assumed that the transitions concern the same event of transitions as in THF-SAINT-16 and Dioxan-SAINT-16.

As summarized in Table 1 all investigated lipids have a low impact on cell viability except for Dioxan-SAINT-12 and Dioxan-SAINT-14 (Table 1). It seems that the choice of the linker influences the viability in the case of short alkyl chains. The dioxane linker leads to a higher toxic effect as compared to the THF or THP linker. This is contrary to the boron lipids B-THF-14 and B-Dioxan-14 where the introduction of an ether function in the hydrocarbon spacer leads to a decrease of toxicity *(25)*.

The increasing alkyl chains lead to a significant decrease of toxicity in the case of THF-SAINT and Dioxan-SAINT lipids. This tendency is not well pronounced for the Pyran-SAINT lipids, however, the toxicity decreases by half from Pyran-SAINT-12 to Pyran-SAINT-16. Previously we found a similar trend for the lipids B-6-14 and B-6-16 *(24)*.

It seems that the linker influences the viability for longer alkyl chains less powerfully because the IC_{50} values are all in the same concentration range (4 mM **±** 1.5 mM). Thus for the SAINT-16 derivatives, the influence on cell viability depends only slightly on the nature of the linker, whereas this is not the case for shorter alkyl chains.

Table 1: IC_{50} values and standard deviations for all of the tested lipids. For the determination of the cell viability hamster V79 fibroblasts and the CellTiter-Glo assay were used.

name	**log IC_{50} ± SD**	**IC_{50} [mM]**
THF-SAINT-12	0.18 ± 0.02	1.5
THF-SAINT-14	0.51 ± 0.07	3.3
THF-SAINT-16	0.68 ± 0.01	4.8
Dioxan-SAINT-12	-0.56 ± 0.03	0.3
Dioxan-SAINT-14	-0.16 ± 0.14	0.7
Dioxan-SAINT-16	0.49 ± 0.02	3.0
Pyran-SAINT-12	0.27 ± 0.04	1.9
Pyran-SAINT-14	0.14 ± 0.02	1.4
Pyran-SAINT-16	0.54 ± 0.03	3.4

Discussion

Synthesis of nine *closo*-dodecaborate cluster containing lipids was achieved. These SAINT derivatives are the first boron lipids with an alkylpyridinium core as lipid backbone. The absence of enzymatically cleavable bonds such as ester or amides suggest a reduced degradation and subsequently a longer retention time in the body. In contrast, the dodecaborate cluster lipids described in previous publications contain bonds in their chemical structure for which an enzymatic degradation by (unspecific) esterases and/or amidases is imaginable. Metabolic *in vivo* studies with lipids carrying radioactive labels in the linker and in the chain moieties would have to be carried out to follow their respective metabolism.

The net charge of liposomes influences the biological properties. The incorporation of negatively charged lipids into the liposomal membrane accelerates the opsonization und consequently the clearance of liposomes from the blood stream *(41)*. The SAINT lipids are the second generation of boron lipids with a single negative net charge. The decrease of lipid charge may, by reduced clearance, lead to longer retention times in the body in comparison to doubly negatively charged dodecaborate cluster lipids. Thus dodecaborate cluster lipids with reduced net charge (up to a neutral molecule) might be desirable in regard to therapeutic efficacy.

The change in the negative net charge does not influence the toxicity of the dodecaborate cluster lipids against cells. Thus the IC_{50} values of the SAINTs lie in the same concentrations range as B-6-14 *(24)*. Studies of cell uptake are in progress for the SAINTs, B-Dioxan-14, B-6-14, and B-6-16, in order to investigate the influence of the different net charges in more detail.

Depending on the preparation temperature the SAINT lipids are able to form closed liposomes in the absence of helper lipids and are stable after storing at 4°C. The liposomes from pure boron lipid are able to transfer high amounts of boron to the tumor. Targeting with tumor-seeking entities probably allows to achieve selective accumulation.

Interestingly, the choice of the linker plays no major role with respect to liposome formation or thermotropic behavior. Recently we reported about the lipids B-THF-14 and B-Dioxan-14 in which only the linker differs. For those lipids the linker influences the vesicle formation as well as the DSC profile *(25)*. The absence of the effect of the linker on toxicity observed here is very unexpected and makes it difficult to propose an optimal linker for further syntheses.

The length of the alkyl chains influences the properties of the lipids with regard to their thermotropic behavior, liposome formation in the absence and in presence of helper lipids, and cell toxicity. Higher temperatures are necessary during the preparation of liposomes when the length of the chains increases. It must be pointed out that the helper and boron lipids should not differ significantly in their tail lengths. Therefore DSPC, which is commonly used as helper lipid for *in vivo* experiments, is suitable for the SAINT-16 derivatives. Longer lipid tails lead to a decrease of toxicity and are consequently recommended for dodecaborate cluster lipids.

All SAINT lipids have been prepared as cesium salts. The purification of the lipids by precipitation from methanol could be achieved by addition of a solution of cesium fluoride in methanol; this is an elegant procedure and consequently recommended for synthesis strategies of boron lipids. In contrast to, e.g., the tetramethylammonium ion (which is toxic *in vivo*), the cesium ion does not carry a substantial toxicity on its own.

The new lipids, with the exception of Dioxan-SAINT-12 and Dioxan-SAINT-14, have low *in vitro* toxicity and hence might represent suitable boron carriers for BNCT. *In vivo* experiments on mice are in progress to proceed to the next stage toward successful treatment with BNCT.

Acknowledgement

The authors gratefully thank Dr. Uwe Schüßler for the ICP-MS measurements. We would also like to thank Lipoid GmbH for generous gifts of lipids. This work has been financially supported by the German Research Council DFG through a joint grant to DG, RS, and RPS.

Supporting information available:

^{1}H NMR spectra of compounds **1c** and **all SAINT lipids**; ^{13}C NMR spectra of compounds **1c** and **all SAINT lipids**; ^{11}B NMR spectra of compounds **1c** and **all SAINT lipids**; ESI mass spectra of compounds **1c** and **all SAINT lipids**; IR spectra of compounds **1c** and **all SAINT lipids**. This material is available free of charge via the Internet at http://pubs.acs.org

References

(1) Barth, R. F. (2003) A critical assessment of boron neutron capture therapy: an overview. *J. Neurooncol.* 62, 1-5.

(2) Koryakin, S. N. (2006) Molecular-biological problems of drug design and mechanism of drug action. *Pharm. Chem. J. 40*, 583-587.

(3) Barth, R. F., Coderre, J. A., Vicente, M. G. H., and Blue, T. E. (2005) Boron neutron capture therapy of cancer: Current status and future prospects. *Clin. Cancer Res. 11*, 3987-4002.

(4) Hawthorne, M. F., and Lee, M. W. (2003) A critical assessment of boron target compounds for boron neutron capture therapy. *J. Neurooncol. 62*, 33-45.

(5) Schinanzi, R. F., and Prusoff, W. H. (1985) Synthesis of 5-(dihydroxyboryl)-2´-deoxyuridine and related boron-containing pyrimidines. *J. Org. Chem. 50*, 841-847.

(6) Yamamoto, Y., Seko, T., Nakamura, H., Nemoto, H., Hojo, H., Mukai N., and Hashimoto, Y. (1992) Synthesis of carboranes containing nucleosides bases. Unexpectedly high

cytostatic and cytocidal toxicity towards cancer cells. *J. Chem. Soc. Chem. Commun. 2*, 157-18.

(7) Peymann, T., Preusse, D., and Gabel, D. (1997) Synthesis of S-glycosides of mercaptoundecahydro-closo-dodecaborate (2-). *In Advances in Neutron Capture Therapy, Volume II, Chemistry and Biology.* (Larsson, B.; Crawford, J.; Weinreich, R., Eds.) pp. 35-37., Elsevier, Amsterdam.

(8) Bregadze, V. I., Sivaev, I. B., Gabel, D., and Wöhrle, D. (2001) Polyhedral boron derivatives of porphyrins and phthalocyanines. *J. Porphyrins Phthalocyanines 5*, 767-781.

(9) Vicente, M. G. H., Wickramasighe, A., Nurco, D. J., Wang, H. J. H., Nawrocky, M. M., Makar, M. S., and Miura, M. (2003) Synthesis, toxicity and biodistribution of two 5,15-di[3,5-(nidocarboranylmethyl)phenyl]porphyrin in EMT-6 tumor bearing mice. *Bioorg. Med. Chem. 11*, 3101-3108.

(10) Fronczek, F. R., and Vicente, M. G. H. (2005) Synthesis and cellular studies of an octa-anionic 5,10,15,20-tetra[3,5(nido-carboranylmethyl)phenyl]porphyrin (H_2OCP) for application in BNCT. *Bioorg. Med. Chem. 13*, 1633-1640.

(11) Hill, J. S., Kahl, S. B., Kaye, A. H., Stylli, S. S., Koo, M-S., Gonzales, M. F., Vardaxis N. J., and Johnson, C. I.(1992) Selective tumor uptake of boronated porphyrin in an animal model of cerebral glioma. *Proc. Natl. Acad. Sci. U.S.A. 89*, 1785-1789.

(12) Hill, J. S., Kahl, S. B., Stylli, S. S., Nakamura, Y., Koo, M-S., and Kaye, A. H. (1995) Selective tumor kill of cerebral glioma by photodynamic therapy using a boronated porphyrin photosensitizer. *Proc. Natl. Acad. Sci. U.S.A. 92*, 12126-12130.

(13) Barth, R. F., Adams, D. M., Soloway, A. H., Alam, F., and Darby, M. V. (1994) Boronated starburst dendrimer-monoclonal antibody immunoconjugates: evaluation as a potential delivery system for neutron capture therapy. *Bioconjugate Chem. 5*, 58-66.

(14) Novick, S., Quastel, M. R., Marcus, S., Chipman, D., Shani, G., Barth, R. F., and Soloway, A. H. (2002) Linkage of boronated polylysine to glycoside moieties of polyclonal antibody; Boronated antibodies as potential delivery agents for neutron capture therapy. *Nucl. Med. Biol. 29*, 159-167.

(15) Wu, G., Barth, R. F., Yang, W., Chatterjee, M., Tjarks, W., Cielsielski, M. J., and Fenstermaker, R. A. (2004) Site-specific conjugation of boron containing dendrimers of anti-EGF receptor monoclonal antibody cetuximab (IMC-C225) and its evaluation as a potential delivery agent for neutron capture therapy. *Bioconjugate Chem. 15*, 185-194.

(16) Pan, X. Q., Wang, H., Shukla, S., Sekido, M., Adams, D. M., Tjarks, W., Barth R. F., and Lee, R. J. (2002) Boron-containing folate receptor-targeted liposomes as potential delivery agents for neutron capture therapy. *Bioconjugate Chem. 13*, 435-442.

(17) Bohl-Kullberg, E., Bergstrand, N., Carlsson, J., Edwards, K., Johnsson, M., Sjöberg S., and Gedda, L. (2002) Development of EGF-conjugated liposomes for targeted delivery or boronated DNA-binding agents. *Bioconjugate Chem. 13*, 737-743.

(18) Maruyama, K., Ishida, O., Kasaoka, S., Takizawa, T., Utoguchi, N., Shinohara, A., Chiba, M., Kobayashi, H., Eriguchi, M., and Yanagie, H. J. (2004) Intracellular targeting of sodium mercaptoundecahydrododecaborate (BSH) to solid tumors by transferrin-PEG liposomes, for boron neutron-capture therapy (BNCT). *J. Controlled Release 98*, 195-207.

(19) Mehta, S. C., Lai, J. C., and Lu, D. R. (1996) Liposomal formulations containing sodium mercaptoundecahydrododecaborate (BSH) for boron neutron capture therapy. *J. Microencapsul. 13*, 269-279.

(20) Feakes, D. A., Shelly, K., Knobler, C. B., and Hawthorne, M. F. (1994) $Na_3[B_{20}H_{17}NH_3]^-$ Synthesis and liposomal delivery to murine tumors. *Proc. Natl. Acad. Sci. U.S.A. 91*, 3029-3033.

(21) Gabel, D., Awad, D., Schaffran, T., Radovan, D., Daraban, D., Damian, L., Winterhalter, M., Karlsson G., and Edwards, K. (2007) The anionic boron cluster $(B_{12}H_{11}SH)^{2-}$ as a means to trigger release of liposome contents. *ChemMedChem 2*, 51-53.

(22) Lee, J.-D., Ueno, M., Miyajima Y., and Nakamura, H. (2007) Synthesis of Boron Cluster Lipids: closo-dodecaborate as an alternative hydrophilic function of boronated liposomes for neutron capture therapy. *Org. Lett. 9*, 323-326.

(23) Nakamura, H., Lee, J.-D., Ueno, M., Miyajima, Y., and Ban, H. S. (2007) Synthesis of closo-dodecaboryl lipids and their liposomal formation for boron neutron capture therapy. *Nanobiotechnol. 3*, 135-145.

(24) Justus, E., Awad, D., Hohnholt, M., Schaffran, T., Edwards, K., Karlsson, G., Damian L., and Gabel., D. (2007) Synthesis, liposomal preparation, and in vitro toxicity of two novel dodecaborate cluster lipids for boron neutron capture therapy. *Bioconjugate Chem. 18*, 1287-1293.

(25) Schaffran, T., Lissel, F., Samatanga, B., Karlsson, G., Burghardt, A., Edwards, K., Winterhalter, M., Peschka-Süss, R., Schubert, R., and Gabel, D. (2009) Dodecaborate cluster lipids with variable headgroups for boron neutron capture therapy: Synthesis, physical–chemical properties and toxicity. *J. Organomet. Chem. 694*, 1708-1712.

(26) Rejman, J., Wagenaar, A., Engberts, J. B. F. N., and Hoekstra, D. (2004) Characterization and transfection properties of lipoplexes stabilized with novel exchangeable polyethylene glycol–lipid conjugates. *Biochim. Biophys. Acta 1660*, 41-52.

(27) Van Zanten, J., Doornbos-van der Meer, B., Audouy, S., Kok, R. J., and de Leij, L. (2004) A nonviral carrier for targeted gene delivery to tumor cells. *Cancer Gene Ther. 11*, 156-164.

(28) Zuhorn, I. S., Bakowsky, U., Polushkin, E., Visser, W. H., Stuart, M. C. A., Engberts, J. B. F. N., and Hoekstra, D. (2005) Nonbilayer phase of lipoplex–membrane mixture determines endosomal escape of genetic cargo and transfection efficiency. *Mol. Ther. 11*, 801-810.

(29) Justus, E., Rischka, K., Wishart, J. F., Werner, K., and Gabel, D. (2008) Trialkylammonio-dodecaborates: Anions for ionic liquids with potassium, lithium and proton as cations. *Chem. Eur. J. 14*, 1918-1923.

(30) King, G. T., and Miller, N. E. (1986). 1,12-Bis(hydroxymethyl)decahydrododecaborate(2-) and $B_{12}H_{10}(CH_2X)_2^{2-}$ and $B_{12}H_{10}(CH_2L)_2$ derivatives. *Inorg. Chem. 25*, 4309-4311.

(31) Sivaev, I. B., Kulikova, N. Y., Nizhnik, E. N., Vichuzhanin, M. V., Starikova, Z. A., Semioshkin, A. A., and Bregadze, V. I. (2008) Practical synthesis of 1,4-dioxane derivative of the closo-dodecaborate anion and its ring opening with acetylenic alkoxides. *J. Organomet. Chem. 693*, 519-525.

(32) Sivaev, I. B., Semioshkin, A. A., Brellochs, B., Sjöberg, S., and Bregatze, V. I. (2000) Synthesis of oxonium derivatives of the dodecahydro-closo-dodecaborate anion $[B_{12}H_{12}]^{2-}$. Tetramethylene oxonium derivative of $[B_{12}H_{12}]^{2-}$ as a convenient precursor for the synthesis of functional compounds for boron nutron captre therapy. *Polyhedron 19*, 627-632.

(33) Peymann, T., Lork, E., and Gabel, D. (1996) Hydroxoundecahydro-closo-dodecaborate (2-) as a nucleophile. Preparation and structural characterization of O-acyl derivatives of Hydroxoundecahydro-closo-dodecaborate (2-). *Inorg. Chem. 35*, 1355-1360.

(34) Meekel, A. A. P., Wagenaar, A., Ŝmisterová, J., Kroeze, J. E., Haadsma, P., Bosgraaf, B., Stuart, M. C. A., Brisson, A., Ruiters, M. H. J., Hoekstra, D., and Engberts, J. B. F. N. (2000) Synthesis of pyridinium amphiphiles used for transfection and some characteristics of amphiphile/DNA complex formation. *Eur. J. Org. Chem.*, 665-673.

(35) Sudhölter, E. J. R., Engberts, J. B. F. N., and de Jeu, W. H. (1982) Thermotropic liquid-crysatlline behavior of some single- and double chained pyridinium amphiphiles. *J. Phys. Chem. 86*, 1908-1913.

(36) Stewart, J. C. (1980) Calorimetric determination of phospholipids with ammonium ferrothiocyanate. *Anal. Biochem. 104*, 10-14.

(37) Semioshkin, A., Nizhnik, E., Godovikov, I., Starikova, Z., and Bregadze, V. (2007) Reactions of oxonium derivatives of $[B_{12}H_{12}]^{2-}$ with amines: Synthesis and structure of novel B_{12}-based ammonium salts and amino acids. *J. Org. Chem. 692*, 4020-4028.

(38) Biltonen, R. L., and Lichtenberg, D. (1993) The use of differential scanning calorimetry as a tool to characterize liposome preparations. *Chem. Phys. Lipids 64*, 129-142.

(39) Chen, S. C., Sturtevant, J. M., and Gaffney, B. (1980) Scanning calorimetric evidence for a third phase transition in phosphatidylcholine bilayers. *Proc. Natl. Acad. Sci. U.S.A. 77*, 5060-5063.

(40) Finegold, L., and Singer, M. A. (1984) Phosphatidylcholine bilayers: Subtransitions in pure and in mixed lipids. *Chem. Phys. Lipids* 35, 291-297.

(41) Levchenko, T. S., Rammohan, R., Lukyanov, A. N., Whiteman, K. R., and Torchilin, V. P. (2002) Liposome clearance in mice: the effect of a separate and combined presence of surface charge and polymer coating. *Int. J. Pharm.* 240, 95-102.

Pyridinium lipids with the dodecaborate cluster as polar head group: Synthesis, characterization of the physical-chemical behavior and cell viability

Tanja Schaffran, Alexander Burghardt, Regine Peschka-Süss, Rolf Schubert, Mathias Winterhalter, Detlef Gabel

Supplementary material

1H-NMR spectra of compounds **1c** and **all SAINT lipids**
13C-NMR spectra of compounds **1c** and **all SAINT lipids**
11B-NMR spectra of compounds **1c** and **all SAINT lipids**
ESI mass spectra of compounds **1c** and **all SAINT lipids**
IR spectra of compounds **1c** and **all SAINT lipids**

1-pentamethyleneoxonium-closo-undecahydrododecaborate (-1), tetrabutylammonium salt (1c).

ESI-MS, negative

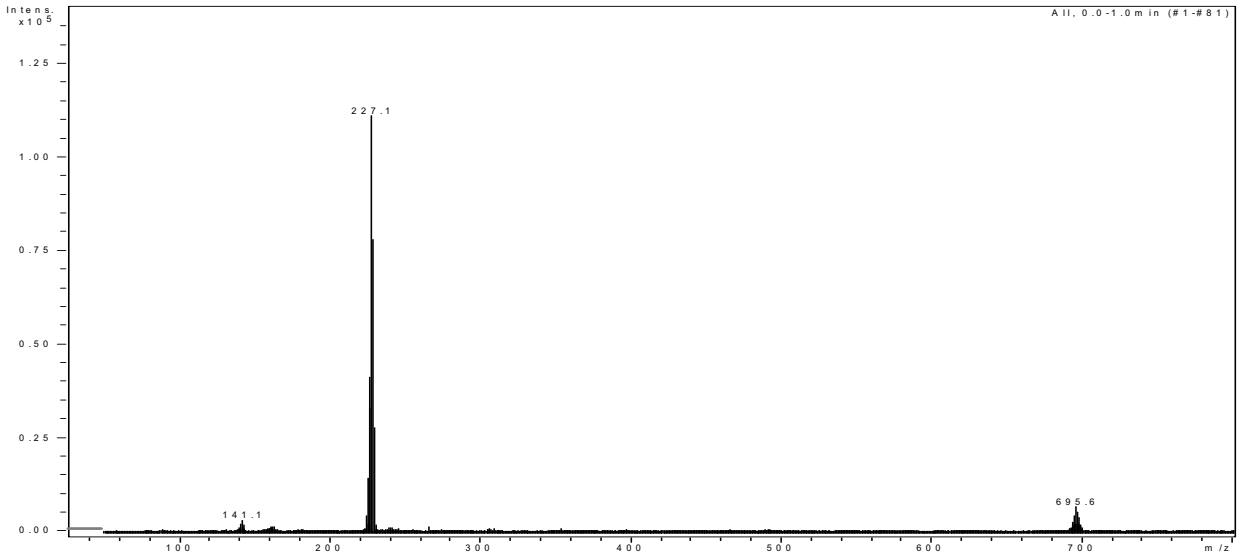

ESI-MS, positive

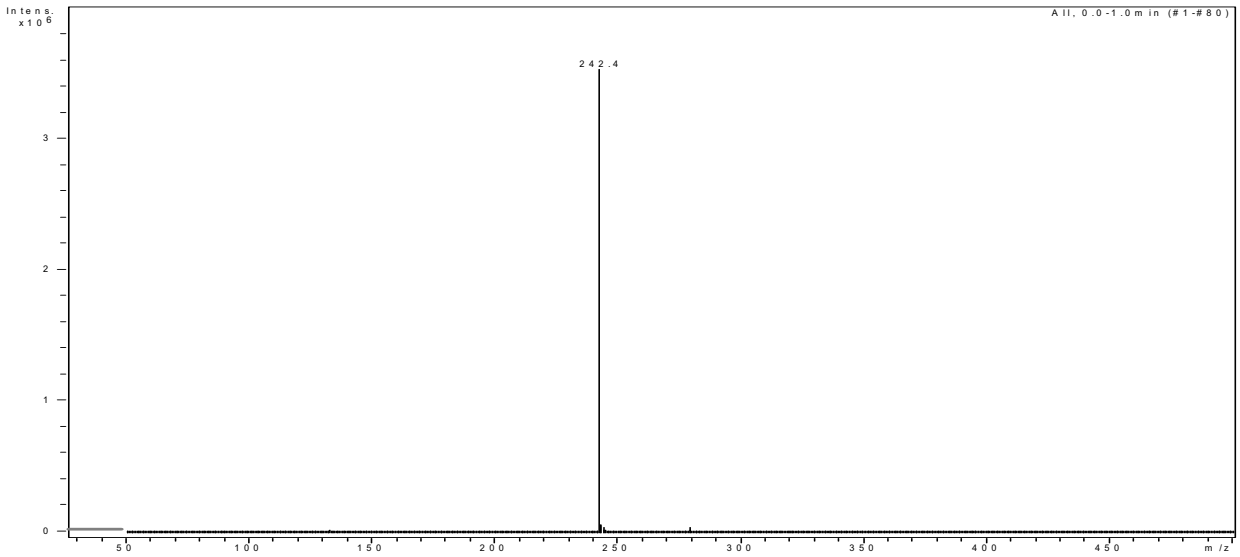

1H-NMR, Acetonitrile-d3

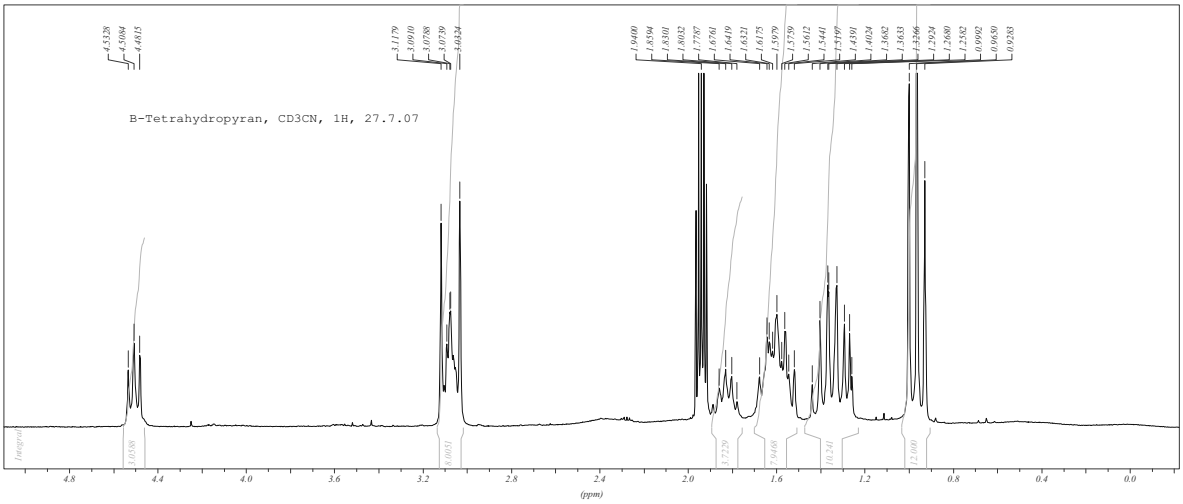

13C-NMR, Acetonitrile-d3

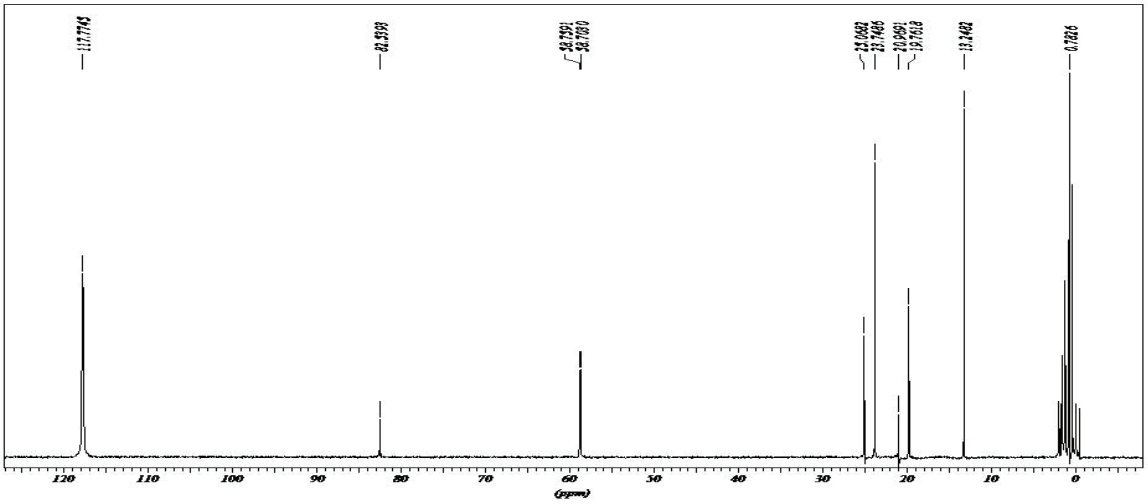

11B-NMR, Acetonitrile-d3

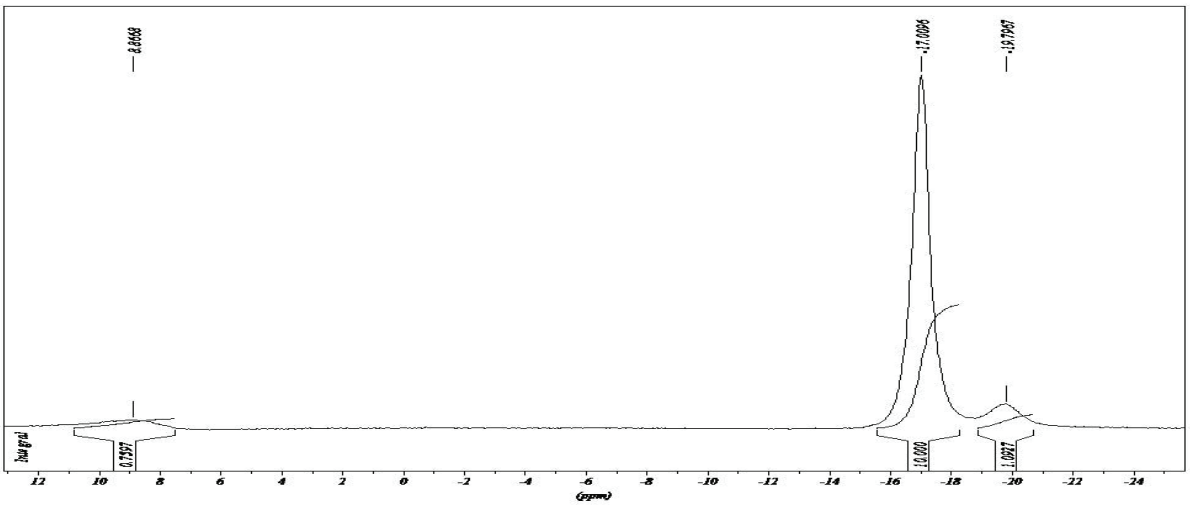

IR-spectrum

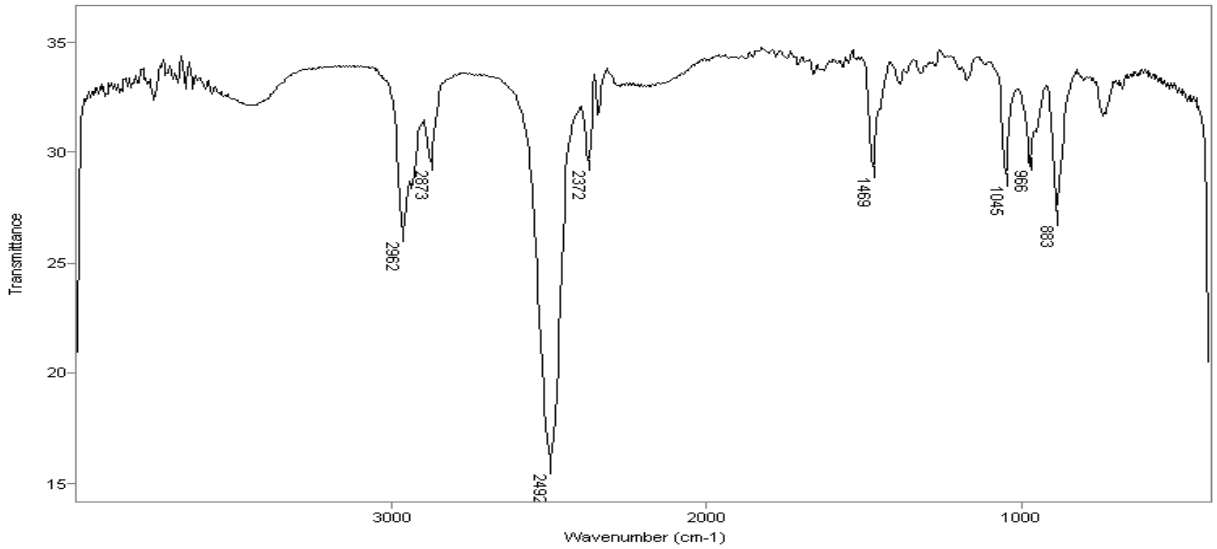

4-(Bisdodecylmethyl)pyridinio-N-butoxy-undecahydro-closo-dodecaborate (-1), cesium salt (THF-SAINT-12).

ESI-MS, negative

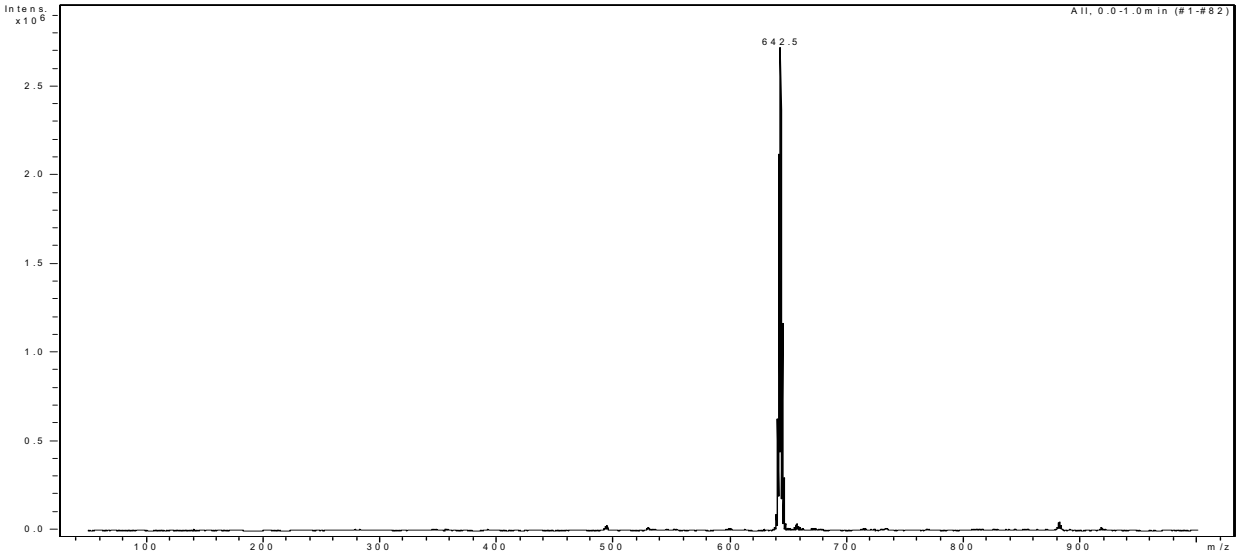

ESI-MS, positive

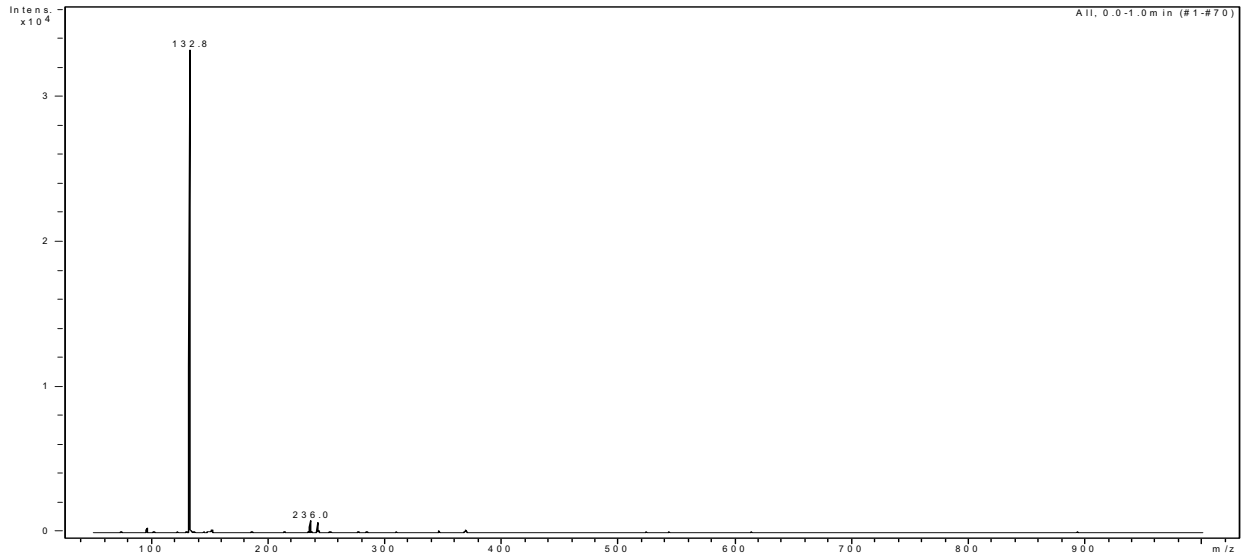

1H-NMR, DMSO-d6

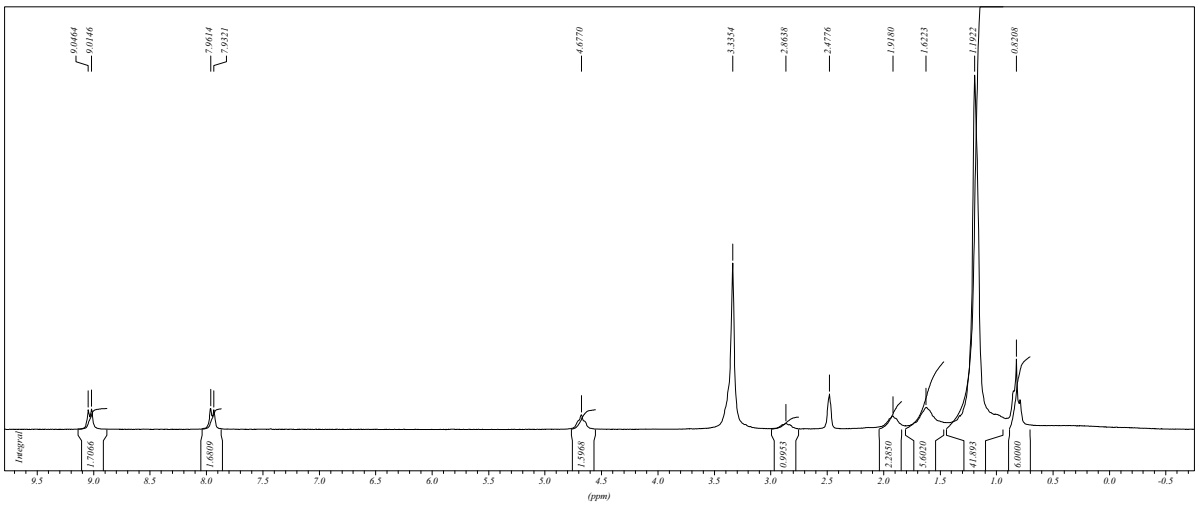

13C-NMR, DMSO-d6

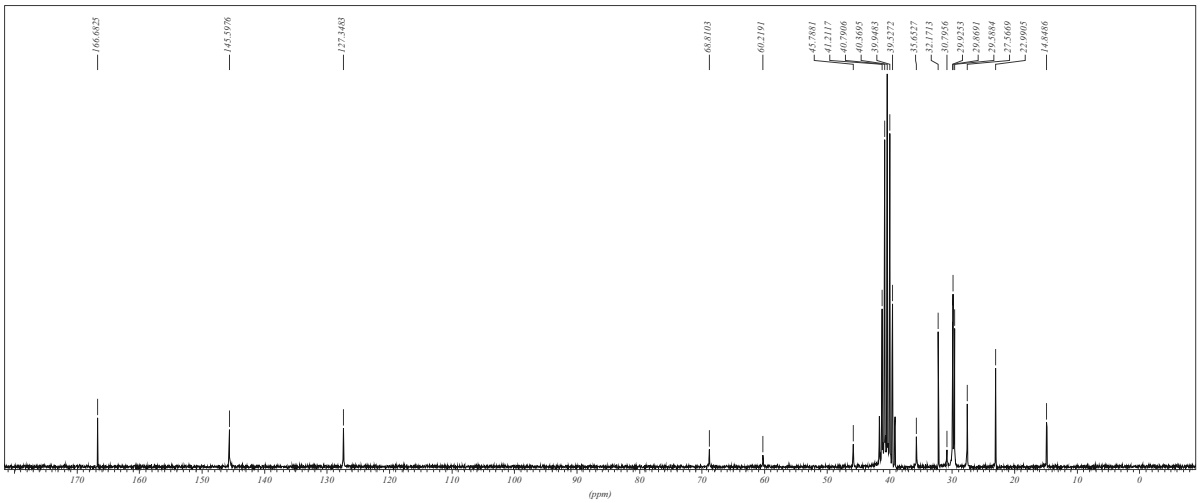

11B-NMR, DMSO-d6

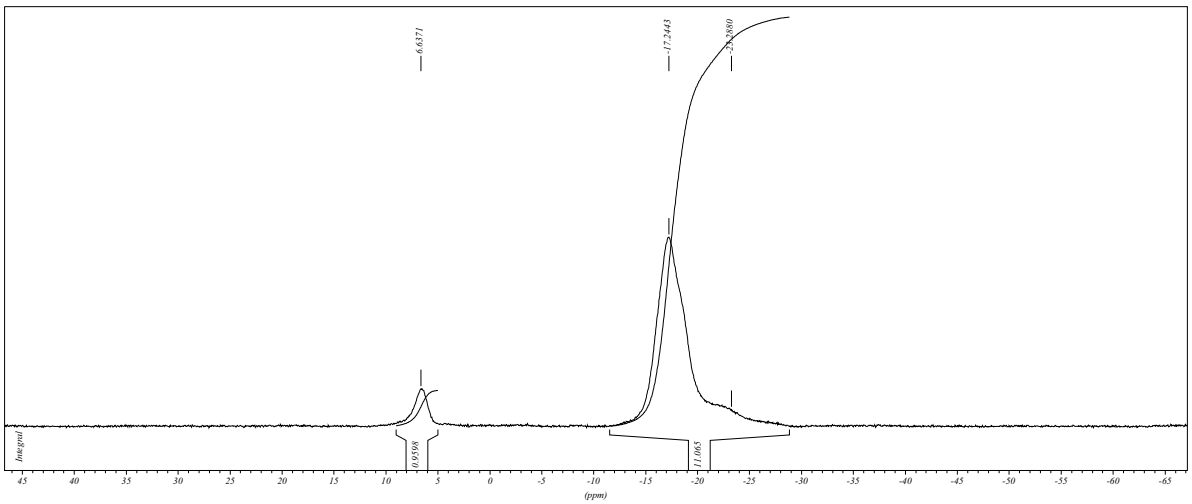

IR-spectrum

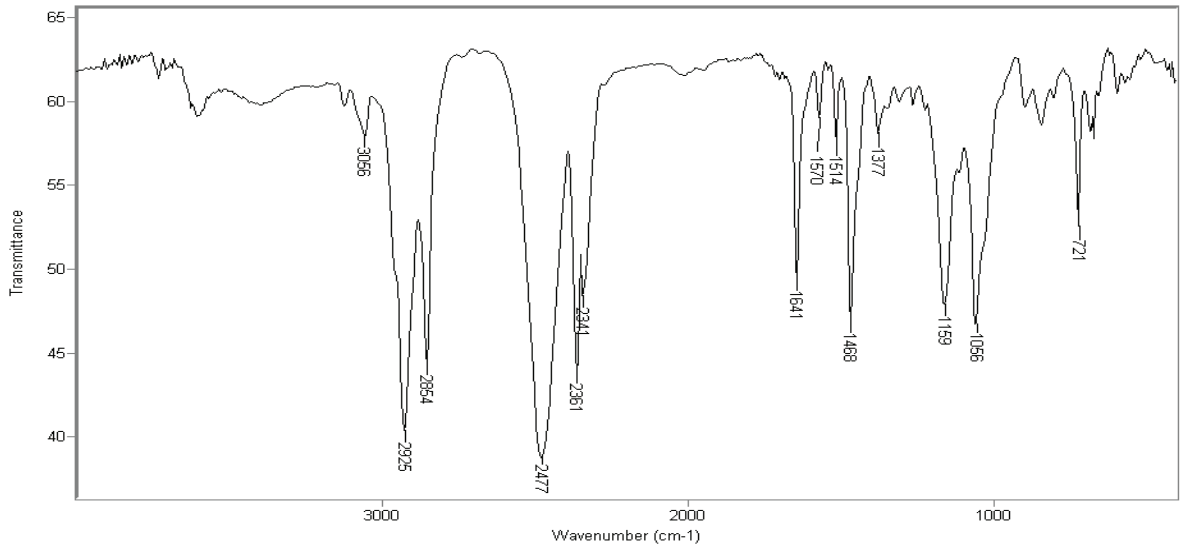

4-(Bisdodecylmethyl)pyridinio-N-ethoxy-ethoxy-undecahydro-closo-dodecaborate (-1), cesium salt (Dioxan-SAINT-12).

ESI-MS, negative

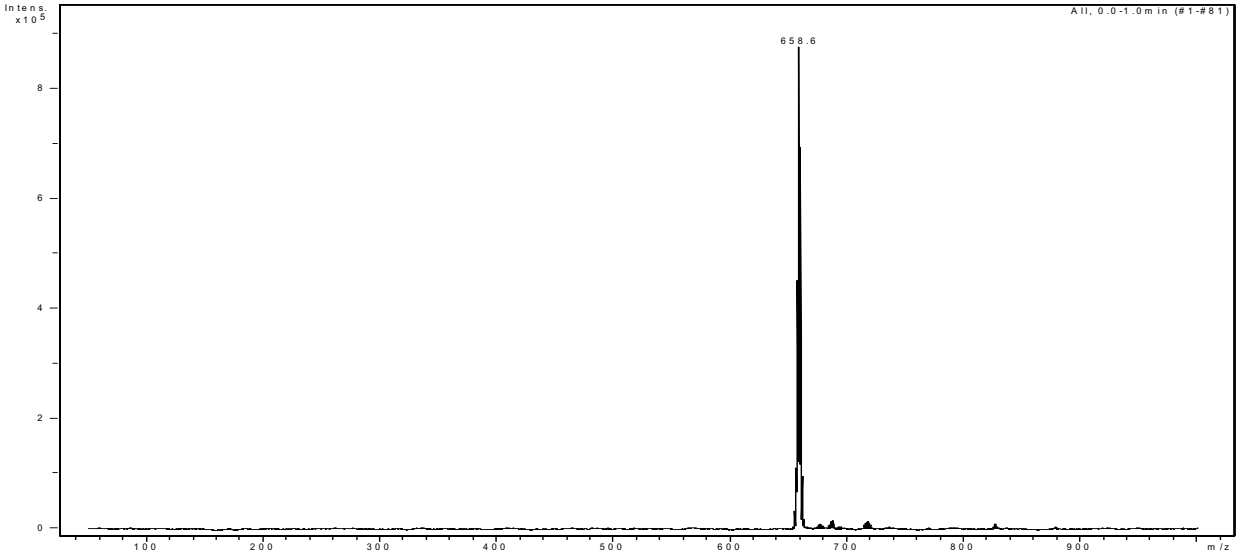

ESI-MS, positive

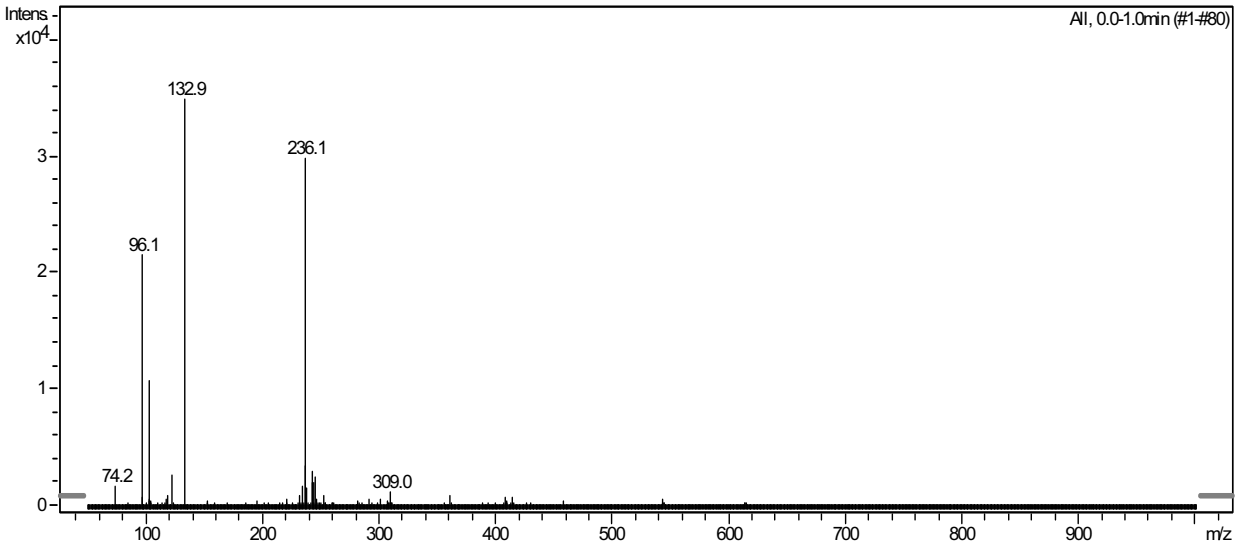

1H-NMR, DMSO-d6

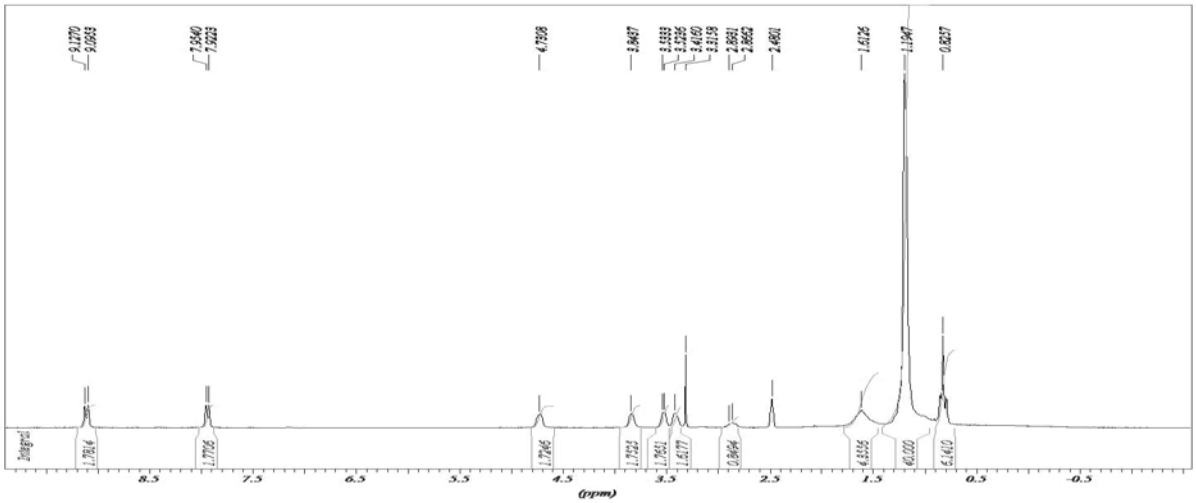

13C-NMR, DMSO-d6

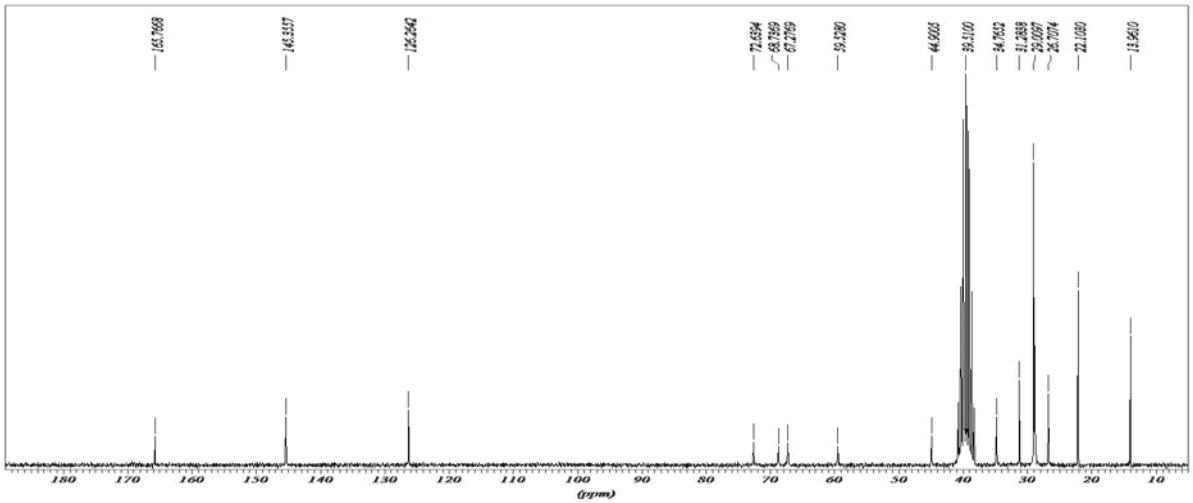

11B-NMR, DMSO-d6

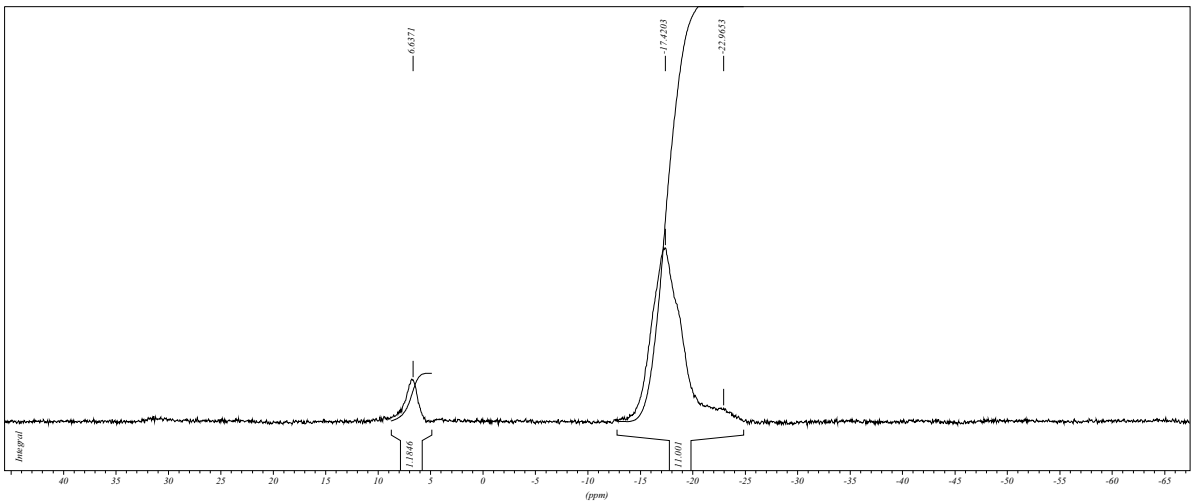

IR-spectrum

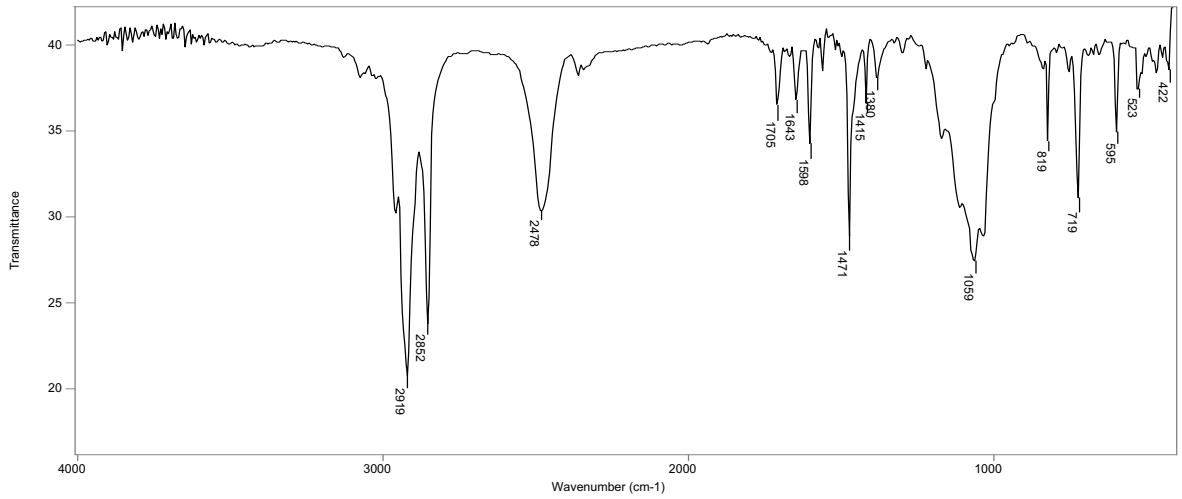

4-(Bisdodecylmethyl)pyridinio-N-pentoxy-undecahydro-closo-dodecaborate (-1), cesium salt (Pyran-SAINT-12).

ESI-MS, negative

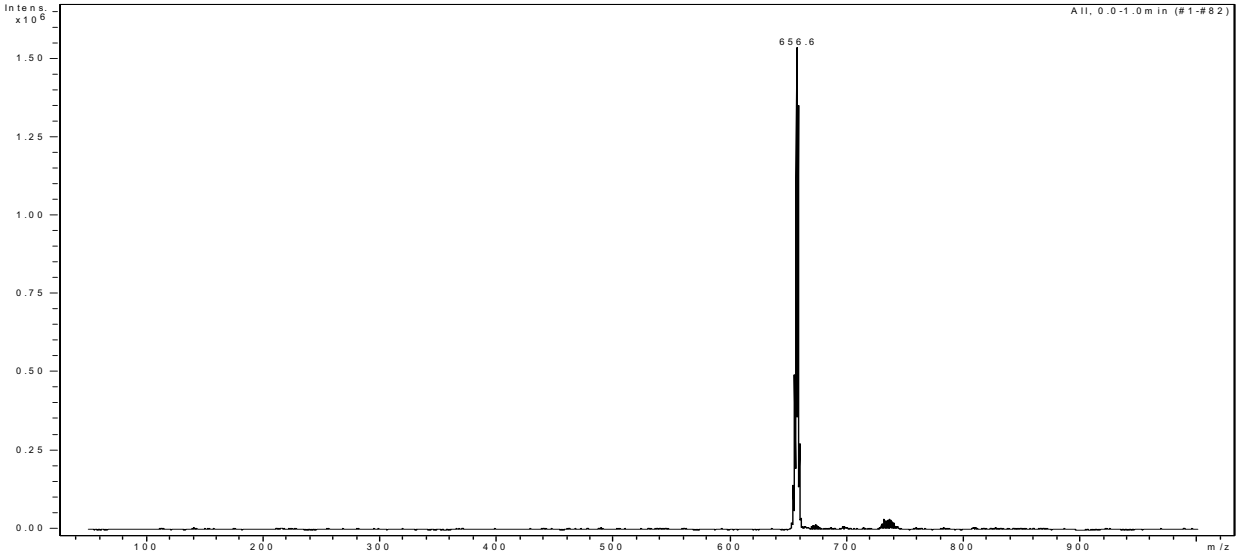

ESI-MS, positive

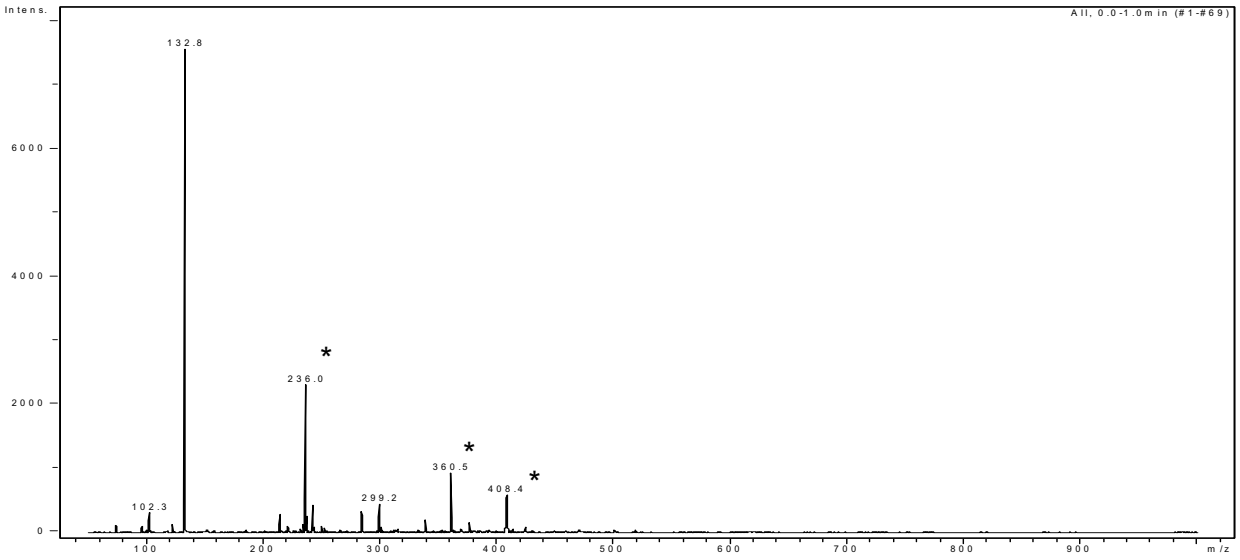

* Impurities in the MS machine.

1H-NMR, DMSO-d6

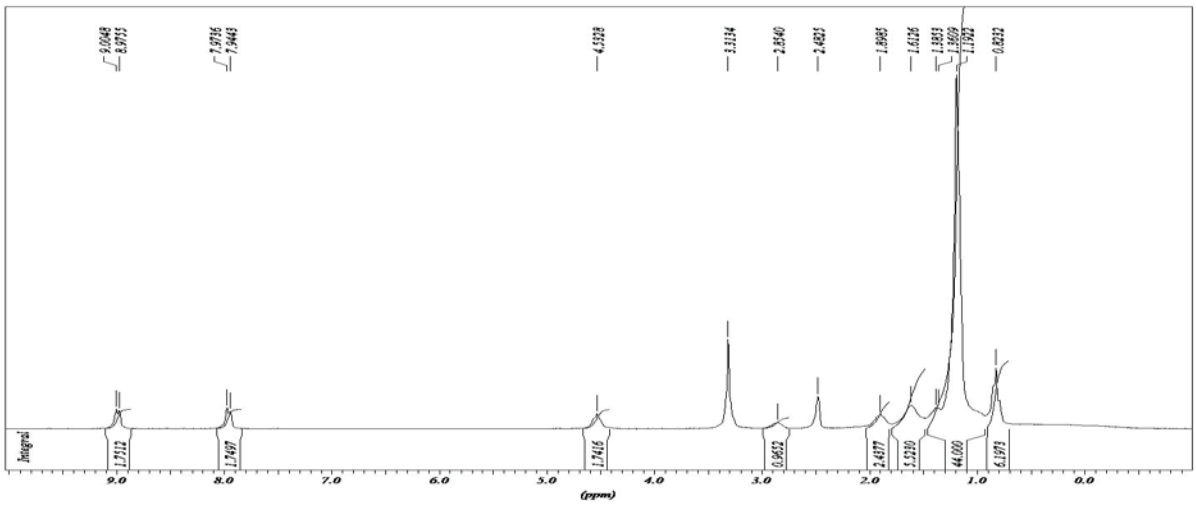

13C-NMR, DMSO-d6

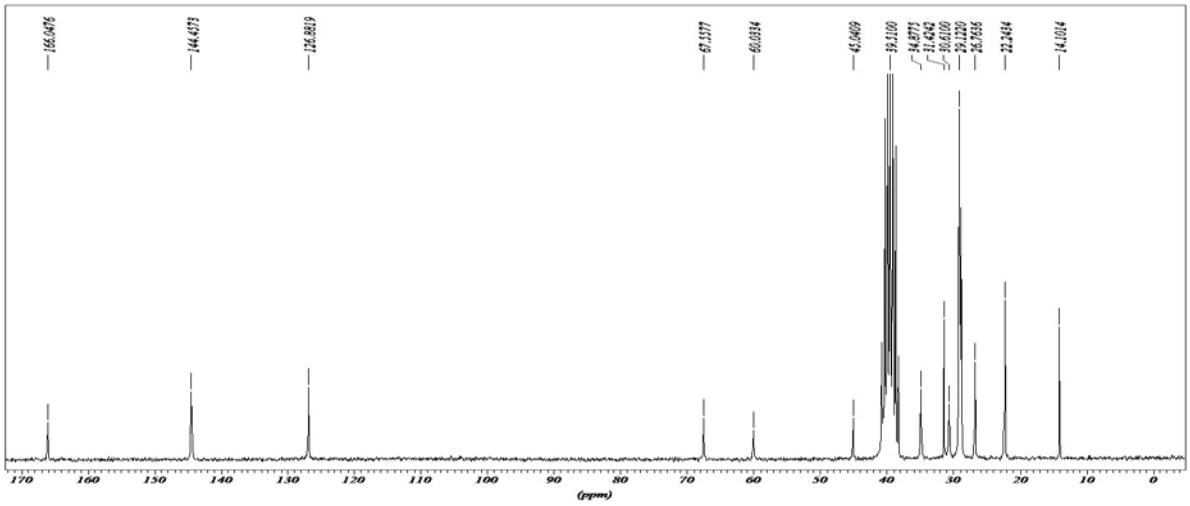

11B-NMR, DMSO-d6

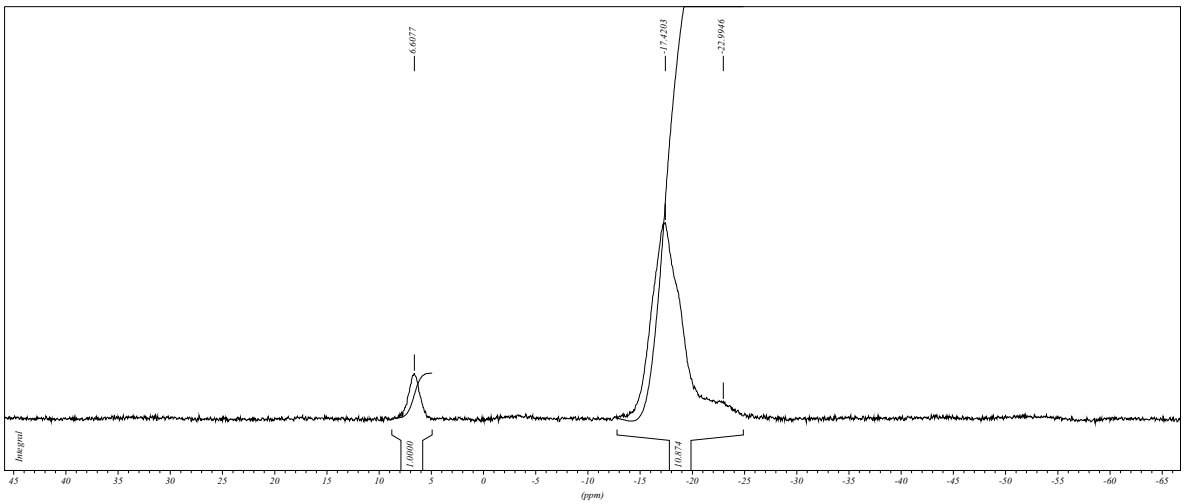

IR-spectrum

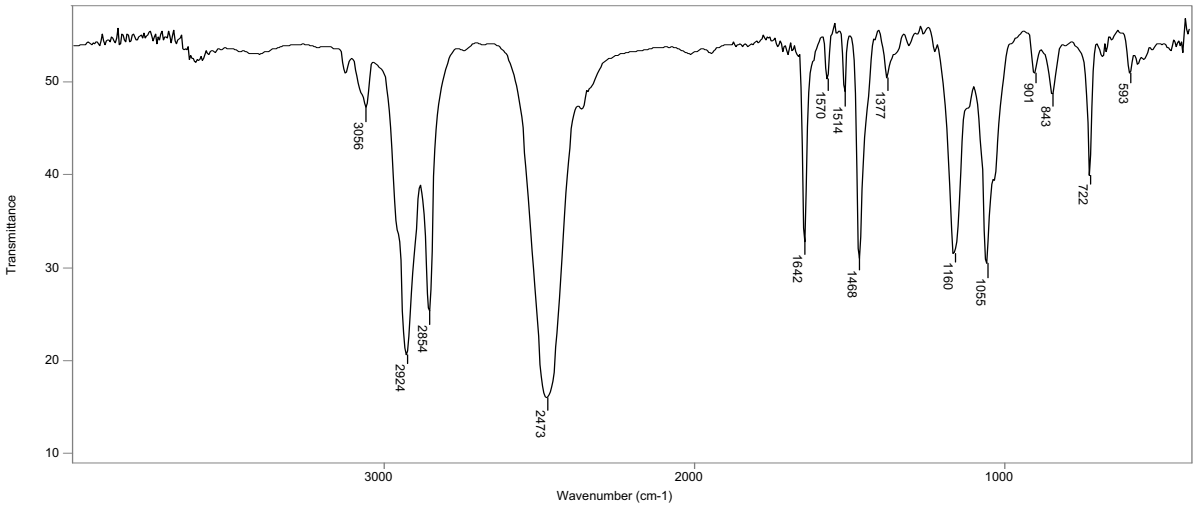

4-(Bistetradecylmethyl)pyridinio-N-butoxy-undecahydro-closo-dodecaborate (-1), cesium salt (THF-SAINT-14).

ESI-MS, negative

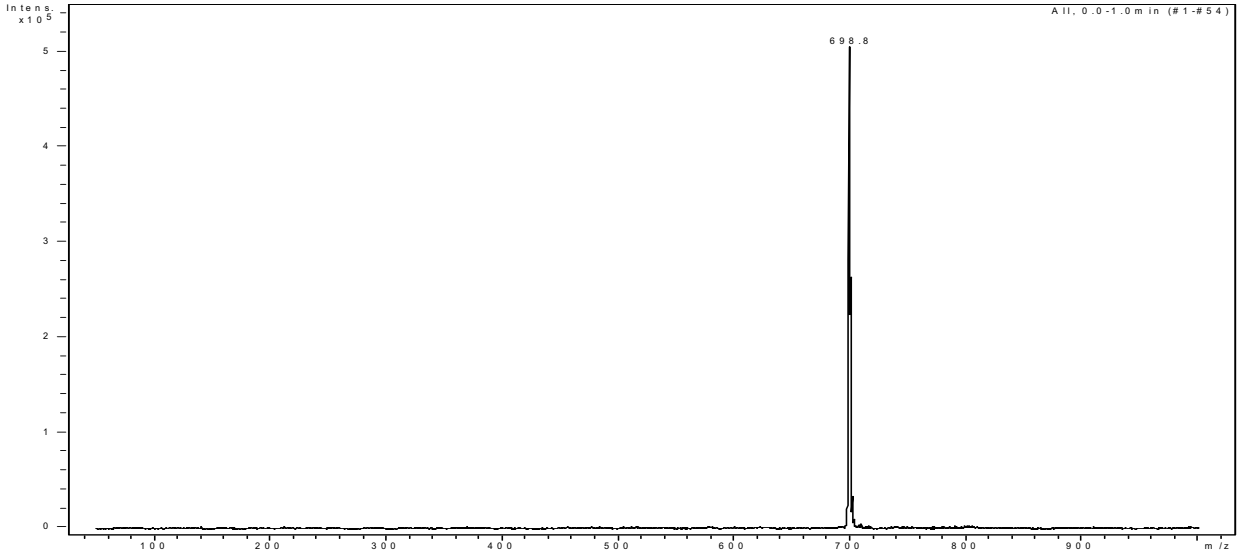

ESI-MS, positive

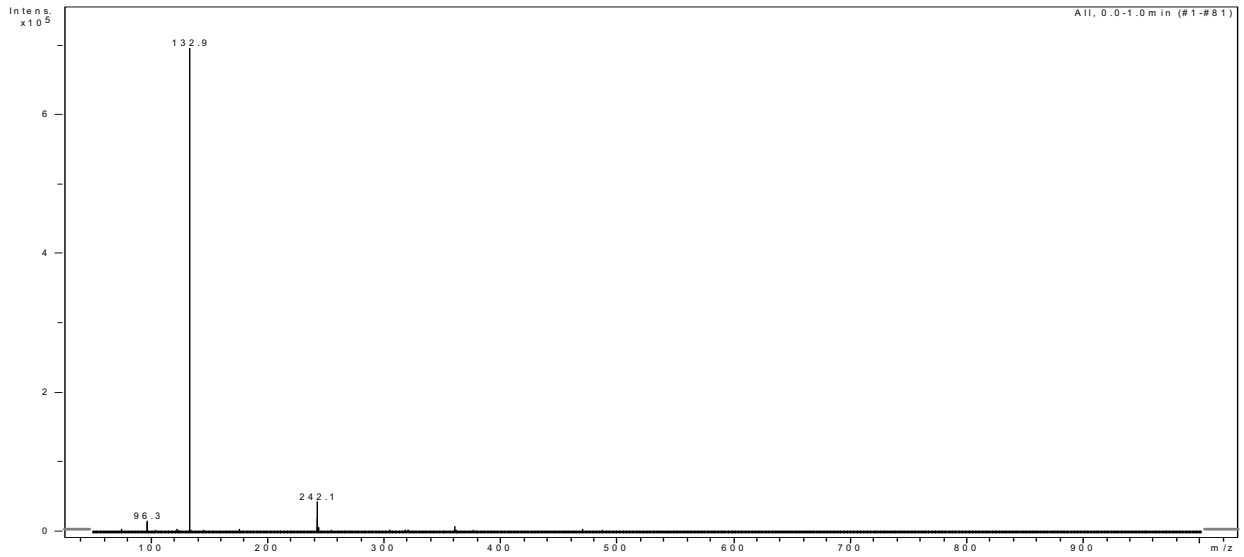

1H-NMR, DMSO-d6

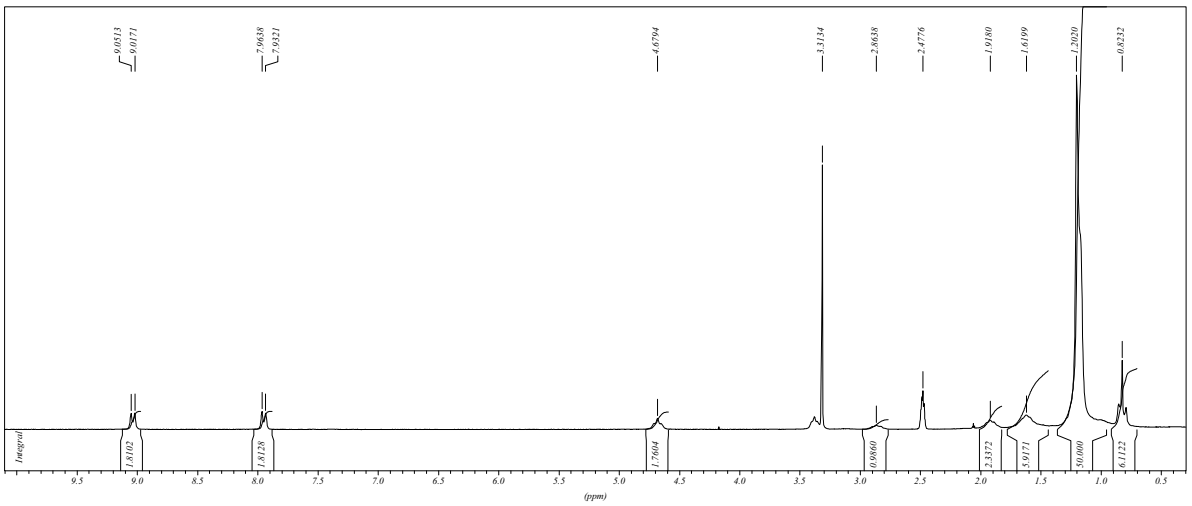

13C-NMR, DMSO-d6

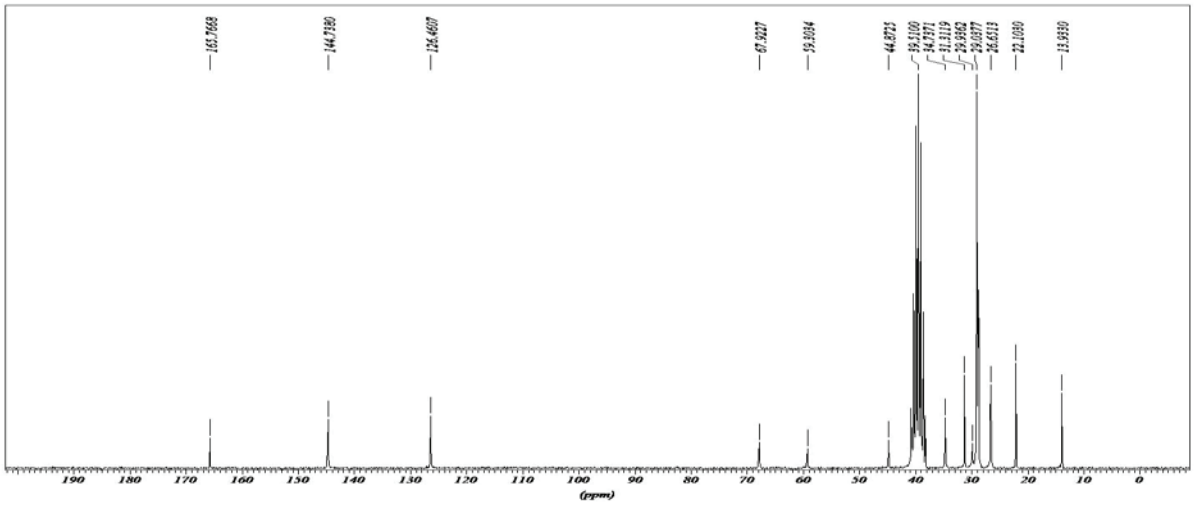

11B-NMR, DMSO-d6

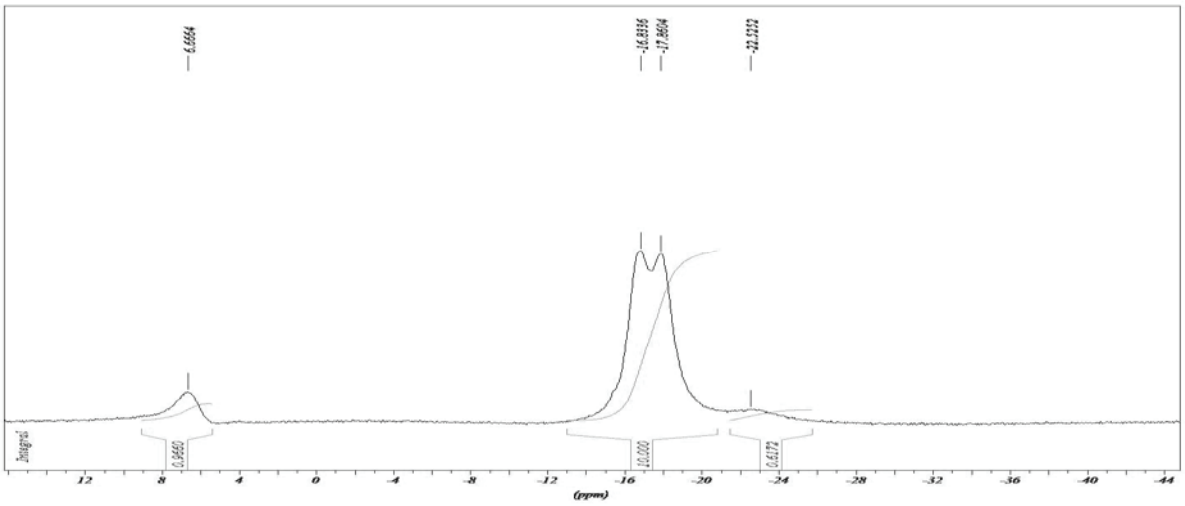

IR-spectrum

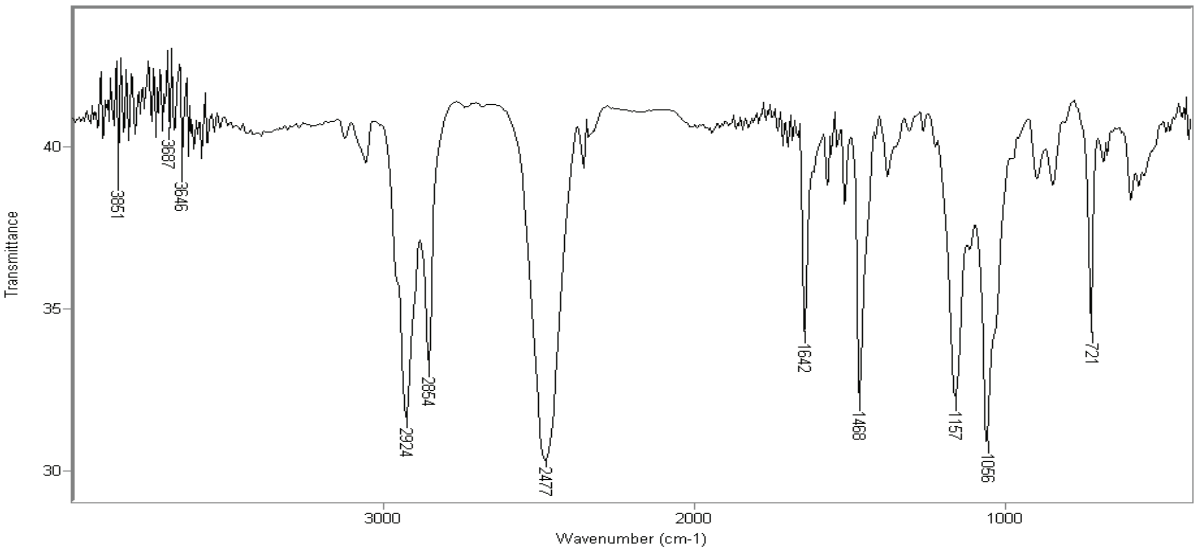

4-(Bistetradecylmethyl)pyridinio-N-ethoxy-ethoxy-undecahydro-closo-dodecaborate (-1), cesium salt (Dioxan-SAINT-14).

ESI-MS, negative

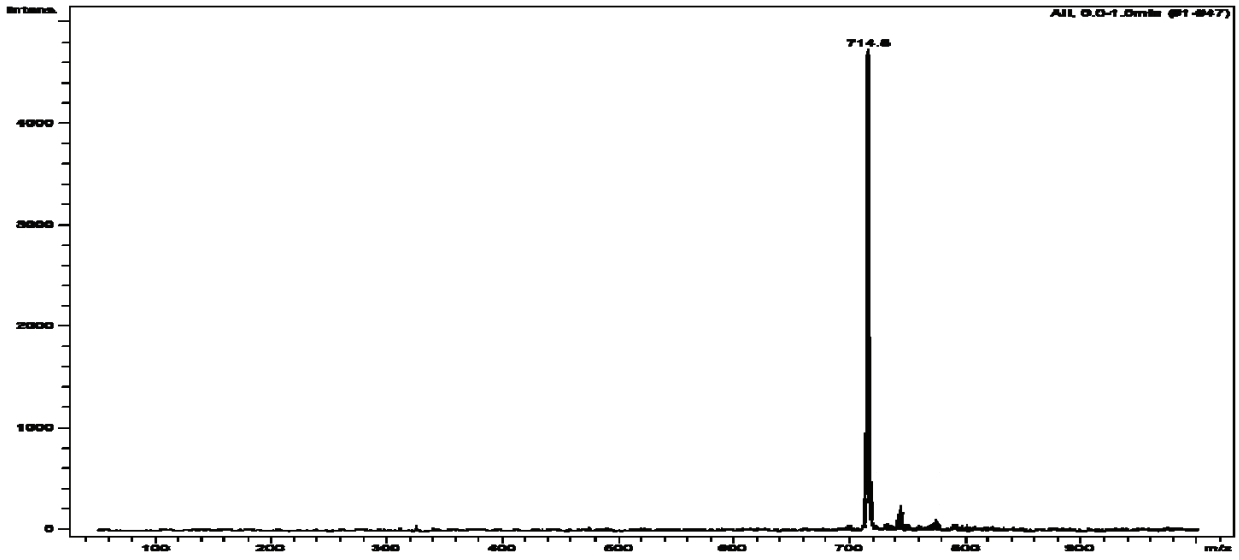

ESI-MS, positive

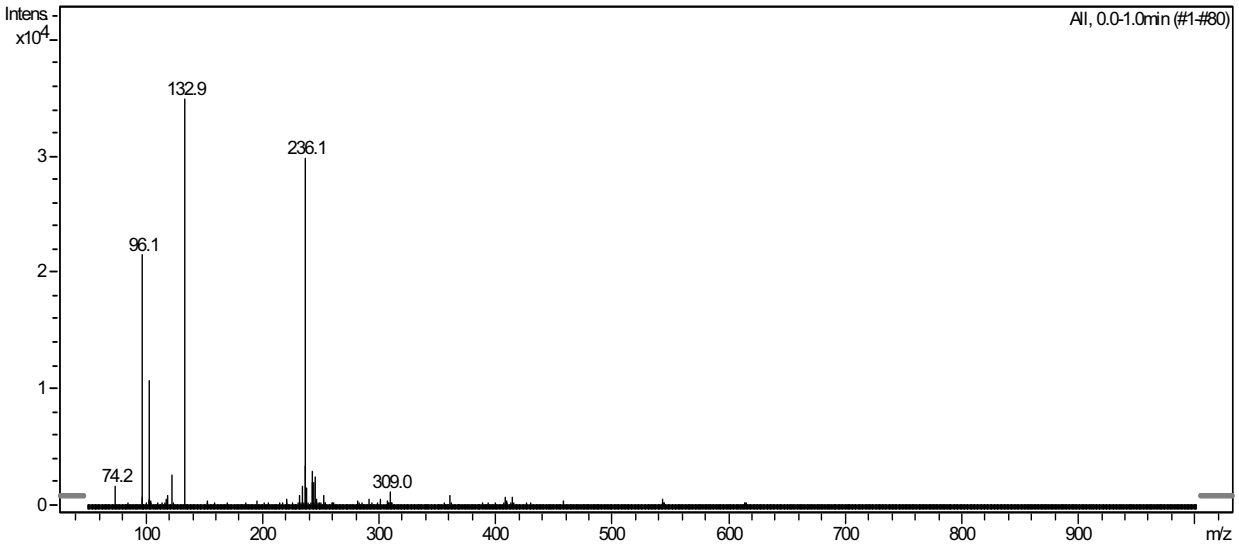

1H-NMR, DMSO-d6

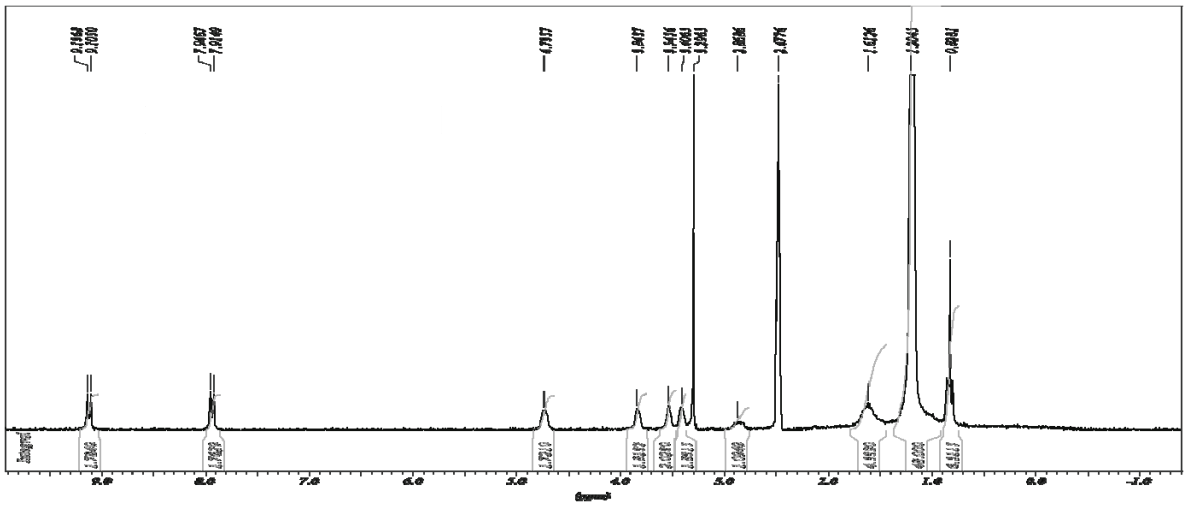

13C-NMR, DMSO-d6

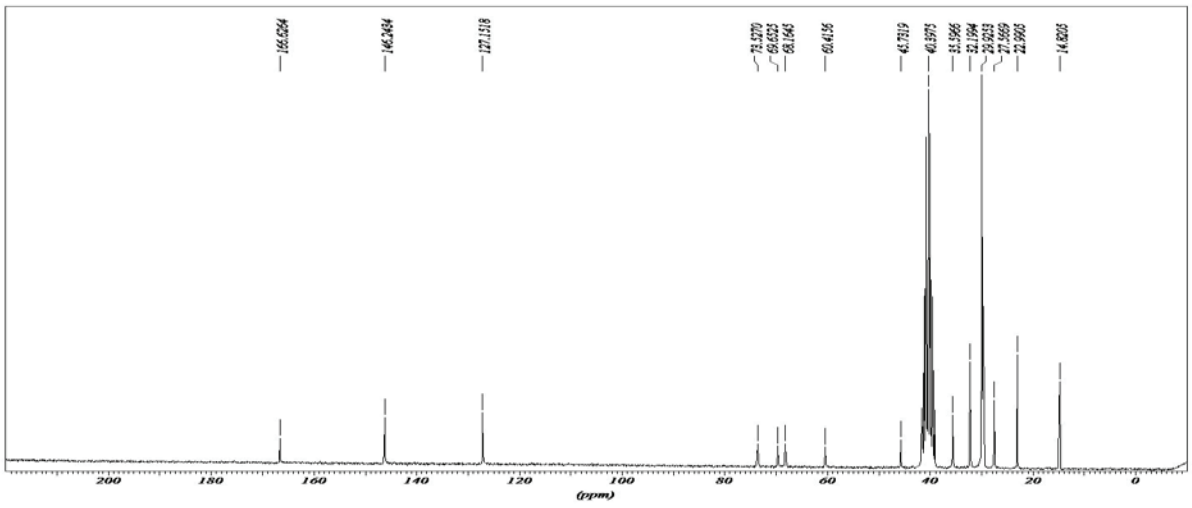

11B-NMR, DMSO-d6

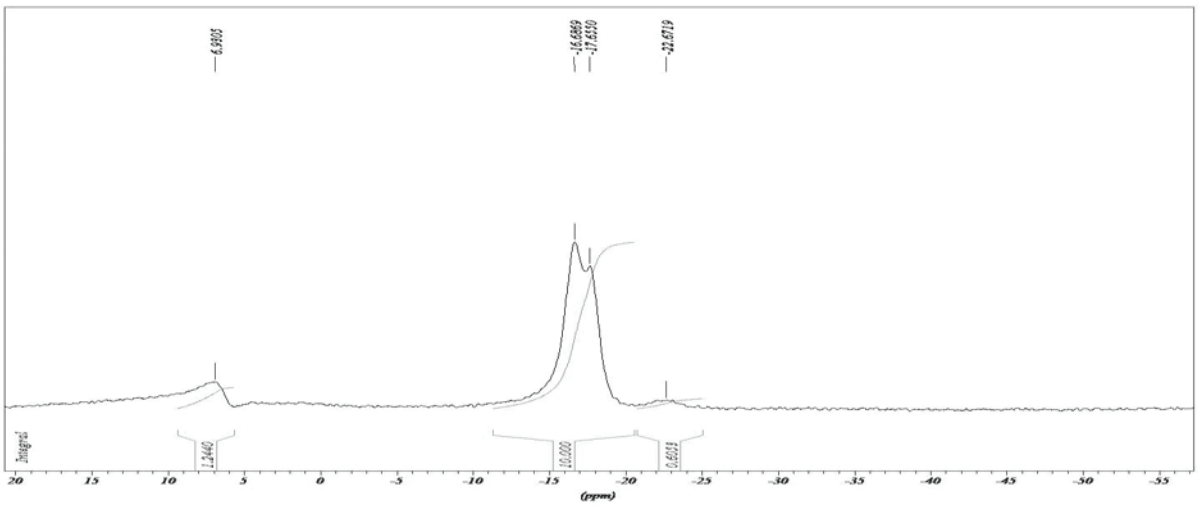

IR-spectrum

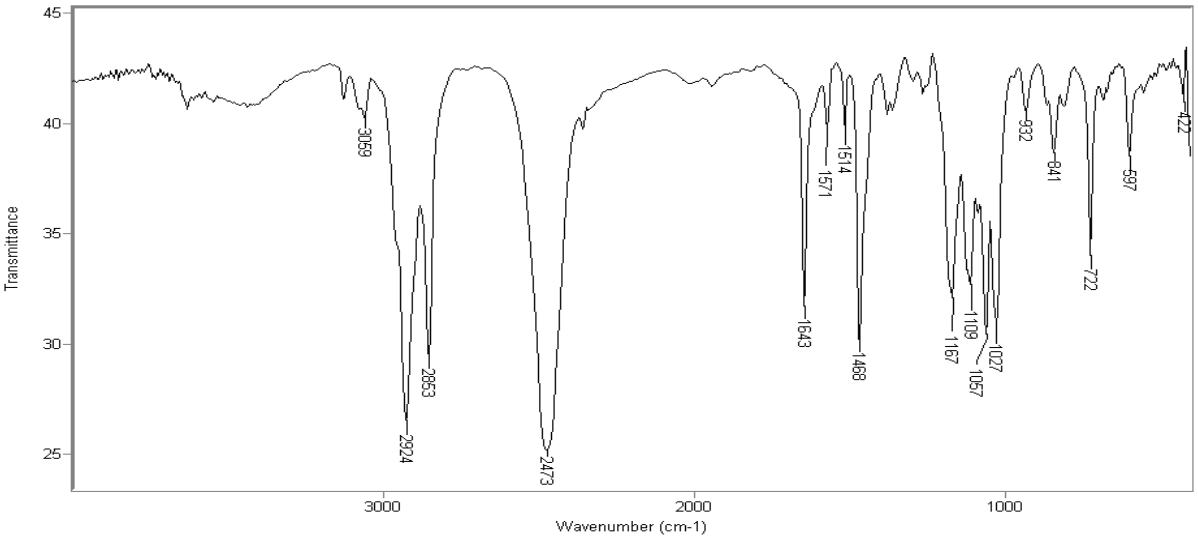

4-(Bistetradecylmethyl)pyridinio-N-pentoxy-undecahydro-closo-dodecaborate (-1), cesium salt (Pyran-SAINT-14).

ESI-MS, negative

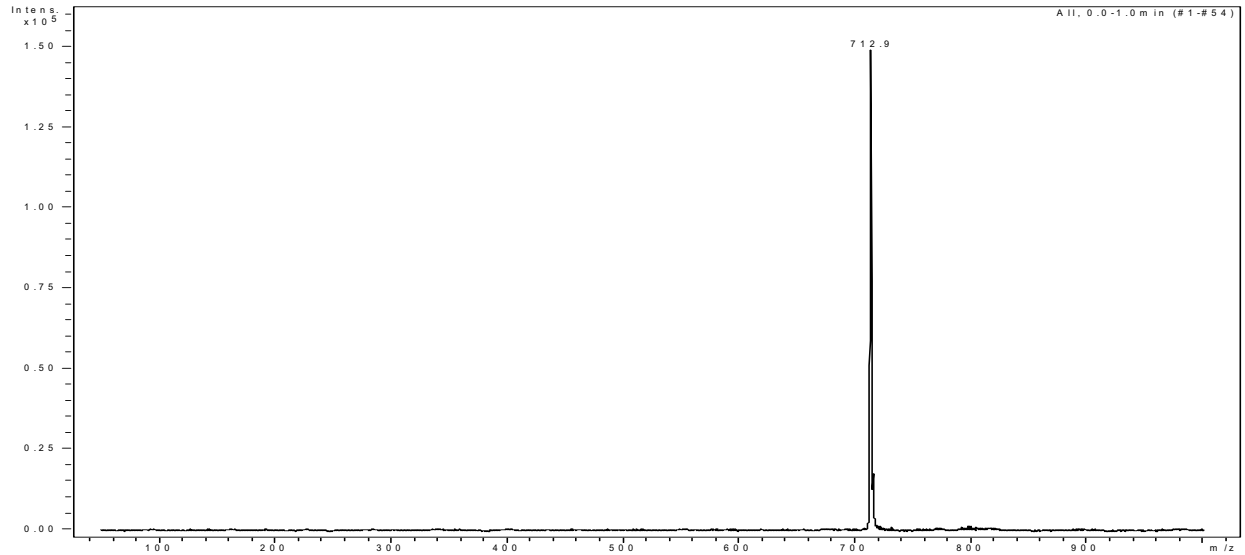

ESI-MS, positive

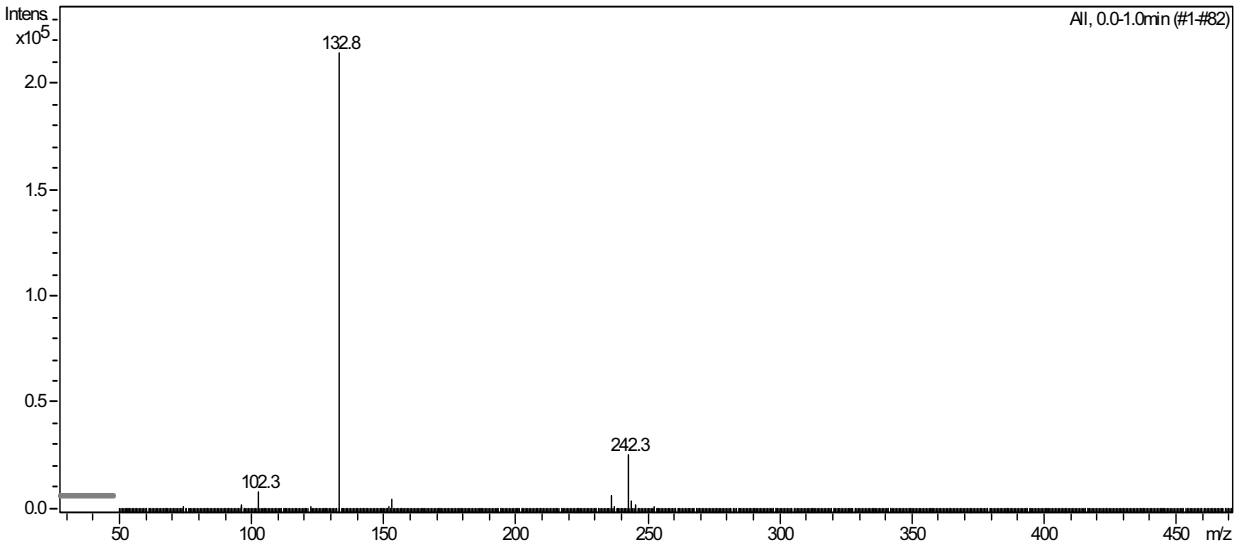

1H-NMR, DMSO-d6

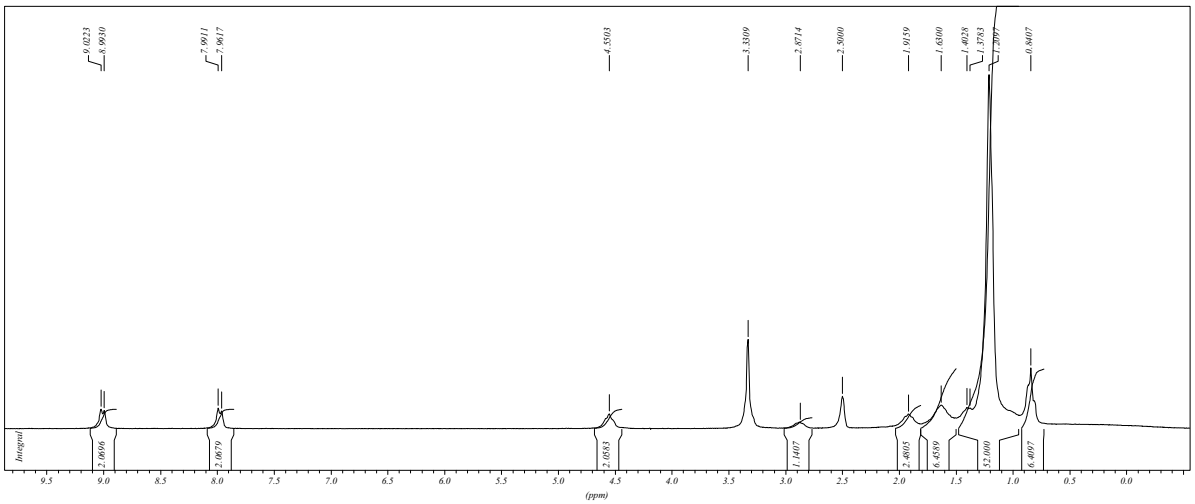

13C-NMR, DMSO-d6

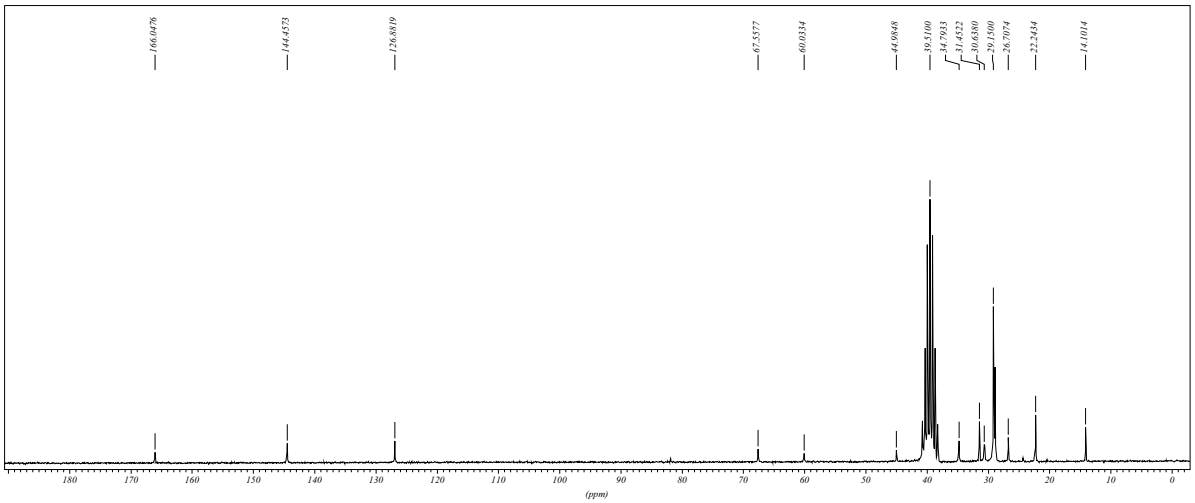

11B-NMR, DMSO-d6

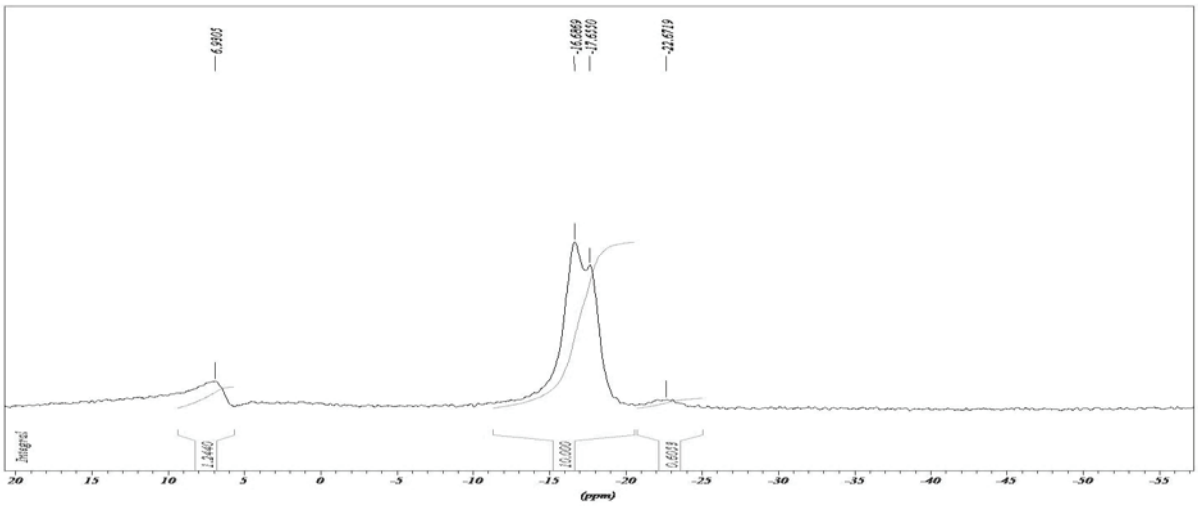

IR-spectrum

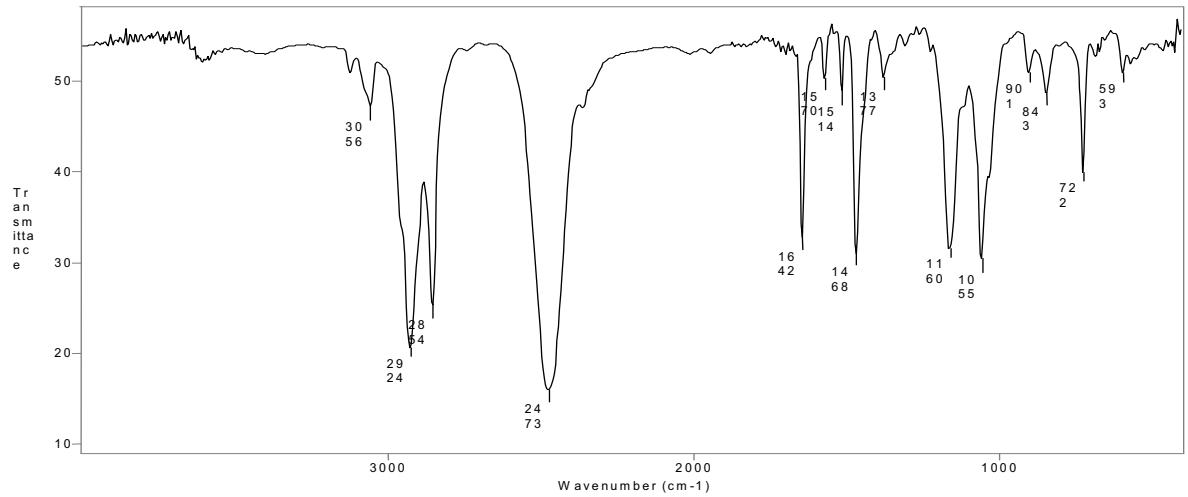

4-(Bishexadecylmethyl)pyridinio-N-butoxy-undecahydro-closo-dodecaborate (-1), cesium salt (THF-SAINT-16).

ESI-MS, negative

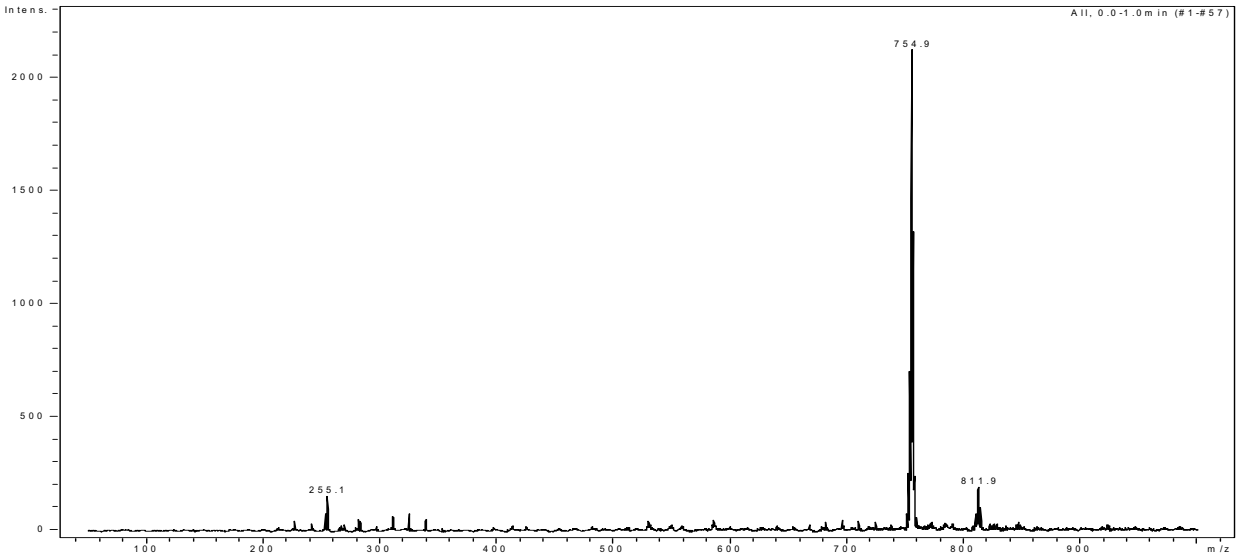

ESI-MS, positive

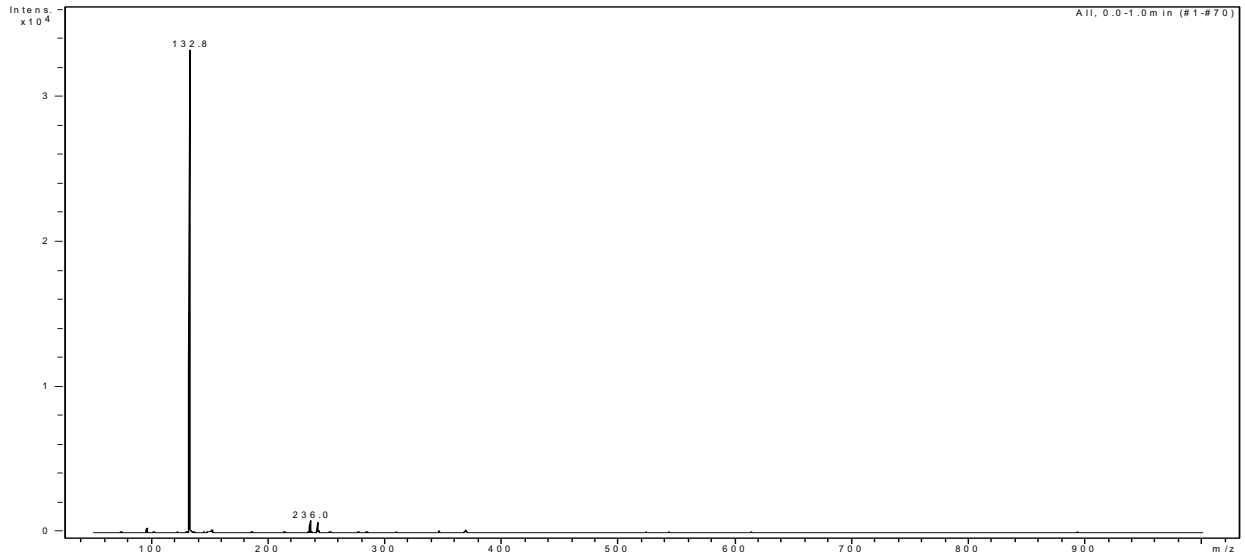

1H-NMR, DMSO-d6

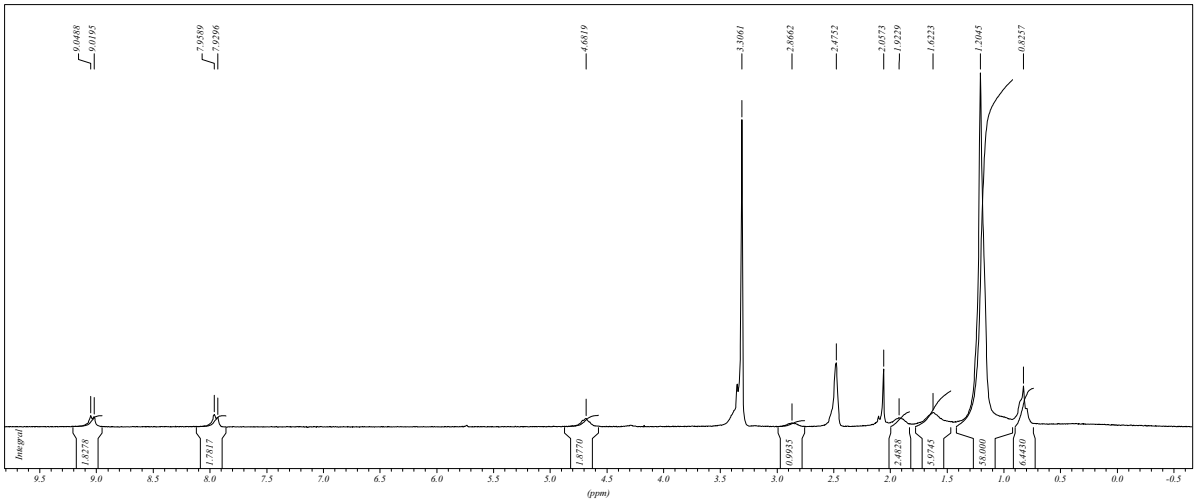

13C-NMR, DMSO-d6

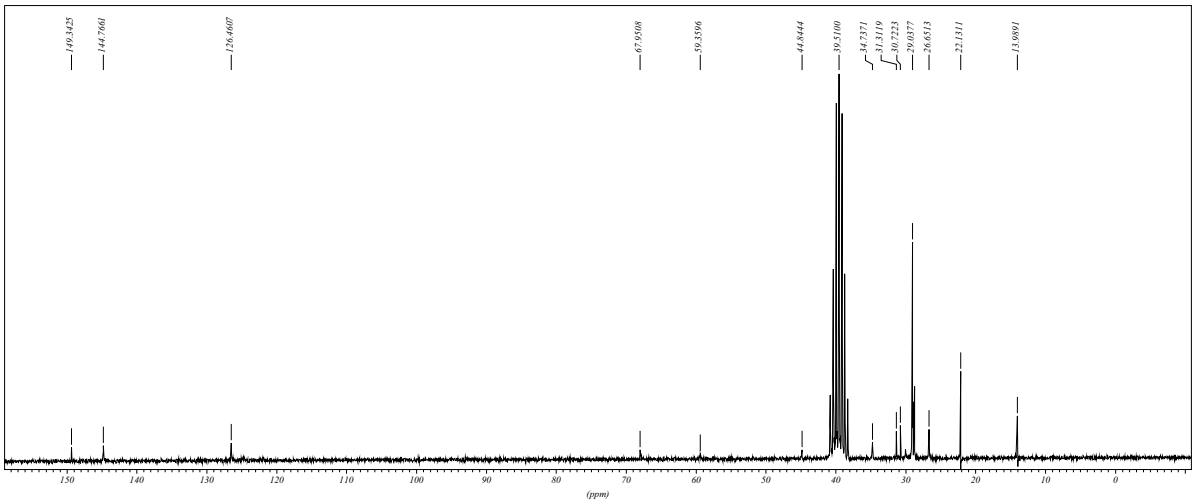

11B-NMR, DMSO-d6

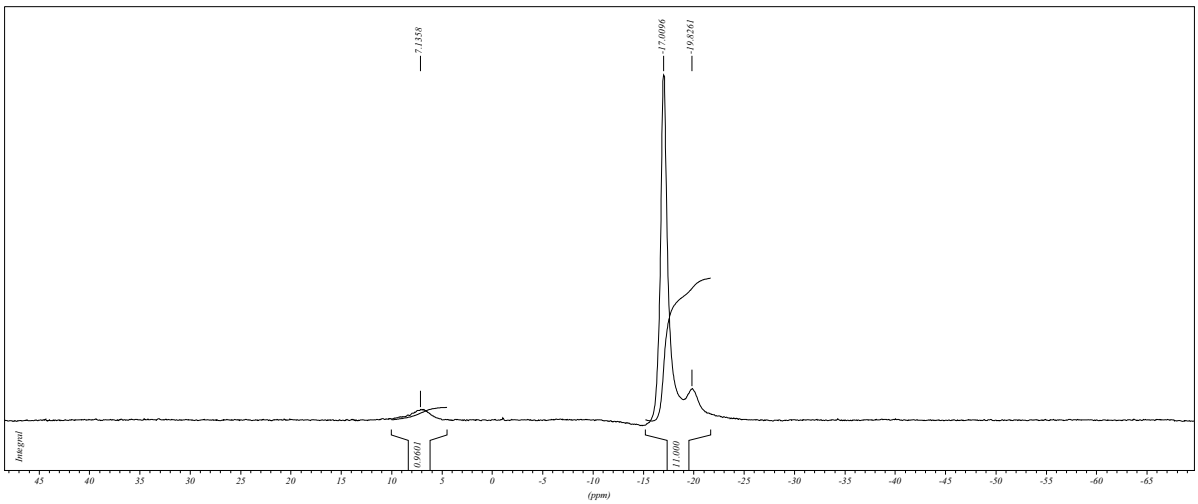

IR-spectrum

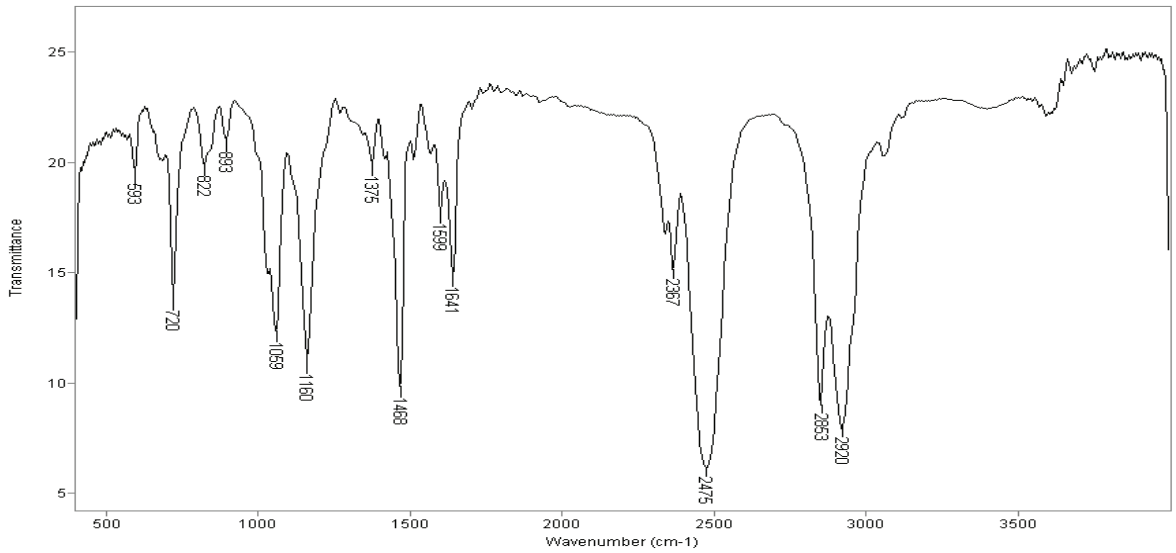

4-(Bishexadecylmethyl)pyridinio-N-ethoxy-ethoxy-undecahydro-closo-dodecaborate (-1), cesium salt (Dioxan-SAINT-16).

ESI-MS, negative

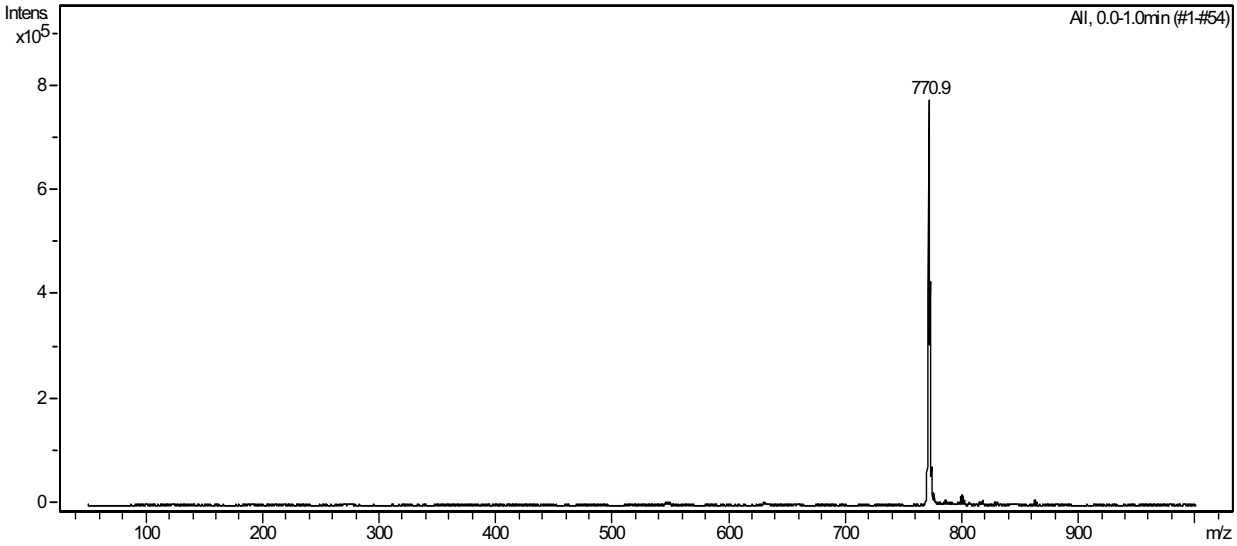

ESI-MS, positive

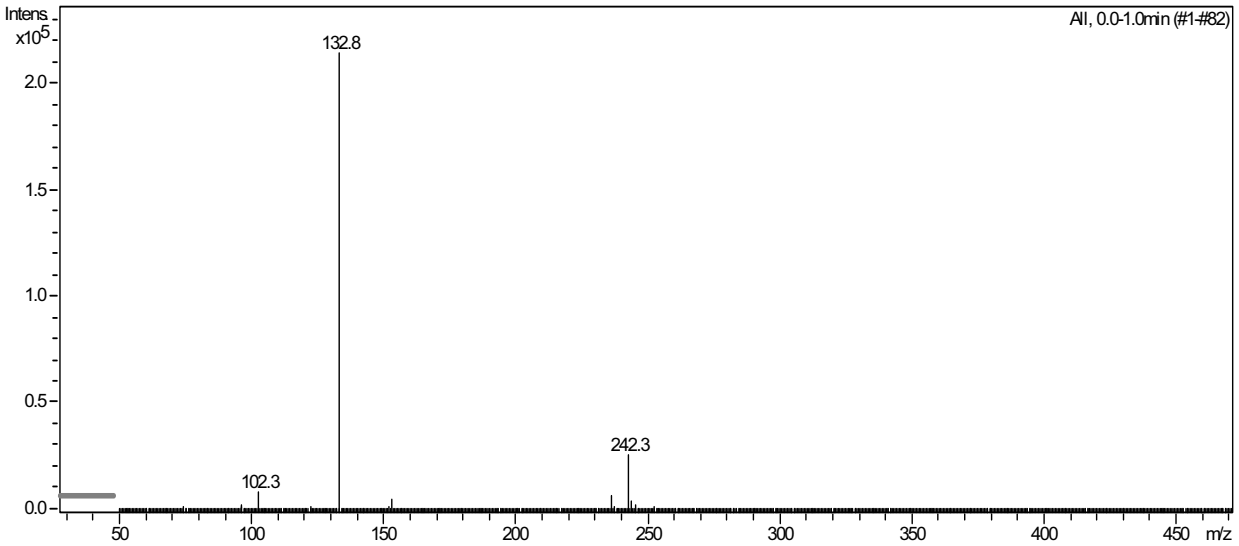

1H-NMR, DMSO-d6

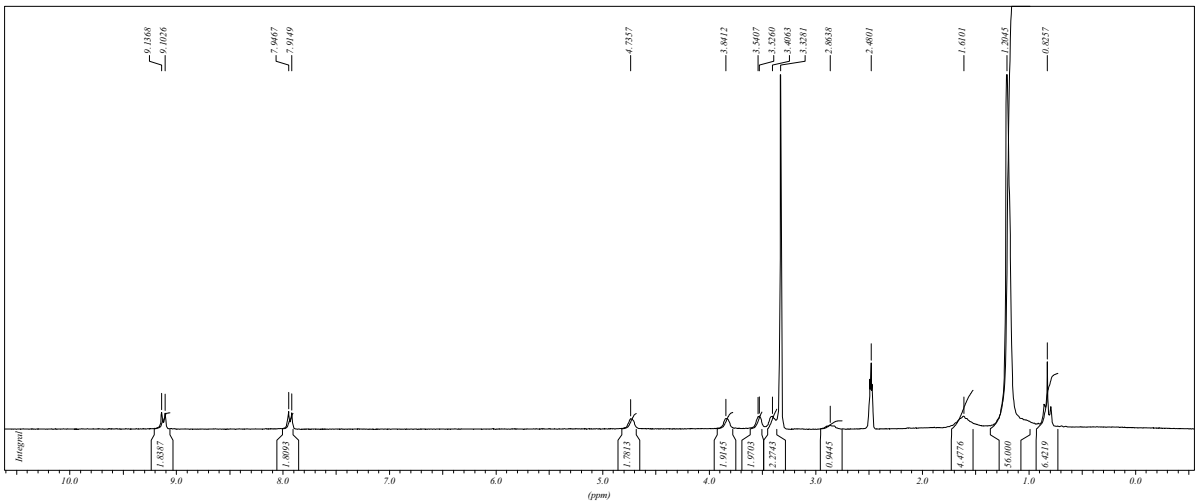

13C-NMR, DMSO-d6

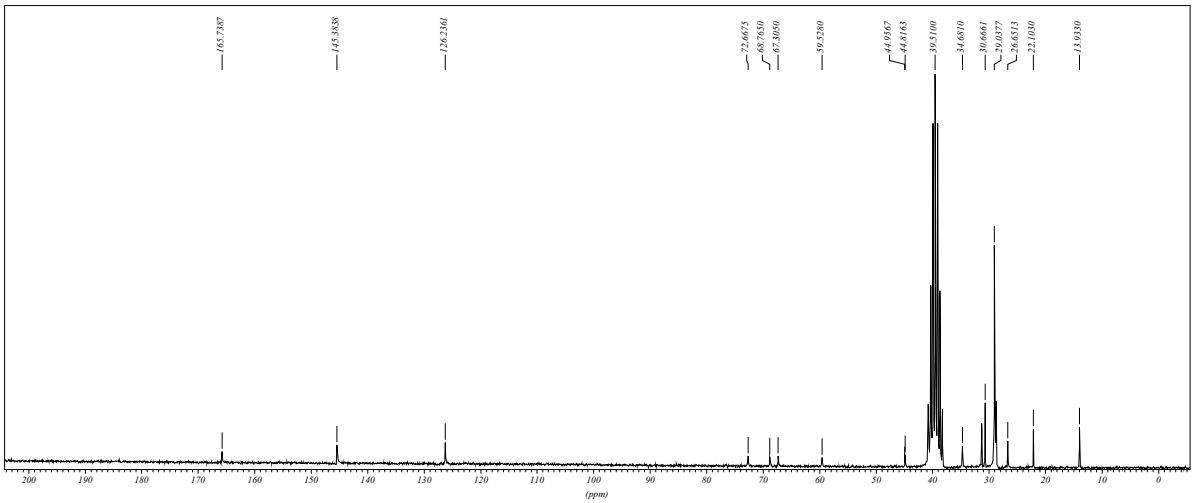

11B-NMR, DMSO-d6

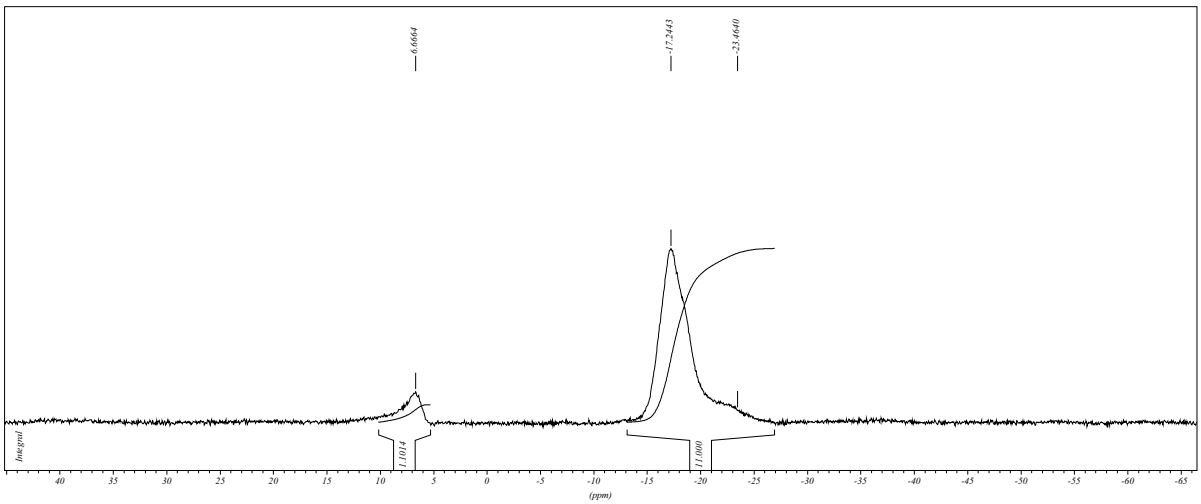

IR-spectrum

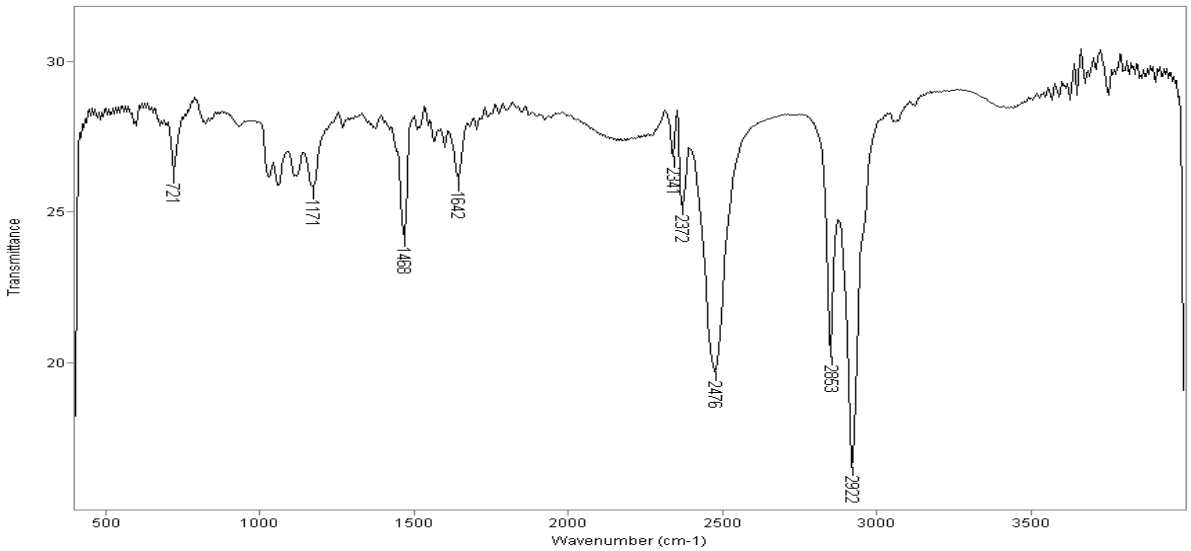

4-(Bishexadecylmethyl)pyridinio-N-pentoxy-undecahydro-closo-dodecaborate (-1), cesium salt (Pyran-SAINT-16).

ESI-MS, negative

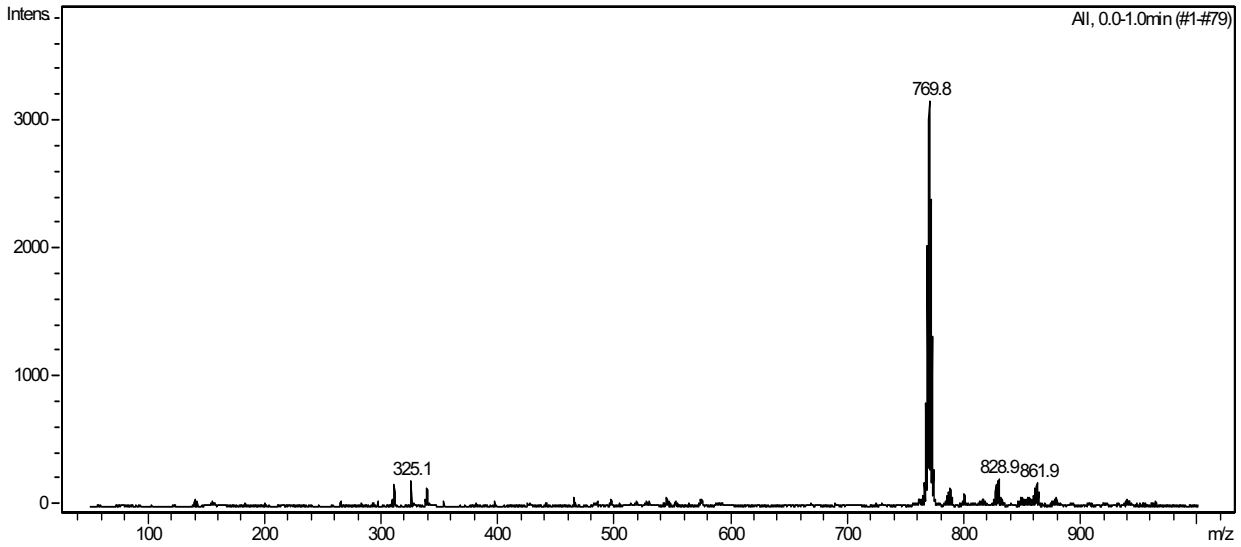

ESI-MS, positive

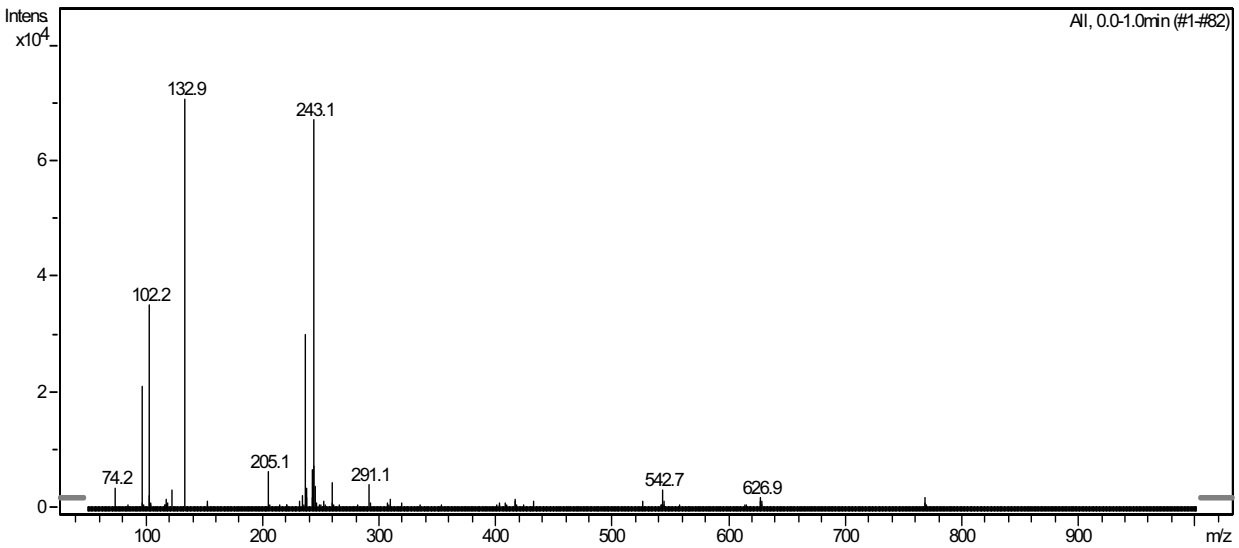

1H-NMR, DMSO-d6

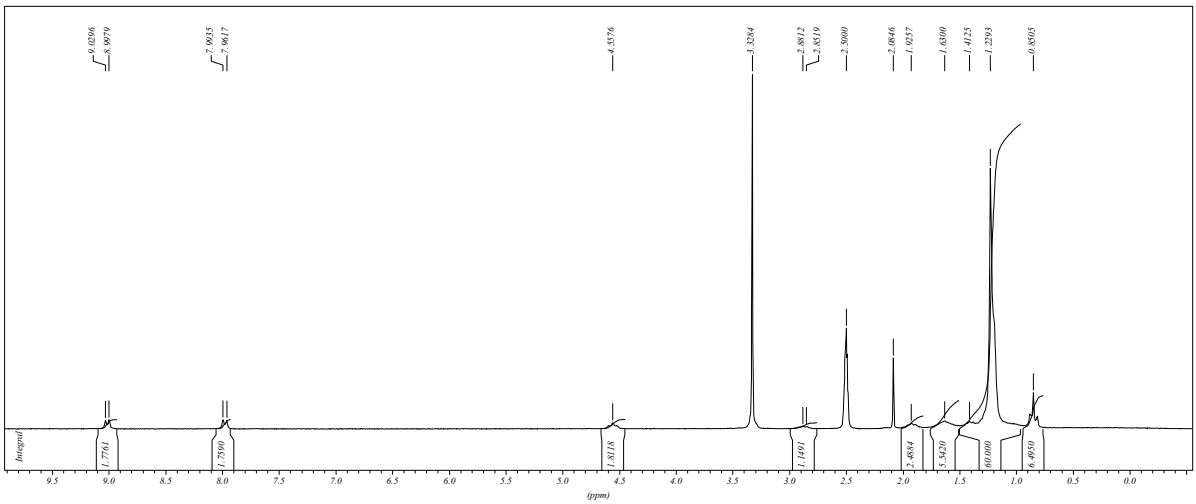

13C-NMR, DMSO-d6

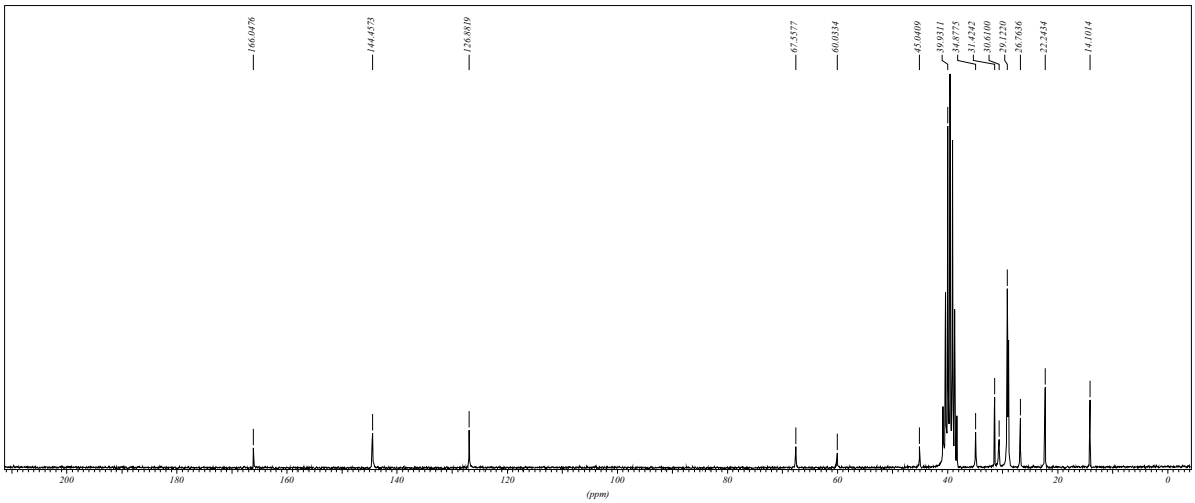

11B-NMR, DMSO-d6

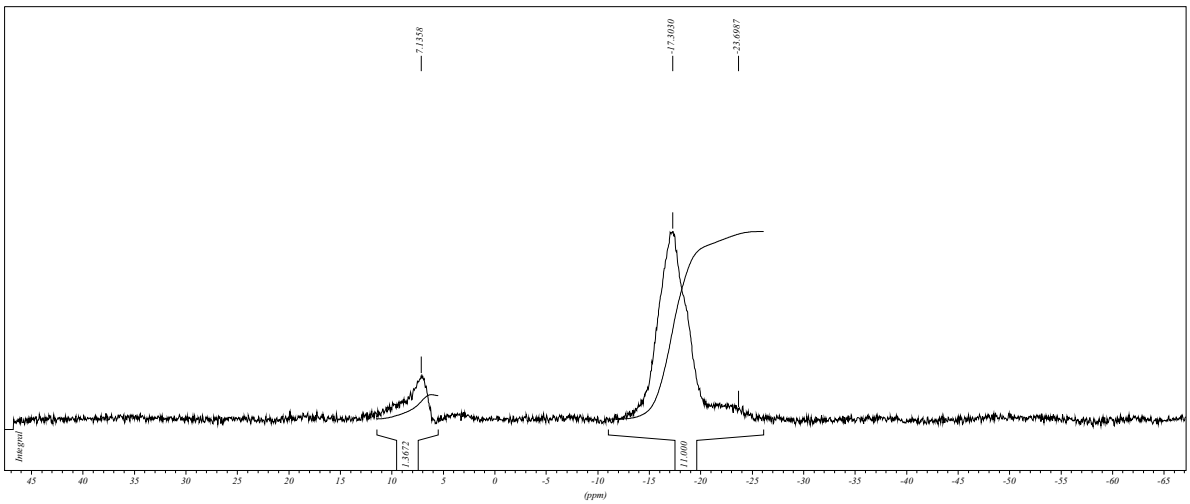

IR-spectrum

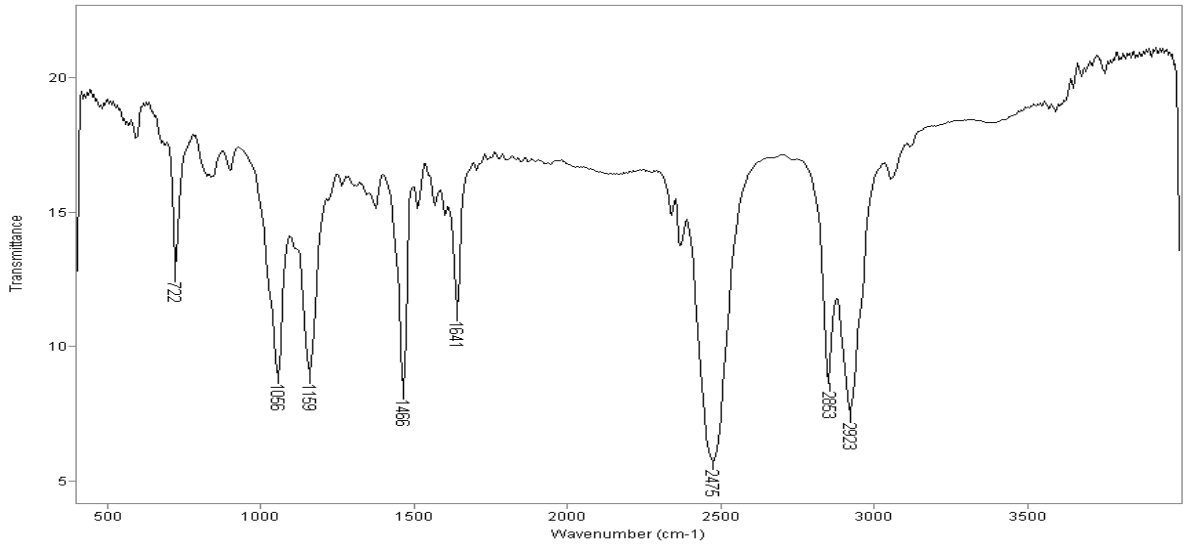
Transmittance
20
15
10
5
722
1056
1159
1466
1641
2475
2853
2923
500
1000
1500
2000
2500
3000
3500
Wavenumber (cm-1)

V

Tumoral hemorrhage induced by dodecaborate cluster lipids

submitted for publication in ChemMedChem

DOI: 10.1002/cmdc.200((will be filled in by the editorial staff))

Tumoral hemorrhage induced by dodecaborate cluster lipids

Tanja Schaffran*[a], Markus Bergmann[b], Ingo Grunwald[c], Regine Peschka-Süss[d], Rolf Schubert[d], Franz M. Wagner[e], and Detlef Gabel[a]

Boron neutron capture therapy (BNCT) is potentially a very effective method for the treatment of localized tumors.[1,2] For this therapy to be successful, boron must be accumulated in concentrations of more than 10 ppm in the target tissue.[3] As the amount of boron in the tumor should be as high as possible, compounds should contain boron units with as many boron atoms as possible. This is best achieved with tumor targeting compounds containing boron clusters, such as the *o*-carborane ($B_{10}C_2$), *nido*-carborane (B_9C_2(1-)) or *closo*-dodecaborate (B_{12}(2-)) clusters. The latter two are ionic, whereas the former is electrically neutral and very hydrophobic. Recently, a number of research groups including ours, have concentrated on the synthesis of lipids containing ionic boron clusters as polar head groups.[4,5,6,7,8,9] The lipids should be ideal carriers of boron when incorporated into liposomes, especially when the liposomes carry a targeting unit such as transferrin or other suitable agents.[10]

Up until now, only two substances are in clinical trials, p-boronophenylalanine (BPA) and $Na_2B_{12}H_{11}SH$ (BSH). However, neither of these achieves good boron concentrations in the tumor[11] and hence they are not optimal boron delivery agents. BSH is well tolerated in patients, and shows low toxicity in mammalian cells. A correspondence between *in vitro* and *in vivo* toxicity, however, does not always exist.

Whereas *in vitro* toxicity is relatively easy to measure, it appears not always to be a good predictor for *in vivo* effects. Li et al.[9] have found for one lipid that *in vivo* toxicity was sufficiently severe to make this lipid of limited if any use for BNCT. Also Nakamura found dose-limiting toxicity with another lipid.[6]

We have tested four newly synthesized lipids of their effects in a mouse tumor model. The lipids are shown in Scheme 1. The lipid B-6-14 carries two negative charges, which are located on the boron cluster, whereas the other lipids have an additional positive charge at some distance from the hydrophobic part. All lipids can form bilayers (either open bilayers or closed vesicles) on their own; in combination with helper lipids, liposomes are formed).[8,12]

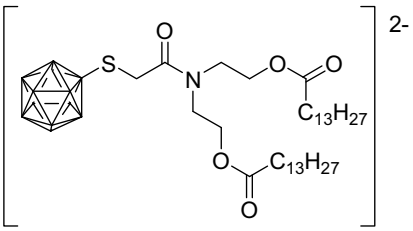

B-6-14

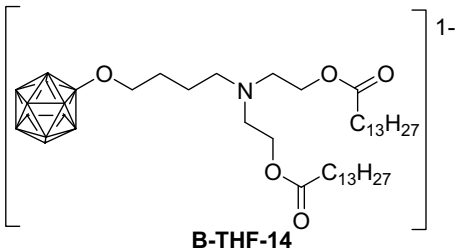

B-THF-14

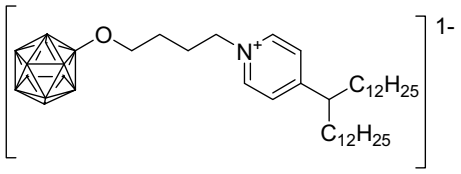

THF-S-12

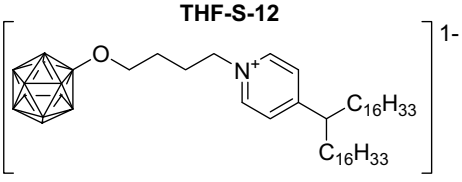

THF-S-16

Scheme 1. Structure of the lipids tested. In the icosahedra, each corner represents a B atom, which carries an additional H atom if not substituted by O or S. The dodecaborate cluster unit $B_{12}H_{11}$ carries a double negative charge.

[a] *Dipl.-Chem. T. Schaffran, Prof. Dr. D. Gabel*
Dept. of Chemistry
University of Bremen
PO Box 330440, D-28334 Bremen
Fax: +49 421 2182871
E-mail: t.schaffran@web.de
[b] *Prof. Dr. M. Bergmann*
Institute of Neuropathology
Klinikum Bremen-Mitte
St.-Jürgenstr. 1, D-28177 Bremen
[c] *Dr. I. Grunwald*
Fraunhofer IFAM
Wiener Straße 12, D-28359 Bremen
[d] *Prof. Dr. R. Peschka-Süss, Prof. Dr. R. Schubert*
Pharmaceutical Technology
University of Freiburg
Hermann-Herder-Str. 9, D-79104 Freiburg i. Br.
[e] *Dipl.-Phys. F.M. Wagner*
ZWE FRM II
Technische Unversitaet Muenchen
Lichtenbergstr. 1, D-85747 Garching

Liposomes were prepared from the lipids in equimolar mixtures with distearoylphosphatidylcholine (DSPC) and cholesterol with 2 mol% DSPE-PEG_{2000} by thin film hydration and extrusion. The liposomal suspension was injected intravenously into the tail vein of mice (Balb/c or C3H, respectively) into which a syngeneic tumor (CT26.WT resp. SCCVII) had been transplanted beforehand.

One lipid, B-THF-14, led to the death of two animals within 5 minutes following the injection. The other three lipids, administered in the same amounts of 20 mg boron/kg body weight, were well tolerated by the animals.

Upon whole-body cryosectioning of the animals, both tumor types were found to be deep-red from blood, for all three lipids (THF-S-12, THF-S-16, B-6-14); in contrast the tumors in non-treated animals consistently showed no macroscopically visible bleeding (Fig. 1). Hemorrhaging occurred rapidly and was visible in the tumor *in situ* within about one hour.

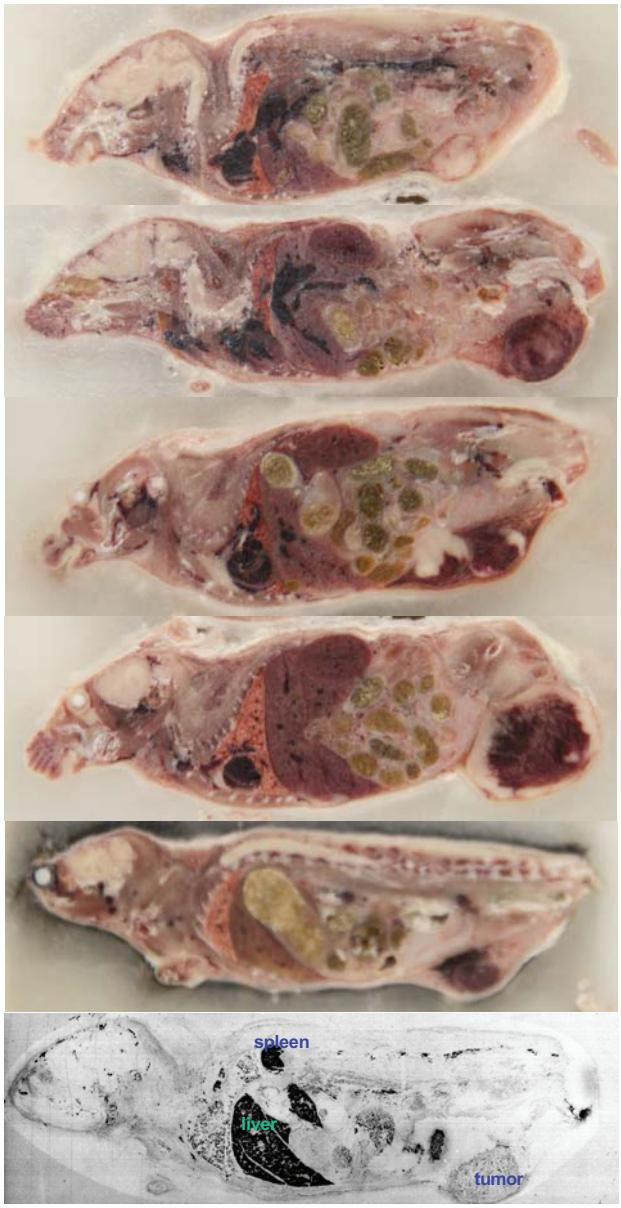

Figure 1. Photographs of mice embedded in CMC during cryo-sectioning. From top to bottom: Balb/c without treatment; Balb/c THF-S-12 3 h post injection; Balb/c THF-S-16 22 h post injection; Balb/c B-6-14 20 h post injection; C3H THF-S-12 4 h post injection. In each animal, the tumor is located at the right lower edge. With no treatment (top), the tumor is lighter in color than muscle. Bottom: Neutron capture radiogram of a section of an animal having received THF-S-12 four hours before sacrifice. Tumor, spleen and liver are labelled. High boron concentrations are indicated by a darker color.

In one animal to which THF-S-12 was administered death occurred within two hours. Upon biopsy, it was found that some of the tumor cells had been injected unintentionally into the peritoneal cavity during subcutaneous implantation and had grown there into numerous tumor nodules. The peritoneum was filled with blood, and thus the animal might have died from severe blood loss.

Neutron capture radiography showed that a lot of boron was taken up in the liver and spleen (despite the fact that the liposomes were pegylated) (bottom picture of Fig. 1). The concentration in the tumor was similar to the concentration in blood.

In histology, the massive hemorrhage was even macroscopically visible (Fig 2.) the red color of the tumors is most probably exclusively associated with extravasated red blood cells.

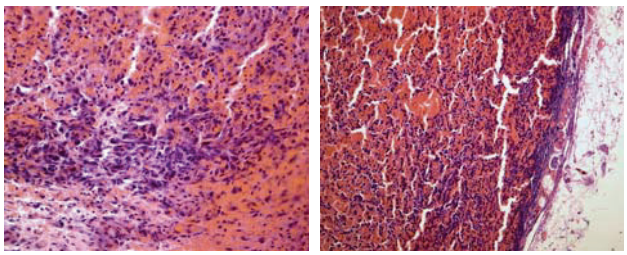

Figure 2. Photographs of histological sections of tumors. Sections were stained with hematoxylin-eosin. left: (S173_8_HE) (20x) right: (S169_08_HE) (20x). In tumors from untreated mice, no hemorrhage was observed.

We assume that the massive hemorrhage observed is caused by destruction of the tumor blood vessels. Such a selective destruction has been observed before by combinations of tumor necrosis factor α (TNFα) in combination with melphalan[13], by multiple doses of doxorubicin-containing liposomes[14], and by a combination of galactosamine and endotoxin.[15] Overexpression of some forms of vascular endothelial growth factor (VEGF) also leads to hemorrhage.[16] As an induction of VEGF production would require at least several hours, we do not consider this to be a likely cause of the effect observed with the boron-containing liposomes.

The liposomes prepared here all have a negative ζ-potential, and are shielded by a PEG layer. Nevertheless, they seem to interact with the walls of the blood vessels, either with the basement membrane or the cells of the endothelial lining.

The induction of tumor hemorrhage for BNCT is not necessarily a desired effect, especially when accompanied, as observed here, with a non-impressive uptake of boron into the tumor. The lipids used here all carry an overall charge of -1 or -2. We therefore intend to prepare boron-containing lipids with no net

charge, or a net charge of +1, to see whether such lipids also cause hemorrhaging. If this were the case, the observed effect might be caused by the amphiphilicity of the lipid, having a hydrophilic dodecaborate cluster in combination with the hydrophobic tails.

Experimental Section

DSPC and DSPE-PEG_{2000} were from Lipoid (Ludwigshafen, Germany). Cholesterol was purchased from Acros Organics (Geel, Belgium).

The used boron lipids were described earlier: B-6-14[7], THF-S-12[12], THF-S-16[12], and B-THF-14[8]. Liposomes were prepared from equimolar mixtures of DSPC, cholesterol and the boron lipid, together with 2 mol% (calculated based on the total amount of lipid) DSPE-PEG_{2000} by hydration and extrusion (21 times through a 100 nm filter) in Hepes-buffered saline solution (pH=7.4). The concentration of total lipid was 100 mM, and the boron lipid concentration was 33.3 mM.

Mice (Balb/c and C3H) were purchased from Charles River (Sulzfeld, Germany). Tumor cells were implanted subcutaneously into the ventral skin. For Balb/c, CT26.WT (American Type Culture Collection CRL-2638) was used. For C3H, SCCVII cells (provided by Dr. Ono, Kyoto University Research Reactor Institute) were used. The tumors were allowed to grow until they reached a diameter of about 0.5 to 1 cm. Animals were allowed free access to food and water. The experiments were approved by the State of Bremen and were carried out in accordance with legal requirements.

Liposomes (100 µL) were injected into the tail vein. After predetermined times, animals were sacrificed. For histology, organs were taken out and preserved immediately in 5% formalin in PBS. For whole-body sectioning[17] the animals were frozen, embedded in 5% carboxymethylcellulose and sectioned in a whole-body cryomicrotome (PMV Instruments, Stockholm, Sweden). The histology sections were prepared in the usual way following paraffin embedding, and stained with hematoxylin/eosin.

Whole-body sections of mice were taken as described in [17]. The freeze-dried sections were placed against a Kodak Pathé LR115 film and irradiated with $4 \cdot 10^{12}$ n cm^{-2} at the FRM II. The films were etched in 10% NaOH, until the holes penetrated the sensitive layer.

The ζ -potential was measured as described by Justus et al.[7]

Acknowledgements

We are grateful to Dr. Ono, Kyoto University Research Reactor Institute, for giving us SCCVII cells. We would like to thank Lipoid GmbH for the gift of DSPC. This work was supported by the German Research Foundation DFG with a joint grant to DG, RS, and RPS.

Keywords: dodecaborate cluster lipids, tumoral hemorrhage, whole body section, *in vivo* toxicity, liposomes

[1] M.F. Hawthorne, *Angew. Chem.* **1993**, 105, 997-1033.

[2] A. H. Soloway, W. Tjarks, B. A. Barnum, F.G. Rong, R. F. Barth, I. M. Codogni, J. G. Wilson, *Chem. Rev*. **1998**, 98, 1515-1562.

[3] R. G. Fairchild, V. P. Bond, *Int. J. Radiat. Oncol. Biol. Phys*. **1985**, 11, 831-840.

[4] H. Nakamura, Y. Miyajima, T. Takei, S. Kasaoka, K. Maruyama, *ChemComm* **2004**, 1910-1911.

[5] H. Nakamura, J.-D. Lee, M. Ueno, Y. Miyajima, H. S. Ban, *Nanobiotechnol.* **2007**, 3, 135-145.

[6] J.-D. Lee, M. Ueno, Y. Miyajima, H. Nakamura, *Org. Lett.* ***2007****, 9*, 323-326.

[7] E. Justus, D. Awad, M. Hohnholt, T. Schaffran, K. Edwards, G. Karlsson, L. Damian, D. Gabel, *Bioconj. Chem*. **2007**, 18, 1287-1293.

[8] T. Schaffran, F. Lissel, B. Samatanga, G. Karlsson, A. Burghardt, K. Edwards, M. Winterhalter, R. Peschka-Süss, R. Schubert, D. Gabel, *J. Organomet. Chem*. **2009**, 694, 1708-1712.

[9] T. Li, J. Hamdie, M. F. Hawthorne, *Bioconj. Chem*. **2006**, 17, 15-20.

[10] K. Maruyama, O. Ishida, S. Kasaoka, T. Takizawa, N. Utoguchi, A. shinohara, M. Chiba, H. Kobayashi, M. Eriguchi, H. Yanagie, *J. Controlled Release* **2004**, 98, 195-207.

[11] S. N. Koryakin, *Pharm. Chem. J.* **2006**, 40, 583-587.

[12] T. Schaffran, A. Burghardt, S. Barnert, R. Peschka-Süss, R. Schubert, M. Winterhalter, D. Gabel, *Bioconj. Chem.* **2009** submitted

[13] S. Hoving, A. L. B. Seynhaeve, S. T. van Tiel, G. aan de Wiel-Ambagtsheer, E. A. de Bruijn, A. M. M. Eggermont, T. L. M. ten Hagen, *Anti-Cancer Drugs* **2006**, 17, 949-959.

[14] R. Zhou, R. Mazurchuk, R. M. Straubinger, *Cancer Res*. **2006**, 62, 2561-2566.

[15] Y. Ito, E. R. Abril, N. W. Bethea, M. K. McCuskey, C. Cover, H. Jaeschke, R. S. McCuskey, *Am. J. Physiol. Gastrointest. Liver Physiol.* **2006**, 291, 211-218.

[16] S.-Y. Cheng, M. Nagane, H.-J. Su Huang, K. C. Webster, *Proc. Natl. Acad. Sci. USA* **1997**, 94, 12081-12087.

[17] D. Gabel, H. Holstein, B. Larsson, L. Gille, G. Ericson, D. Sacker, P. Som, R. G. Fairchild, *Cancer Res.* **1987**, 47, 5451-5454.

Received: ((will be filled in by the editorial staff))
Published online: ((will be filled in by the editorial staff))

9. Declaration

The work described in this thesis is my own work, unless otherwise stated or mentioned in the references. The thesis was written by myself and nobody else.

_____

Tanja Schaffran

Bremen, the 27th of April, 2009